

# **Sparsity Models for Signals: Theory and Applications**

Raja Giryes



# Sparsity Models for Signals: Theory and Applications

Research Thesis

Submitted in Partial Fulfillment of the Requirements for  
the Degree of Doctor of Philosophy

Raja Giryes

Submitted to the Senate of the Technion—Israel Institute of Technology

Adar Aleph 5774

Haifa

February 2014



This Research Thesis was done under the supervision of Prof. Michael Elad  
in the Computer Science Department at the Technion.

I would like to express my gratitude to Prof. Michael Elad for his good instructions, directions, patience, and the open door he always had. His unique pleasant personality, care for the other, and uncompromising character which is satisfied with nothing except excellency created a very comfortable sphere which led to a challenging and enjoyable research experience for me.

I want to thank my co-authors for fascinating collaborations that have deepened my understanding and widened my worldview: Remi Gribonval, Mike Davies, Volkan Cevher, Sangnam Nam and Deanna Needell. I am grateful to my colleagues for many inspiring discussions and brainstorming sessions: Zvika Ben-Haim, Tomer Peleg, Idan Ram, Boaz Ophir, Amir Adler, Matan Protter, Ron Rubinstein, Yossi Shtok, Ori Bryt, Javier Turek, Guy Rosman, Dan Raviv and Anastasia Dubrovina. I am indebted to Freddy Bruckstein and Ron Kimmell for the many helpful and eye-opening tips. I am thankful also to Nir Ailon, Jalal Fadili, Yoram Bresler and Yaniv Plan for many fruitful conversations.

I would like to express my gratitude to my dear wife Shireen for her support, love, patience, endurance and encouragement. I can only be grateful to God for such an excellent wife I have found (Proverbs 31). I want to thank my father Hani and his wife Rana for their encouragement, advice and cherish during all the period, and my parents in law Michel and Louise that supported me all the way. I cannot forget to mention my mother Samira of blessed memory who put in me the will to study and investigate while always remembering the words of the verse: "Train up a child in the way he should go, and when he is old he will not depart from it." (Proverbs 22:6)

I would like to thank my siblings and friends for their support, good advice and prayers during the past four years. I am grateful to my office-mates Tamar Zemach, Eyal Kibbar and Yaniv Romano for their interesting conversations and friendliness.

The Generous Financial Help of the Azrieli Foundation and the Technion is Gratefully Acknowledged



Dedicated to the blessed memory of my mother Samira Giryes which is no longer with us, but whose impact is still visible.

The results shown in this thesis have been published and appeared in the following articles:

- R. Giryes and M. Elad, *RIP-based near-oracle performance guarantees for SP, CoSaMP, and IHT,* *IEEE Transactions on Signal Processing*, vol.60, no.3, pp.1465-1468, March 2012 [1]. Journal Impact Factor (JIF) = 2.831. Jouran Rank (JR) = 25/243.
- R. Giryes and V. Cevher, *"Online performance guarantees for sparse recovery,"* in *Proc. IEEE International Conference on Acoustics, Speech and Signal Processing (ICASSP)*, 22-27 May, 2011 [2].
- R. Giryes and M. Elad, *"Denoising with greedy-like pursuit algorithms,"* in *Proc. European Signal Processing Conference (EUSIPCO)*, Barcelona, Spain, Aug. 29, 2011 [3].
- R. Giryes, S. Nam, M. Elad, R. Gribonval and M.E. Davies, *"Greedy-like algorithms for the cospase analysis model,"* *The Special Issue in LAA on Sparse Approximate Solution of Linear Systems*, 2013 [4]. JIF = 0.968. JR = 84/247.
- R. Giryes, S. Nam, R. Gribonval, M. E. Davies, *"Iterative cospase projection algorithms for the recovery of cospase vectors,"* in *Proc. European Signal Processing Conference (EUSIPCO)*, Barcelona, Spain, Aug. 29, 2011 [5].
- R. Giryes and M. Elad, *"CoSaMP and SP for the cospase analysis model,"* in *Proc. European Signal Processing Conference (EUSIPCO)*, Bucharest, Romania, Aug. 27-31, 2012 [6].
- R. Giryes and M. Elad, *"Can we allow linear dependencies in the dictionary in the synthesis framework?,"* in *Proc. IEEE International Conference on Acoustics, Speech and Signal Processing (ICASSP)*, 26-31 May, 2013 [7].
- R. Giryes and M. Elad, *"Iterative hard thresholding with near optimal projection for signal recovery,"* In *Proc. 10th International Conference on Sampling Theory and Applications (SAMPTA)*, 1-5, July, 2013 [8].
- R. Giryes and M. Elad, *"OMP performance with highly coherent dictionaries,"* in *Proc. 10th International Conference on Sampling Theory and Applications (SAMPTA)*, 1-5, July, 2013 [9].
- R. Giryes and M. Elad, *"Sparsity based Poisson denoising,"* in *Proc. IEEE 27-th Convention of Electronics and Electrical Engineers in Israel (IEEEI'12)*, Eilat, Israel, Nov. 2012 [10].
- R. Giryes and D. Needell, *"Greedy signal space methods for incoherence and beyond,"* Submitted, 2013 [11].

- R. Giryes, "Greedy algorithm for the analysis transform domain," Submitted, 2013 [12].
- R. Giryes and M. Elad, "Sparsity based Poisson denoising with dictionary learning," Submitted, 2013 [13].

If I ... can fathom all mysteries and all knowledge,  
and if I have a faith that can move mountains,  
but do not have love, I am nothing.  
And now these three remain: faith, hope and love.  
But the greatest of these is love.

1 Corinthians 13 (NIV)

# Contents

<b>Abstract</b>	<b>1</b>
<b>Notation</b>	<b>3</b>
<b>1 Introduction</b>	<b>7</b>
1.1 Overview . . . . .	7
1.2 Dissertation Contributions . . . . .	11
1.2.1 Greedy like Algorithms - Near Oracle Performance . . . . .	11
1.2.2 Analysis Greedy-Like Algorithms . . . . .	12
1.2.3 Signal Space Recovery . . . . .	12
1.2.4 Operating in the Transform Domain . . . . .	13
1.2.5 Poisson Data Modeling . . . . .	13
1.3 Dissertation Structure . . . . .	13
<b>2 Background</b>	<b>15</b>
2.1 The Sparse Recovery Problem . . . . .	15
2.2 The Synthesis Approach . . . . .	16
2.2.1 $\ell_0$ Uniqueness . . . . .	16
2.2.2 $\ell_0$ Stability . . . . .	17
2.3 Approximation Techniques . . . . .	17
2.3.1 $\ell_1$ -Relaxation . . . . .	18
2.3.2 The Greedy Approach . . . . .	18
2.3.3 Greedy-Like Techniques . . . . .	18
2.4 Performance Analysis – Basic Tools . . . . .	20
2.5 Theoretical Guarantees for Adversarial Noise . . . . .	22
2.6 Random versus Adversarial Noise . . . . .	23
2.7 Other Signal Models . . . . .	24

2.7.1	The Matrix Completion Problem . . . . .	24
2.7.2	The Cosparse Analysis Model . . . . .	25
2.7.3	Poisson Noise Model . . . . .	27
<b>3</b>	<b>Greedy-Like Algorithms – Near Oracle Performance</b>	<b>31</b>
3.1	Preliminaries . . . . .	32
3.2	Near Oracle Performance of the Algorithms . . . . .	34
3.2.1	Near Oracle Performance of the SP Algorithm . . . . .	34
3.2.2	Near Oracle Performance of the CoSaMP Algorithm . . . . .	37
3.2.3	Near Oracle Performance of the IHT Algorithm . . . . .	40
3.2.4	Bounds on the Expected Error . . . . .	44
3.3	Experiments . . . . .	45
3.4	Extension to the Non-Exact Sparse Case . . . . .	49
3.5	Summary . . . . .	50
<b>4</b>	<b>Greedy-Like Methods for the Cosparse Analysis Model</b>	<b>53</b>
4.1	O-RIP Definition and its Properties . . . . .	55
4.2	Near Optimal Projections . . . . .	59
4.2.1	Cosupport Selection by Thresholding . . . . .	60
4.2.2	Optimal Analysis Projection Operators . . . . .	62
4.3	New Analysis Algorithms . . . . .	66
4.3.1	Analysis Greedy-Like Methods . . . . .	66
4.3.2	The Unitary Case . . . . .	69
4.3.3	Relaxed Versions for High Dimensional Problems . . . . .	70
4.4	Performance Guarantees . . . . .	70
4.4.1	AIHT and AHTP Guarantees . . . . .	73
4.4.2	ACoSaMP Guarantees . . . . .	76
4.4.3	ASP Guarantees . . . . .	80
4.4.4	Non-Exact Cosparse Case . . . . .	81
4.4.5	Theorem Conditions . . . . .	82
4.4.6	Comparison to Other Works . . . . .	83
4.5	Experiments . . . . .	84
4.5.1	Targeted Cosparsity . . . . .	84
4.5.2	Phase Diagrams for Synthetic Signals in the Noiseless Case . . . . .	85

<i>CONTENTS</i>	ix
4.5.3 Reconstruction of High Dimensional Images in the Noisy Case . . . . .	87
4.6 Discussion and Summary . . . . .	88
<b>5 The Signal Space Paradigm</b>	<b>91</b>
5.1 Preliminaries . . . . .	92
5.2 D-RIP Properties . . . . .	94
5.3 Revisiting $\ell_0$ for Signal Recovery . . . . .	96
5.3.1 Uniqueness for Signal Recovery . . . . .	96
5.3.2 $\ell_0$ -Stability for Signal Recovery . . . . .	97
5.4 New Coherence Definition . . . . .	98
5.5 $\epsilon$ -Orthogonal Matching Pursuit . . . . .	99
5.6 $\epsilon$ -OMP Recovery Guarantees . . . . .	99
5.7 Signal Space Algorithms . . . . .	105
5.8 SSSoSaMP Guarantees . . . . .	106
5.8.1 Theorem Conditions . . . . .	108
5.8.2 SSSoSaMP Theorem . . . . .	108
5.8.3 Near Optimal Projection Examples . . . . .	110
5.9 Experimental Results . . . . .	115
5.10 Discussion and Summary . . . . .	116
<b>6 The Analysis Transform Domain Strategy</b>	<b>121</b>
6.1 Preliminary Lemma . . . . .	123
6.2 Transform Domain Iterative Hard Thresholding . . . . .	124
6.3 Frame Guarantees . . . . .	125
6.4 Discussion and Summary . . . . .	129
<b>7 Poisson Noise Model</b>	<b>131</b>
7.1 Poisson Sparsity Model . . . . .	133
7.2 Sparse Poisson Denoising Algorithm (SPDA) . . . . .	135
7.3 Experiments . . . . .	140
7.4 Discussion and Summary . . . . .	148
<b>8 Epilog</b>	<b>149</b>

<b>A Proofs for Chapter 3</b>	<b>153</b>
A.1 Proof of Theorem 3.2.1 – Inequality (3.4) . . . . .	153
A.2 Proof of Inequality (A.1) . . . . .	153
A.3 Proof of Inequality (A.2) . . . . .	156
A.4 Proof of Inequality (3.15) . . . . .	157
<b>B Proofs for Chapter 4</b>	<b>161</b>
B.1 Proofs of Theorem 4.1.7 and Theorem 4.1.8 . . . . .	161
B.2 Proof of Lemma 4.4.6 . . . . .	162
B.3 Proof of Lemma 4.4.7 . . . . .	164
B.4 Proof of Lemma 4.4.10 . . . . .	166
B.5 Proof of Lemma 4.4.11 . . . . .	167
B.6 Proof of Lemma 4.4.12 . . . . .	168
<b>C Proofs for Chapter 5</b>	<b>173</b>
C.1 Proof of Lemma 5.8.5 . . . . .	173
C.2 Proof of Lemma 5.8.6 . . . . .	174
C.3 Proof of Lemma 5.8.7 . . . . .	175
<b>Bibliography</b>	<b>179</b>

# List of Figures

2.1	Poisson noisy versions of the image <i>peppers</i> with different peak values. From left to right: Peaks 0.1, 1, 4 and 10. . . . .	29
3.1	The coefficients in (3.4) and (3.8) as functions of $\delta_{3k}$ . . . . .	35
3.2	The constants of the SP and CoSaMP algorithms as a function of $\delta_{4k}$ . . . . .	40
3.3	The constants of the SP, IHT and DS algorithms as a function of $\delta_{3k}$ . . . . .	43
3.4	The squared-error as achieved by the SP, the CoSaMP and the IHT algorithms as a function of the cardinality. The graphs also show the theoretical guarantees and the oracle performance. . . . .	46
3.5	The mean-squared-error of the SP, the CoSaMP and the IHT algorithms as a function of the cardinality. . . . .	47
3.6	The squared-error as achieved by the SP, the CoSaMP and the IHT algorithms as a function of the noise variance. The graphs also show the theoretical guarantees and the oracle performance. . . . .	48
3.7	The mean-squared-error of the SP, the CoSaMP and the IHT algorithms as a function of the noise variance. . . . .	49
4.1	Comparison between projection using thresholding cosupport selection and optimal cosupport selection. As it can be seen the thresholding projection error is much larger than the optimal projection error by a factor much larger than 1 . . .	61
4.2	Recovery rate for a random tight frame with $p = 144$ and $d = 120$ . From left to right, up to bottom: AIHT with a constant step-size, AIHT with an adaptive changing step-size, AHTP with a constant step-size, AHTP with an adaptive changing step-size, ACoSaMP with $a = \frac{2\ell-p}{\ell}$ , ACoSaMP with $a = 1$ , ASP with $a = \frac{2\ell-p}{\ell}$ , ASP with $a = 1$ , A- $\ell_1$ -minimization and GAP. . . . .	86

4.3	Recovery rate for a random tight frame with $p = 240$ and $d = 120$ (up) and a finite difference operator (bottom). From left to right: AIHT and AHTP with an adaptive changing step-size, and ACoSaMP and ASP with $a = 1$ . . . . .	87
4.4	From left to right, to to bottom: Shepp Logan phantom image, AIHT reconstruction using 35 radial lines, noisy image with SNR of 20 and recovered image using RASP and only 22 radial lines. Note that for the noiseless case RASP and RACoSaMP get a perfect reconstruction using only 15 radial lines. . . . .	89
5.1	Correlation size (inner product) in a sorted order of one atom of the 4 times redundant-DFT dictionary with the other atoms. Note that the x-axis is in a log-scale. . . . .	115
5.2	Recovery rate for SSCoSaMP (Thresholding), SSCoSaMP ( $\epsilon$ -Thresholding) with $\epsilon = \sqrt{0.1}$ , SSCoSaMP (OMP), SSCoSaMP ( $\epsilon$ -OMP) with $\epsilon = \sqrt{0.1}$ and $\epsilon$ -OMP with $\epsilon = \sqrt{0.1}$ for a random $m \times 1024$ Gaussian matrix $\mathbf{M}$ and a 4 times overcomplete DFT matrix $\mathbf{D}$ . The signal is 8-sparse and on the left the coefficients of the original signal are clustered whereas on the right they are separated. . . . .	117
5.3	Recovery rate for SSCoSaMP ( $\epsilon$ -Thresholding) with different values of $\epsilon$ for a random $m \times 1024$ Gaussian matrix $\mathbf{M}$ and a 4 times overcomplete DFT matrix $\mathbf{D}$ . The signal is 8-sparse and on the left the coefficients of the original signal are clustered whereas on the right they are separated. . . . .	118
5.4	Recovery rate for SSCoSaMP ( $\epsilon$ -OMP) with different values of $\epsilon$ for a random $m \times 1024$ Gaussian matrix $\mathbf{M}$ and a 4 times overcomplete DFT matrix $\mathbf{D}$ . The signal is 8-sparse and on the left the coefficients of the original signal are clustered whereas on the right they are separated. . . . .	119
7.1	The piecewise constant image used for the offline training of the initial dictionary. For each range of peak values the image is scaled appropriately. . . . .	138
7.2	The proposed sparse Poisson denoising algorithm (SPDA). . . . .	139
7.3	Test images used in this chapter. From left to right: Saturn, Flag, Cameraman, House, Swoosh, Peppers, Bridge and Ridges. . . . .	140
7.4	Denoising of <i>flag</i> with peak = 1. The PSNR is of the presented recovered images. . . . .	141
7.5	Samples of atoms from the dictionary $\mathbf{D}$ learned using SPDA for <i>flag</i> with peak= 1. . . . .	142
7.6	Denoising of <i>ridges</i> with peak = 0.1. The PSNR is of the presented recovered images. . . . .	142

7.7 Denoising of *Saturn* with peak = 0.2. The PSNR is of the presented recovered images. . . . . 144

7.8 Denoising of *house* with peak = 2. The PSNR is of the presented recovered images. 145



# Abstract

Many signal and image processing applications have benefited remarkably from the theory of sparse representations. In its classical form this theory models signal as having a sparse representation under a given dictionary – this is referred to as the “Synthesis Model”. In this work we focus on greedy methods for the problem of recovering a signal from a set of deteriorated linear measurements. We consider four different sparsity frameworks that extend the aforementioned synthesis model: (i) The cosparse analysis model; (ii) the signal space paradigm; (iii) the transform domain strategy; and (iv) the sparse Poisson noise model.

Our algorithms of interest in the first part of the work are the greedy-like schemes: CoSaMP, subspace pursuit (SP), iterative hard thresholding (IHT) and hard thresholding pursuit (HTP). It has been shown for the synthesis model that these can achieve a stable recovery under some RIP (restricted isometry property) based assumptions in the case that the noise is additive and adversarial. In this work we extend these results in several important ways:

(a) For the case that the noise is random white Gaussian we show that CoSaMP, SP and IHT achieve near-oracle performance, closing a gap between greedy algorithms and relaxation based techniques.

(b) We propose analysis variants for the greedy-like techniques. Assuming the availability of a near optimal projection scheme for the cosparse model, we provide performance guarantees for these algorithms. Our theoretical study relies on a RIP adapted to the context of the cosparse analysis model.

(c) We consider the recovery performance in the synthesis framework when the signal, rather than the representation, is the objective. We develop new uniqueness and stability conditions. We propose a variant of orthogonal matching pursuit (OMP) and give reconstruction guarantees for it using a generalized coherence definition. Then we study the recently proposed signal space CoSaMP (SSCoSaMP) and provide recovery guarantees that hold in several settings including those when the dictionary is incoherent or structurally coherent. These results align more closely with traditional results for representation recovery and improve upon

previous work in the signal space setting.

(d) One drawback of the results for the analysis greedy-like algorithms is that they do not hold for frames as the analysis dictionary, while the existing guarantees for relaxation based methods do cover frames. We propose a variant of IHT that operates in the analysis transform domain and provide guarantees that close this gap.

In the last part of our work we look at the Poisson denoising problem. We propose to harness sparse-representation modeling of image patches for this denoising task, handling severe SNR scenarios. We employ an exponential sparsity model, as recently proposed by Salmon *et al.*, relying directly on the true noise statistics. Our scheme uses a greedy pursuit, with boot-strapping based stopping criterion, and dictionary learning within the denoising process, leading to state-of-the-art-results.

# Notation

Throughout the document, scalars are denoted by italicized letters, as in  $m$  or  $K$ ; vectors are denoted by boldface lowercase letters, as in  $\mathbf{x}$ ; and matrices are denoted by boldface uppercase letters, as in  $\mathbf{A}$ . The  $i$ th component of a vector  $\mathbf{x}$  is denoted  $x_i$ . The state of the vector  $\alpha$  in the  $t$  –  $th$  iteration is denoted by  $\alpha^t$ .

$\ \cdot\ _2$	the euclidean norm for vectors and the spectral ( $2 \rightarrow 2$ ) norm for matrices.
$\ \cdot\ _1$	$\ell_1$ norm - sums the absolute values of a vector.
$\ \cdot\ _0$	$l_0$ pseudo-norm – counts the number of nonzero elements.
$\mathbf{x}$	original unknown signal of size $d$ which is either $\ell$ -cosparsity or has a $k$ -sparse representation $\alpha$ .
$k$	signal sparsity.
$\ell$	signal cosparsity.
$r$	signal corank.
$\alpha$	sparse representation of $\mathbf{x}$ of size $n$ .
$\mathbf{y}$	measured signal of size $m$ .
$\mathbf{e}$	additive noise.
$\mathbf{v}$	general vector of size $d$ which is either $\ell$ -cosparsity or has a $k$ -sparse representation.
$\mathbf{u}$	general vector of size $d$ which is either $\ell$ -cosparsity or has a $k$ -sparse representation.
$\mathbf{z}$	general vector in the signal domain of size $d$ .
$\mathbf{w}$	general vector in the representation or the analysis transform domain.
$\hat{\alpha}$	reconstructed representation.
$\hat{\alpha}_{alg}$	recovered representation by method $alg$ . If clear from context, we may use just $\hat{\alpha}$ .
$\hat{\mathbf{x}}$	reconstructed signal.
$\hat{\mathbf{x}}_{alg}$	reconstructed signal by algorithm $alg$ . If clear from context, we may use just $\hat{\mathbf{x}}$ .

$\varepsilon$	$\ell_2$ noise energy (if $\mathbf{e}$ is bounded adversarial).
$\sigma^2$	noise variance (if $\mathbf{e}$ is Gaussian).
$\mathbf{M}$	measurement matrix of size $m \times d$ .
$\sigma_{\mathbf{M}}$	largest singular value of $\mathbf{M}$ , i.e., $\sigma_{\mathbf{M}}^2 = \ \mathbf{M}^* \mathbf{M}\ _2$ .
$\mathbf{D}$	synthesis dictionary of size $d \times n$ .
$\Omega$	analysis dictionary in matrix representation of size $p \times d$ .
$\mathbf{I}$	identity matrix.
$[p]$	the set of integers $[1 \dots p]$ .
$\text{supp}(\mathbf{w})$	support set of $\mathbf{w}$ (subset of $[d]$ ) – contains the locations of the non-zeros in $\mathbf{w}$ .
$ \text{supp}(\mathbf{w}) $	size of the set $\text{supp}(\mathbf{w})$ .
$\text{supp}(\mathbf{w}, k)$	support of the largest $k$ magnitude elements in $\mathbf{w}$ .
$\text{supp}(\Omega \mathbf{v})$	cosupport set of $\mathbf{v}$ (subset of $[d]$ ) – contains the locations of the zeros in $\Omega \mathbf{v}$ .
$\text{cosupp}(\Omega \mathbf{z}, \ell)$	cosupport of the smallest $\ell$ magnitude elements in $\Omega \mathbf{z}$ .
$\Lambda$	cosupport of $\mathbf{x}$ (if $\mathbf{x}$ is cosparse) – a subset of $[p]$ . $ \Lambda  \geq \ell$ .
$[\cdot]_k$	hard thresholding operator – keeps the largest $k$ -elements in a vector.
$\Lambda^C$	complementary set of $\Lambda$ .
$T$	if $\mathbf{x}$ is cosparse then $\Lambda^C$ (subset of $[p]$ ), otherwise support of $\mathbf{x}$ (subset of $[n]$ ).
$T - \tilde{T}$	set of all the elements contained in $T$ but not in $\tilde{T}$ .
$\alpha_T$	a sub-vector of $\alpha$ with <i>elements</i> corresponding to the set of indices in $T$ .
$\mathbf{D}_T$	a sub-matrix of $\mathbf{D}$ with <i>columns</i> corresponding to the set of indices in $T$ .
$\Omega_\Lambda$	a sub-matrix of $\Omega$ with <i>rows</i> <sup>1</sup> corresponding to the set of indices in $\Lambda$ .
$\text{range}(\mathbf{D})$	range of $\mathbf{D}$ .
$\text{rank}(\mathbf{D})$	rank of matrix $\mathbf{D}$ .
$\delta_{\mathbf{D},k}^D$	D-RIP constant for synthesis dictionary $\mathbf{D}$ and sparsity $k$ .
$\delta_k$	RIP constant for sparsity $k$ . If clear from context, can denote also the D-RIP.
$\delta_\ell = \delta_{\Omega,\ell}^O$	O-RIP constant for analysis dictionary $\Omega$ and cosparsity $\ell$ .
$\mathbf{P}$	projection matrix.
$\mathbf{Q}$	projection matrix.
$\mathbf{P}_T$	for a given $\mathbf{D}$ , $\mathbf{P}_T = \mathbf{D}_T \mathbf{D}_T^\dagger$ is orthogonal projection onto $\text{range}(\mathbf{D}_T)$ .
$\mathbf{P}_\Lambda$	for a given $\Omega$ , $\mathbf{P}_\Lambda = \Omega_\Lambda^\dagger \Omega_\Lambda$ is orthogonal projection onto $\text{range}(\Omega_\Lambda^*)$ .
$\mathbf{Q}_\Lambda$	for a given $\Omega$ , $\mathbf{Q}_\Lambda = \mathbf{I} - \Omega_\Lambda^\dagger \Omega_\Lambda$ is orthogonal projection onto the orthogonal complement of $\text{range}(\Omega_\Lambda^*)$ .

$\mathcal{L}_\ell = \mathcal{L}_{\Omega, \ell}$	set of $\ell$ -cosparsity cosupports, $\{\Lambda \subseteq [p],  \Lambda  \geq \ell\}$ .
$\mathcal{L}_r^{\text{corank}} = \mathcal{L}_{\Omega, r}^{\text{corank}}$	set of all cosupports with corank $r$ , $\{\Lambda \subseteq [p], \text{rank}(\mathbf{\Omega}_\Lambda) \geq r\}$ .
$\mathcal{W}_\Lambda$	subspace spanned by a cosparsity set $\Lambda$ , $\text{span}^\perp(\mathbf{\Omega}_\Lambda) = \{\mathbf{Q}_\Lambda \mathbf{z}, \mathbf{z} \in \mathbb{R}^d\}$ .
$\mathcal{A}_\ell = \mathcal{A}_{\Omega, \ell}$	union of subspaces of $\ell$ -cosparsity vectors, $\bigcup_{\Lambda \in \mathcal{L}_{\Omega, \ell}} \mathcal{W}_\Lambda$ .
$\mathcal{A}_r^{\text{corank}} = \mathcal{A}_{\Omega, r}^{\text{corank}}$	union of subspaces of all vectors with corank $r$ , $\bigcup_{\Lambda \in \mathcal{L}_{\Omega, r}^{\text{corank}}} \mathcal{W}_\Lambda$ .
$\text{trace}(\mathbf{A})$	the sum of the diagonal elements of the matrix $\mathbf{A}$ .
$\text{conv } S$	convex hull of set $S$ .
$\mathcal{S}_\ell^*(\cdot)$	optimal cosupport (of size $\ell$ ) selection procedure.
$\hat{\mathcal{S}}_\ell(\cdot)$	near-optimal cosupport (of size $\ell$ ) selection procedure.



# Chapter 1

## Introduction

### 1.1 Overview

In the past ten years the idea that signals can be represented sparsely had a great impact on the fields of signal and image processing. This new model led to a long series of novelties: new sampling theory has been developed [14] together with new tools for handling signals in different types of applications, such as image denoising [15], image deblurring [16], super-resolution [17], radar [18], medical imaging [19] and astronomy [20], to name a few [21]. Remarkably, in most of these fields the sparsity based techniques achieve state-of-the-art results.

In the classical sparsity model, the signal  $\mathbf{x} \in \mathbb{R}^d$  is assumed to have a  $k$ -sparse representation  $\boldsymbol{\alpha} \in \mathbb{R}^n$  under a given dictionary  $\mathbf{D} \in \mathbb{R}^{d \times n}$ . Formally,

$$\mathbf{x} = \mathbf{D}\boldsymbol{\alpha}, \quad \|\boldsymbol{\alpha}\|_0 \leq k, \quad (1.1)$$

where  $\|\cdot\|_0$  is the  $\ell_0$ -pseudo norm that counts the number of non-zero entries in a vector. Notice, that the non-zero elements in  $\boldsymbol{\alpha}$  corresponds to a set of columns that creates a low-dimensional subspace in which  $\mathbf{x}$  resides. This paradigm is denoted as the synthesis model.

Recently, a new sparsity framework has been introduced: the analysis one [22, 23]. In this model, we look at the coefficients of  $\boldsymbol{\Omega}\mathbf{x}$ , the coefficients of the signal after applying the transform  $\boldsymbol{\Omega} \in \mathbb{R}^{p \times d}$  on it. The sparsity of the signal is measured by the number of zeros in  $\boldsymbol{\Omega}\mathbf{x}$ . We say that a signal is  $\ell$ -cosparse if  $\boldsymbol{\Omega}\mathbf{x}$  has  $\ell$  zero elements. Formally,

$$\|\boldsymbol{\Omega}\mathbf{x}\|_0 \leq p - \ell. \quad (1.2)$$

Note that each zero element in  $\boldsymbol{\Omega}\mathbf{x}$  corresponds to a row in  $\boldsymbol{\Omega}$  to which the signal is orthogonal and all these rows define a subspace the signal is orthogonal to. Similar to the synthesis

model, when the number of zeros is large the signal's subspace is of low dimension. Though the zeros are those that define the subspace, in some cases it is more convenient to use the number of non-zeros as done in [24, 25].

In certain applications, it is more natural and effective to use the analysis framework, as it addresses the signal directly. In the denoising problem, a very common strategy is the total variation (TV) denoising [26] which belongs to the analysis framework [23, 4, 27]. For the deblurring problem, a significant improvement over the state-of-the-art has been achieved by the use of the analysis model [16]. In general, each model implies a different prior on the signal. Thus, the answer to the question which one to use depends heavily on the specific settings of the problem at hand.

The main setup in which the above models have been used is the recovery problem of the form

$$\mathbf{y} = \mathbf{M}\mathbf{x} + \mathbf{e}, \quad (1.3)$$

where  $\mathbf{y} \in \mathbb{R}^m$  is a given set of measurements,  $\mathbf{M} \in \mathbb{R}^{m \times d}$  is the measurement matrix and  $\mathbf{e} \in \mathbb{R}^d$  is an additive noise, which is assumed to be either adversarial bounded noise [14, 21, 28, 29], or with a certain given distribution such as Gaussian [30, 31]. The goal is to recover  $\mathbf{x}$  from  $\mathbf{y}$  and this is the focus of our work.

Note that it is impossible without a prior knowledge to recover  $\mathbf{x}$  from  $\mathbf{y}$  in the case  $m < d$ , or to have an effective denoising when  $\mathbf{e}$  is random with a known distribution. Hence, having a prior, such as the sparsity one, is vital for these tasks. Both the synthesis and the analysis models lead to (different) minimization problems that provide estimates for the original signal  $\mathbf{x}$ .

In the synthesis model, the signal is recovered by its representation, using

$$\hat{\mathbf{a}}_{S-\ell_0} = \underset{\mathbf{w} \in \mathbb{R}^n}{\operatorname{argmin}} \|\mathbf{w}\|_0 \quad s.t. \quad \|\mathbf{y} - \mathbf{MD}\mathbf{w}\|_2 \leq \lambda_{\mathbf{e}}, \quad (1.4)$$

where  $\lambda_{\mathbf{e}}$  is an upper bound for  $\|\mathbf{e}\|_2$  if the noise is bounded and adversarial. Otherwise, it is a scalar dependent on the noise distribution [30, 31, 32]. The recovered signal is simply  $\hat{\mathbf{x}}_{S-\ell_0} = \mathbf{D}\hat{\mathbf{a}}_{S-\ell_0}$ . In analysis, we have the following minimization problem:

$$\hat{\mathbf{x}}_{A-\ell_0} = \underset{\mathbf{v} \in \mathbb{R}^d}{\operatorname{argmin}} \|\mathbf{\Omega}\mathbf{v}\|_0 \quad s.t. \quad \|\mathbf{y} - \mathbf{M}\mathbf{v}\|_2 \leq \lambda_{\mathbf{e}}. \quad (1.5)$$

The values of  $\lambda_{\mathbf{e}}$  are selected as before depending on the noise properties.

Note the differences between synthesis and analysis. In the former we use an indirect estimation for the signal as we work with its representation, while in the latter we get a direct estimate since the minimization is done in the signal domain.

Both (1.4) and (1.5) are NP-hard problems [23, 33]. Hence, approximation techniques are required. These are divided mainly into two categories: relaxation methods and greedy algorithms. In the first category we find the  $\ell_1$ -relaxation [22, 34, 35], which includes LASSO [36], basis pursuit (BP) [34], and the Dantzig selector (DS) [30], where the latter has been proposed only for synthesis context. The  $\ell_1$ -relaxation leads to the following minimization problems for synthesis and analysis respectively:

$$\hat{\mathbf{a}}_{S-\ell_1} = \underset{\mathbf{w} \in \mathbb{R}^n}{\operatorname{argmin}} \|\mathbf{w}\|_1 \quad s.t. \quad \|\mathbf{y} - \mathbf{MD}\mathbf{w}\|_2 \leq \lambda_{\mathbf{e}}, \quad (1.6)$$

$$\hat{\mathbf{x}}_{A-\ell_1} = \underset{\mathbf{v} \in \mathbb{R}^d}{\operatorname{argmin}} \|\mathbf{\Omega}\mathbf{v}\|_1 \quad s.t. \quad \|\mathbf{y} - \mathbf{M}\mathbf{v}\|_2 \leq \lambda_{\mathbf{e}}. \quad (1.7)$$

Among the synthesis greedy strategies we mention orthogonal matching pursuit (OMP) [37, 38], compressive sampling matching pursuit (CoSaMP) [39], subspace pursuit (SP) [40], iterative hard thresholding (IHT) [41] and hard thresholding pursuit (HTP) [42]. In analysis we find the GAP algorithm [23], the counterpart of OMP.

An important question to ask is what are the recovery guarantees that exist for these methods. Two main tools were used for answering this question in the synthesis context. The first is the mutual-coherence which is the maximal inner product between columns in  $\mathbf{MD}$  after normalization [43], and the second is the restricted isometry property [28]. It has been shown that under some conditions on the mutual-coherence or the RIP of  $\mathbf{MD}$ , the approximation algorithms lead to a stable recovery in the adversarial noise case [14, 28, 39, 40, 41, 42, 44, 45], and to an effective denoising in the random Gaussian case [30, 31, 46].

The advantage of the RIP conditions over the coherence ones is that there exist measurement matrices with  $m = O(k \log(n/k))$  that satisfy the RIP conditions [28, 47], while with the coherence the number of measurements is required to be at least  $O(k^2)$  [48]. Hence, in this work we focus mainly on the RIP. It is defined as:

**Definition 1.1.1 (Restricted Isometry Property (RIP) [28])** *A matrix  $\mathbf{A} \in \mathbb{R}^{m \times n}$  has the RIP with a constant  $\delta_k$ , if  $\delta_k$  is the smallest constant that satisfies*

$$(1 - \delta_k) \|\mathbf{w}\|_2^2 \leq \|\mathbf{A}\mathbf{w}\|_2^2 \leq (1 + \delta_k) \|\mathbf{w}\|_2^2, \quad (1.8)$$

whenever  $\mathbf{w} \in \mathbb{R}^n$  is  $k$ -sparse.

The RIP based guarantees for the above synthesis techniques in the adversarial noise case read as follows: If  $\delta_{ak} \leq \delta_{\text{alg}}$ , where  $a > 1$  and  $\delta_{\text{alg}} < 1$  are constants depending on the conditions for each technique, then

$$\|\hat{\mathbf{a}}_{\text{alg}} - \mathbf{a}\|_2^2 \leq C_{\text{alg}} \|\mathbf{e}\|_2^2, \quad (1.9)$$

where  $\hat{\mathbf{a}}_{\text{alg}}$  is the recovered representation by one of the methods and  $C_{\text{alg}} > 2$  is a constant depending on  $\delta_{ak}$ , which differs for each method.

Similar results have been provided for the case where the noise is random white Gaussian with variance  $\sigma^2$ . In this case the reconstruction error is guaranteed to be  $O(k \log(n) \sigma^2)$  [30, 31] – only constant times  $\log(n)$  away from the oracle estimator that foreknows the support of the original signal, i.e., the locations of the non-zero elements of  $\mathbf{a}$ . Unlike in the adversarial noise case, these guarantees hold only for the relaxation based algorithms and not for the greedy ones. Indeed, similar bounds have been provided for OMP and thresholding but those rely on the coherence and the magnitude of the coefficients of the original signal [46, 49].

Turning to the adversarial noise case in the analysis framework, we find guarantees similar to the synthesis ones. Note that as the analysis model treats the signal directly, the guarantees are in terms of the signal and not its representation as in (1.9). The conditions of these guarantees rely on a specific extension of the RIP, referred to as the D-RIP [24].

It has been shown for the analysis  $\ell_1$ -minimization [24, 50, 51] that if  $\mathbf{\Omega}$  is a frame then under some D-RIP conditions we have recovery guarantees similar to (1.9) but in terms of the signal recovery error. A similar result has been proposed for the two dimensional (2D) anisotropic total variation (TV), which is an analysis  $\ell_1$ -minimization problem with the 2D discrete gradient as an operator [27].

As we have seen before, here as well a gap exists between relaxation and greedy techniques as no similar guarantees have been proposed for the latter methods. Indeed, ERC-like recovery conditions have been proposed for GAP in [23]. However, unlike the D-RIP, these are not known to be satisfied for any analysis operator that is not unitary (for unitary operators the analysis model coincides with the synthesis one). Hence, the gap is not closed by the GAP algorithm.

As both OMP and GAP fail to provide theoretical recovery performance which are comparable to the relaxation based techniques in the synthesis and analysis recovery problems, it would be interesting to see whether the greedy-like techniques – CoSaMP, SP, IHT and HTP – or an analysis version developed for them can close these gaps. A clue that this is possi-

ble is the fact they were the first to close such a gap in the adversarial noise case in synthesis [39, 40, 41, 42].

It is worth noting that another gap exists between synthesis and analysis. While the random noise case has been considered in synthesis, no result exists in analysis for this case apart from one that analyzes thresholding in the case of  $\mathbf{M} = \mathbf{I}$  and relies on the signal statistics [52]. Since so many parallels exist between the two frameworks, it is likely that a result for analysis, which is not dependent on the signal statistics and treats also the case  $\mathbf{M} \neq \mathbf{I}$ , should be available.

Another venue in which the sparse model has been used is the Poisson denoising problem. This problem appears in various imaging applications, such as low-light photography, medical imaging and microscopy. In cases of high SNR, several transformations exist so as to approximately convert the Poisson noise into an additive i.i.d. Gaussian noise, for which many effective algorithms are available. However, in a low SNR regime, these transformations are significantly less accurate, and a strategy that relies directly on the true noise statistics is required. A recent work by Salmon *et al.* [20, 53] took this route, proposing a patch-based exponential image representation model. Its integration with a GMM (Gaussian mixture model) based approach has provided state-of-the-art results.

In the Gaussian denoising regime, dictionary learning based denoising strategies [54] have achieved better denoising performance than the GMM based one [55]. This gives us a clue that using a dictionary learning based method, with the new exponential model, should lead to a better Poisson denoising performance.

## 1.2 Dissertation Contributions

This dissertation has two main parts. In the first one, it bridges the gap between greedy techniques and relaxation based methods, and even proposes guarantees that are not known to hold for the relaxation strategies. In the second part, state-of-the-art results for the Poisson denoising problem are obtained using a dictionary learning based technique.

We turn to present our contributions in more details.

### 1.2.1 Greedy like Algorithms - Near Oracle Performance

We start with an average case denoising performance study for Subspace Pursuit (SP), CoSaMP and IHT in the context of the synthesis model. This effort considers the recovery of a noisy signal, with the assumptions that (i) it is corrupted by an additive random white Gaussian noise;

and (ii) it has a  $k$ -sparse representation with respect to a known dictionary  $\mathbf{D}$ . The proposed treatment is based on the RIP, establishing a near-oracle performance guarantee for each of these algorithms. The results for the three algorithms differ in the bounds' constants and in the cardinality requirement (the upper bound on  $k$  for which the claim is true). Also, despite the fact that SP, CoSaMP, and IHT are greedy-like methods, our developed performance guarantees resemble those obtained for the relaxation-based methods (DS and BP), suggesting, among other things, that the performance is independent of the sparse representation entries contrast and magnitude.

### 1.2.2 Analysis Greedy-Like Algorithms

As mentioned before, a prominent question brought up by the cospase analysis model is the analysis pursuit problem – the need to find a signal belonging to this model, given a set of corrupted measurements of it. Several pursuit methods have already been proposed based on  $\ell_1$ -relaxation and the greedy approach. We pursue this question further, and propose a new family of pursuit algorithms for the cospase analysis model, mimicking the greedy-like methods CoSaMP, SP, IHT and HTP. Assuming the availability of a near optimal projection scheme that finds the nearest cospase subspace to any vector, we provide performance guarantees for these algorithms. Our theoretical study relies on a RIP adapted to the context of the cospase analysis model. We explore empirically the performance of these algorithms by adopting a plain thresholding projection, demonstrating their competitive performance.

### 1.2.3 Signal Space Recovery

Most of the work dealing with the synthesis sparse recovery problem has focused on the reconstruction of the signal's representation as the means for recovering the signal itself. This approach forced the dictionary to be of low coherence and with no linear dependencies between its columns. In the analysis model the focus is on the signal, and thus linear dependencies in the analysis dictionary are in fact permitted and found to be beneficial. We show theoretically that the same holds also for signal recovery in the synthesis setup. We start with the  $\ell_0$ -synthesis minimization problem, providing new uniqueness and stability conditions for it. Then we introduce a new mutual coherence definition for signal recovery, showing that a modified version of OMP can recover sparsely represented signals of a dictionary with very high correlations between pairs of columns. We show how the derived results apply to the plain OMP algorithm.

We end by analyzing a signal space version of CoSaMP. Previous work has relied on the existence of fast and accurate projections that allow one to identify the most relevant atoms in a dictionary for any given signal, up to a very strict accuracy. When the dictionary is highly overcomplete, no such projections are currently known in general; the requirements on such projections do not even hold for incoherent or well-behaved dictionaries. We provide an alternative study which enforces assumptions on these projections that hold in several settings including those when the dictionary is incoherent or structurally coherent. These results align more closely with traditional results in the standard sparse recovery literature and improve upon previous work in the signal space setting.

#### 1.2.4 Operating in the Transform Domain

Our results for the analysis greedy-like schemes provide guarantees for dictionaries that have a near optimal projection procedure using greedy-like algorithms. However, no claims have been given for frames. We propose a greedy-like technique that operates in the transform domain, unlike the previous analysis greedy-like methods that operate in the signal domain, and provide guarantees that close the gap between greedy and relaxation techniques showing that the proposed method achieves a stable recovery for frames as operators. In addition, we treat the case where the noise is random and provide denoising guarantees for it, closing a gap between the synthesis and analysis frameworks.

#### 1.2.5 Poisson Data Modeling

For the task of Poisson denoising we propose to harness sparse-representation modeling to overlapping image patches, adopting the same exponential idea proposed by Salmon *et al.* [20, 53]. Our scheme uses a greedy pursuit with boot-strapped stopping condition and dictionary learning within the denoising process. The reconstruction performance of the proposed scheme is competitive with leading methods in high SNR, and achieving state-of-the-art results in cases of low SNR.

### 1.3 Dissertation Structure

This thesis is organized as follows: In Chapter 2 we set the stage for our work, giving a detailed background on the different sparsity models. In the background and later chapters, we

repeat some of the definitions/equations that already appeared before. We do so for enhancing the readability of this thesis. In Chapter 3 we present near-oracle performance guarantees for the greedy-like methods. Chapter 4 presents the analysis greedy-like algorithms with their near optimal projection based theoretical guarantees. Chapter 5 introduces the synthesis signal space paradigm with new uniqueness and stability results for the  $\ell_0$ -minimization problem. It proposes an OMP variant with claims about its recovery performance. It ends with a new study of the signal space CoSaMP, developing new theoretical guarantees for it. In Chapter 6 we present a new greedy-like method that operates in the analysis transform domain. We show that this technique inherits reconstruction guarantees for frames as analysis operators. In Chapter 7 we turn to the Poisson denoising problem. We propose a new denoising strategy and show its novelty in various synthetic experiments. We conclude our work in Chapter 8.

Various portions of the research presented in this dissertation were previously published in [4, 56, 1, 2, 3, 5, 6, 7, 8, 9, 11, 12, 10, 13].

## Chapter 2

# Background

### 2.1 The Sparse Recovery Problem

Many natural signals and images have been observed to be inherently low dimensional despite their possibly very high ambient signal dimension. It is by now well understood that this phenomenon lies at the heart of the success of numerous methods in signal and image processing. Sparsity-based models for signals offer an elegant and clear way to enforce such inherent low-dimensionality, explaining their high popularity in recent years. These models consider the signal  $\mathbf{x} \in \mathbb{R}^d$  as belonging to a finite union of subspaces of dimension  $k \ll d$  [57]. In this thesis we shall focus on two such approaches – the synthesis and the cosparsity analysis models – and develop pursuit methods for them.

Before we dive into the details of the model assumed and the pursuit problem, let us first define the following generic inverse problem that will accompany us throughout this work: For some unknown signal  $\mathbf{x} \in \mathbb{R}^d$ , an incomplete set of linear observations  $\mathbf{y} \in \mathbb{R}^m$  (incomplete implies  $m < d$ ) is available via

$$\mathbf{y} = \mathbf{M}\mathbf{x} + \mathbf{e}, \tag{2.1}$$

where the vector  $\mathbf{e} \in \mathbb{R}^m$  is an additive noise, which is assumed to be a bounded adversarial disturbance that satisfies  $\|\mathbf{e}\|_2 \leq \varepsilon$ , or a random vector – e.g., white Gaussian noise with zero mean and variance  $\sigma^2$ . The task is to recover or approximate  $\mathbf{x}$ . In the noiseless setting where  $\mathbf{e} = 0$ , this amounts to solving  $\mathbf{y} = \mathbf{M}\mathbf{x}$ . Of course, a simple fact in linear algebra tells us that this problem admits infinitely many solutions (since  $m < d$ ). Therefore, when all we have is the observation  $\mathbf{y}$  and the measurement/observation matrix  $\mathbf{M} \in \mathbb{R}^{m \times d}$ , we are in a hopeless situation to recover  $\mathbf{x}$ .

## 2.2 The Synthesis Approach

This is where “sparse signal models” come into play. In the sparse synthesis model, the signal  $\mathbf{x}$  is assumed to have a very sparse representation in a given fixed dictionary  $\mathbf{D} \in \mathbb{R}^{d \times n}$ . In other words, there exists  $\boldsymbol{\alpha}$  with few non-zero entries, as counted by the “ $\ell_0$ -norm”  $\|\boldsymbol{\alpha}\|_0$ , such that

$$\mathbf{x} = \mathbf{D}\boldsymbol{\alpha}, \quad \text{and} \quad k := \|\boldsymbol{\alpha}\|_0 \ll d. \quad (2.2)$$

Having this knowledge we can write down our measurements as

$$\mathbf{y} = \mathbf{A}\boldsymbol{\alpha} + \mathbf{e}, \quad \text{and} \quad k := \|\boldsymbol{\alpha}\|_0 \ll d, \quad (2.3)$$

where  $\mathbf{A} = \mathbf{M}\mathbf{D}$ . Hence, with the assumption that the noise has a bounded energy  $\varepsilon$ , we can solve (2.1) by simply using

$$\hat{\boldsymbol{\alpha}}_{S-\ell_0} = \underset{\mathbf{w}}{\operatorname{argmin}} \|\mathbf{w}\|_0 \quad \text{subject to} \quad \|\mathbf{y} - \mathbf{A}\mathbf{w}\|_2 \leq \varepsilon, \quad (2.4)$$

and  $\hat{\mathbf{x}}_{\ell_0} = \mathbf{D}\hat{\boldsymbol{\alpha}}_{S-\ell_0}$ . In the noiseless case ( $\varepsilon = 0$ ) this minimization problem becomes

$$\hat{\boldsymbol{\alpha}}_{S-\ell_0} = \underset{\mathbf{w}}{\operatorname{argmin}} \|\mathbf{w}\|_0 \quad \text{subject to} \quad \mathbf{y} = \mathbf{A}\mathbf{w}. \quad (2.5)$$

Two important properties that were explored for the  $\ell_0$ -problem [58, 59] are the uniqueness of its solution and the stability of the solution under bounded adversarial noise. In this section we survey the existing results for representation recovery. We present the results with no proofs, since these proofs are available in the literature. Furthermore, the proof of a more generalized result appears in Section 5.3 in this thesis.

### 2.2.1 $\ell_0$ Uniqueness

Given a signal’s representation  $\boldsymbol{\alpha}$  with a cardinality  $k$  ( $\|\boldsymbol{\alpha}\|_0 \leq k$ ) we are interested to know whether it is the unique solution of (2.5). In other words, whether there exists another representation  $\tilde{\boldsymbol{\alpha}} \neq \boldsymbol{\alpha}$  with a cardinality at most  $k$  such that  $\mathbf{A}\boldsymbol{\alpha} = \mathbf{A}\tilde{\boldsymbol{\alpha}}$ . An answer for this question has been given in [43] using the definition of the Spark of a matrix:

**Definition 2.2.1 (Definition 1 in [43])** *Given a matrix  $\mathbf{A}$ , we define  $\operatorname{spark}(\mathbf{A})$  as the smallest possible number of columns from  $\mathbf{A}$  that are linearly dependent.*

This definition provides us with a sharp uniqueness condition for the representation reconstruction:

**Theorem 2.2.2 (Corollary 3 in [43])** *Let  $\mathbf{y} = \mathbf{A}\boldsymbol{\alpha}$ . If  $\|\boldsymbol{\alpha}\|_0 < \operatorname{spark}(\mathbf{A})/2$  then  $\boldsymbol{\alpha}$  is the unique solution of (2.5).*

### 2.2.2 $\ell_0$ Stability

In the case where noise exists in the measurement, the uniqueness of the solution is no longer the question since we cannot recover the original signal exactly. Instead, we ask whether the reconstruction is stable, i.e., whether the  $\ell_2$ -distance between the estimated signal's representation and the original one is proportional to the noise power  $\varepsilon$ . In order to establish that, we use the restricted isometry property (RIP) [28, 29]. The RIP can be seen as an extension of the Spark, which allows noisy case analysis.

**Definition 2.2.3** *A matrix  $\mathbf{A}$  satisfies the RIP condition with parameter  $\delta_k$  if it is the smallest value that satisfies*

$$(1 - \delta_k) \|\boldsymbol{\alpha}\|_2^2 \leq \|\mathbf{A}\boldsymbol{\alpha}\|_2^2 \leq (1 + \delta_k) \|\boldsymbol{\alpha}\|_2^2 \quad (2.6)$$

for any  $k$ -sparse vector  $\boldsymbol{\alpha}$ .

The connection between the RIP and the Spark is the following. Given a matrix  $\mathbf{A}$ ,  $k < \text{spark}(\mathbf{A})$  if  $\delta_k < 1$  [29]. Having the RIP, it is straight forward to have a stability condition for the representation reconstruction using (2.4).

**Theorem 2.2.4** *Let  $\mathbf{y} = \mathbf{A}\boldsymbol{\alpha} + \mathbf{e}$  where  $\|\mathbf{e}\|_2 \leq \varepsilon$ ,  $\mathbf{A}$  satisfies the RIP condition with  $\delta_{2k}$  and  $\|\boldsymbol{\alpha}\|_0 \leq k$ . If  $\delta_{2k} < 1$  then the solution  $\hat{\boldsymbol{\alpha}}_{S-\ell_0}$  of (2.4) is stable. More specifically,*

$$\|\boldsymbol{\alpha} - \hat{\boldsymbol{\alpha}}_{S-\ell_0}\|_2 \leq \frac{2\varepsilon}{\sqrt{1 - \delta_{2k}}}. \quad (2.7)$$

The real restriction by the condition  $\delta_{2k} < 1$  is the lower RIP bound as the upper one can be always satisfied by rescaling the columns of  $\mathbf{A}$ . Hence, this condition can be satisfied if all sets of  $2k$ -columns in  $\mathbf{A}$  are independent.

## 2.3 Approximation Techniques

At a first glance, the result in Theorem 2.2.4 is promising. However, this observation is practical only under the assumption that the solution of (2.4) is feasible. Indeed, the problem in (2.4) is quite hard and problematic [14, 21, 35, 60]. A straight forward search for its solution is a NP hard problem as it requires a combinatorial search over all the possible supports of  $\boldsymbol{\alpha}$  [33, 61]. For this reason, approximation algorithms have been proposed – these are often referred to as pursuit algorithms.

### 2.3.1 $\ell_1$ -Relaxation

One popular pursuit approach is based on  $\ell_1$  relaxation and known as the Basis Pursuit (BP) [34] or the Lasso [36]. By replacing the  $\ell_0$  with  $\ell_1$  norm, we get the  $\ell_1$ -synthesis problem

$$\hat{\boldsymbol{\alpha}}_{S-\ell_1} = \operatorname{argmin} \|\boldsymbol{\alpha}\|_1 \quad \text{s.t.} \quad \|\mathbf{y} - \mathbf{A}\boldsymbol{\alpha}\|_2 \leq \varepsilon, \quad (2.8)$$

with  $\hat{\mathbf{x}}_{S-\ell_1} = \mathbf{D}\hat{\boldsymbol{\alpha}}_{S-\ell_1}$ . This minimizing problem has an equivalent form, known as Basis Pursuit Denoising (BPDN) [34] :

$$\min_{\mathbf{w}} \frac{1}{2} \|\mathbf{y} - \mathbf{A}\mathbf{w}\|_2^2 + \gamma_{BPDN} \|\mathbf{w}\|_1, \quad (2.9)$$

where  $\gamma_{BPDN}$  is a constant related to  $\varepsilon$ . Another  $\ell_1$ -based relaxed algorithm is the Dantzig Selector (DS), as proposed in [30]. The DS aims at solving

$$\min_{\mathbf{w}} \|\mathbf{w}\|_1 \quad \text{subject to} \quad \|\mathbf{A}^*(\mathbf{y} - \mathbf{A}\mathbf{w})\|_\infty \leq \varepsilon_{DS}, \quad (2.10)$$

where  $\varepsilon_{DS}$  is a constant related to the noise power.

### 2.3.2 The Greedy Approach

A different pursuit approach towards the approximation of the solution of (2.4) is the greedy strategy [33, 37, 38, 62], leading to algorithms such as thresholding (Thr), Matching Pursuit (MP), Orthogonal Matching Pursuit (OMP) and regularized OMP (ROMP) [63].

Thresholding selects the support  $\hat{T}_{\text{thresh}}$  to be the locations of the largest  $k$  entries in  $|\mathbf{A}^*\mathbf{y}|$  (element-wise absolute value on each entry). Then it sets  $(\hat{\boldsymbol{\alpha}}_{\text{thresh}})_{\hat{T}_{\text{thresh}}^c} = 0$  and  $(\hat{\boldsymbol{\alpha}}_{\text{thresh}})_{\hat{T}_{\text{thresh}}} = \mathbf{A}_{\hat{T}_{\text{thresh}}}^\dagger \mathbf{y}$ , where  $(\hat{\boldsymbol{\alpha}}_{\text{thresh}})_{\hat{T}_{\text{thresh}}}$  and  $\mathbf{A}_{\hat{T}_{\text{thresh}}}$  are a sub-vector and a sub-matrix that contain only the entries and columns involved in the support  $\hat{T}_{\text{thresh}}$ , and  $\hat{T}_{\text{thresh}}^c$  symbolizes the complementary set of  $\hat{T}_{\text{thresh}}$ .

MP and OMP build the solution  $\boldsymbol{\alpha}$  one non-zero entry at a time, while greedily aiming to reduce the residual error  $\|\mathbf{y} - \mathbf{A}\mathbf{w}\|_2^2$ . ROMP is a variant of OMP that may add more than one element in each iteration. OMP is described in Algorithm 1, where  $\mathbf{a}_i$  denotes the  $i$ -th column of  $\mathbf{A}$ .

### 2.3.3 Greedy-Like Techniques

A different yet related approach is the greedy-like family of algorithms. Among these we have compressive sampling matching pursuit (CoSaMP) [39], subspace pursuit (SP) [40], iterative hard thresholding (IHT) [41] and hard thresholding pursuit (HTP) [42].

**Algorithm 1** Orthogonal Matching Pursuit (OMP)

**Input:**  $k, \mathbf{A} \in \mathbb{R}^{m \times n}$  and  $\mathbf{y} \in \mathbb{R}^m$ , where  $\mathbf{y} = \mathbf{A}\boldsymbol{\alpha} + \mathbf{e}$ ,  $\|\boldsymbol{\alpha}\|_0 \leq k$  and  $\mathbf{e}$  is an additive noise.

**Output:**  $\hat{\boldsymbol{\alpha}}_{\text{OMP}}$ :  $k$ -sparse approximation of  $\boldsymbol{\alpha}$ .

Initialize estimate  $\hat{\boldsymbol{\alpha}}^0 = \mathbf{0}$ , residual  $\mathbf{r}^0 = \mathbf{y}$ , support  $\hat{T}^0 = \emptyset$  and set  $t = 0$ .

**while**  $t \leq k$  **do**

$t = t + 1$ .

New support element:  $i^t = \operatorname{argmax}_{1 \leq i \leq n} |\mathbf{a}_i^*(\mathbf{r}^{t-1})|$ .

Extend support:  $\hat{T}^t = \hat{T}^{t-1} \cup \{i^t\}$ .

Calculate a new estimate:  $\hat{\boldsymbol{\alpha}}_{\hat{T}^t}^t = \mathbf{A}_{\hat{T}^t}^\dagger \mathbf{y}$  and  $\hat{\boldsymbol{\alpha}}_{(\hat{T}^t)^c}^t = \mathbf{0}$ .

Calculate a new residual:  $\mathbf{r}^t = \mathbf{y} - \mathbf{A}\hat{\boldsymbol{\alpha}}^t$ .

**end while**

Form the final solution  $\hat{\boldsymbol{\alpha}}_{\text{OMP}} = \hat{\boldsymbol{\alpha}}^k$ .

These differ from MP and OMP in two important ways: (i) Rather than accumulating the desired solution one element at a time, a group of non-zeros is identified and added together; and (ii) As opposed to the MP and OMP, these algorithms enable removal of elements from the detected support. The first part of the dissertation focuses on this specific family of methods, as it poses an interesting compromise between the simplicity of the greedy methods and the strong abilities of the relaxation algorithms.

The greedy-like strategies use a prior knowledge about the cardinality  $k$  and actually aim at approximating a variant of (2.4)

$$\operatorname{argmin}_{\mathbf{w}} \|\mathbf{y} - \mathbf{A}\mathbf{w}\|_2^2 \quad \text{subject to} \quad \|\mathbf{w}\|_0 \leq k. \quad (2.11)$$

For simplicity we shall present the greedy-like pursuit algorithms without specifying the stopping criterion. Any standard stopping criterion, like residual's size or relative iteration change, can be used. More details can be found in [39, 40].

*IHT and HTP:* IHT [41] and HTP [42] are presented in Algorithm 2, where  $\operatorname{supp}(\mathbf{w}_g, k)$  is the support of the largest  $k$  magnitude elements in  $\boldsymbol{\alpha}$ . Each IHT iteration is composed of two basic steps. The first is a gradient step, with a step size  $\mu_t$ , in the direction of minimizing  $\|\mathbf{y} - \mathbf{A}\mathbf{w}\|_2^2$ . The step size can be either constant in all iterations ( $\mu^t = \mu$ ) or changing [64]. The result vector  $\mathbf{w}_g$  is not guaranteed to be sparse and thus the second step of IHT projects  $\mathbf{w}_g$  to the closest  $k$ -sparse subspace by keeping its largest  $k$  elements. The HTP takes a different strategy in the projection step. Instead of using a simple projection to the closest  $k$ -sparse subspace, HTP selects the vector in this subspace that minimizes  $\|\mathbf{y} - \mathbf{A}\mathbf{w}\|_2^2$  [42, 65].

---

**Algorithm 2** Iterative Hard Thresholding (IHT) and Hard Thresholding Pursuit (HTP)

---

**Input:**  $k, \mathbf{A}, \mathbf{y}$  where  $\mathbf{y} = \mathbf{A}\boldsymbol{\alpha} + \mathbf{e}$ ,  $k$  is the cardinality of  $\boldsymbol{\alpha}$  and  $\mathbf{e}$  is an additive noise.**Output:**  $\hat{\boldsymbol{\alpha}}_{\text{IHT}}$  or  $\hat{\boldsymbol{\alpha}}_{\text{HTP}}$ :  $k$ -sparse approximation of  $\boldsymbol{\alpha}$ .Initialize representation  $\hat{\boldsymbol{\alpha}}^0 = \mathbf{0}$  and set  $t = 0$ .**while** halting criterion is not satisfied **do** $t = t + 1$ .Perform a gradient step:  $\mathbf{w}_g = \hat{\boldsymbol{\alpha}}^{t-1} + \mu^t \mathbf{A}^*(\mathbf{y} - \mathbf{A}\hat{\boldsymbol{\alpha}}^{t-1})$ Find a new support:  $T^t = \text{supp}(\mathbf{w}_g, k)$ Calculate a new estimate:  $\hat{\boldsymbol{\alpha}}_{T^t}^t = (\mathbf{w}_g)_{T^t}$  for IHT or  $\hat{\boldsymbol{\alpha}}_{T^t}^t = \mathbf{A}_{T^t}^\dagger \mathbf{y}$  for HTP, and  $\hat{\boldsymbol{\alpha}}_{(T^t)^c}^t = 0$ .**end while**Form the final solution  $\hat{\boldsymbol{\alpha}}_{\text{IHT}} = \hat{\boldsymbol{\alpha}}^t$  for IHT and  $\hat{\boldsymbol{\alpha}}_{\text{HTP}} = \hat{\boldsymbol{\alpha}}^t$  for HTP.

---

*CoSaMP and SP:* CoSaMP [39] and SP [40] are presented in Algorithm 3. The difference between these two techniques is similar to the difference between IHT and HTP. Unlike IHT and HTP, the estimate for the support of  $\boldsymbol{\alpha}$  in each CoSaMP and SP iteration is computed by observing the residual  $\mathbf{y}_{\text{resid}}^t = \mathbf{y} - \mathbf{A}\hat{\boldsymbol{\alpha}}^t$ . In each iteration, CoSaMP and SP detect new support indices from the residual by taking those with the largest elements in  $|\mathbf{A}^* \mathbf{y}_{\text{resid}}^t|$ . They add the new indices to the already estimated support set from the previous iteration, creating a new estimated support  $\tilde{T}^t$  with cardinality larger than  $k$ . Having the updated support, in a similar way to the projection in HTP, an objective aware projection is performed resulting with an estimate  $\mathbf{w}$  for  $\boldsymbol{\alpha}$  that is supported on  $\tilde{T}^t$ . Since we know that  $\boldsymbol{\alpha}$  is  $k$ -sparse we want to project  $\mathbf{w}$  to a  $k$ -sparse subspace. CoSaMP does it by simple hard thresholding like in IHT. SP does it by an objective aware projection similar to HTP.

## 2.4 Performance Analysis – Basic Tools

Recall that we aim at recovering the (deterministic!) sparse representation vector  $\boldsymbol{\alpha}$ . We measure the quality of the approximate solution  $\hat{\boldsymbol{\alpha}}$  by the Mean-Squared-Error (MSE)

$$\text{MSE}(\hat{\boldsymbol{\alpha}}) = E \|\boldsymbol{\alpha} - \hat{\boldsymbol{\alpha}}\|_2^2, \quad (2.12)$$

where the expectation is taken over the distribution of the noise. If the noise is adversarial then the MSE turns to be the squared error  $\|\boldsymbol{\alpha} - \hat{\boldsymbol{\alpha}}\|_2^2$  (with no mean). Therefore, our goal is to get as small as possible error. The question is, how small can it be? In order to answer this question, we may rely on two features that characterize the matrix  $\mathbf{A}$  – the mutual-coherence  $\mu$  (the

**Algorithm 3** Subspace Pursuit (SP) and CoSaMP

**Input:**  $k, \mathbf{A}, \mathbf{y}$  where  $\mathbf{y} = \mathbf{A}\boldsymbol{\alpha} + \mathbf{e}$ ,  $k$  is the cardinality of  $\boldsymbol{\alpha}$  and  $\mathbf{e}$  is an additive noise.  $a = 1$  (SP),  $a = 2$  (CoSaMP).

**Output:**  $\hat{\boldsymbol{\alpha}}_{\text{CoSaMP}}$  or  $\hat{\boldsymbol{\alpha}}_{\text{SP}}$ :  $k$ -sparse approximation of  $\boldsymbol{\alpha}$ .

Initialize the support  $T^0 = \emptyset$ , the residual  $\mathbf{y}_{\text{resid}}^0 = \mathbf{y}$  and set  $t = 0$ .

**while** halting criterion is not satisfied **do**

$t = t + 1$ .

Find new support elements:  $T_\Delta = \text{supp}(\mathbf{A}^* \mathbf{y}_{\text{resid}}^{t-1}, ak)$ .

Update the support:  $\tilde{T}^t = T^{t-1} \cup T_\Delta$ .

Compute a temporary representation:  $\mathbf{w} = \mathbf{A}_{\tilde{T}^t}^+ \mathbf{y}$ .

Prune small entries:  $T^t = \text{supp}(\mathbf{w}, k)$ .

Calculate a new estimate:  $\hat{\boldsymbol{\alpha}}_{T^t}^t = \mathbf{w}_{T^t}$  for CoSaMP or  $\hat{\boldsymbol{\alpha}}_{T^t}^t = \mathbf{A}_{T^t}^+ \mathbf{y}$  for SP, and  $\hat{\boldsymbol{\alpha}}_{(T^t)^c}^t = 0$ .

Update the residual:  $\mathbf{y}_{\text{resid}}^t = \mathbf{y} - \mathbf{A}\hat{\boldsymbol{\alpha}}^t$ .

**end while**

Form the final solution  $\hat{\boldsymbol{\alpha}}_{\text{CoSaMP}} = \hat{\boldsymbol{\alpha}}^t$  for CoSaMP and  $\hat{\boldsymbol{\alpha}}_{\text{SP}} = \hat{\boldsymbol{\alpha}}^t$  for SP.

maximal absolute inner product between columns of  $\mathbf{A}$  after normalization) and the Restricted Isometry Property (RIP). These two measures are related by  $\delta_k \leq (k-1)\mu$  [46]. The RIP is a stronger descriptor of  $\mathbf{A}$  as it characterizes groups of  $k$  columns from  $\mathbf{A}$ , whereas the mutual-coherence “sees” only pairs. On the other hand, computing  $\mu$  is easy, while the evaluation of  $\delta_k$  is prohibitive in most cases. An exception to this are random matrices  $\mathbf{A}$  for which the RIP constant is known (with high probability). For example, if the entries of  $\sqrt{m}\mathbf{A}$  are drawn from a white Gaussian distribution<sup>1</sup> and  $m \geq Ck \log(n/k)/\varepsilon_k^2$ , or if its rows are drawn uniformly from the  $N \times N$  unitary discrete Fourier transform (DFT) and

$$m \geq \frac{Ck \log^5 n \cdot \log(\varepsilon_k^{-1})}{\varepsilon_k^2}, \quad (2.13)$$

where  $C$  is a certain constant<sup>2</sup>, then with a very high probability  $\delta_k \leq \varepsilon_k$  [28, 47]. For details about other matrices that satisfy the RIP condition we refer the reader to [66, 67, 68, 69].

<sup>1</sup>The multiplication by  $\sqrt{m}$  comes to normalize the columns of the effective dictionary  $\mathbf{A}$ .

<sup>2</sup>Throughout the dissertation we use  $C$  to denote a constant. By the abuse of notation, at each occurrence it may admit a different value.

## 2.5 Theoretical Guarantees for Adversarial Noise

We return now to the question we posed above: how small can the recovery error be? There are various attempts to bound the MSE of pursuit algorithms. Early works considered the adversarial case, where the noise can admit any form as long as its norm is bounded [14, 35, 70, 71]. These works gave bounds on the reconstruction error in the form of a constant factor ( $C > 1$ ) multiplying the noise power,

$$\|\boldsymbol{\alpha} - \hat{\boldsymbol{\alpha}}\|_2^2 \leq C \cdot \|\mathbf{e}\|_2^2. \quad (2.14)$$

Notice that the cardinality of the representation plays no role in this bound, and all the noise energy is manifested in the final error.

One such example is the work by Candès and Tao, reported in [29], which analyzed the  $\ell_1$ -minimization (BP) error. They have shown that if the dictionary  $\mathbf{A}$  satisfies  $\delta_k + \delta_{2k} + \delta_{3k} < 1$  then the MSE is bounded by a constant times the energy of the noise, as shown above. The condition on the RIP was improved to  $\delta_{2k} < 0.4931$  in [28, 45, 72, 73]. Similar tighter bounds are  $\delta_{1.625k} < \sqrt{2} - 1$  and  $\delta_{3k} < 4 - 2\sqrt{3}$  [74], or  $\delta_k < 0.307$  [75]. The advantage of using the RIP in the way described above is that it gives a uniform guarantee: it is related only to the dictionary and sparsity level.

Note that the bound in (2.14) is in terms of the representation. If the dictionary  $\mathbf{D}$  is a unitary matrix then the same bound holds also for the signal error. The above statement was extended also for incoherent redundant dictionaries in [76].

Next in line to be analyzed are the greedy methods (MP, OMP, Thr) [14, 70]. Unlike the  $\ell_1$ -relaxation, these algorithms were shown to be more sensitive, incapable of providing a uniform guarantee for the reconstruction. Rather, beyond the dependence on the properties of  $\mathbf{A}$  and the sparsity level, the guarantees obtained depend also on the ratio between the noise power and the absolute values of the signal representation entries.

Interestingly, the greedy-like approach, as practiced in the ROMP, the CoSaMP, the SP, and the IHT algorithms, was found to be closer in spirit to the  $\ell_1$ -relaxation, all leading to uniform guarantees on the bounded MSE. The ROMP was the first of these algorithms to be analyzed [63], leading to the more strict requirement  $\delta_{2k} < 0.03/\sqrt{\log k}$ . The CoSaMP [39] and the SP [40] that came later have similar RIP conditions without the  $\log k$  factor, where the SP result is slightly better. Its condition is based on  $\delta_{3k}$  whereas the CoSaMP result uses  $\delta_{4k}$ . The IHT algorithm was also shown to have a uniform guarantee for bounded error of the same flavor as

shown above [41]. Recently, a RIP based guarantee was developed also for OMP, when applied with  $30k$  iterations [44].

## 2.6 Random versus Adversarial Noise

All the results mentioned above deal with an adversarial noise, and therefore give bounds that are related only to the noise power with a coefficient  $C$  that is larger than 1, implying that no effective denoising is to be expected. This is natural since we consider the worst case results, where the noise can be concentrated in the places of the non-zero elements of the sparse vector. To obtain better results, one must change the perspective and consider a random noise drawn from a certain distribution.

We start by considering an oracle estimator that knows the support of  $\alpha$ , i.e. the locations of the  $k$  non-zeros in this vector. The oracle estimator obtained as a direct solution of the problem posed in (2.3) is easily given by

$$\hat{\alpha}_{oracle} = \mathbf{A}_T^\dagger \mathbf{y}, \quad (2.15)$$

where  $T$  is the support of  $\alpha$ . Its MSE is given by [30]

$$\text{MSE}(\hat{\alpha}_{oracle}) = E \|\alpha - \hat{\alpha}_{oracle}\|_2^2 = E \|\mathbf{A}_T^\dagger \mathbf{e}\|_2^2, \quad (2.16)$$

where we now assume  $\mathbf{e}$  to be random. Assuming that each entry in it is i.i.d Gaussian distributed with zero-mean and variance  $\sigma^2$ , the error in (2.16) becomes

$$\begin{aligned} \text{MSE}(\hat{\alpha}_{oracle}) &= E \|\mathbf{A}_T^\dagger \mathbf{e}\|_2^2 \\ &= \text{trace} \left\{ (\mathbf{A}_T^* \mathbf{A}_T)^{-1} \right\} \sigma^2. \end{aligned} \quad (2.17)$$

Hence, using the RIP we have

$$\frac{1}{1 + \delta_k} k \sigma^2 \leq E \|\mathbf{A}_T^\dagger \mathbf{e}\|_2^2 \leq \frac{1}{1 - \delta_k} k \sigma^2. \quad (2.18)$$

This is the smallest possible error, and it is proportional to the number of non-zeros  $k$  multiplied by  $\sigma^2$ . It is natural to ask how close do we get to this best error by practical pursuit methods that do not assume the knowledge of the support. This brings us to the next discussion.

The first to realize this and exploit this alternative point of view were Candès and Tao in the work reported in [30] that analyzed the DS algorithm. As mentioned above, the noise was assumed to be random zero-mean white Gaussian noise with a known variance  $\sigma^2$ . For the

choice  $\varepsilon_{DS} = \sqrt{2(1+a)\log n} \cdot \sigma$ , and requiring  $\delta_{2k} + \delta_{3k} < 1$ , the minimizer of (2.10),  $\hat{\alpha}_{DS}$ , was shown to obey

$$\|\alpha - \hat{\alpha}_{DS}\|_2^2 \leq C_{DS}^2 \cdot (2(1+a)\log n) \cdot k\sigma^2, \quad (2.19)$$

with probability exceeding  $1 - (\sqrt{\pi(1+a)\log n} \cdot n^a)^{-1}$ , where  $C_{DS} = 4/(1 - 2\delta_{3k})$ .<sup>3</sup> Up to a constant and a  $\log n$  factor, this bound is the same as the oracle's one in (2.16). The  $\log n$  factor in (2.19) is unavoidable, as proven in [32], and therefore this bound is optimal up to a constant factor.

A similar result is presented in [31] for BPDN. For the choice  $\gamma_{BPDN} = \sqrt{8\sigma^2(1+a)\log n}$ , and requiring  $\delta_{2k} + 3\delta_{3k} < 1$ , the solution of (2.9) satisfies

$$\|\alpha - \hat{\alpha}_{BPDN}\|_2^2 \leq C_{BPDN}^2 \cdot (2(1+a)\log n) \cdot k\sigma^2 \quad (2.20)$$

with probability exceeding  $1 - n^{-a}$ . This result is weaker than the one obtained for the DS in two ways: (i) It gives a smaller probability of success; and (ii) The constant  $C_{BPDN}$  is larger, as shown in [46] ( $C_{BPDN} \geq 32/\kappa^4$ , where  $\kappa < 1$  is defined in [31]).

Mutual-Coherence based results for DS and BP were derived in [46, 49]. In [46] results were developed also for the greedy algorithms – OMP and thresholding. These results rely on the contrast and magnitude of the entries of  $\alpha$ . Denoting by  $\hat{\alpha}_{greedy}$  the reconstruction result of thresholding and OMP, we have

$$\|\alpha - \hat{\alpha}_{greedy}\|_2^2 \leq C_{greedy}^2 \cdot (2(1+a)\log n) \cdot k\sigma^2, \quad (2.21)$$

with probability exceeds  $1 - (\sqrt{\pi(1+a)\log n} \cdot n^a)^{-1}$ , where  $C_{greedy} \leq 2$ . This result is true for OMP and thresholding under the condition

$$\frac{|\alpha_{min}| - 2\sigma\sqrt{2(1+a)\log n}}{(2k-1)\mu} \geq \begin{cases} |\alpha_{min}| & \text{OMP} \\ |\alpha_{max}| & \text{THR} \end{cases}, \quad (2.22)$$

where  $|\alpha_{min}|$  and  $|\alpha_{max}|$  are the minimal and maximal non-zero absolute entries in  $\alpha$ .

## 2.7 Other Signal Models

### 2.7.1 The Matrix Completion Problem

A problem which is a variant of (2.1) is the matrix completion problem. In this problem, by abuse of notation,  $\mathbf{x} \in \mathbb{R}^{d_1 \times d_2}$  is a matrix and  $\mathbf{M}$  is a sampling operator that keeps only several

<sup>3</sup>In [30] a slightly different constant was presented.

elements from the matrix  $\mathbf{x}$ . In order to recover  $\mathbf{x}$  from  $\mathbf{y}$  an additional prior is needed also in this case, since without it the system has an infinite number of solutions.

As in the synthesis framework, also in the matrix completion problem a low dimensionality model is imposed on  $\mathbf{x}$ . In the former discussion we have looked at the sparsity of the signal, measured by counting the number of non-zeros in its representation. Here, the matrix  $\mathbf{x}$  is assumed to have a low rank and we recover it by solving

$$\hat{\mathbf{x}}_r = \underset{\mathbf{z} \in \mathbb{R}^{d_1 \times d_2}}{\operatorname{argmin}} \operatorname{rank}(\mathbf{z}) \quad \text{subject to} \quad \|\mathbf{y} - \mathbf{M}\mathbf{z}\|_F \leq \epsilon, \quad (2.23)$$

where  $\|\cdot\|_F$  is the Frobenius norm. Just like (2.4) is NP-hard, solving (2.23) is a NP-hard problem as well [77].

As before, approximation strategies exist also for (2.23). Noticing that the rank of a matrix is the number of its non-zero singular values, i.e, the  $\ell_0$ -pseudo norm of the vector of its singular values, one can replace the  $\ell_0$  with  $\ell_1$  as done in the synthesis case in (2.8). This result with the following convex optimization problem:

$$\hat{\mathbf{x}}_* = \underset{\mathbf{z} \in \mathbb{R}^{d_1 \times d_2}}{\operatorname{argmin}} \|\mathbf{z}\|_* \quad \text{subject to} \quad \|\mathbf{y} - \mathbf{M}\mathbf{z}\|_F \leq \epsilon, \quad (2.24)$$

where  $\|\cdot\|_*$  is the nuclear norm that returns the sum of the singular values of a matrix. Candès and Recht have shown in [78] that under some proper assumptions on  $\mathbf{M}$ , the solution of (2.24) gives a stable estimation of the original matrix, i.e.,

$$\|\hat{\mathbf{x}}_* - \mathbf{x}\|_F \leq C_* \|\mathbf{e}\|_F, \quad (2.25)$$

for a certain constant  $C_*$ . In particular, in the noiseless case ( $\|\mathbf{e}\|_F = 0$ ) the original matrix is recovered exactly. Other approximation methods exist for the matrix completion problem [79], such as ADMiRA (a CoSaMP variant) [80], SET (a SP variant) [81] and NIHT (an IHT variant) [82].

## 2.7.2 The Cosparse Analysis Model

Recently, a new signal model called the *cosparse analysis model* was proposed in [23, 83]. The model can be summarized as follows: For a given analysis operator  $\mathbf{\Omega} \in \mathbb{R}^{p \times d}$ , referred to as the analysis dictionary, a signal  $\mathbf{x} \in \mathbb{R}^d$  belongs to the cosparse analysis model with cosparsity  $\ell$  if

$$\ell := p - \|\mathbf{\Omega}\mathbf{x}\|_0. \quad (2.26)$$

The quantity  $\ell$  is the number of rows in  $\Omega$  that are orthogonal to the signal. The signal  $\mathbf{x}$  is said to be  $\ell$ -cosparsely, or simply cosparsely. We denote the indices of the zeros of the analysis representation as the *cosupport*  $\Lambda$  and the sub-matrix that contains the rows from  $\Omega$  that belong to  $\Lambda$  by  $\Omega_\Lambda$ . As the definition of cosparsity suggests, the emphasis of the cosparsely analysis model is on the zeros of the analysis representation vector  $\Omega\mathbf{x}$ . This contrasts the emphasis on ‘few non-zeros’ in the synthesis model (2.2). It is clear that in the case where every  $\ell$  rows in  $\Omega$  are independent,  $\mathbf{x}$  resides in a subspace of dimension  $d - \ell$  that consists of vectors orthogonal to the rows of  $\Omega_\Lambda$ . In the general case where dependencies occur between the rows of  $\Omega$ , the dimension of this subspace is  $d$  minus the rank of  $\Omega_\Lambda$ . This is similar to the behavior in the synthesis case where a  $k$ -sparse signal lives in a  $k$ -dimensional space. Thus, for this model to be effective, we assume a large value of  $\ell$ .

In the analysis model, recovering  $\mathbf{x}$  from the corrupted measurements is done by solving the following minimization problem [22]:

$$\mathbf{x}_{A-\ell_0} = \underset{\mathbf{x}}{\operatorname{argmin}} \|\Omega\mathbf{x}\|_0 \quad \text{subject to} \quad \|\mathbf{y} - \mathbf{M}\mathbf{x}\|_2 \leq \varepsilon. \quad (2.27)$$

Solving this problem is NP-hard [23], just as in the synthesis case, and thus approximation methods are required. As before, we can use an  $\ell_1$  relaxation to (2.27), replacing the  $\ell_0$  with  $\ell_1$  in (2.27) [22, 23, 24, 25]. This algorithm has been analyzed using the D-RIP. This tool is an extension of the RIP that by its definition “belongs to the synthesis context”. However, as we shall see hereafter, it has been used for studying the  $\ell_1$ -analysis minimization by setting  $\mathbf{D} = \Omega^\dagger$ .

**Definition 2.7.1 (D-RIP [24])** *A matrix  $\mathbf{M}$  has the D-RIP with a dictionary  $\mathbf{D}$  and a constant  $\delta_k = \delta_{\mathbf{D},k}^D$ , if  $\delta_{\mathbf{D},k}^D$  is the smallest constant that satisfies*

$$(1 - \delta_{\mathbf{D},k}^D) \|\mathbf{D}\mathbf{w}\|_2^2 \leq \|\mathbf{M}\mathbf{D}\mathbf{w}\|_2^2 \leq (1 + \delta_{\mathbf{D},k}^D) \|\mathbf{D}\mathbf{w}\|_2^2, \quad (2.28)$$

whenever  $\mathbf{w}$  is  $k$ -sparse.

Note that though the D-RIP is also a function of  $\mathbf{D}$  we abuse notation and, if clear from the context, use the same symbol  $\delta_k$  for the D-RIP as the regular RIP.

It has been shown that if  $\Omega$  is a frame with frame constants  $A$  and  $B$ ,  $\mathbf{D} = \Omega^\dagger$  and  $\delta_{\mathbf{D},ak}^D \leq \delta_{A-\ell_1}(a, A, B)$  then

$$\|\hat{\mathbf{x}}_{A-\ell_1} - \mathbf{x}\|_2^2 \leq C_{A-\ell_1} \left( \|\mathbf{e}\|_2^2 + \frac{\|\Omega\mathbf{x} - [\Omega\mathbf{x}]_k\|_1^2}{k} \right), \quad (2.29)$$

where the operator  $[\cdot]_k$  is a hard thresholding operator that keeps the largest  $k$  elements in a vector, and  $a \geq 1$ ,  $\delta_{A-\ell_1}(a, A, B)$  and  $C_{A-\ell_1}$  are some constants. A similar result has been proposed for analysis  $\ell_1$ -minimization with  $\Omega_{2D-DIF}$ , the two dimensional finite different operator that corresponds to the discrete gradient in 2D, also known as the anisotropic total variation (TV). Notice that unlike in synthesis, the recovery guarantees in analysis are for the signal as the recovery operates in the signal domain.

Another approximation option is the greedy approach. A greedy algorithm called Greedy Analysis Pursuit (GAP) has been developed in [23, 83, 84] and somehow mimics OMP [38, 62] with a form of iterative reweighted least Squares (IRLS) [85]. Other alternatives for OMP, backward greedy (BG) and orthogonal BG (OBG), were presented in [86] for the case that  $\mathbf{M}$  is the identity. For the same case, the parallel to the thresholding technique was analyzed in [52].

More details about the analysis framework appear in Chapters 4 and 6.

### 2.7.3 Poisson Noise Model

The last framework we consider relies on a different measurement model than the one in (2.1). In the new setup there is no measurement matrix  $\mathbf{M}$ . The noise in the system is Poisson distributed and hence not additive.

Poisson noise appears in many applications such as night vision, computed tomography (CT), fluorescence microscopy, astrophysics and spectral imaging. Given a Poisson noisy image  $\mathbf{y} \in \mathbb{R}^d$  (represented as a column-stacked vector), our task is to recover the original true image  $\mathbf{x} \in \mathbb{R}^d$ , where the  $i$ -th pixel in  $\mathbf{y}$ ,  $\mathbf{y}[i]$ , is a Poisson distributed random variable with mean and variance  $\mathbf{x}[i]$ , i.e.,

$$P(\mathbf{y}[i]|\mathbf{x}[i]) = \begin{cases} \frac{(\mathbf{x}[i])^{\mathbf{y}[i]}}{\mathbf{y}[i]!} \exp(-\mathbf{x}[i]) & \mathbf{x}[i] > 0 \\ \delta_0(\mathbf{y}[i]) & \mathbf{x}[i] = 0, \end{cases} \quad (2.30)$$

where  $\delta_0$  is the Kronecker delta function. Notice that Poisson noise is not additive and its strength is dependent on the image intensity. Lower intensity in the image yields a stronger noise as the SNR in each pixel is  $\sqrt{\mathbf{x}[i]}$ . Thus, it is natural to define the noise power in an image by its peak value, the maximal value in  $\mathbf{x}$ .

Many schemes for recovering  $\mathbf{x}$  from  $\mathbf{y}$  [87, 88, 89] rely on transformations, such as Anscombe [90] and Fisz [91], that convert the Poisson denoising problem into a Gaussian one, for which plenty of methods exist (e.g. [55, 92, 93]). The noise becomes white Gaussian with unit variance.

The problem with these approximations is the fact that they hold true only when the measured pixels have high intensity [20, 53, 88], i.e. when a high photon count is measured in the detectors. As a thumb rule, these transformations are efficient only when the peak value in  $x$  is larger than 4 [20]. In this case the noise looks very similar to a Gaussian one. When the peak value is smaller, the structure of the noisy image is quite different, with many zero pixels and others that have very small (integer) values. As an example, when the peak equals 0.1 we have almost a binary image, containing mainly either zeros or ones. Fig 2.1 shows noisy versions of *peppers* with different peak values. It can be seen that indeed, as the peak value increases, the noise "looks" more and more like Gaussian.

In this work we aim at denoising Poisson noisy images with  $\text{peak} < 4$  where Anscombe or Fisz is less effective. For this purpose the noise statistics should be treated directly. This approach is taken in [20, 53] in the non-local PCA (NLPCA) and non-local sparse PCA (NLSPCA) algorithms. More details in Chapter 7.

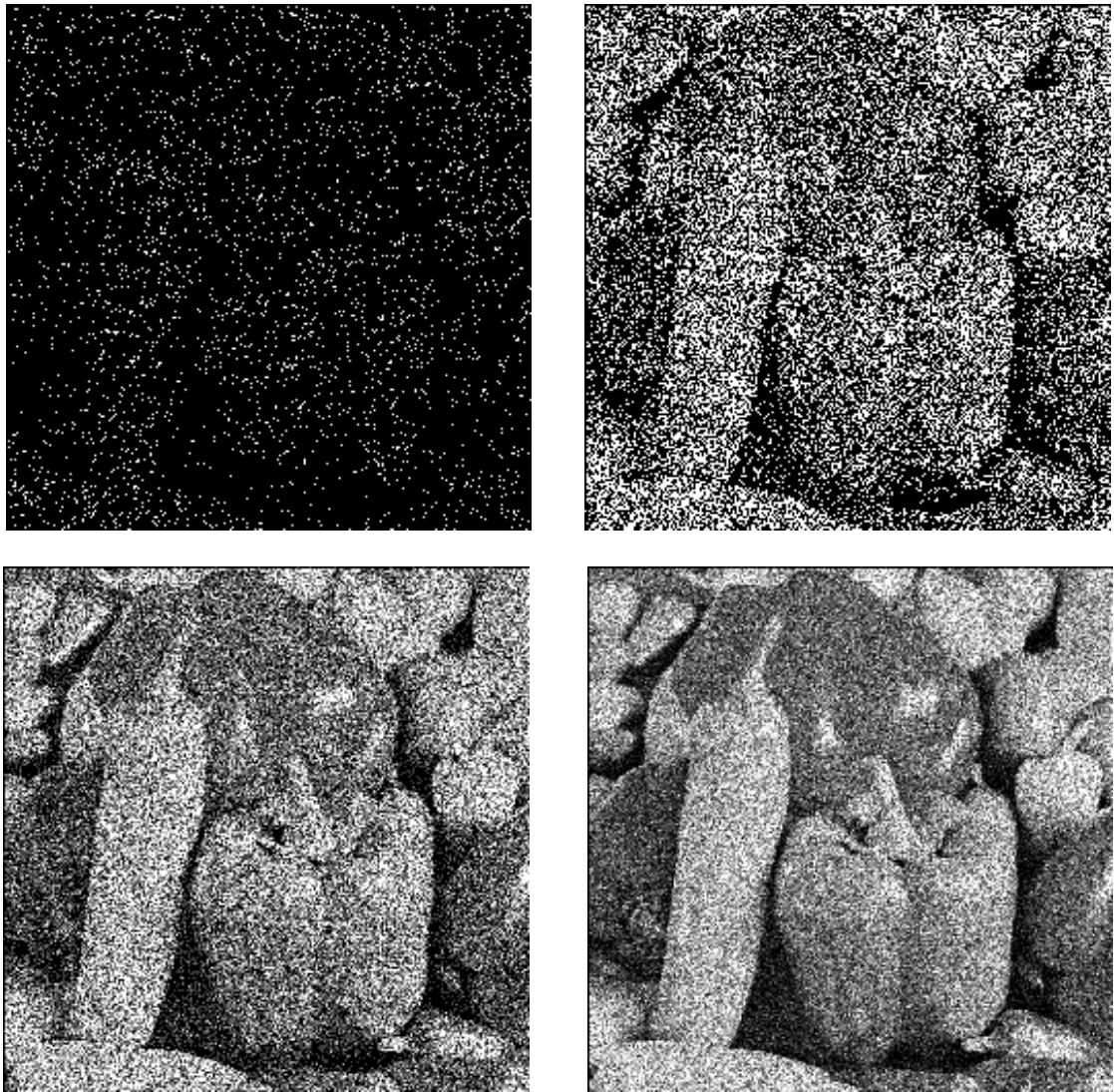


Figure 2.1: Poisson noisy versions of the image *peppers* with different peak values. From left to right: Peaks 0.1, 1, 4 and 10.



## Chapter 3

# Greedy-Like Algorithms – Near Oracle Performance

The results shown in this chapter have been published and appeared in the following articles:

- R. Giryes and M. Elad, "RIP-based near-oracle performance guarantees for subspace-pursuit, CoSaMP, and iterative hard-thresholding," *Technion CS-2010-23 Technical Report, 2010* [56].
- R. Giryes and M. Elad, "RIP-based near-oracle performance guarantees for SP, CoSaMP, and IHT," *IEEE Transactions on Signal Processing, vol.60, no.3, pp.1465-1468, March 2012* [1].
- R. Giryes and V. Cevher, "Online performance guarantees for sparse recovery," in *Proc. IEEE International Conference on Acoustics, Speech and Signal Processing (ICASSP), 22-27 May, 2011* [2].
- R. Giryes and M. Elad, "Denoising with greedy-like pursuit algorithms," in *Proc. European Signal Processing Conference (EUSIPCO), Barcelona, Spain, Aug. 29, 2011* [3].

We have seen in Section 2.6 that the success of greedy algorithms is dependent on the magnitude of the entries of  $\alpha$  and the noise power, which is not the case for the DS and BPDN. It seems that there is a need for pursuit algorithms that, on one hand, will enjoy the simplicity and ease of implementation as in the greedy methods, while being guaranteed to perform as well as the BPDN and DS. Could the greedy-like methods serve this purpose? The answer was

shown to be positive for the adversarial noise assumption, but these results are too weak, as they do not show the true denoising effect that such algorithms may lead to. In this Chapter we show that the answer remains positive for the random noise assumption.

More specifically, we present RIP-based near-oracle performance guarantees for the SP, CoSaMP and IHT algorithms (in this order). We show that these algorithms get uniform guarantees, just as for the relaxation based methods (the DS and BPDN). We present the study that leads to these results and we provide explicit values for the constants in the obtained bounds.

The importance of the obtained bounds is in showing that using the greedy-like methods we can recover signals with an effective reduction of the additive noise. In the case of an adversarial noise, such a guarantee does not exist. Furthermore, the obtained results suggest that the reconstruction results' error behaves like the oracle's error up to a  $\log n$  and a constant factor.

The organization of this chapter is as follows: Section 3.1 presents notations and preliminary results used in our theoretical analysis. In Section 3.2 we develop RIP-based bounds for the SP, CoSaMP and IHT algorithms for the adversarial case. Then we show how we can derive from these a new set of guarantees for near oracle performance that consider the noise as random. We develop fully the steps for the SP, and outline the steps needed to get the results for the CoSaMP and IHT. In Section 3.3 we present some experiments that show the actual performance of the three methods, and a comparison between the theoretical bounds and the empirical performance. In Section 3.4 we consider the nearly-sparse case, extending all the above results. Section 3.5 concludes this chapter.

### 3.1 Preliminaries

The proofs for this chapter use several propositions from [39, 40]. We bring these in this section, so as to keep the discussion complete. In the propositions,  $\mathbf{P}_T = \mathbf{A}_T \mathbf{A}_T^\dagger$  is the orthogonal projection onto the subspace spanned by the columns of  $\mathbf{A}_T$  and  $\mathbf{Q}_T = \mathbf{I} - \mathbf{P}_T$  is the orthogonal projection onto the corresponding orthogonal subspace. The support of a  $k$ -sparse vector  $\boldsymbol{\alpha}$  is denoted by  $\text{supp}(\boldsymbol{\alpha})$  and its size by  $|\text{supp}(\boldsymbol{\alpha})|$  (By abuse of notation  $|\cdot|$  is the absolute value for a scalar and the number of elements for a given set).

**Proposition 3.1.1** [Proposition 3.1 in [39]] Suppose that  $\mathbf{A}$  has a restricted isometry constant  $\delta_k$ . Let

$T$  be an arbitrary set of  $k$  indices or fewer. Then

$$\begin{aligned}\|\mathbf{A}_T^* \mathbf{y}\|_2 &\leq \sqrt{1 + \delta_k} \|\mathbf{y}\|_2 \\ \|\mathbf{A}_T^\dagger \mathbf{y}\|_2 &\leq \frac{1}{\sqrt{1 - \delta_k}} \|\mathbf{y}\|_2 \\ \|\mathbf{A}_T^* \mathbf{A}_T \mathbf{w}\|_2 &\stackrel{\leq}{\geq} (1 \pm \delta_k) \|\mathbf{w}\|_2 \\ \left\| (\mathbf{A}_T^* \mathbf{A}_T)^{-1} \mathbf{w} \right\|_2 &\stackrel{\leq}{\geq} \frac{1}{1 \pm \delta_k} \|\mathbf{w}\|_2\end{aligned}$$

where the last two statements contain upper and lower bounds, depending on the sign chosen.

**Proposition 3.1.2** [Lemma 1 in [40]] *Consequences of the RIP:*

1. (Monotonicity of  $\delta_k$ ) For any two integers  $k \leq k'$ ,  $\delta_k \leq \delta_{k'}$ .
2. (Near-orthogonality of columns) Let  $I, J \subset \{1, \dots, n\}$  be two disjoint sets ( $I \cap J = \emptyset$ ). Suppose that  $\delta_{|I|+|J|} < 1$ . For arbitrary vectors  $\mathbf{a} \in \mathbb{R}^{|I|}$  and  $\mathbf{b} \in \mathbb{R}^{|J|}$ ,

$$|\langle \mathbf{A}_I \mathbf{a}, \mathbf{A}_J \mathbf{b} \rangle| \leq \delta_{|I|+|J|} \|\mathbf{a}\|_2 \|\mathbf{b}\|_2$$

and

$$\|\mathbf{A}_I^* \mathbf{A}_J \mathbf{b}\|_2 \leq \delta_{|I|+|J|} \|\mathbf{b}\|_2.$$

**Proposition 3.1.3** [Lemma 2 in [40]] *Projection and Residue:*

1. (Orthogonality of the residue) For an arbitrary vector  $\mathbf{y} \in \mathbb{R}^m$  and a sub-matrix  $\mathbf{A}_I \in \mathbb{R}^{m \times k}$  of full column-rank, let  $\mathbf{y}_{\text{resid}} = \mathbf{Q}_I \mathbf{y}$ . Then  $\mathbf{A}_I^* \mathbf{y}_r = 0$ .
2. (Approximation of the projection residue) Consider a matrix  $\mathbf{A} \in \mathbb{R}^{m \times n}$ . Let  $I, J \subset \{1, \dots, n\}$  be two disjoint sets,  $I \cap J = \emptyset$ , and suppose that  $\delta_{|I|+|J|} < 1$ . Let  $\mathbf{y} \in \text{span}(\mathbf{A}_I)$ ,  $\mathbf{y}_P = \mathbf{P}_J \mathbf{y}$  and  $\mathbf{y}_{\text{resid}} = \mathbf{Q}_J \mathbf{y}$ . Then

$$\|\mathbf{y}_P\|_2 \leq \frac{\delta_{|I|+|J|}}{1 - \delta_{\max(|I|, |J|)}} \|\mathbf{y}\|_2$$

and

$$\left(1 - \frac{\delta_{|I|+|J|}}{1 - \delta_{\max(|I|, |J|)}}\right) \|\mathbf{y}\|_2 \leq \|\mathbf{y}_r\|_2 \leq \|\mathbf{y}\|_2.$$

**Proposition 3.1.4** [Corollary 3.3 in [39]] Suppose that  $\mathbf{A}$  has an RIP constant  $\delta_{\tilde{k}}$ . Let  $T_1$  be an arbitrary set of indices, and let  $\boldsymbol{\alpha}$  be a vector. Provided that  $\tilde{k} \geq |T_1 \cup \text{supp}(\boldsymbol{\alpha})|$ , we obtain that

$$\left\| \mathbf{A}_{T_1}^* \mathbf{A}_{T_1^c} \boldsymbol{\alpha}_{T_1^c} \right\|_2 \leq \delta_{\tilde{k}} \left\| \boldsymbol{\alpha}_{T_1^c} \right\|_2. \quad (3.1)$$

## 3.2 Near Oracle Performance of the Algorithms

Our goal in this section is to find error bounds for the SP, CoSaMP and IHT reconstructions given the measurement from

$$\mathbf{y} = \mathbf{A}\boldsymbol{\alpha} + \mathbf{e}, \quad \text{and} \quad k := \|\boldsymbol{\alpha}\|_0 \ll d. \quad (3.2)$$

We first find bounds for the case where  $\mathbf{e}$  is an adversarial noise using the same techniques used in [39, 40]. In these works and in [41], the reconstruction error has been bounded by a constant times the noise power in the same form as in (2.14). In this chapter, we derive a bound that is a constant times  $\|\mathbf{A}_{T_e}^* \mathbf{e}\|_2$ , where  $T_e$  is the subset of columns of size  $k$  in  $\mathbf{A}$  that gives the maximum correlation with the noise vector  $\mathbf{e}$ , namely,

$$T_e = \operatorname{argmax}_{T \mid |T|=k} \|\mathbf{A}_T^* \mathbf{e}\|_2. \quad (3.3)$$

Armed with this bound, we will change perspective and look at the case where  $\mathbf{e}$  is a white Gaussian noise, and derive a near-oracle performance result of the same form as the one of DS in (2.19), using the same tools used in [30] for DS.

### 3.2.1 Near Oracle Performance of the SP Algorithm

We begin with the SP pursuit method, as described in Algorithm 3. SP holds a temporal solution with  $k$  non-zero entries, and in each iteration it adds an additional set of  $k$  candidate non-zeros that are most correlated with the residual, and prunes this list back to  $k$  elements by choosing the dominant ones. We use a constant number of iterations as a stopping criterion but different stopping criteria can be sought, as presented in [40]. In the theorem,  $T - T^t$  is the set of all the elements contained in  $T$  but not in  $T^t$ .

**Theorem 3.2.1** *The SP solution at the  $t$ -th iteration satisfies the recurrence inequality*

$$\|\boldsymbol{\alpha}_{T-T^t}\|_2 \leq \frac{2\delta_{3k}(1+\delta_{3k})}{(1-\delta_{3k})^3} \|\boldsymbol{\alpha}_{T-T^{t-1}}\|_2 + \frac{6-6\delta_{3k}+4\delta_{3k}^2}{(1-\delta_{3k})^3} \|\mathbf{A}_{T_e}^* \mathbf{e}\|_2. \quad (3.4)$$

For  $\delta_{3k} \leq 0.139$  this leads to

$$\|\boldsymbol{\alpha}_{T-T^t}\|_2 \leq 0.5 \|\boldsymbol{\alpha}_{T-T^{t-1}}\|_2 + 8.22 \|\mathbf{A}_{T_e}^* \mathbf{e}\|_2. \quad (3.5)$$

*Proof:* The proof of the inequality in (3.4) is given in Appendix A.1. Note that the recursive formula given (3.4) has two coefficients, both functions of  $\delta_{3k}$ . Fig. 3.1 shows these coefficients

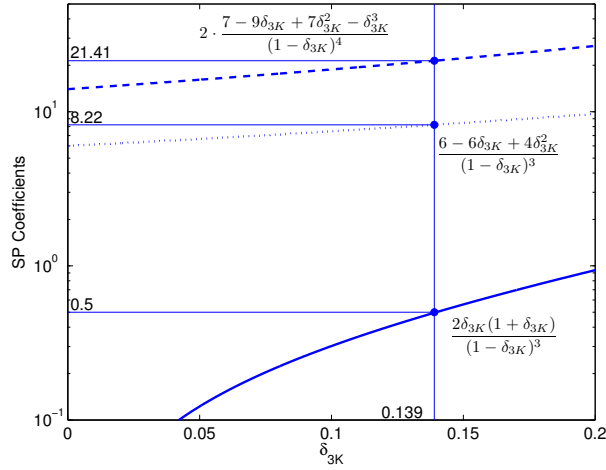


Figure 3.1: The coefficients in (3.4) and (3.8) as functions of  $\delta_{3k}$ .

as a function of  $\delta_{3k}$ . As can be seen, under the condition  $\delta_{3k} \leq 0.139$ , it holds that the coefficient multiplying  $\|\alpha_{T-T^{t-1}}\|_2$  is lesser or equal to 0.5, while the coefficient multiplying  $\|\mathbf{A}_{T_e}^* \mathbf{e}\|_2$  is lesser or equal to 8.22, which completes our proof.  $\square$

**Corollary 3.2.2** *Under the condition  $\delta_{3k} \leq 0.139$ , the SP algorithm satisfies*

$$\|\alpha_{T-T^t}\|_2 \leq 2^{-t} \|\alpha\|_2 + 2 \cdot 8.22 \|\mathbf{A}_{T_e}^* \mathbf{e}\|_2. \quad (3.6)$$

*In addition, After at most*

$$t^* = \left\lceil \log_2 \left( \frac{\|\alpha\|_2}{\|\mathbf{A}_{T_e}^* \mathbf{e}\|_2} \right) \right\rceil \quad (3.7)$$

*iterations, the solution  $\hat{\alpha}_{SP}$  leads to an accuracy*

$$\|\alpha - \hat{\alpha}_{SP}\|_2 \leq C_{SP} \|\mathbf{A}_{T_e}^* \mathbf{e}\|_2, \quad (3.8)$$

*where*

$$C_{SP} = 2 \cdot \frac{7 - 9\delta_{3k} + 7\delta_{3k}^2 - \delta_{3k}^3}{(1 - \delta_{3k})^4} \leq 21.41 \quad (3.9)$$

*Proof:* Starting with (3.5), and applying it recursively we obtain

$$\begin{aligned} \|\alpha_{T-T^t}\|_2 &\leq 0.5 \|\alpha_{T-T^{t-1}}\|_2 + 8.22 \|\mathbf{A}_{T_e}^* \mathbf{e}\|_2 \\ &\leq 0.5^2 \|\alpha_{T-T^{t-2}}\|_2 + 8.22 \cdot (0.5 + 1) \|\mathbf{A}_{T_e}^* \mathbf{e}\|_2 \\ &\leq \dots \leq 0.5^k \|\alpha_{T-T^{t-k}}\|_2 + 8.22 \cdot \left( \sum_{j=0}^{k-1} 0.5^j \right) \|\mathbf{A}_{T_e}^* \mathbf{e}\|_2. \end{aligned} \quad (3.10)$$

Setting  $k = t$  leads easily to (3.6), since  $\|\alpha_{T-T^0}\|_2 = \|\alpha_T\|_2 = \|\alpha\|_2$ .

Plugging the number of iterations  $t^*$  as in (3.7) to (3.6) yields<sup>1</sup>

$$\begin{aligned} \|\alpha_{T-T^{t^*}}\|_2 &\leq 2^{-t^*} \|\alpha\|_2 + 2 \cdot \frac{6 - 6\delta_{3k} + 4\delta_{3k}^2}{(1 - \delta_{3k})^3} \|\mathbf{A}_{T^c}^* \mathbf{e}\|_2 \\ &\leq \left(1 + 2 \cdot \frac{6 - 6\delta_{3k} + 4\delta_{3k}^2}{(1 - \delta_{3k})^3}\right) \|\mathbf{A}_{T^c}^* \mathbf{e}\|_2. \end{aligned} \quad (3.11)$$

We define  $\hat{T} \triangleq T^{t^*}$  and bound the reconstruction error  $\|\alpha - \hat{\alpha}_{SP}\|_2$ . First, notice that  $\|\alpha\|_2 = \|\alpha_{\hat{T}}\|_2 + \|\alpha_{T-\hat{T}}\|_2$ , simply because the true support  $T$  can be divided into  $\hat{T}$  and the complementary part,  $T - \hat{T}$ . Using the facts that  $\hat{\alpha}_{SP} = \mathbf{A}_{\hat{T}}^\dagger \mathbf{y}$ ,  $\mathbf{y} = \mathbf{A}_T \alpha_T + \mathbf{e}$ , and the triangle inequality, we get

$$\begin{aligned} \|\alpha - \hat{\alpha}_{SP}\|_2 &\leq \left\| \alpha_{\hat{T}} - \mathbf{A}_{\hat{T}}^\dagger \mathbf{y} \right\|_2 + \|\alpha_{T-\hat{T}}\|_2 \\ &= \left\| \alpha_{\hat{T}} - \mathbf{A}_{\hat{T}}^\dagger (\mathbf{A}_T \alpha_T + \mathbf{e}) \right\|_2 + \|\alpha_{T-\hat{T}}\|_2 \\ &\leq \left\| \alpha_{\hat{T}} - \mathbf{A}_{\hat{T}}^\dagger \mathbf{A}_T \alpha_T \right\|_2 + \left\| \mathbf{A}_{\hat{T}}^\dagger \mathbf{e} \right\|_2 + \|\alpha_{T-\hat{T}}\|_2. \end{aligned} \quad (3.12)$$

We proceed by breaking the term  $\mathbf{A}_T \alpha_T$  into the sum  $\mathbf{A}_{T \cap \hat{T}} \alpha_{T \cap \hat{T}} + \mathbf{A}_{T-\hat{T}} \alpha_{T-\hat{T}}$ , and obtain

$$\begin{aligned} \|\alpha - \hat{\alpha}_{SP}\|_2 &\leq \left\| \alpha_{\hat{T}} - \mathbf{A}_{\hat{T}}^\dagger \mathbf{A}_{T \cap \hat{T}} \alpha_{T \cap \hat{T}} \right\|_2 + \left\| \mathbf{A}_{\hat{T}}^\dagger \mathbf{A}_{T-\hat{T}} \alpha_{T-\hat{T}} \right\|_2 \\ &\quad + \left\| (\mathbf{A}_{\hat{T}}^* \mathbf{A}_{\hat{T}})^{-1} \mathbf{A}_{\hat{T}}^* \mathbf{e} \right\|_2 + \|\alpha_{T-\hat{T}}\|_2. \end{aligned} \quad (3.13)$$

The first term in the above inequality vanishes, since  $\mathbf{A}_{T \cap \hat{T}} \alpha_{T \cap \hat{T}} = \mathbf{A}_{\hat{T}} \alpha_{\hat{T}}$  (recall that  $\alpha_{\hat{T}}$  outside the support  $T$  has zero entries that do not contribute to the multiplication). Thus, we get that  $\alpha_{\hat{T}} - \mathbf{A}_{\hat{T}}^\dagger \mathbf{A}_{T \cap \hat{T}} \alpha_{T \cap \hat{T}} = \alpha_{\hat{T}} - \mathbf{A}_{\hat{T}}^\dagger \mathbf{A}_{\hat{T}} \alpha_{\hat{T}} = 0$ . The second term can be bounded using Propositions 3.1.1 and 3.1.2,

$$\begin{aligned} \left\| \mathbf{A}_{\hat{T}}^\dagger \mathbf{A}_{T-\hat{T}} \alpha_{T-\hat{T}} \right\|_2 &= \left\| (\mathbf{A}_{\hat{T}}^* \mathbf{A}_{\hat{T}})^{-1} \mathbf{A}_{\hat{T}}^* \mathbf{A}_{T-\hat{T}} \alpha_{T-\hat{T}} \right\|_2 \\ &\leq \frac{1}{1 - \delta_k} \left\| \mathbf{A}_{\hat{T}}^* \mathbf{A}_{T-\hat{T}} \alpha_{T-\hat{T}} \right\|_2 \leq \frac{\delta_{2k}}{1 - \delta_k} \|\alpha_{T-\hat{T}}\|_2. \end{aligned}$$

Similarly, the third term is bounded using Propositions 3.1.1, and we obtain

$$\begin{aligned} \|\alpha - \hat{\alpha}_{SP}\|_2 &\leq \left(1 + \frac{\delta_{2k}}{1 - \delta_k}\right) \|\alpha_{T-\hat{T}}\|_2 + \frac{1}{1 - \delta_k} \|\mathbf{A}_{\hat{T}}^* \mathbf{e}\|_2 \\ &\leq \frac{1}{1 - \delta_{3k}} \|\alpha_{T-\hat{T}}\|_2 + \frac{1}{1 - \delta_{3k}} \|\mathbf{A}_{\hat{T}}^* \mathbf{e}\|_2, \end{aligned}$$

<sup>1</sup>Note that we have replaced the constant 8.22 with the equivalent expression that depends on  $\delta_{3k}$  – see (3.4).

where we have replaced  $\delta_k$  and  $\delta_{2k}$  with  $\delta_{3k}$ , thereby bounding the existing expression from above. Plugging (3.11) into this inequality leads to

$$\begin{aligned}\|\boldsymbol{\alpha} - \hat{\boldsymbol{\alpha}}_{SP}\|_2 &\leq \frac{1}{1 - \delta_{3k}} \left( 2 + 2 \cdot \frac{6 - 6\delta_{3k} + 4\delta_{3k}^2}{(1 - \delta_{3k})^3} \right) \|\mathbf{A}_{T_e}^* \mathbf{e}\|_2 \\ &= 2 \cdot \frac{7 - 9\delta_{3k} + 7\delta_{3k}^2 - \delta_{3k}^3}{(1 - \delta_{3k})^4} \|\mathbf{A}_{T_e}^* \mathbf{e}\|_2.\end{aligned}$$

Applying the condition  $\delta_{3k} \leq 0.139$  on this equation leads to the result in (3.8).  $\square$

For practical use we may suggest a simpler term for  $t^*$ . Since  $\|\mathbf{A}_{T_e}^* \mathbf{e}\|_2$  is defined by the subset that gives the maximal correlation with the noise, and it appears in the denominator of  $t^*$ , it can be replaced with the average correlation, thus  $t^* \approx \lceil \log_2 \left( \|\boldsymbol{\alpha}\|_2 / \sqrt{k}\sigma \right) \rceil$ .

Now that we have a bound for the SP algorithm for the adversarial case, we proceed and consider a bound for the random noise case, which will lead to a near-oracle performance guarantee for the SP algorithm.

**Theorem 3.2.3** *Assume that  $\mathbf{e}$  is a white Gaussian noise vector with variance  $\sigma^2$  and that the columns of  $\mathbf{A}$  are normalized. If the condition  $\delta_{3k} \leq 0.139$  holds, then with probability exceeding  $1 - (\sqrt{\pi(1+a)} \log n \cdot n^a)^{-1}$  we obtain*

$$\|\boldsymbol{\alpha} - \hat{\boldsymbol{\alpha}}_{SP}\|_2^2 \leq C_{SP}^2 \cdot (2(1+a) \log n) \cdot k\sigma^2. \quad (3.14)$$

*Proof:* Following Section 3 in [30] it holds true that  $\mathbf{P} \left( \sup_i |\mathbf{A}_i^* \mathbf{e}| > \sigma \cdot \sqrt{2(1+a) \log n} \right) \leq 1 - (\sqrt{\pi(1+a)} \log n \cdot n^a)^{-1}$ . Combining this with (3.8), and bearing in mind that  $|T_e| = k$ , we get the stated result.  $\square$

As can be seen, this result is similar to the one posed in [30] for the Dantzig-Selector, but with a different constant – the one corresponding to DS is  $\approx 5.5$  for the RIP requirement used for the SP. For both algorithms, smaller values of  $\delta_{3k}$  provide smaller constants.

### 3.2.2 Near Oracle Performance of the CoSaMP Algorithm

We continue with the CoSaMP pursuit method, as described in Algorithm 3. CoSaMP, in a similar way to the SP, holds a temporal solution with  $k$  non-zero entries, with the difference that in each iteration it adds an additional set of  $2k$  (instead of  $k$ ) candidate non-zeros that are most correlated with the residual. Another difference is that after the pruning step in SP we use a matrix inversion in order to calculate a new projection for the  $k$  dominant elements, while in

CoSaMP we just take the biggest  $k$  elements. Here also, we use a constant number of iterations as a stopping criterion while different stopping criteria can be sought, as presented in [39].

In the analysis of the CoSaMP that comes next, we follow the same steps as for the SP to derive a near-oracle performance guarantee. Since the proofs are very similar to those of the SP, and those found in [39], we omit most of the derivations and present only the differences.

**Theorem 3.2.4** *The CoSaMP solution at the  $t$ -th iteration satisfies the recurrence inequality<sup>2</sup>*

$$\|\boldsymbol{\alpha} - \hat{\boldsymbol{\alpha}}_{\text{CoSaMP}}^t\|_2 \leq \frac{4\delta_{4k}}{(1 - \delta_{4k})^2} \|\boldsymbol{\alpha} - \hat{\boldsymbol{\alpha}}_{\text{CoSaMP}}^{t-1}\|_2 + \frac{14 - 6\delta_{4k}}{(1 - \delta_{4k})^2} \|\mathbf{A}_{T_e}^* \mathbf{e}\|_2 \quad (3.15)$$

For  $\delta_{4k} \leq 0.1$  this leads to

$$\|\boldsymbol{\alpha} - \hat{\boldsymbol{\alpha}}_{\text{CoSaMP}}^t\|_2 \leq 0.5 \|\boldsymbol{\alpha} - \hat{\boldsymbol{\alpha}}_{\text{CoSaMP}}^{t-1}\|_2 + 16.6 \|\mathbf{A}_{T_e}^* \mathbf{e}\|_2. \quad (3.16)$$

*Proof:* The proof of the inequality in (3.15) is given in Appendix A.4. In a similar way to the proof in the SP case, under the condition  $\delta_{4k} \leq 0.1$ , it holds that the coefficient multiplying  $\|\boldsymbol{\alpha} - \hat{\boldsymbol{\alpha}}_{\text{CoSaMP}}^{t-1}\|_2$  is smaller or equal to 0.5, while the coefficient multiplying  $\|\mathbf{A}_{T_e}^* \mathbf{e}\|_2$  is smaller or equal to 16.6, which completes our proof.  $\square$

**Corollary 3.2.5** *Under the condition  $\delta_{4k} \leq 0.1$ , the CoSaMP algorithm satisfies*

$$\|\boldsymbol{\alpha} - \hat{\boldsymbol{\alpha}}_{\text{CoSaMP}}^t\|_2 \leq 2^{-t} \|\boldsymbol{\alpha}\|_2 + 2 \cdot 16.6 \|\mathbf{A}_{T_e}^* \mathbf{e}\|_2. \quad (3.17)$$

In addition, After at most

$$t^* = \left\lceil \log_2 \left( \frac{\|\boldsymbol{\alpha}\|_2}{\|\mathbf{A}_{T_e}^* \mathbf{e}\|_2} \right) \right\rceil \quad (3.18)$$

iterations, the solution  $\hat{\boldsymbol{\alpha}}_{\text{CoSaMP}}$  leads to an accuracy

$$\|\boldsymbol{\alpha} - \hat{\boldsymbol{\alpha}}_{\text{CoSaMP}}^t\|_2 \leq C_{\text{CoSaMP}} \|\mathbf{A}_{T_e}^* \mathbf{e}\|_2, \quad (3.19)$$

where

$$C_{\text{CoSaMP}} = \frac{29 - 14\delta_{4k} + \delta_{4k}^2}{(1 - \delta_{4k})^2} \leq 34.1. \quad (3.20)$$

---

<sup>2</sup>The observant reader will notice a delicate difference in terminology between this theorem and Theorem 3.2.1. While here the recurrence formula is expressed with respect to the estimation error,  $\|\boldsymbol{\alpha} - \hat{\boldsymbol{\alpha}}_{\text{CoSaMP}}^t\|_2$ , Theorem 3.2.1 uses a slightly different error measure,  $\|\boldsymbol{\alpha}_{T-T^t}\|_2$ .

*Proof:* Starting with (3.16), and applying it recursively, in the same way as was done in the proof of Corollary 3.2.5, we obtain

$$\|\boldsymbol{\alpha} - \hat{\boldsymbol{\alpha}}_{\text{CoSaMP}}^t\|_2 \leq 0.5^k \|\boldsymbol{\alpha} - \hat{\boldsymbol{\alpha}}_{\text{CoSaMP}}^{t-k}\|_2 + 16.6 \cdot \left( \sum_{j=0}^{k-1} 0.5^j \right) \|\mathbf{A}_{T_e}^* \mathbf{e}\|_2. \quad (3.21)$$

Setting  $k = t$  leads easily to (3.17), since  $\|\boldsymbol{\alpha} - \hat{\boldsymbol{\alpha}}_{\text{CoSaMP}}^0\|_2 = \|\boldsymbol{\alpha}\|_2$ .

Plugging the number of iterations  $t^*$  as in (3.18) to (3.17) yields<sup>3</sup>

$$\begin{aligned} \|\boldsymbol{\alpha} - \hat{\boldsymbol{\alpha}}_{\text{CoSaMP}}^t\|_2 &\leq 2^{-t^*} \|\boldsymbol{\alpha}\|_2 + 2 \cdot \frac{14 - 6\delta_{4k}}{(1 - \delta_{4k})^2} \|\mathbf{A}_{T_e}^* \mathbf{e}\|_2 \\ &\leq \left( 1 + 2 \cdot \frac{14 - 6\delta_{4k}}{(1 - \delta_{4k})^2} \right) \|\mathbf{A}_{T_e}^* \mathbf{e}\|_2 \leq \frac{29 - 14\delta_{4k} + \delta_{4k}^2}{(1 - \delta_{4k})^2} \|\mathbf{A}_{T_e}^* \mathbf{e}\|_2. \end{aligned}$$

Applying the condition  $\delta_{4k} \leq 0.1$  on this equation leads to the result in (3.19).  $\square$

As for the SP, we move now to the random noise case, which leads to a near-oracle performance guarantee for the CoSaMP algorithm.

**Theorem 3.2.6** *Assume that  $\mathbf{e}$  is a white Gaussian noise vector with variance  $\sigma^2$  and that the columns of  $\mathbf{A}$  are normalized. If the condition  $\delta_{4k} \leq 0.1$  holds, then with probability exceeding  $1 - (\sqrt{\pi(1+a)} \log n \cdot n^a)^{-1}$  we obtain*

$$\|\boldsymbol{\alpha} - \hat{\boldsymbol{\alpha}}_{\text{CoSaMP}}\|_2^2 \leq C_{\text{CoSaMP}}^2 \cdot (2(1+a) \log n) \cdot k\sigma^2. \quad (3.22)$$

*Proof:* The proof is identical to the one of Theorem 3.2.6.  $\square$

Fig. 3.2 shows a graph of  $C_{\text{CoSaMP}}$  as a function of  $\delta_{4k}$ . In order to compare the CoSaMP to SP, we also introduce in this figure a graph of  $C_{\text{SP}}$  versus  $\delta_{4k}$  (replacing  $\delta_{3k}$ ). Since  $\delta_{3k} \leq \delta_{4k}$ , the constant  $C_{\text{SP}}$  is actually better than the values shown in the graph, and yet, it can be seen that even in this case we get  $C_{\text{SP}} < C_{\text{CoSaMP}}$ . In addition, the requirement for the SP is expressed with respect to  $\delta_{3k}$ , while the requirement for the CoSaMP is stronger and uses  $\delta_{4k}$ .

With comparison to the results presented in [46] for OMP and thresholding, the results obtained for CoSaMP and SP are uniform, and expressed only with respect to the properties of the dictionary  $\mathbf{A}$ . These algorithms' validity is not dependent on the values of the input vector  $\boldsymbol{\alpha}$ , its energy, or the noise power. The condition used is the RIP, which implies constraints only on the used dictionary and the sparsity level.

<sup>3</sup>As before, we replace the constant 16.6 with the equivalent expression that depends on  $\delta_{4k}$  – see (3.15).

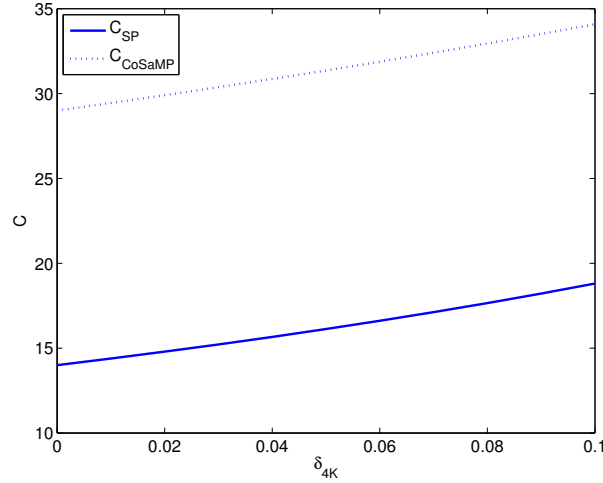


Figure 3.2: The constants of the SP and CoSaMP algorithms as a function of  $\delta_{4k}$

### 3.2.3 Near Oracle Performance of the IHT Algorithm

The IHT algorithm, presented in Algorithm 2, uses a different strategy than SP and CoSaMP. It applies only multiplications by  $\mathbf{A}$  and  $\mathbf{A}^*$ , and a hard thresholding operator. In each iteration it calculates a new representation and keeps its  $k$  largest elements. As for SP and CoSaMP, here as well we employ a fixed number of iterations as a stopping criterion.

Similar results, as of the SP and CoSaMP methods, can be sought for the IHT method. Again, the proofs are very similar to the ones shown before for SP and CoSaMP and thus only the differences are presented.

**Theorem 3.2.7** *The IHT solution at the  $t$ -th iteration satisfies the recurrence inequality*

$$\|\boldsymbol{\alpha} - \hat{\boldsymbol{\alpha}}_{IHT}^t\|_2 \leq \sqrt{8}\delta_{3k} \|\boldsymbol{\alpha} - \hat{\boldsymbol{\alpha}}_{IHT}^{t-1}\|_2 + 4 \|\mathbf{A}_{T_e}^* \mathbf{e}\|_2. \quad (3.23)$$

For  $\delta_{3k} \leq \frac{1}{\sqrt{32}}$  this leads to

$$\|\boldsymbol{\alpha} - \hat{\boldsymbol{\alpha}}_{IHT}^t\|_2 \leq 0.5 \|\boldsymbol{\alpha} - \hat{\boldsymbol{\alpha}}_{IHT}^{t-1}\|_2 + 4 \|\mathbf{A}_{T_e}^* \mathbf{e}\|_2. \quad (3.24)$$

For the proof we introduce the definition of

$$T_{\mathbf{e},b} = \operatorname{argmax}_{T \mid |T|=bk} \|\mathbf{A}_T^* \mathbf{e}\|_2. \quad (3.25)$$

It is a generalization of  $T_e$ , where  $T$  in (3.3) is of size  $bk$ ,  $b \in \mathbb{N}$ . It is clear that  $\|\mathbf{A}_{T_{\mathbf{e},b}}^* \mathbf{e}\|_2 \leq b \|\mathbf{A}_{T_e}^* \mathbf{e}\|_2$ .

*Proof:* Our proof is based on the proof of Theorem 5 in [41]. By the triangle inequality we have

$$\|\boldsymbol{\alpha} - \hat{\boldsymbol{\alpha}}_{IHT}^t\|_2 \leq \|\boldsymbol{\alpha} - (\mathbf{w}_g)_{T \cup T^t}\|_2 + \|\hat{\boldsymbol{\alpha}}_{IHT}^t - (\mathbf{w}_g)_{T \cup T^t}\|_2. \quad (3.26)$$

Since  $\hat{\boldsymbol{\alpha}}_{IHT}^t$  is the best  $k$ -sparse approximation for  $\mathbf{w}_g$  and in particular also for  $(\mathbf{w}_g)_{T \cup T^t}$ , as  $\hat{\boldsymbol{\alpha}}_{IHT}^t$  is support on  $T^t$ , we have

$$\|\boldsymbol{\alpha} - \hat{\boldsymbol{\alpha}}_{IHT}^t\|_2 \leq 2 \|\boldsymbol{\alpha}_{T \cup T^t} - (\mathbf{w}_g)_{T \cup T^t}\|_2, \quad (3.27)$$

where we use the fact that  $\boldsymbol{\alpha}$  is supported on  $T$  and thus  $\boldsymbol{\alpha} = \boldsymbol{\alpha}_{T \cup T^t}$ . Using the definitions of  $\mathbf{w}_g$  and  $\mathbf{r}^t \triangleq \boldsymbol{\alpha} - \hat{\boldsymbol{\alpha}}_{IHT}^t$  with the last inequality, it holds that

$$\begin{aligned} \|\boldsymbol{\alpha} - \hat{\boldsymbol{\alpha}}_{IHT}^t\|_2 &\leq 2 \left\| \boldsymbol{\alpha}_{T \cup T^t} - \hat{\boldsymbol{\alpha}}_{T \cup T^t}^{t-1} - \mathbf{A}_{T \cup T^t}^* \mathbf{A} \mathbf{r}^{t-1} - \mathbf{A}_{T \cup T^t}^* \mathbf{e} \right\|_2 \\ &= 2 \left\| \mathbf{r}_{T \cup T^t}^{t-1} - \mathbf{A}_{T \cup T^t}^* \mathbf{A} \mathbf{r}^{t-1} - \mathbf{A}_{T \cup T^t}^* \mathbf{e} \right\|_2, \end{aligned} \quad (3.28)$$

where the equality emerges from the definition  $\mathbf{w}_g = \hat{\boldsymbol{\alpha}}_{IHT}^{t-1} + \mathbf{A}^*(\mathbf{y} - \mathbf{A} \hat{\boldsymbol{\alpha}}_{IHT}^{t-1}) = \hat{\boldsymbol{\alpha}}_{IHT}^{t-1} + \mathbf{A}^*(\mathbf{A} \boldsymbol{\alpha} + \mathbf{e} - \mathbf{A} \hat{\boldsymbol{\alpha}}_{IHT}^{t-1})$ .

The support of  $\mathbf{r}^{t-1}$  is over  $T \cup T^{t-1}$  and thus it is also over  $T \cup T^t \cup T^{t-1}$ . Based on this, we can divide  $\mathbf{A} \mathbf{r}^{t-1}$  into a part supported on  $T^{t-1} - T^t \cup T$  and a second part supported on  $T^t \cup T$ . Using this and the triangle inequality with (3.28), we obtain

$$\begin{aligned} \|\boldsymbol{\alpha} - \hat{\boldsymbol{\alpha}}_{IHT}^t\|_2 &\leq 2 \left\| \mathbf{r}_{T \cup T^t}^{t-1} - \mathbf{A}_{T \cup T^t}^* \mathbf{A} \mathbf{r}^{t-1} \right\|_2 + 2 \|\mathbf{A}_{T \cup T^t}^* \mathbf{e}\|_2 \\ &= 2 \left\| (\mathbf{I} - \mathbf{A}_{T \cup T^t}^* \mathbf{A}_{T \cup T^t}) \mathbf{r}_{T \cup T^t}^{t-1} - \mathbf{A}_{T \cup T^t}^* \mathbf{A}_{T^{t-1} - T \cup T^t} \mathbf{r}_{T^{t-1} - T \cup T^t}^{t-1} \right\|_2 + 2 \|\mathbf{A}_{T \cup T^t}^* \mathbf{e}\|_2 \\ &\leq 2 \left\| (\mathbf{I} - \mathbf{A}_{T \cup T^t}^* \mathbf{A}_{T \cup T^t}) \mathbf{r}_{T \cup T^t}^{t-1} \right\|_2 + 2 \left\| \mathbf{A}_{T \cup T^t}^* \mathbf{A}_{T^{t-1} - T \cup T^t} \mathbf{r}_{T^{t-1} - T \cup T^t}^{t-1} \right\|_2 + 2 \|\mathbf{A}_{T_e, 2}^* \mathbf{e}\|_2 \\ &\leq 2\delta_{2k} \left\| \mathbf{r}_{T \cup T^t}^{t-1} \right\|_2 + 2\delta_{3k} \left\| \mathbf{r}_{T^{t-1} - T \cup T^t}^{t-1} \right\|_2 + 4 \|\mathbf{A}_{T_e}^* \mathbf{e}\|_2. \end{aligned} \quad (3.29)$$

The last inequality holds because the eigenvalues of  $(\mathbf{I} - \mathbf{A}_{T \cup T^t}^* \mathbf{A}_{T \cup T^t})$  are in the range  $[-\delta_{2k}, \delta_{2k}]$ , the size of the set  $T \cup T^t$  is smaller than  $2k$ , the sets  $T \cup T^t$  and  $T^{t-1} - T \cup T^t$  are disjoint, and of total size of these together is equal or smaller than  $3k$ . Note that we have used the definition of  $T_{e,2}$  as given in (3.25).

We proceed by observing that  $\left\| \mathbf{r}_{T^{t-1} - T \cup T^t}^{t-1} \right\|_2 + \left\| \mathbf{r}_{T \cup T^t}^{t-1} \right\|_2 \leq \sqrt{2} \|\mathbf{r}^{t-1}\|_2$ , since these vectors are orthogonal. Using the fact that  $\delta_{2k} \leq \delta_{3k}$  we get (3.23) from (3.29). Finally, under the condition  $\delta_{3k} \leq 1/\sqrt{32}$ , it holds that the coefficient multiplying  $\left\| \boldsymbol{\alpha} - \hat{\boldsymbol{\alpha}}_{IHT}^{t-1} \right\|_2$  is smaller or equal to 0.5, which completes our proof.  $\square$

**Corollary 3.2.8** Under the condition  $\delta_{3k} \leq 1/\sqrt{32}$ , the IHT algorithm satisfies

$$\|\boldsymbol{\alpha} - \hat{\boldsymbol{\alpha}}_{IHT}^t\|_2 \leq 2^{-t} \|\boldsymbol{\alpha}\|_2 + 8 \|\mathbf{A}_{T_e}^* \mathbf{e}\|_2. \quad (3.30)$$

In addition, After at most

$$t^* = \left\lceil \log_2 \left( \frac{\|\boldsymbol{\alpha}\|_2}{\|\mathbf{A}_{T_e}^* \mathbf{e}\|_2} \right) \right\rceil \quad (3.31)$$

iterations, the solution  $\hat{\boldsymbol{\alpha}}_{IHT}$  leads to an accuracy

$$\|\boldsymbol{\alpha} - \hat{\boldsymbol{\alpha}}_{IHT}^t\|_2 \leq C_{IHT} \|\mathbf{A}_{T_e}^* \mathbf{e}\|_2, \quad (3.32)$$

where

$$C_{IHT} = 9. \quad (3.33)$$

*Proof:* The proof is obtained following the same steps as in Corollaries 3.2.2 and 3.2.5.  $\square$

Finally, considering a random noise instead of an adversarial one, we get a near-oracle performance guarantee for the IHT algorithm, as was achieved for the SP and CoSaMP.

**Theorem 3.2.9** Assume that  $\mathbf{e}$  is a white Gaussian noise with variance  $\sigma^2$  and that the columns of  $\mathbf{A}$  are normalized. If the condition  $\delta_{3k} \leq 1/\sqrt{32}$  holds, then with probability exceeding  $1 - (\sqrt{\pi(1+a)} \log n \cdot n^a)^{-1}$  we obtain

$$\|\boldsymbol{\alpha} - \hat{\boldsymbol{\alpha}}_{IHT}\|_2^2 \leq C_{IHT}^2 \cdot (2(1+a) \log n) \cdot k\sigma^2. \quad (3.34)$$

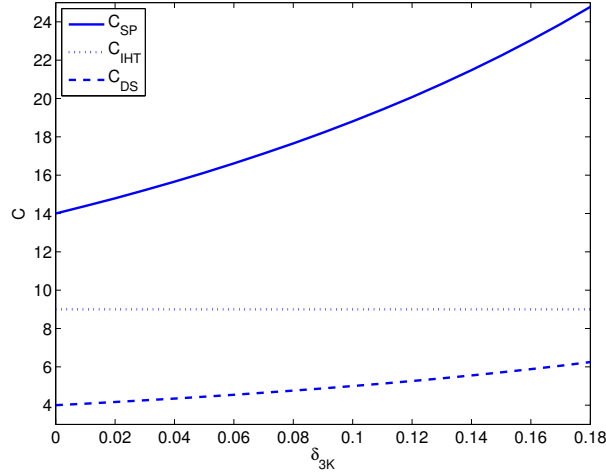
*Proof:* The proof is identical to the one of Theorem 3.2.6.  $\square$

A comparison between the constants achieved by the IHT, SP and DS is presented in Fig. 3.3. The CoSaMP constant was omitted since it is bigger than the one of the SP and it is dependent on  $\delta_{4k}$  instead of  $\delta_{3k}$ . The figure shows that the constant values of IHT and DS are better than that of the SP (and as such better than the one of the CoSaMP), and that the one of the DS is the smallest. It is interesting to note that the constant of the IHT is independent of  $\delta_{3k}$ .

In table 3.1 we summarize the performance guarantees of several different algorithms – the DS [30], the BP [31], and the three algorithms analyzed in this chapter.

We can observe the following:

1. In terms of the RIP: DS and BP are the best, then IHT, then SP and last is CoSaMP.
2. In terms of the constants in the bounds: the smallest constant is achieved by DS. Then come IHT, SP, CoSaMP and BP in this order.

Figure 3.3: The constants of the SP, IHT and DS algorithms as a function of  $\delta_{3k}$ 

Alg.	RIP Condition	Probability of Correctness	Constant	The Obtained Bound
DS	$\delta_{2k} + \delta_{3k} \leq 1$	$1 - (\sqrt{\pi(1+a)} \log n \cdot n^a)^{-1}$	$\frac{4}{1-2\delta_{3k}}$	$C_{DS}^2 \cdot (2(1+a) \log n) \cdot k\sigma^2$
BP	$\delta_{2k} + 3\delta_{3k} \leq 1$	$1 - (n^a)^{-1}$	$> \frac{32}{\kappa^4}$	$C_{BP}^2 \cdot (2(1+a) \log n) \cdot k\sigma^2$
SP	$\delta_{3k} \leq 0.139$	$1 - (\sqrt{\pi(1+a)} \log n \cdot n^a)^{-1}$	$\leq 21.41$	$C_{SP}^2 \cdot (2(1+a) \log n) \cdot k\sigma^2$
CoSaMP	$\delta_{4k} \leq 0.1$	$1 - (\sqrt{\pi(1+a)} \log n \cdot n^a)^{-1}$	$\leq 34.2$	$C_{CoSaMP}^2 \cdot (2(1+a) \log n) \cdot k\sigma^2$
IHT	$\delta_{3k} \leq \frac{1}{\sqrt{32}}$	$1 - (\sqrt{\pi(1+a)} \log n \cdot n^a)^{-1}$	9	$C_{IHT}^2 \cdot (2(1+a) \log n) \cdot k\sigma^2$

Table 3.1: Near oracle performance guarantees for the DS, BP, SP, CoSaMP and IHT techniques.

3. In terms of the probability: all have the same probability except the BP which gives a weaker guarantee.
4. Though the CoSaMP has a weaker guarantee compared to the SP, it has an efficient implementation that saves the matrix inversion in the algorithm.<sup>4</sup>

For completeness of the discussion here, we also refer to algorithms' complexity: the IHT is the cheapest, CoSaMP and SP come next with a similar complexity (with a slight advantage to CoSaMP). DS and BP seem to be the most complex.

Interestingly, in the guarantees of the OMP and the thresholding in [46] better constants are obtained. However, these results, as mentioned before, holds under mutual-coherence based conditions, which are more restricting. In addition, their validity relies on the magnitude of the

<sup>4</sup>The proofs of the guarantees in this chapter are not valid for this case, though it is not hard to extend them for it.

entries of  $\boldsymbol{\alpha}$  and the noise power, which is not correct for the results presented in this section for the greedy-like methods. Furthermore, though we get bigger constants with these methods, the conditions are not tight, as will be seen in Section 3.3.

### 3.2.4 Bounds on the Expected Error

So far we have seen that with high probability the greedy-like algorithms achieve near oracle performance. It is interesting to ask whether we can derive a similar bound on the expected error. The next theorem shows that the answer to this question is positive<sup>5</sup>.

**Theorem 3.2.10** *For a  $k$ -sparse vector  $\boldsymbol{\alpha}$ , assuming that  $\mathbf{e}$  is a zero-mean white Gaussian noise vector with variance  $\sigma^2$  and that  $n > 3^6$ , if the condition  $\delta_{bk} \leq \delta$  holds, then after at most  $t^* = \lceil \log_2 \left( \|\boldsymbol{\alpha}\|_2 / \|\mathbf{A}_{T_e}^* \mathbf{e}\|_2 \right) \rceil$  iterations*

$$E \|\boldsymbol{\alpha} - \hat{\boldsymbol{\alpha}}\|_2^2 \leq 4C^2(1+a) \log n \cdot k\sigma^2. \quad (3.35)$$

where  $b = 3$  and  $\delta = 0.139$  for SP;  $b = 4$  and  $\delta = 0.1$  for CoSaMP; and  $b = 3$  and  $\delta = 1/\sqrt{32}$  for IHT. The constant  $C$  is the one from Corollaries 3.2.2, 3.2.5 and 3.2.8 (summarized in Table 3.1).

*Proof:* Utilizing simple rules of probability theory with the result of Theorems 3.2.3, 3.2.6 and 3.2.9 as a first step and of Corollaries 3.2.2, 3.2.5 and 3.2.8 as a second step give

$$\begin{aligned} E \|\boldsymbol{\alpha} - \hat{\boldsymbol{\alpha}}\|_2^2 &\leq \mathbf{P} \left( \sup_i |\mathbf{A}_i^* \mathbf{e}| < \sigma \sqrt{2(1+a) \log n} \right) \cdot 2C^2(1+a) \log n \cdot k\sigma^2 \\ &\quad + E_{\sup_i |\mathbf{A}_i^* \mathbf{e}| > \sigma \sqrt{2(1+a) \log n}} \|\boldsymbol{\alpha} - \hat{\boldsymbol{\alpha}}\|_2^2 \\ &\leq 2C^2(1+a) \log n \cdot k\sigma^2 + C^2 E_{\sup_i |\mathbf{A}_i^* \mathbf{e}| > \sigma \sqrt{2(1+a) \log n}} \|\mathbf{D}_T^* \mathbf{e}\|_2^2. \end{aligned} \quad (3.36)$$

The facts that the supremum in the last inequality is over  $n$  elements and that the support of  $T^7$  is of size  $k$  leads to

$$\begin{aligned} E_{\sup_i |\mathbf{A}_i^* \mathbf{e}| > \sigma \sqrt{2(1+a) \log n}} \|\mathbf{A}_T^* \mathbf{e}\|_2^2 &\leq n \cdot E_{\substack{|\mathbf{A}_1^* \mathbf{e}| > \sigma \sqrt{2(1+a) \log n} \\ |\mathbf{A}_i^* \mathbf{e}| < |\mathbf{A}_1^* \mathbf{e}|, 2 \leq i \leq k}} \|\mathbf{A}_T^* \mathbf{e}\|_2^2 \\ &\leq nk \cdot E_{|\mathbf{A}_1^* \mathbf{e}| > \sigma \sqrt{2(1+a) \log n}} (\mathbf{A}_1^* \mathbf{e})^2. \end{aligned} \quad (3.37)$$

<sup>5</sup>Similar result for DS appears in [32].

<sup>6</sup>The assumption that  $n > 3$  is non-crucial for the proof and is used only for getting a better constant.

<sup>7</sup>We assume with no loss of generality that  $T = \{1, \dots, k\}$ .

Since the columns of  $\mathbf{A}$  are normalized and  $\mathbf{e}$  is a zero-mean white Gaussian noise with variance  $\sigma^2$ , we have that  $\mathbf{A}_1^* \mathbf{e} \sim n(0, \sigma^2)$ . Using the symmetry of the Gaussian distribution we have that

$$\begin{aligned} E_{|\mathbf{A}_1^* \mathbf{e}| > \sigma \cdot \sqrt{2(1+a) \log n}} (\mathbf{A}_1^* \mathbf{e})^2 &= 2 \int_{\sigma \cdot \sqrt{2(1+a) \log n}}^{\infty} \frac{x^2}{\sqrt{2\pi\sigma^2}} e^{-\frac{x^2}{2\sigma^2}} dx \\ &\leq 2\sigma \sqrt{2(1+a) \log n} e^{-\frac{\sigma^2 \cdot 2(1+a) \log n}{4\sigma^2}} \cdot \int_{\sigma \cdot \sqrt{2(1+a) \log n}}^{\infty} \frac{x}{\sqrt{2\pi\sigma^2}} e^{-\frac{x^2}{4\sigma^2}} dx \\ &= 2\sigma \sqrt{2(1+a) \log n} n^{-(1+a)} \int_{\frac{(1+a) \log n}{2}}^{\infty} \sqrt{\frac{2\sigma^2}{\pi}} e^{-t} dt = 2\sigma^2 \sqrt{\frac{2}{\pi}} \sqrt{2(1+a) \log n} n^{-(1+a)}. \end{aligned} \quad (3.38)$$

The inequality follows from the fact that  $\frac{x^2}{\sqrt{2\pi\sigma^2}} e^{-\frac{x^2}{2\sigma^2}} = x e^{-\frac{x^2}{4\sigma^2}} \cdot \frac{x}{\sqrt{2\pi\sigma^2}} e^{-\frac{x^2}{4\sigma^2}}$  and that the maximum of  $x e^{-\frac{x^2}{4\sigma^2}}$  in the range  $[\sigma \cdot \sqrt{2(1+a) \log n}, \infty)$  is achieved in the point  $x = \sigma \cdot \sqrt{2(1+a) \log n}$ . The equalities holds due to simple arithmetics and changing of variables in the integral with  $t = \frac{x^2}{4\sigma^2}$ .

By summing all the above and observing that  $\frac{2}{\pi \log n} < 1$  when  $n > 3$ , we get the desired result.  $\square$

We note that though the proof is presented only for the greedy-like algorithms, as this is the scope of this chapter, it can be easily used to extend the results of the other algorithms that guarantee near-oracle performance with high probability.

### 3.3 Experiments

In our experiments we use a random dictionary with entries drawn from the canonical normal distribution. The columns of the dictionary are normalized and the dimensions are  $m = 512$  and  $n = 1024$ . The vector  $\alpha$  is generated by selecting a support uniformly at random. Then the elements in the support are generated using the following model<sup>8</sup>:

$$\alpha_i = 10\epsilon_i(1 + |n_i|) \quad (3.39)$$

where  $\epsilon_i$  is  $\pm 1$  with probability 0.5, and  $n_i$  is a canonical normal random variable. The support and the non-zero values are statistically independent. We repeat each experiment 1500 times.

In the first experiment we calculate the error of the SP, CoSaMP and IHT methods for different sparsity levels. The noise variance is set to  $\sigma = 1$ . Fig. 3.4 presents the squared-error  $\|\alpha - \hat{\alpha}\|_2^2$  of all the instances of the experiment for the three algorithms. Our goal is to show that with high-probability the error obtained is bounded by the guarantees we have developed. For each algorithm we add the theoretical guarantee and the oracle performance. As can

<sup>8</sup>This model is taken from the experiments section in [30].

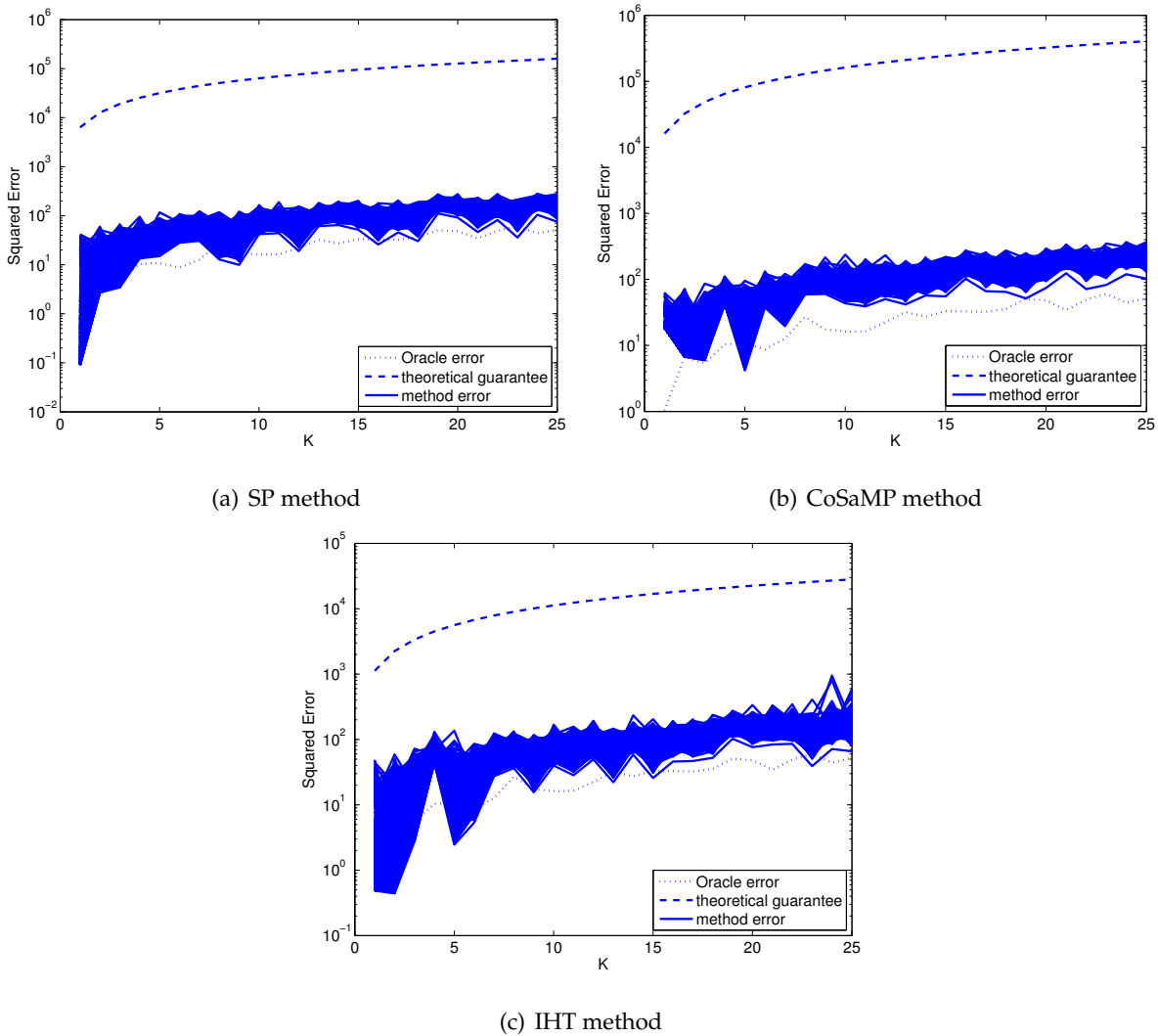
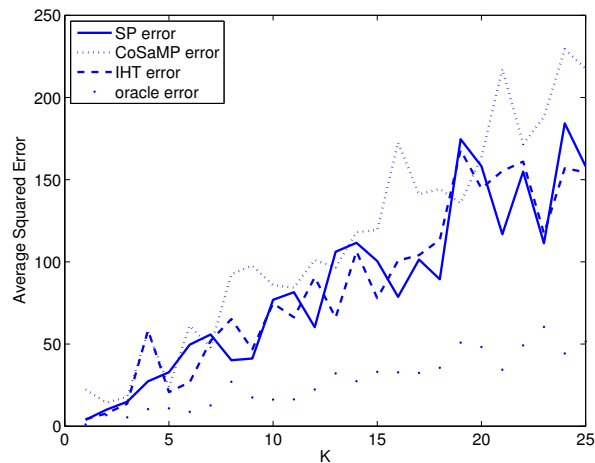


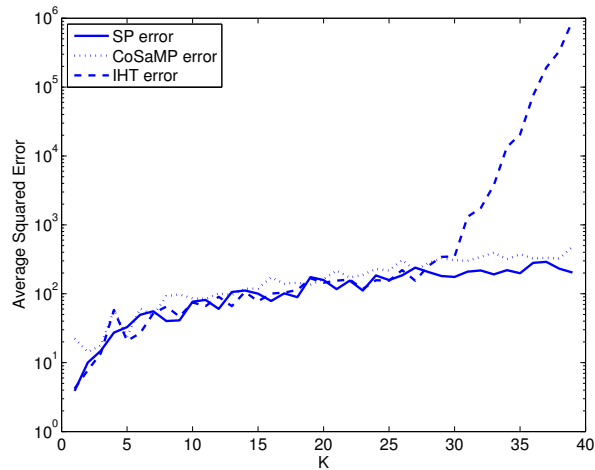
Figure 3.4: The squared-error as achieved by the SP, the CoSaMP and the IHT algorithms as a function of the cardinality. The graphs also show the theoretical guarantees and the oracle performance.

be seen, the theoretical guarantees are too loose and the actual performance of the algorithms is much better. However, we see that both the theoretical and the empirical performance curves show a proportionality to the oracle error. Note that the actual performance of the algorithms' may be better than the oracle's – this happens because the oracle is the Maximum-Likelihood Estimator (MLE) in this case [94], and by adding a bias one can perform even better in some cases.

Fig. 3.5(a) presents the mean-squared-error (by averaging all the experiments) for the range where the RIP-condition seems to hold, and Fig. 3.5(b) presents this error for a wider range, where it is likely to be violated. It can be seen that in the average case, though the algorithms



(a) RIP condition satisfied



(b) RIP condition not satisfied

Figure 3.5: The mean-squared-error of the SP, the CoSaMP and the IHT algorithms as a function of the cardinality.

get different constants in their bounds, they achieve almost the same performance. We also see a near-linear curve describing the error as a function of  $k$ . Finally, we observe that the SP and the CoSaMP, which were shown to have worse constants in theory, have better performance and are more stable in the case where the RIP-condition do not hold anymore.

In a second experiment we calculate the error of the SP, the CoSaMP and the IHT methods for different noise variances. The sparsity is set to  $k = 10$ . Fig. 3.6 presents the error of all the instances of the experiment for the three algorithms. Here as well we add the theoretical guarantee and the oracle performance. As we saw before, the guarantee is not tight but the error is proportional to the oracle estimator's error.

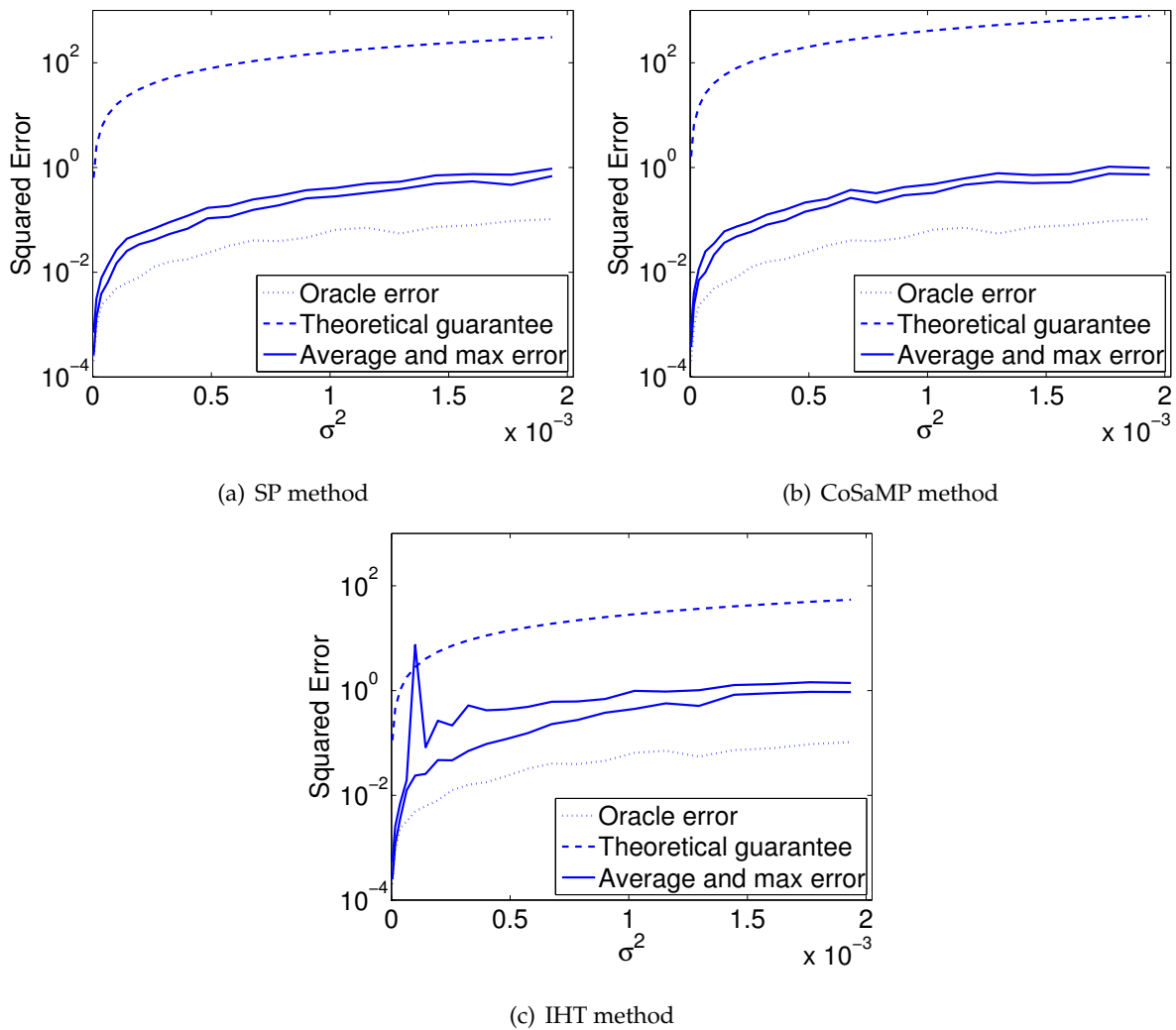


Figure 3.6: The squared-error as achieved by the SP, the CoSaMP and the IHT algorithms as a function of the noise variance. The graphs also show the theoretical guarantees and the oracle performance.

Fig. 3.7 presents the mean-squared-error as a function of the noise variance, by averaging over all the experiments. It can be seen that the error behaves linearly with respect to the variance, as expected from the theoretical analysis. Again we see that the constants are not tight and that the algorithms behave in a similar way. Finally, we note that the algorithms succeed in meeting the bounds even in very low signal-to-noise ratios, where simple greedy algorithms are expected to fail.

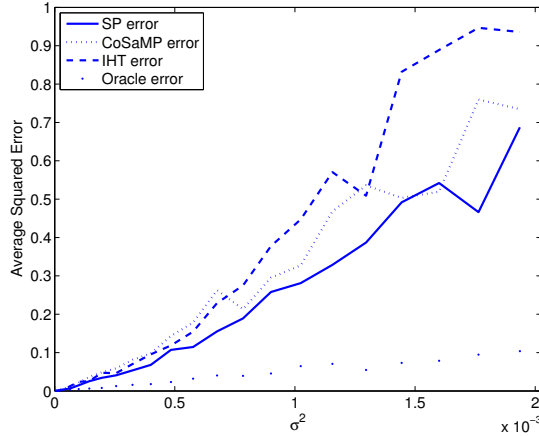


Figure 3.7: The mean-squared-error of the SP, the CoSaMP and the IHT algorithms as a function of the noise variance.

### 3.4 Extension to the Non-Exact Sparse Case

In the case where  $\alpha$  is not exactly  $k$ -sparse, our analysis has to change. Following the work reported in [39], we have the following error bounds for all algorithms (with the different RIP conditions and constants):

**Theorem 3.4.1** *If  $\mathbf{e}$  is a zero-mean white Gaussian noise vector with variance  $\sigma^2$ , then after at most  $t^* = \lceil \log_2 \left( \|\alpha\|_2 / \|\mathbf{A}_T^* \mathbf{e}\|_2 \right) \rceil$  iterations and under the appropriate RIP conditions, the reconstruction result,  $\hat{\alpha}$ , of SP, CoSaMP and IHT, satisfies*

$$E \|\alpha - \hat{\alpha}\|_2^2 \leq 4C^2(1+a) \log n \cdot k\sigma^2 + 4C^2 \left( \|\alpha - \alpha_T\|_2 + \frac{1}{\sqrt{k}} \|\alpha - \alpha_T\|_1 \right)^2, \quad (3.40)$$

where  $T$  denotes the support of the  $k$  largest elements in  $\alpha$  and  $C$  is the constant from Corollaries 3.2.2, 3.2.5 and 3.2.8.

*Proof:* Proposition 3.5 from [39] provides us with the following claim

$$\|\mathbf{A}\alpha\|_2 \leq \sqrt{1 + \delta_k} \left( \|\alpha\|_2 + \frac{1}{\sqrt{k}} \|\alpha\|_1 \right). \quad (3.41)$$

When  $\alpha$  is a non-exact  $k$ -sparse vector we get that the effective error in our results becomes  $\tilde{\mathbf{e}} = \mathbf{e} + \mathbf{A}(\alpha - \alpha_T)$ . Thus, using the error bounds of the algorithms (Equations (3.8), (3.19) and (3.32)) with the inequality in (3.41) and the relation  $\|\alpha - \hat{\alpha}\|_2 \leq \|\alpha_T - \hat{\alpha}\|_2 + \|\alpha - \alpha_T\|_2$ , we

have

$$\begin{aligned}
E \|\boldsymbol{\alpha} - \hat{\boldsymbol{\alpha}}\|_2^2 &\leq E \left( C \|\mathbf{A}_{T_e}^* \tilde{\mathbf{e}}\|_2 + \|\boldsymbol{\alpha} - \boldsymbol{\alpha}_T\|_2 \right)^2 \\
&\leq C^2 E \left( \|\mathbf{A}_{T_e}^* \mathbf{e}\|_2 + \sqrt{1 + \delta_k} \|\mathbf{A}(\boldsymbol{\alpha} - \boldsymbol{\alpha}_T)\|_2 + \frac{1}{C} \|\boldsymbol{\alpha} - \boldsymbol{\alpha}_T\|_2 \right)^2 \\
&\leq C^2 E \left( \|\mathbf{A}_{T_e}^* \mathbf{e}\|_2 + (1 + \delta_k) \|\boldsymbol{\alpha} - \boldsymbol{\alpha}_T\|_2 + \frac{1 + \delta_k}{\sqrt{k}} \|\boldsymbol{\alpha} - \boldsymbol{\alpha}_T\|_1 + \frac{1}{C} \|\boldsymbol{\alpha} - \boldsymbol{\alpha}_T\|_2 \right)^2.
\end{aligned} \tag{3.42}$$

Using the fact that  $E\mathbf{e} = 0$  and similar steps to those taken in Theorem 3.2.10 gives

$$\begin{aligned}
E \|\boldsymbol{\alpha} - \hat{\boldsymbol{\alpha}}\|_2^2 &\leq 4C^2(1 + a) \log n \cdot k\sigma^2 \\
&\quad + C^2 \left( \left( \frac{1}{C} + 1 + \delta_k \right) \|\boldsymbol{\alpha} - \boldsymbol{\alpha}_T\|_2 + \frac{1 + \delta_k}{\sqrt{k}} \|\boldsymbol{\alpha} - \boldsymbol{\alpha}_T\|_1 \right)^2.
\end{aligned} \tag{3.43}$$

Since the RIP condition for all the algorithms satisfies  $\delta_k \leq 0.5$  and  $C \geq 2$ , plugging this into (3.43) gives (3.40), which concludes the proof.  $\square$

Embarking from (3.42) and using (3.43) for the first term, we obtain also the inequality

$$E \|\boldsymbol{\alpha} - \hat{\boldsymbol{\alpha}}\|_2^2 \leq 4C(1 + a) \log n \cdot k\sigma^2 + \left( \|\boldsymbol{\alpha} - \boldsymbol{\alpha}_T\|_2 + C \|\mathbf{A}_{T_e}^\dagger \mathbf{A}(\boldsymbol{\alpha} - \boldsymbol{\alpha}_T)\|_2 \right)^2. \tag{3.44}$$

**Remark 3.4.2** For a  $k$ -sparse vector  $\boldsymbol{\alpha}$ , by applying the SP, CoSaMP and IHT algorithms with  $k = \sum_i I(|\boldsymbol{\alpha}_i| > \sigma)$  ( $I$  is the indicator function and  $\boldsymbol{\alpha}_i$  is the  $i$ -th element in  $\boldsymbol{\alpha}$ ) one can easily get from (3.44) a bound of the form  $E \|\boldsymbol{\alpha} - \hat{\boldsymbol{\alpha}}\|_2^2 \leq 4(1 + a)C^2 \log n \cdot \sum \min(\boldsymbol{\alpha}_i^2, \sigma^2)$ . This bound is proportional to a better oracle that for small elements of  $\boldsymbol{\alpha}$  estimates 0. Unlike the regular oracle that uses the support of the original vector  $\boldsymbol{\alpha}$ , this oracle uses the support that minimizes the MSE. Its MSE is lower bounded by  $0.5 \sum \min(\boldsymbol{\alpha}_i^2, \sigma^2)$  [32, 30].

### 3.5 Summary

In this chapter we have presented near-oracle performance guarantees for three greedy-like algorithms – Subspace Pursuit, CoSaMP, and Iterative Hard-Thresholding. The approach taken in our analysis is an RIP-based (as opposed to mutual-coherence) and uses the existing worst case guarantees of these algorithms. Our study leads to uniform guarantees for the three algorithms explored, i.e., the near-oracle error bounds are dependent only on the dictionary properties (RIP constant) and the sparsity level of the sought solution. In addition, those bounds hold also for the MSE of the reconstruction and not only with high probability for the squared error, as was done in previous works for other algorithms. We have also presented a simple extension of our results to the case where the representation is only approximately sparse.

Note that the near oracle performance bounds do not only improve the “pre-run recovery guarantees”, but are quite useful in exploring various data error and solution sparsity trade-offs. For example, for compressible signals (the representation is not exactly  $k$ -sparse but has decreasing coefficients according to a given distribution) the parameter  $k$  should be specified to the greedy-like techniques. We have shown that this parameter can be automatically tuned by using a prior knowledge on the distribution of the representation together with the developed near-oracle bounds [2].



## Chapter 4

# Greedy-Like Methods for the Cospase Analysis Model

The results shown in this chapter have been published and appeared in the following articles:

- R. Giryes, S. Nam, M. Elad, R. Gribonval and M.E. Davies, "Greedy-like algorithms for the cospase analysis model," *The Special Issue in LAA on Sparse Approximate Solution of Linear Systems*, 2013 [4].
- R. Giryes, S. Nam, R. Gribonval, M. E. Davies, "Iterative cospase projection algorithms for the recovery of cospase vectors," in *Proc. European Signal Processing Conference (EUSIPCO), Barcelona, Spain, Aug. 29, 2011* [5].
- R. Giryes and M. Elad, "CoSaMP and SP for the cospase analysis model," in *Proc. European Signal Processing Conference (EUSIPCO), Bucharest, Romania, Aug. 27-31, 2012* [6].

In Section 2.7.2 we have described several pursuit algorithms that have been developed for the cospase analysis model. Instead of developing new methods from scratch, we propose in this chapter a general recipe for "converting synthesis pursuit methods" into analysis ones. Encouraged by the developed results for the greedy-like techniques in the previous chapter, we apply this recipe on these strategies – constructing methods that will imitate the family of greedy-like algorithms. This chapter introduces these algorithms: analysis IHT (AIHT), analysis HTP (AHTP), analysis CoSaMP (ACoSaMP) and Analysis SP (ASP).

The main contribution of this chapter is our result on the stability of these analysis pursuit

algorithms. We show that after a finite number of iterations and for a given constant  $c_0$ , the reconstruction result  $\hat{\mathbf{x}}$  of AIHT, AHTP, ACoSaMP and ASP all satisfy

$$\|\mathbf{x} - \hat{\mathbf{x}}\|_2 \leq c_0 \|\mathbf{e}\|_2, \quad (4.1)$$

under a RIP-like condition on  $\mathbf{M}$  and the assumption that we are given a good near optimal projection scheme. Note that this result is posed in terms of the signal error and not the one of the representation. The reason is that in the analysis model, unlike the synthesis one, we focus on the signal directly.

A recovery error bound is also given for the case where  $\mathbf{x}$  is only nearly  $\ell$ -cosparse. Similar results for the  $\ell_1$  analysis appear in [24, 25]. More details about the relation between these papers and our results will be given in Section 4.4.

In addition to our theoretical results we demonstrate the performance of the four pursuit methods under a thresholding based simple projection scheme. Both our theoretical and empirical results show that linear dependencies in  $\Omega$  that result with a larger cosparsity in the signal  $\mathbf{x}$ , lead to a better reconstruction performance. *This suggests that, as opposed to the synthesis case, strong linear dependencies within  $\Omega$  are desired.*

This chapter is organized as follows:

- In Section 4.1 we define the operator RIP (O-RIP) for the analysis model, proving that it has similar characteristics to the original RIP.
- In Section 4.2 the notion of near optimal projection is proposed and some nontrivial operators for which a tractable optimal projection exists are exhibited. Both the O-RIP and the near optimal projection are used throughout this chapter as a main force for deriving our theoretical results.
- In Section 4.3 the four pursuit algorithms for the cosparse analysis framework are defined, using a general recipe for converting synthesis methods into analysis ones.
- In Section 4.4 we derive the success guarantees for all the above algorithms in a unified way. Note that the provided results can be easily adapted to other union-of-subspaces models given near optimal projection schemes for them, in the same fashion done for IHT with an optimal projection scheme in [95]. The relation between the obtained results and existing work appears in this section as well.

- Empirical performance of these algorithms is demonstrated in Section 4.5 in the context of the cosparsity signal recovery problem. We use a simple thresholding as the near optimal projection scheme in the greedy-like techniques.
- Section 4.6 discusses the presented results and concludes this chapter.

## 4.1 O-RIP Definition and its Properties

Before entering into the definition of the O-RIP, we bring some definitions and notations which are used throughout this chapter:

- $\sigma_{\mathbf{M}}$  is the largest singular value of  $\mathbf{M}$ , i.e.,  $\sigma_{\mathbf{M}}^2 = \|\mathbf{M}^* \mathbf{M}\|_2$ .
- Given a cosupport set  $\Lambda$ ,  $\mathbf{\Omega}_{\Lambda}$  is a sub-matrix of  $\mathbf{\Omega}$  with the *rows*<sup>1</sup> that belong to  $\Lambda$ .
- For given vectors  $\mathbf{v}, \mathbf{z} \in \mathbb{R}^d$  and an analysis dictionary  $\mathbf{\Omega}$ ,  $\text{cosupp}(\mathbf{\Omega}\mathbf{v})$  returns the cosupport of  $\mathbf{\Omega}\mathbf{v}$  and  $\text{cosupp}(\mathbf{\Omega}\mathbf{z}, \ell)$  returns the index set of  $\ell$  smallest (in absolute value) elements in  $\mathbf{\Omega}\mathbf{z}$ . If more than  $\ell$  elements are zero all of them are returned. In the case where the  $\ell$ -th smallest entry is equal to the  $\ell + 1$  smallest entry, one of them is chosen arbitrarily.
- $\mathbf{Q}_{\Lambda} = \mathbf{I} - \mathbf{\Omega}_{\Lambda}^{\dagger} \mathbf{\Omega}_{\Lambda}$  is the orthogonal projection onto the orthogonal complement of  $\text{range}(\mathbf{\Omega}_{\Lambda}^*)$ .
- $\mathbf{P}_{\Lambda} = \mathbf{I} - \mathbf{Q}_{\Lambda} = \mathbf{\Omega}_{\Lambda}^{\dagger} \mathbf{\Omega}_{\Lambda}$  is the orthogonal projection onto  $\text{range}(\mathbf{\Omega}_{\Lambda}^*)$ .
- A cosupport  $\Lambda$  has a corank  $r$  if  $\text{rank}(\mathbf{\Omega}_{\Lambda}) = r$ . A vector  $\mathbf{v}$  has a corank  $r$  if its cosupport has a corank  $r$ .
- $[p]$  denotes the set of integers  $[1 \dots p]$ .
- $\mathcal{L}_{\Omega, \ell} = \{\Lambda \subseteq [p], |\Lambda| \geq \ell\}$  is the set of  $\ell$ -cosparsity cosupports and  $\mathcal{L}_{\Omega, r}^{\text{corank}} = \{\Lambda \subseteq [p], \text{rank}(\mathbf{\Omega}_{\Lambda}) \geq r\}$  is the set of all cosupports with corresponding corank  $r$ .
- $\mathcal{W}_{\Lambda} = \text{span}^{\perp}(\mathbf{\Omega}_{\Lambda}) = \{\mathbf{Q}_{\Lambda} \mathbf{z}, \mathbf{z} \in \mathbb{R}^d\}$  is the subspace spanned by a cosparsity set  $\Lambda$ .
- $\mathcal{A}_{\Omega, \ell} = \bigcup_{\Lambda \in \mathcal{L}_{\Omega, \ell}} \mathcal{W}_{\Lambda}$  is the union of subspaces of  $\ell$ -cosparsity vectors and  $\mathcal{A}_{\Omega, r}^{\text{corank}} = \bigcup_{\Lambda \in \mathcal{L}_{\Omega, r}^{\text{corank}}} \mathcal{W}_{\Lambda}$  is the union of subspaces of all vectors with corank  $r$ . In the case that

---

<sup>1</sup>By abuse of notation we use the same notation for the selection sub-matrices of rows and columns. The selection will be clear from the context since in analysis the focus is always on the rows and in synthesis on the columns.

every  $\ell$  rows of  $\Omega$  are independent it is clear that  $\mathcal{A}_{\Omega,\ell} = \mathcal{A}_{\Omega,r}^{\text{corank}}$ . When it will be clear from the context, we will remove  $\Omega$  from the subscript.

- $\mathbf{x} \in \mathbb{R}^d$  denotes the original unknown  $\ell$ -cosparse vector and  $\Lambda$  its cosupport.
- $\mathbf{v}, \mathbf{u} \in \mathcal{A}_\ell$  are used to denote general  $\ell$ -cosparse vectors and  $\mathbf{z} \in \mathbb{R}^d$  is used to denote a general vector.

We now turn to define the O-RIP, which parallels the regular RIP as used in [28]. This property is very important for the study of the pursuit algorithms in this chapter and it holds for a large family of matrices  $\mathbf{M}$ , as we will see hereafter.

**Definition 4.1.1** *A matrix  $\mathbf{M}$  has the O-RIP with an operator  $\Omega$  and a constant  $\delta_\ell = \delta_{\Omega,\ell}^O$ , if  $\delta_{\Omega,\ell}^O$  is the smallest constant that satisfies*

$$(1 - \delta_{\Omega,\ell}^O) \|\mathbf{v}\|_2^2 \leq \|\mathbf{M}\mathbf{v}\|_2^2 \leq (1 + \delta_{\Omega,\ell}^O) \|\mathbf{v}\|_2^2, \quad (4.2)$$

whenever  $\Omega\mathbf{v}$  has at least  $\ell$  zeroes.

Note that though  $\delta_\ell$  is also a function of  $\Omega$  we abuse notation and use the same symbol for the O-RIP as the regular RIP. It will be clear from the context which of them we refer to and what  $\Omega$  is in use with the O-RIP.

A similar property that looks at the corank of the vectors can be defined as follows.

**Definition 4.1.2** *A matrix  $\mathbf{M}$  has the corank-O-RIP with a constant  $\delta_r^{\text{corank}}$ , if  $\delta_r^{\text{corank}}$  is the smallest constant that satisfies*

$$(1 - \delta_r^{\text{corank}}) \|\mathbf{u}\|_2^2 \leq \|\mathbf{M}\mathbf{u}\|_2^2 \leq (1 + \delta_r^{\text{corank}}) \|\mathbf{u}\|_2^2 \quad (4.3)$$

whenever the corank of  $\mathbf{u}$  with respect to  $\Omega$  is greater or equal to  $r$ .

The O-RIP, like the regular RIP, inherits several key properties. We present only those related to  $\delta_\ell$ , while very similar characteristics can be derived also for the corank-O-RIP. The first property we pose is an immediate corollary of the  $\delta_\ell$  definition.

**Corollary 4.1.3** *If  $\mathbf{M}$  has the O-RIP with a constant  $\delta_\ell$  then*

$$\|\mathbf{M}\mathbf{Q}_\Lambda\|_2^2 \leq 1 + \delta_\ell \quad (4.4)$$

for any  $\Lambda \in \mathcal{L}_\ell$ .

*Proof:* Any  $\mathbf{v} \in \mathcal{A}_\ell$  can be represented as  $\mathbf{v} = \mathbf{Q}_\Lambda \mathbf{z}$  with  $\Lambda \in \mathcal{L}_\ell$  and  $\mathbf{z} \in \mathbb{R}^d$ . Thus, the O-RIP in (4.2) can be reformulated as

$$(1 - \delta_\ell) \|\mathbf{Q}_\Lambda \mathbf{z}\|_2^2 \leq \|\mathbf{M} \mathbf{Q}_\Lambda \mathbf{z}\|_2^2 \leq (1 + \delta_\ell) \|\mathbf{Q}_\Lambda \mathbf{z}\|_2^2 \quad (4.5)$$

for any  $\mathbf{z} \in \mathbb{R}^d$  and  $\Lambda \in \mathcal{L}_\ell$ . Since  $\mathbf{Q}_\Lambda$  is a projection  $\|\mathbf{Q}_\Lambda \mathbf{z}\|_2^2 \leq \|\mathbf{z}\|_2^2$ . Combining this with the right inequality in (4.5) gives

$$\|\mathbf{M} \mathbf{Q}_\Lambda \mathbf{z}\|_2^2 \leq (1 + \delta_\ell) \|\mathbf{z}\|_2^2 \quad (4.6)$$

for any  $\mathbf{z} \in \mathbb{R}^d$  and  $\Lambda \in \mathcal{L}_\ell$ . The first inequality in (4.4) follows from (4.6) by the definition of the spectral norm.  $\square$

**Lemma 4.1.4** *For  $\tilde{\ell} \leq \ell$  it holds that  $\delta_\ell \leq \delta_{\tilde{\ell}}$ .*

*Proof:* Since  $\mathcal{A}_\ell \subseteq \mathcal{A}_{\tilde{\ell}}$  the claim is immediate.  $\square$

**Lemma 4.1.5**  *$\mathbf{M}$  has the O-RIP if and only if*

$$\|\mathbf{Q}_\Lambda (\mathbf{I} - \mathbf{M}^* \mathbf{M}) \mathbf{Q}_\Lambda\|_2 \leq \delta_\ell \quad (4.7)$$

for any  $\Lambda \in \mathcal{L}_\ell$ .

*Proof:* The proof is similar to the one of the regular RIP as appears in [45]. As a first step we observe that Definition 4.1.1 is equivalent to requiring

$$\left| \|\mathbf{M} \mathbf{v}\|_2^2 - \|\mathbf{v}\|_2^2 \right| \leq \delta_\ell \|\mathbf{v}\|_2^2 \quad (4.8)$$

for any  $\mathbf{v} \in \mathcal{A}_\ell$ . The latter is equivalent to

$$\left| \|\mathbf{M} \mathbf{Q}_\Lambda \mathbf{z}\|_2^2 - \|\mathbf{Q}_\Lambda \mathbf{z}\|_2^2 \right| \leq \delta_\ell \|\mathbf{Q}_\Lambda \mathbf{z}\|_2^2 \quad (4.9)$$

for any set  $\Lambda \in \mathcal{L}_\ell$  and any  $\mathbf{z} \in \mathbb{R}^d$ , since  $\mathbf{Q}_\Lambda \mathbf{z} \in \mathcal{A}_\ell$ . Next we notice that

$$\|\mathbf{M} \mathbf{Q}_\Lambda \mathbf{z}\|_2^2 - \|\mathbf{Q}_\Lambda \mathbf{z}\|_2^2 = \mathbf{z}^* \mathbf{Q}_\Lambda \mathbf{M}^* \mathbf{M} \mathbf{Q}_\Lambda \mathbf{z} - \mathbf{z}^* \mathbf{Q}_\Lambda \mathbf{z} = \langle \mathbf{Q}_\Lambda (\mathbf{M}^* \mathbf{M} - \mathbf{I}) \mathbf{Q}_\Lambda \mathbf{z}, \mathbf{z} \rangle.$$

Since  $\mathbf{Q}_\Lambda (\mathbf{M}^* \mathbf{M} - \mathbf{I}) \mathbf{Q}_\Lambda$  is Hermitian we have that

$$\max_{\mathbf{z}} \frac{|\langle \mathbf{Q}_\Lambda (\mathbf{M}^* \mathbf{M} - \mathbf{I}) \mathbf{Q}_\Lambda \mathbf{z}, \mathbf{z} \rangle|}{\|\mathbf{z}\|_2} = \|\mathbf{Q}_\Lambda (\mathbf{M}^* \mathbf{M} - \mathbf{I}) \mathbf{Q}_\Lambda\|_2. \quad (4.10)$$

Thus we have that Definition 4.1.1 is equivalent to (4.7) for any set  $\Lambda \in \mathcal{L}_\ell$ .  $\square$

**Corollary 4.1.6** *If  $\mathbf{M}$  has the O-RIP then*

$$\|\mathbf{Q}_{\Lambda_1}(\mathbf{I} - \mathbf{M}^*\mathbf{M})\mathbf{Q}_{\Lambda_2}\|_2 \leq \delta_{\ell}, \quad (4.11)$$

for any  $\Lambda_1$  and  $\Lambda_2$  such that  $\Lambda_1 \cap \Lambda_2 \in \mathcal{L}_{\ell}$ .

*Proof:* Since  $\Lambda_1 \cap \Lambda_2 \subseteq \Lambda_1$  and  $\Lambda_1 \cap \Lambda_2 \subseteq \Lambda_2$

$$\|\mathbf{Q}_{\Lambda_1}(\mathbf{I} - \mathbf{M}^*\mathbf{M})\mathbf{Q}_{\Lambda_2}\|_2 \leq \|\mathbf{Q}_{\Lambda_2 \cap \Lambda_1}(\mathbf{I} - \mathbf{M}^*\mathbf{M})\mathbf{Q}_{\Lambda_2 \cap \Lambda_1}\|_2.$$

Using Lemma 4.1.5 completes the proof.  $\square$

As we will see later, we need the O-RIP constant to be small. Thus, we are interested to know for which matrices this holds true. In the synthesis case, where  $\mathbf{\Omega}$  is unitary and the O-RIP is identical to the RIP, it was shown for certain family of random matrices, such as matrices with Bernoulli or Subgaussian ensembles, that for any value of  $\varepsilon_k$  if  $m \geq C_{\varepsilon_k} k \log(\frac{m}{k\varepsilon_k})$  then  $\delta_k \leq \varepsilon_k$  [28, 76, 96], where  $\delta_k$  is the RIP constant and  $C_{\varepsilon_k}$  is a constant depending on  $\varepsilon_k$  and  $\mathbf{M}$ . A similar result for the same family of random matrices holds for the analysis case. The result is a special case of the result presented in [95].

**Theorem 4.1.7 (Theorem 3.3 in [95])** *Fix  $\mathbf{\Omega} \in \mathbb{R}^{p \times d}$  and let  $\mathbf{M} \in \mathbb{R}^{m \times d}$  be a random matrix such that for any  $\mathbf{z} \in \mathbb{R}^d$  and  $0 < \tilde{\varepsilon} \leq \frac{1}{3}$  it satisfies*

$$P\left(\left|\|\mathbf{M}\mathbf{z}\|_2^2 - \|\mathbf{z}\|_2^2\right| \geq \tilde{\varepsilon} \|\mathbf{z}\|_2^2\right) \leq e^{-\frac{C_{\mathbf{M}} m \tilde{\varepsilon}}{2}}, \quad (4.12)$$

where  $C_{\mathbf{M}} > 0$  is a constant. For any value of  $\varepsilon_r > 0$ , if

$$m \geq \frac{32}{C_{\mathbf{M}} \varepsilon_r^2} \left( \log(|\mathcal{L}_r^{\text{corank}}|) + (d-r) \log(9/\varepsilon_r) + t \right), \quad (4.13)$$

then  $\delta_r^{\text{corank}} \leq \varepsilon_r$  with probability exceeding  $1 - e^{-t}$ .

The above theorem is important since it shows that a large family of random matrices – similar to those having the RIP with high probability<sup>2</sup> – has a small O-RIP constant with high probability. In a recent work it was even shown that by randomizing the signs of the columns

<sup>2</sup>Note that, depending on  $\mathbf{\Omega}$ , the family of random matrices that have the RIP with high probability may not coincide with the family of random matrices that have the O-RIP with high probability. For example, take  $\mathbf{M}$  a partial random Fourier matrix (known to have RIP),  $\mathbf{\Omega}$  as the orthogonal Fourier basis and select any vector in the Fourier basis. With reasonably high probability, this vector is not included in the selected rows and will be orthogonal to all rows of  $\mathbf{M}$ . Thus, the O-RIP will not hold with any constant smaller than 1.

in the matrices that have the RIP we get new matrices that also have the RIP [97]. A similar process can be carried also with the O-RIP matrices. Thus, requiring the O-RIP constant to be small, as will be done hereafter, is legitimate.

For completeness we present a proof for theorem 4.1.7 in Appendix B.1 using the proof techniques in [76, 96, 98]. We include in it also the proof of Theorem 4.1.8 to follow. In the case that  $\Omega$  is in general position  $|\mathcal{L}_r^{\text{corank}}| = \binom{p}{r} \leq \left(\frac{ep}{p-r}\right)^{p-r}$  (inequality is by Stirling's formula) and thus  $m \geq (p-r) \log\left(\frac{ep}{p-r}\right)$ . Since we want  $m$  to be smaller than  $d$  we need  $p-r$  to be smaller than  $d$ . This limits the size of  $p$  for  $\Omega$  since  $r$  cannot be greater than  $d$ . Thus, we present a variation of the theorem which states the results in terms of  $\delta_\ell$  and  $\ell$  instead of  $\delta_r^{\text{corank}}$  and  $r$ . The following theorem is also important because of the fact that our theoretical results are in terms of  $\delta_\ell$  and not  $\delta_r^{\text{corank}}$ . It shows that  $\delta_\ell$  is small in the same family of matrices that guarantees  $\delta_r^{\text{corank}}$  to be small.

**Theorem 4.1.8** *Under the same setup of Theorem 4.1.7, for any  $\varepsilon_\ell > 0$  if*

$$m \geq \frac{32}{C_M \varepsilon_\ell^2} \left( (p-\ell) \log \left( \frac{9p}{(p-\ell)\varepsilon_\ell} \right) + t \right), \quad (4.14)$$

*then  $\delta_\ell \leq \varepsilon_\ell$  with probability exceeding  $1 - e^{-t}$ .*

We note that when  $\Omega$  is in general position,  $\ell$  cannot be greater than  $d$  and thus  $p$  cannot be greater than  $2d$  [23]. For this reason, if we want to have large values for  $p$  we should allow linear dependencies between the rows of  $\Omega$ . In this case the cosparsity of the signal can be greater than  $d$ . This explains why linear dependencies are a favorable thing in analysis dictionaries [86]. In Section 4.5 we shall see that also empirically we get a better recovery when  $\Omega$  contains linear dependencies.

## 4.2 Near Optimal Projections

As we will see hereafter, in the proposed algorithms we will face the following problem: Given a general vector  $\mathbf{z} \in \mathbb{R}^d$ , we would like to find an  $\ell$ -cosparse vector that is closest to it in the  $\ell_2$ -norm sense. In other words, we would like to project the vector to the closest  $\ell$ -cosparse subspace. Given the cosupport  $\Lambda$  of this space the solution is simply  $\mathbf{Q}_\Lambda \mathbf{z}$ . Thus, the problem of finding the closest  $\ell$ -cosparse vector turns to be the problem of finding the cosupport of the closest  $\ell$ -cosparse subspace. We denote the procedure of finding this cosupport by

$$\mathcal{S}_\ell^*(\mathbf{z}) = \underset{\Lambda \in \mathcal{L}_\ell}{\operatorname{argmin}} \|\mathbf{z} - \mathbf{Q}_\Lambda \mathbf{z}\|_2^2. \quad (4.15)$$

In the representation domain in the synthesis case, the support of the closest  $k$ -sparse subspace is found simply by hard thresholding, i.e., taking the support of the  $k$ -largest elements. However, in the analysis case calculating (4.15) is NP-complete with no efficient method for doing it for a general  $\Omega$  [99]. Thus an approximation procedure  $\hat{S}_\ell$  is needed. For this purpose we introduce the definition of a near-optimal projection [5].

**Definition 4.2.1** A procedure  $\hat{S}_\ell$  implies a near-optimal projection  $\mathbf{Q}_{\hat{S}_\ell(\cdot)}$  with a constant  $C_\ell$  if for any  $\mathbf{z} \in \mathbb{R}^d$

$$\left\| \mathbf{z} - \mathbf{Q}_{\hat{S}_\ell(\mathbf{z})} \mathbf{z} \right\|_2^2 \leq C_\ell \left\| \mathbf{z} - \mathbf{Q}_{S_\ell^*(\mathbf{z})} \mathbf{z} \right\|_2^2. \quad (4.16)$$

A clear implication of this definition is that if  $\hat{S}_\ell$  implies a near-optimal projection with a constant  $C_\ell$  then for any vector  $\mathbf{z} \in \mathbb{R}^d$  and an  $\ell$ -cosparsive vector  $\mathbf{v} \in \mathbb{R}^d$

$$\left\| \mathbf{z} - \mathbf{Q}_{\hat{S}_\ell(\mathbf{z})} \mathbf{z} \right\|_2^2 \leq C_\ell \left\| \mathbf{z} - \mathbf{v} \right\|_2^2. \quad (4.17)$$

Similarly to the O-RIP, the above discussion can be directed also for finding the closest vector with corank  $r$  defining  $S_r^{\text{corank}^*}$  and near optimal projection for this case in a very similar way to (4.15) and Definition 4.2.1 respectively.

Having a near-optimal cosupport selection scheme for a general operator is still an open problem and we leave it for a future work. It is possible that this is also NP-complete. We start by describing a simple thresholding rule that can be used with any operator. Even though it does not have any known (near) optimality guarantee besides the case of unitary operators, the numerical section will show it performs well in practice. Then we present two tractable algorithms for finding the optimal cosupport for two non-trivial analysis operators, the one dimensional finite difference operator  $\Omega_{1\text{D-DIF}}$  [100] and the fused Lasso operator  $\Omega_{\text{FUS}}$  [101].

Later in the chapter, we propose theoretical guarantees for algorithms that use operators that has an optimal or a near-optimal cosupport selection scheme. We leave the theoretical study of the thresholding technique for a future work but demonstrate its performance empirically in Section 4.5 where this rule is used showing that also when near-optimality is not at hand reconstruction is feasible.

### 4.2.1 Cosupport Selection by Thresholding

One intuitive option for cosupport selection is the simple thresholding

$$\hat{S}_\ell(\mathbf{z}) = \text{cosupp}(\Omega \mathbf{z}, \ell), \quad (4.18)$$

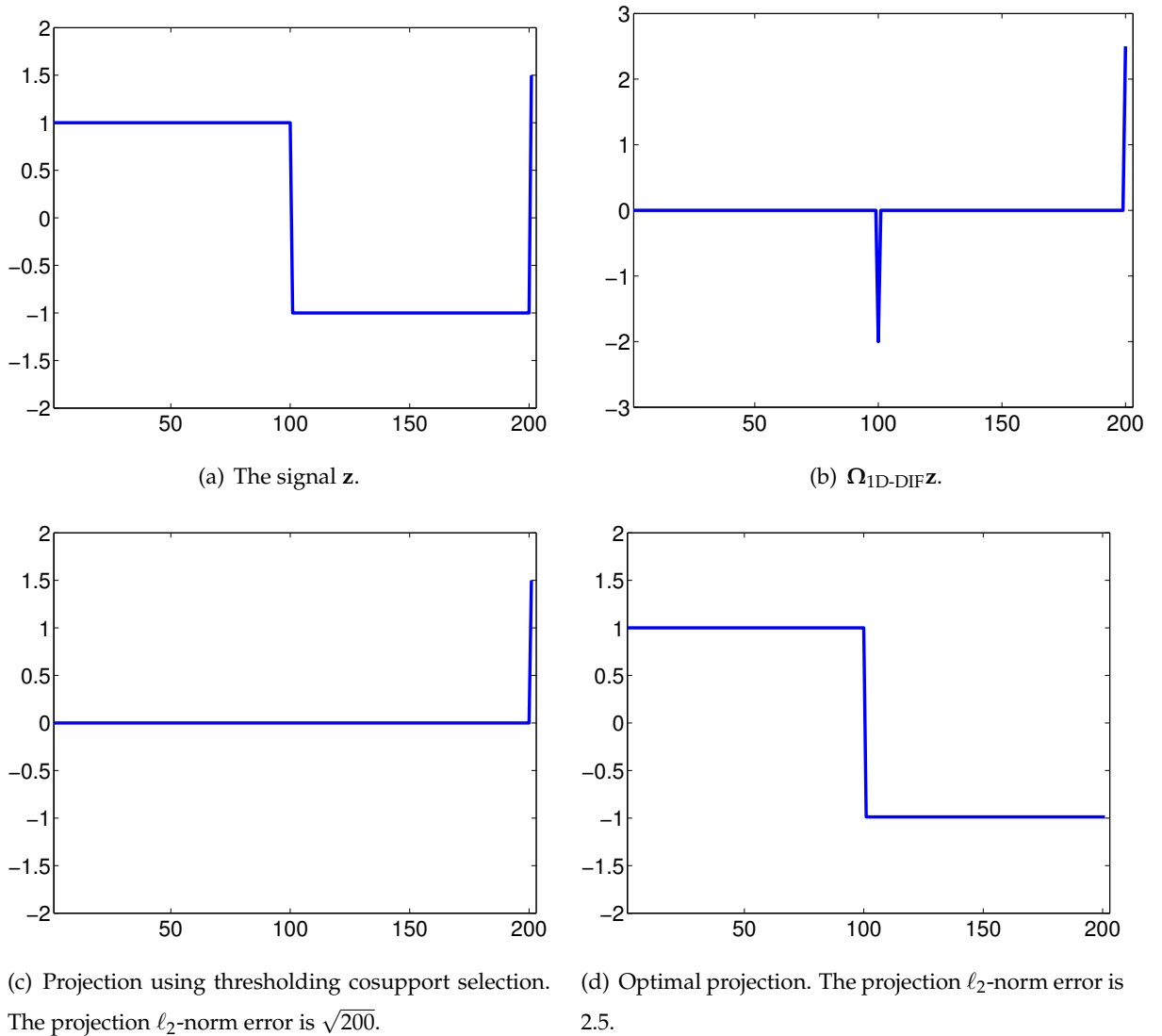


Figure 4.1: Comparison between projection using thresholding cosupport selection and optimal cosupport selection. As it can be seen the thresholding projection error is much larger than the optimal projection error by a factor much larger than 1

which selects as a cosupport the indices of the  $\ell$  smallest elements after applying  $\Omega$  on  $\mathbf{z}$ . As mentioned above, this selection method is optimal for unitary analysis operators where it coincides with the hard thresholding used in synthesis. However, in the general case this selection method is not guaranteed to give the optimal cosupport. Its near optimality constant  $C_\ell$  is not close to one and is equal to the fraction of the largest and smallest singular values (which are not zero) of the submatrices composed of  $\ell$  rows from  $\Omega$  [5].

One example for an operator for which the thresholding is sub-optimal is the 1D-finite

difference operator  $\Omega_{1D-DIF}$ . This operator is defined as:

$$\Omega_{1D-DIF} = \begin{pmatrix} -1 & 1 & \cdots & & & \\ \vdots & -1 & 1 & & & \\ & & & \ddots & & \\ & & & & -1 & 1 \end{pmatrix} \quad (4.19)$$

In this case, given a signal  $\mathbf{z}$ , applying  $\Omega_{1D-DIF}$  on it, results with a vector of coefficients that represents the differences in the signal. The thresholding selection method selects the indices of the  $\ell$  smallest elements in  $\Omega\mathbf{z}$  as the cosupport.

To demonstrate the sub-optimality of thresholding for  $\Omega_{1D-DIF}$  we use the signal  $\mathbf{z} \in \mathbb{R}^{201}$  in Fig 4.1(a) as an example. It contains 100 times one, 100 times minus one and 1.5 as the last element. Note that thresholding provides a non-optimal cosupport estimate even in the simple case of  $\ell = 199$ . It selects the cosupport to be the first 199 coefficients in  $\Omega_{1D-DIF}\mathbf{z}$  that appears in Fig 4.1(b). This selected cosupport implies that the first 200 entries in the projected vector should equal each other. Since orthogonal projection minimizes the  $\ell_2$  distance between the projected vector and the original vector, the value of these entries would be zero which is the average of the first 200 entries of  $\mathbf{z}$ . The projected vector is presented in Fig 4.1(c). Its error in the  $\ell_2$ -norm sense is  $\sqrt{200}$ . By selecting the cosupport to be the first 99 elements and last 100 elements we result with the projected vector in Fig. 4.1(d), which has a projection error 2.491. As this error is smaller than the one of thresholding, it is clear that thresholding is sub-optimal for  $\Omega_{1D-DIF}$ . In a similar way it is also sub-optimal for the 2D-finite difference operator  $\Omega_{2D-DIF}$  that returns the vertical and horizontal differences of a two dimensional signal.

Although thresholding is not an optimal selection scheme, it can still be used in practice with operators that are not known to have an efficient optimal or good near-optimal cosupport selection program. The use of thresholding with  $\Omega_{2D-DIF}$  and frames, which are both examples for such operators, is illustrated in Section 4.5 demonstrating that also when a good projection is not at hand, good reconstruction is still possible.

## 4.2.2 Optimal Analysis Projection Operators

As mentioned above, in general it would appear that determining the optimal projection is computationally difficult with the only general solution being to fully enumerate the projections onto all possible cosupports. Here we highlight two cases where it is relatively easy (polynomial complexity) to calculate the optimal cosparse projection.

**Case 1: 1D Finite Difference**

For the 1D finite difference operator the analysis operator is not redundant ( $p = d - 1$ ) but neither is it invertible. As we have seen, a simple thresholding does not provide us with the optimal cosparsity projection. Thus, in order to determine the best  $\ell$ -cosparsity approximation for a given vector  $\mathbf{z}$  we take another route and note that we are looking for the closest (in the  $\ell_2$ -norm sense to  $\mathbf{z}$ ) piecewise constant vector with  $p - \ell$  change-points. This problem has been solved previously in the signal processing literature using dynamic programming (DP), see for example [100]. Thus for this operator it is possible to calculate the best cosparsity representation in  $\mathcal{O}(d^2)$  operations. The existence of a DP solution follows from the ordered localized nature of the finite difference operator. To the best of our knowledge, there is no known extension to 2D finite difference.

**Case 2: Fused Lasso Operator**

A redundant operator related to the 1D finite difference operator is the so-called fused Lasso operator, usually used with analysis  $\ell_1$ -minimization [101]. This usually takes the form:

$$\mathbf{\Omega}_{\text{FUS}} = \begin{pmatrix} \mathbf{\Omega}_{\text{1D-DIF}} \\ \varepsilon \mathbf{I} \end{pmatrix}. \quad (4.20)$$

Like  $\mathbf{\Omega}_{\text{1D-DIF}}$  this operator works locally and therefore we can expect to derive a DP solution to the approximation problem. This is presented below.

**Remark 4.2.2** *Note that in terms of the cosparsity model the  $\varepsilon$  parameter plays no role. This is in contrast to the traditional convex optimization solutions where the value of  $\varepsilon$  is pivotal [25]. It is possible to mimic the  $\varepsilon$  dependence within the cosparsity framework by considering a generalized fused Lasso operator of the form:*

$$\mathbf{\Omega}_{\varepsilon\text{FUS}} = \begin{pmatrix} \mathbf{\Omega}_{\text{1D-DIF}} \\ \mathbf{\Omega}_{\text{1D-DIF}} \\ \vdots \\ \mathbf{\Omega}_{\text{1D-DIF}} \\ \mathbf{I} \end{pmatrix}. \quad (4.21)$$

where the number of repetitions of the  $\mathbf{\Omega}_{\text{1D-DIF}}$  operator (and possibly the  $\mathbf{I}$  operator) can be selected to mimic a weight on the number of nonzero coefficients of each type. For simplicity we only consider the case indicated by (4.20)

### A Recursive Solution to the Optimal Projection for $\Omega_{\text{FUS}}$

Rather than working directly with the operator  $\Omega_{\text{FUS}}$  we make use of the following observation. An  $\ell$ -cosparse vector  $\mathbf{v}$  (or  $k$ -sparse vector) for  $\Omega_{\text{FUS}}$  is a piecewise constant vector with  $k_1$  change points and  $k_2$  non-zero entries such that  $k_1 + k_2 = k = p - \ell$ , where  $p = 2d - 1$ . To understand better the relation between  $k_1$  and  $k_2$ , notice that  $k_1 = 0$  implies equality of all entries, so  $k_2 = 0$  or  $d$ , hence  $\ell = p$  or  $d - 1$ . Conversely, considering  $d \leq \ell < p$  or  $0 \leq \ell < d - 1$  implies  $k_1 \neq 0$ . It also implies that there is at least one nonzero value, hence  $k_2 \neq 0$ .

Thus, an  $\ell$ -cosparse vector  $\mathbf{v}$  for  $\Omega_{\text{FUS}}$  can be parameterized in terms of a set of change points,  $\{n_i\}_{i=0:k_1+1}$ , and a set of constants,  $\{\mu_i\}_{i=1:k_1+1}$ , such that:

$$\mathbf{v}_j = \mu_i, n_{i-1} < j \leq n_i \quad (4.22)$$

with the convention that  $n_0 = 0$  and  $n_{k_1+1} = d$ , unless stated otherwise. We will also make use of the indicator vector,  $\mathbf{s}$ , defined as:

$$\mathbf{s}_i = \begin{cases} 0 & \text{if } \mu_i = 0, \\ 1 & \text{otherwise} \end{cases} \quad \text{for } 1 \leq i \leq k_1 + 1. \quad (4.23)$$

Using this alternative parametrization we can write the minimum distance between a vector  $\mathbf{z}$  and the set of  $k$ -sparse fused Lasso coefficients as:

$$F_k(\mathbf{z}) = \min_{1 \leq k_1 \leq k} \min_{\substack{\{n_i\}_{i=1:k_1} \\ \{\mu_i\}_{i=1:k_1+1} \\ n_{k_1} < d}} \sum_{i=1}^{k_1+1} \sum_{j=n_{i-1}+1}^{n_i} (\mathbf{z}_j - \mu_i)^2, \quad (4.24)$$

subject to  $\sum_{i=1}^{k_1+1} \mathbf{s}_i (n_i - n_{i-1}) = k - k_1$

Although this looks a formidable optimization task we now show that it can be computed recursively through a standard DP strategy, modifying the arguments in [100].

Let us define the optimal cost,  $I_k(L, \omega, k_1)$ , for the vector  $[\mathbf{z}_1, \dots, \mathbf{z}_L]^T$  with  $k_1$  change points and  $\mathbf{s}_{k_1+1} = \omega$ , as:

$$I_k(L, \omega, k_1) = \min_{\substack{\{n_i\}_{i=1:k_1} \\ \{\mathbf{s}_i\}_{i=1:k_1+1} \\ n_{k_1} < L, n_{k_1+1} = L \\ \mathbf{s}_{k_1+1} = \omega}} \sum_{i=1}^{k_1+1} \sum_{j=n_{i-1}+1}^{n_i} (\mathbf{z}_j - \mu_i)^2, \quad (4.25)$$

subject to  $\sum_{i=1}^{k_1+1} \mathbf{s}_i (n_i - n_{i-1}) = k - k_1$

and  $\mu_i = \frac{\mathbf{s}_i}{n_i - n_{i-1}} \sum_{l=n_{i-1}+1}^{n_i} \mathbf{z}_l$

where we have set  $\mu_i$  to the optimal sample means. Notice that calculating  $I_k(L, \omega, k_1)$  is easy for  $k_1 \leq k \leq 1$ . Thus, we calculate it recursively considering two separate scenarios:

**Case 1:**  $\omega = 0$  where the last block of coefficients are zero. This gives:

$$I_k(L, 0, k_1) = \min_{n_{k_1} < L} \left( \sum_{j=n_{k_1}+1}^L (\mathbf{z}_j)^2 + \min_{\substack{\{n_i\}_{i=1:k_1-1} \\ \{\mathbf{s}_i\}_{i=1:k_1-1} \\ n_{k_1-1} < n_{k_1} \\ \mathbf{s}_{k_1} = 1}} \sum_{i=1}^{k_1} \sum_{j=n_{i-1}+1}^{n_i} (\mathbf{z}_j - \mu_i)^2 \right), \quad (4.26)$$

subject to  $\sum_{i=1}^{k_1} \mathbf{s}_i (n_i - n_{i-1}) = (k-1) - (k_1-1)$

and  $\mu_i = \frac{\mathbf{s}_i}{n_i - n_{i-1}} \sum_{l=n_{i-1}+1}^{n_i} \mathbf{z}_l$ ,

(noting that if  $\mathbf{s}_{k_1+1} = 0$  then  $\mathbf{s}_{k_1} = 1$  since otherwise  $n_{k_1}$  would not have been a change point). This simplifies to the recursive formula:

$$I_k(L, 0, k_1) = \min_{n_{k_1} < L} \left( \sum_{j=n_{k_1}+1}^L (\mathbf{z}_j)^2 + I_{k-1}(n_{k_1}, 1, k_1 - 1) \right) \quad (4.27)$$

**Case 2:**  $\omega = 1$  when the final block of coefficients are non-zero we have:

$$I_k(L, 1, k_1) = \min_{\substack{n_{k_1} < L \\ n_{k_1}+1=L \\ \mathbf{s}_{k_1}}} \left( \sum_{j=n_{k_1}+1}^L (\mathbf{z}_j - \mu_{k_1+1})^2 + \min_{\substack{\{n_i\}_{i=1:k_1-1} \\ \{\mathbf{s}_i\}_{i=1:k_1-1} \\ n_{k_1-1} < n_{k_1}}} \sum_{i=1}^{k_1} \sum_{j=n_{i-1}+1}^{n_i} (\mathbf{z}_j - \mu_i)^2 \right), \quad (4.28)$$

subject to  $\sum_{i=1}^{k_1} \mathbf{s}_i (n_i - n_{i-1}) = (k-L+n_{k_1}-1) - (k_1-1)$

and  $\mu_i = \frac{\mathbf{s}_i}{n_i - n_{i-1}} \sum_{l=n_{i-1}+1}^{n_i} \mathbf{z}_l$ .

This simplifies to the recursive relationship:

$$I_k(L, 1, k_1) = \min_{\substack{n_{k_1} < L \\ \mathbf{s}_{k_1}}} \left( \sum_{j=n_{k_1}+1}^L (\mathbf{z}_j - \mu_{k_1+1})^2 + I_{k-L+n_{k_1}-1}(n_{k_1}, \mathbf{s}_{k_1}, k_1 - 1) \right) \quad (4.29)$$

subject to  $\mu_{k_1+1} = \sum_{l=n_{k_1}+1}^L \mathbf{z}_l / (L - n_{k_1})$

Equations (4.27) and (4.29) are sufficient to enable the calculation of the optimal projection in polynomial time, starting with  $k_1 \leq k \leq 1$  and recursively evaluating the costs for  $k \geq k_1 \geq 1$ . Finally, we have  $F_k(\mathbf{z}) = \min_{k_1 \leq k, \omega \in \{0,1\}} I_k(d, \omega, k_1)$ .

Synthesis operation name	Synthesis operation	Analysis operation name	Analysis operation
Support selection	Largest $k$ elements: $T = \text{supp}(\cdot, k)$	Cosupport selection	Using a near optimal projection: $\Lambda = \hat{\mathcal{S}}_\ell(\cdot)$
Orthogonal Projection of $\mathbf{z}$ to a $k$ -sparse subspace with support $T$	$\mathbf{z}_T$	Orthogonal projection of $\mathbf{z}$ to an $\ell$ -cosparse subspace with cosupport $\Lambda$	$\mathbf{Q}_\Lambda \mathbf{z}$
Objective aware projection to a $k$ -sparse subspace with support $T$	$\mathbf{M}_T^\dagger \mathbf{y} = \arg\min_{\mathbf{v}} \ \mathbf{y} - \mathbf{M}\mathbf{v}\ _2^2$ s.t. $\mathbf{v}_{T^c} = 0$	Objective aware projection to an $\ell$ -cosparse subspace with cosupport $\Lambda$	$\arg\min_{\mathbf{v}} \ \mathbf{y} - \mathbf{M}\mathbf{v}\ _2^2$ s.t. $\mathbf{Q}_\Lambda \mathbf{v} = 0$
Support of $\mathbf{v}_1 + \mathbf{v}_2$ where $\text{supp}(\mathbf{v}_1) = T_1$ and $\text{supp}(\mathbf{v}_2) = T_2$	$\text{supp}(\mathbf{v}_1 + \mathbf{v}_2) \subseteq T_1 \cup T_2$	Cosupport of $\mathbf{v}_1 + \mathbf{v}_2$ where $\text{cosupp}(\mathbf{v}_1) = \Lambda_1$ and $\text{cosupp}(\mathbf{v}_2) = \Lambda_2$	$\text{cosupp}(\mathbf{v}_1 + \mathbf{v}_2) \supseteq \Lambda_1 \cap \Lambda_2$
Maximal size of $T_1 \cup T_2$ where $ T_1  \leq k_1$ and $ T_2  \leq k_2$	$ T_1 \cup T_2  \leq k_1 + k_2$	Minimal size of $\Lambda_1 \cap \Lambda_2$ where $ \Lambda_1  \geq \ell_1$ and $ \Lambda_2  \geq \ell_2$	$ \Lambda_1 \cap \Lambda_2  \geq \ell_1 + \ell_2 - p$

Table 4.1: Parallel synthesis and analysis operations

### 4.3 New Analysis Algorithms

#### 4.3.1 Analysis Greedy-Like Methods

Given the synthesis greedy-like pursuits, we would like to define their analysis counterparts. For this task we need to ‘translate’ each synthesis operation into an analysis one. This gives us a general recipe for converting algorithms between the two schemes. The parallel lines between the schemes are presented in Table 4.1. Those become more intuitive and clear when we keep in mind that while the synthesis approach focuses on the non-zeros, the analysis concentrates on the zeros.

For clarity we dwell a bit more on the equivalences. For the cosupport selection, as mentioned in Section 4.2, computing the optimal cosupport is a combinatorial problem and thus the approximation  $\hat{\mathcal{S}}_\ell$  is used. Having a selected cosupport  $\Lambda$ , the projection to its corresponding cosparsity subspace becomes trivial, given by  $\mathbf{Q}_\Lambda$ .

Given two vectors  $\mathbf{v}_1 \in \mathcal{A}_{\ell_1}$  and  $\mathbf{v}_2 \in \mathcal{A}_{\ell_2}$  such that  $\Lambda_1 = \text{cosupp}(\mathbf{\Omega}\mathbf{v}_1)$  and  $\Lambda_2 = \text{cosupp}(\mathbf{\Omega}\mathbf{v}_2)$ , we know that  $|\Lambda_1| \geq \ell_1$  and  $|\Lambda_2| \geq \ell_2$ . Denoting  $T_1 = \text{supp}(\mathbf{\Omega}\mathbf{v}_1)$  and  $T_2 = \text{supp}(\mathbf{\Omega}\mathbf{v}_2)$  it is clear that  $\text{supp}(\mathbf{\Omega}(\mathbf{v}_1 + \mathbf{v}_2)) \subseteq T_1 \cup T_2$ . Noticing that  $\text{supp}(\cdot) = \text{cosupp}(\cdot)^C$  it is clear that  $|T_1| \leq p - \ell_1$ ,  $|T_2| \leq p - \ell_2$  and  $\text{cosupp}(\mathbf{\Omega}(\mathbf{v}_1 + \mathbf{v}_2)) \supseteq (T_1 \cup T_2)^C = T_1^C \cap T_2^C = \Lambda_1 \cap \Lambda_2$ . From the last equality we can also deduce that  $|\Lambda_1 \cap \Lambda_2| = p - |T_1 \cup T_2| \geq p - (p - \ell_1) - (p - \ell_2) = \ell_1 + \ell_2 - p$ .

With the above observations we can develop the analysis versions of the greedy-like algorithms. As in the synthesis case, we do not specify a stopping criterion. Any stopping criterion used for the synthesis versions can be used also for the analysis ones.

---

**Algorithm 4** Analysis Iterative Hard Thresholding (AIHT) and Analysis Hard Thresholding Pursuit (AHTP)

---

**Input:**  $\ell, \mathbf{M}, \mathbf{\Omega}, \mathbf{y}$  where  $\mathbf{y} = \mathbf{M}\mathbf{x} + \mathbf{e}$ ,  $\ell$  is the cosparsity of  $\mathbf{x}$  under  $\mathbf{\Omega}$  and  $\mathbf{e}$  is the additive noise.

**Output:**  $\hat{\mathbf{x}}_{\text{AIHT}}$  or  $\hat{\mathbf{x}}_{\text{AHTP}}$ :  $\ell$ -cosparsity approximation of  $\mathbf{x}$ .

Initialize estimate  $\hat{\mathbf{x}}^0 = \mathbf{0}$  and set  $t = 0$ .

**while** halting criterion is not satisfied **do**

$t = t + 1$ .

Perform a gradient step:  $\mathbf{x}_g = \hat{\mathbf{x}}^{t-1} + \mu^t \mathbf{M}^*(\mathbf{y} - \mathbf{M}\hat{\mathbf{x}}^{t-1})$

Find a new cosupport:  $\hat{\Lambda}^t = \hat{\mathcal{S}}_\ell(\mathbf{x}_g)$

Calculate a new estimate:  $\hat{\mathbf{x}}_{\text{AIHT}}^t = \mathbf{Q}_{\hat{\Lambda}^t} \mathbf{x}_g$  for AIHT, and  $\hat{\mathbf{x}}_{\text{AHTP}}^t = \text{argmin}_{\tilde{\mathbf{x}}} \|\mathbf{y} - \mathbf{M}\tilde{\mathbf{x}}\|_2^2$  s.t.

$\mathbf{\Omega}_{\hat{\Lambda}^t} \tilde{\mathbf{x}} = 0$  for AHTP.

**end while**

Form the final solution  $\hat{\mathbf{x}}_{\text{AIHT}} = \hat{\mathbf{x}}_{\text{AIHT}}^t$  for AIHT and  $\hat{\mathbf{x}}_{\text{AHTP}} = \hat{\mathbf{x}}_{\text{AHTP}}^t$  for AHTP.

---

*AIHT and AHTP:* Analysis IHT (AIHT) and analysis HTP (AHTP) are presented in Algorithm 4. As in the synthesis case, the choice of the gradient stepsize  $\mu^t$  is crucial: If  $\mu^t$ 's are chosen too small, the algorithm gets stuck at a wrong solution and if too large, the algorithm diverges. We consider two options for  $\mu^t$ .

In the first we choose  $\mu^t = \mu$  for some constant  $\mu$  for all iterations. A theoretical discussion

on how to choose  $\mu$  properly is given in Section 4.4.1.

The second option is to select a different  $\mu$  in each iteration. One way for doing it is to choose an ‘optimal’ stepsize  $\mu^t$  by solving the following problem

$$\mu^t := \underset{\mu}{\operatorname{argmin}} \|\mathbf{y} - \mathbf{M}\hat{\mathbf{x}}^t\|_2^2. \quad (4.30)$$

Since  $\hat{\Lambda}^t = \hat{\mathcal{S}}_\ell(\hat{\mathbf{x}}^{t-1} + \mu^t \mathbf{M}^*(\mathbf{y} - \mathbf{M}\hat{\mathbf{x}}^{t-1}))$  and  $\hat{\mathbf{x}}^t = \mathbf{Q}_{\hat{\Lambda}^t}(\mathbf{x}_g)$ , the above requires a line search over different values of  $\mu$  and along the search  $\hat{\Lambda}^t$  might change several times. A simpler way is an adaptive step size selection as proposed in [64] for IHT. In a heuristical way we limit the search to the cosupport  $\tilde{\Lambda} = \hat{\mathcal{S}}_\ell(\mathbf{M}^*(\mathbf{y} - \mathbf{M}\hat{\mathbf{x}}^{t-1})) \cap \hat{\Lambda}^{t-1}$ . This is the intersection of the cosupport of  $\hat{\mathbf{x}}^{t-1}$  with the  $\ell$ -cosparsive cosupport of the estimated closest  $\ell$ -cosparsive subspace to  $\mathbf{M}^*(\mathbf{y} - \mathbf{M}\hat{\mathbf{x}}^{t-1})$ . Since  $\hat{\mathbf{x}}^{t-1} = \mathbf{Q}_{\tilde{\Lambda}}\hat{\mathbf{x}}^{t-1}$ , finding  $\mu$  turns to be

$$\mu^t := \underset{\mu}{\operatorname{argmin}} \left\| \mathbf{y} - \mathbf{M}(\hat{\mathbf{x}}^{t-1} + \mu \mathbf{Q}_{\tilde{\Lambda}} \mathbf{M}^*(\mathbf{y} - \mathbf{M}\hat{\mathbf{x}}^{t-1})) \right\|_2^2. \quad (4.31)$$

This procedure of selecting  $\mu^t$  does not require a line search and it has a simple closed form solution.

To summarize, there are three main options for the step size selection:

- Constant step-size selection – uses a constant step size  $\mu^t = \mu$  in all iterations.
- Optimal changing step-size selection – uses different values for  $\mu^t$  in each iterations by minimizing  $\|\mathbf{y} - \mathbf{M}\hat{\mathbf{x}}^t\|_2$ .
- Adaptive changing step-size selection – uses (4.31).

*ACoSaMP and ASP:* analysis CoSaMP (ACoSaMP) and analysis SP (ASP) are presented in Algorithm 5. The stages are parallel to those of the synthesis CoSaMP and SP. We dwell a bit more on the meaning of the parameter  $a$  in the algorithms. This parameter determines the size of the new cosupport  $\Lambda_\Delta$  in each iteration.  $a = 1$  means that the size is  $\ell$  and according to Table 4.1 it is equivalent to  $a = 1$  in the synthesis as done in SP in which we select new  $k$  indices for the support in each iteration. In synthesis CoSaMP we use  $a = 2$  and select  $2k$  new elements.  $2k$  is the maximal support size of two added  $k$ -sparse vectors. The corresponding minimal size in the analysis case is  $2\ell - p$  according to Table 4.1. For this setting we need to choose  $a = \frac{2\ell - p}{\ell}$ .

**Algorithm 5** Analysis Subspace Pursuit (ASP) and Analysis CoSaMP (ACoSaMP)

**Input:**  $\ell, \mathbf{M}, \Omega, \mathbf{y}, a$  where  $\mathbf{y} = \mathbf{M}\mathbf{x} + \mathbf{e}$ ,  $\ell$  is the cosparsity of  $\mathbf{x}$  under  $\Omega$  and  $\mathbf{e}$  is the additive noise.

**Output:**  $\hat{\mathbf{x}}_{\text{ACoSaMP}}$  or  $\hat{\mathbf{x}}_{\text{ASP}}$ :  $\ell$ -cosparse approximation of  $\mathbf{x}$ .

Initialize the cosupport  $\Lambda^0 = \{i, 1 \leq i \leq p\}$ , the residual  $\mathbf{y}_{\text{resid}}^0 = \mathbf{y}$  and set  $t = 0$ .

**while** halting criterion is not satisfied **do**

$t = t + 1$ .

Find new cosupport elements:  $\Lambda_\Delta = \hat{\mathcal{S}}_{a\ell}(\mathbf{M}^* \mathbf{y}_{\text{resid}}^{t-1})$ .

Update the cosupport:  $\tilde{\Lambda}^t = \hat{\Lambda}^{t-1} \cap \Lambda_\Delta$ .

Compute a temporary estimate:  $\mathbf{w} = \operatorname{argmin}_{\tilde{\mathbf{x}}} \|\mathbf{y} - \mathbf{M}\tilde{\mathbf{x}}\|_2^2$  s.t.  $\Omega_{\tilde{\Lambda}^t} \tilde{\mathbf{x}} = 0$ .

Enlarge the cosupport:  $\hat{\Lambda}^t = \hat{\mathcal{S}}_\ell(\mathbf{w})$ .

Calculate a new estimate:  $\hat{\mathbf{x}}_{\text{ACoSaMP}}^t = \mathbf{Q}_{\hat{\Lambda}^t} \mathbf{w}$  for ACoSaMP, and

$\hat{\mathbf{x}}_{\text{ASP}}^t = \operatorname{argmin}_{\tilde{\mathbf{x}}} \|\mathbf{y} - \mathbf{M}\tilde{\mathbf{x}}\|_2^2$  s.t.  $\Omega_{\hat{\Lambda}^t} \tilde{\mathbf{x}} = 0$  for ASP.

Update the residual:  $\mathbf{y}_{\text{resid}}^t = \mathbf{y} - \mathbf{M}\hat{\mathbf{x}}_{\text{ACoSaMP}}^t$  for ACoSaMP, and  $\mathbf{y}_{\text{resid}}^t = \mathbf{y} - \mathbf{M}\hat{\mathbf{x}}_{\text{ASP}}^t$  for ASP.

**end while**

Form the final solution  $\hat{\mathbf{x}}_{\text{ACoSaMP}} = \hat{\mathbf{x}}_{\text{ACoSaMP}}^t$  for ACoSaMP and  $\hat{\mathbf{x}}_{\text{ASP}} = \hat{\mathbf{x}}_{\text{ASP}}^t$  for ASP.

### 4.3.2 The Unitary Case

For  $\Omega = \mathbf{I}$  the synthesis and the analysis greedy-like algorithms become equivalent. This is easy to see since in this case we have  $p = d, k = d - \ell, \Lambda = T^C, \mathbf{Q}_\Lambda \mathbf{x} = \mathbf{x}_T$  and  $T_1 \cup T_2 = \Lambda_1 \cap \Lambda_2$  for  $\Lambda_1 = T_1^C$  and  $\Lambda_2 = T_2^C$ . In addition,  $\hat{\mathcal{S}}_\ell = \mathcal{S}_\ell^*$  finds the closest  $\ell$ -cosparse subspace by simply taking the smallest  $\ell$  elements. Using similar arguments, also in the case where  $\Omega$  is a unitary matrix the analysis methods coincide with the synthesis ones. In order to get exactly the same algorithms  $\mathbf{A}$  is replaced with  $\mathbf{M}\Omega^*$  in the synthesis techniques and the output is multiplied by  $\Omega^*$ .

Based on this observation, we can deduce that in this case the guarantees of the synthesis greedy-like methods apply also for the analysis ones in a trivial way. Thus, it is tempting to assume that the last should have similar guarantees based on the O-RIP. In the next section we develop such claims.

### 4.3.3 Relaxed Versions for High Dimensional Problems

Before moving to the next section we mention a variation of the analysis greedy-like techniques. In AHTP, ACoSaMP and ASP we need to solve the constrained minimization problem  $\min_{\tilde{\mathbf{x}}} \|\mathbf{y} - \mathbf{M}\tilde{\mathbf{x}}\|_2^2$  s.t.  $\|\mathbf{\Omega}_\Lambda \tilde{\mathbf{x}}\|_2^2 = 0$ . For high dimensional signals this problem is hard to solve and we suggest to replace it with minimizing  $\|\mathbf{y} - \mathbf{M}\tilde{\mathbf{x}}\|_2^2 + \lambda \|\mathbf{\Omega}_\Lambda \tilde{\mathbf{x}}\|_2^2$ , where  $\lambda$  is a relaxation constant. This results in a relaxed version of the algorithms. We refer hereafter to these versions as relaxed AHTP (RAHTP) relaxed ASP (RASP) and relaxed ACoSaMP (RACoSaMP).

## 4.4 Performance Guarantees

In this section we provide theoretical guarantees for the reconstruction performance of the analysis greedy-like methods. For AIHT and AHTP we study both the constant step-size and the optimal step-size selections. For ACoSaMP and ASP the analysis is made for  $a = \frac{2\ell-p}{\ell}$ , but we believe that it can be extended also to other values of  $a$ , such as  $a = 1$ . The performance guarantees we provide are summarized in the following two theorems. The first theorem, for AIHT and AHTP, is a simplified version of Theorem 4.4.5 and the second theorem, for ASP and ACoSaMP, is a combination of Corollaries 4.4.9 and 4.4.14, all of which appear hereafter along with their proofs. Before presenting the theorems we recall the problem we aim at solving:

**Definition 4.4.1 (Problem  $\mathcal{P}$ -Analysis)** *Consider a measurement vector  $\mathbf{y} \in \mathbb{R}^m$  such that  $\mathbf{y} = \mathbf{M}\mathbf{x} + \mathbf{e}$  where  $\mathbf{x} \in \mathbb{R}^d$  is  $\ell$ -cosparse,  $\mathbf{M} \in \mathbb{R}^{m \times d}$  is a degradation operator and  $\mathbf{e} \in \mathbb{R}^m$  is a bounded additive noise. The largest singular value of  $\mathbf{M}$  is  $\sigma_{\mathbf{M}}$  and its O-RIP constant is  $\delta_\ell$ . The analysis operator  $\mathbf{\Omega} \in \mathbb{R}^{p \times d}$  is given and fixed. A procedure  $\hat{S}_\ell$  for finding a cosupport that implies a near optimal projection with a constant  $C_\ell$  is assumed to be at hand. Our task is to recover  $\mathbf{x}$  from  $\mathbf{y}$ . The recovery result is denoted by  $\hat{\mathbf{x}}$ .*

**Theorem 4.4.2 (Stable Recovery of AIHT and AHTP)** *Consider the problem  $\mathcal{P}$ -Analysis and apply either AIHT or AHTP with a certain constant step-size or an optimal changing step-size, obtaining  $\hat{\mathbf{x}}^t$  after  $t$  iterations. If*

$$\frac{(C_\ell - 1)\sigma_{\mathbf{M}}^2}{C_\ell} < 1 \quad (4.32)$$

and

$$\delta_{2\ell-p} < \delta_1(C_\ell, \sigma_{\mathbf{M}}^2),$$

where  $\delta_1(C_\ell, \sigma_{\mathbf{M}}^2)$  is a constant guaranteed to be greater than zero whenever (4.32) is satisfied and  $C_\ell$  is the near-optimal projection constant for cosparsity  $\ell$  (Definition 4.2.1), then after a finite number of iterations  $t^*$

$$\left\| \mathbf{x} - \hat{\mathbf{x}}^{t^*} \right\|_2 \leq c_1 \|\mathbf{e}\|_2, \quad (4.33)$$

implying that these algorithms lead to a stable recovery. The constant  $c_1$  is a function of  $\delta_{2\ell-p}$ ,  $C_\ell$  and  $\sigma_{\mathbf{M}}^2$ , and the constant step-size used is dependent on  $\delta_1(C_\ell, \sigma_{\mathbf{M}}^2)$ .

**Theorem 4.4.3 (Stable Recovery of ASP and ACoSaMP)** Consider the problem  $\mathcal{P}$ -Analysis and apply either ACoSaMP or ASP with  $a = \frac{2\ell-p}{\ell}$ , obtaining  $\hat{\mathbf{x}}^t$  after  $t$  iterations. If

$$\frac{(C_{\hat{\mathcal{S}}}^2 - 1)\sigma_{\mathbf{M}}^2}{C_{\hat{\mathcal{S}}}^2} < 1, \quad (4.34)$$

and

$$\delta_{4\ell-3p} < \delta_2(C_{\hat{\mathcal{S}}}, \sigma_{\mathbf{M}}^2),$$

where  $C_{\hat{\mathcal{S}}} = \max(C_\ell, C_{2\ell-p})$  and  $\delta_2(C_{\hat{\mathcal{S}}}, \sigma_{\mathbf{M}}^2)$  is a constant guaranteed to be greater than zero whenever (4.34) is satisfied, then after a finite number of iterations  $t^*$

$$\left\| \mathbf{x} - \hat{\mathbf{x}}^{t^*} \right\|_2 \leq c_2 \|\mathbf{e}\|_2, \quad (4.35)$$

implying that these algorithms lead to a stable recovery. The constant  $c_2$  is a function of  $\delta_{4\ell-3p}$ ,  $C_\ell$ ,  $C_{2\ell-p}$  and  $\sigma_{\mathbf{M}}^2$ .

Before we proceed to the proofs, let us comment on the constants in the above theorems. Their values can be calculated using Theorem 4.4.5, and Corollaries 4.4.9 and 4.4.14. In the case where  $\mathbf{\Omega}$  is a unitary matrix, (4.32) and (4.34) are trivially satisfied since  $C_\ell = C_{2\ell-p} = 1$ . In this case the O-RIP conditions become  $\delta_{2\ell-p} < \delta_1(1, \sigma_{\mathbf{M}}^2) = 1/3$  for AIHT and AHTP, and  $\delta_{4\ell-3p} < \delta_2(1, \sigma_{\mathbf{M}}^2) = 0.0156$  for ACoSaMP and ASP. In terms of synthesis RIP for  $\mathbf{M}\mathbf{\Omega}^*$ , the condition  $\delta_{2\ell-p} < 1/3$  parallels  $\delta_{2k}(\mathbf{M}\mathbf{\Omega}^*) < 1/3$  and similarly  $\delta_{4\ell-3p} < 0.0156$  parallels  $\delta_{4k}(\mathbf{M}\mathbf{\Omega}^*) < 0.0156$ . Note that the condition we pose for AIHT and AHTP in this case is the same as the one presented for synthesis IHT with a constant step size [102]. Better reference constants were achieved in the synthesis case for all four algorithms and thus we believe that there is still room for improvement of the reference constants in the analysis context.

In the non-unitary case, the value of  $\sigma_{\mathbf{M}}$  plays a vital role, though we believe that this is just an artifact of our proof technique. For a random Gaussian matrix whose entries are i.i.d with

a zero-mean and a variance  $\frac{1}{m}$ ,  $\sigma_{\mathbf{M}}$  behaves like  $\frac{d}{m} \left(1 + \sqrt{\frac{d}{m}}\right)$ . This is true also for other types of distributions for which the fourth moment is known to be bounded [103]. For example, for  $d/m = 1.5$  we have found empirically that  $\sigma_{\mathbf{M}}^2 \simeq 5$ . In this case we need  $C_\ell \leq \frac{5}{4}$  for (4.32) to hold and  $C_\mathcal{S} \leq 1.118$  for (4.34) to hold, and both are quite demanding on the quality of the near-optimal projection. For  $C_\ell = C_\mathcal{S} = 1.05$  we have the conditions  $\delta_{2\ell-p} \leq 0.289$  for AIHT and AHTP, and  $\delta_{4\ell-3p} \leq 0.0049$  for ACoSaMP and ASP; and for  $C_\ell = C_\mathcal{S} = 1.1$  we have  $\delta_{2\ell-p} \leq 0.24$  for AIHT and AHTP, and  $\delta_{4\ell-3p} \leq 0.00032$  for ACoSaMP and ASP.

As in the synthesis case, the O-RIP requirements for the theoretical bounds of AIHT and AHTP are better than those for ACoSaMP and ASP. In addition, in the migration from the synthesis to the analysis we lost more precision in the bounds for ACoSaMP and ASP than in those of AIHT and AHTP. In particular, even in the case where  $\mathbf{\Omega}$  is the identity we do not coincide with any of the synthesis parallel RIP reference constants. We should also remember that the synthesis bound for SP is in terms of  $\delta_{3k}$  and not  $\delta_{4k}$  [40]. Thus, we expect that it will be possible to give a condition for ASP in terms of  $\delta_{3\ell-2p}$  with better reference constants. However, our main interest in this chapter is to show the existence of such bounds, and in Section 4.4.5 we dwell more on their meaning.

We should note that here and elsewhere we can replace the conditions on  $\delta_{2\ell-p}$  and  $\delta_{4\ell-3p}$  in the theorems to conditions on  $\delta_{2r-p}^{\text{corank}}$  and  $\delta_{4r-3p}^{\text{corank}}$  and the proofs will be almost the same<sup>3</sup>. In this case we will be analyzing a version of the algorithms which is driven by the corank instead of the cosparsity. This would mean we need the near-optimal projection to be in terms of the corank. In the case where  $\mathbf{\Omega}$  is in a general position, there is no difference between the cosparsity  $\ell$  and the corank  $r$ . However, when we have linear dependencies in  $\mathbf{\Omega}$  the two measures differ and an  $\ell$ -cosparse vector is not necessarily a vector with a corank  $r$ .

As we will see hereafter, our recovery conditions require  $\delta_{2\ell-p}$  and  $\delta_{4\ell-3p}$  to be as small as possible and for this we need  $2\ell - p$  and  $4\ell - 3p$  to be as large as possible. Thus, we need  $\ell$  to be as close as possible to  $p$  and for highly redundant  $\mathbf{\Omega}$  this cannot be achieved without having linear dependencies in  $\mathbf{\Omega}$ . Apart from the theoretical advantage of linear dependencies in  $\mathbf{\Omega}$ , we also show empirically that an analysis dictionary with linear dependencies has better recovery rate than analysis dictionary in a general position of the same dimension. Thus, we deduce that linear dependencies in  $\mathbf{\Omega}$  lead to better bounds and restoration performance.

---

<sup>3</sup>At a first glance one would think that the conditions should be in terms of  $\delta_{2r-d}^{\text{corank}}$  and  $\delta_{4r-3d}^{\text{corank}}$ . However, given two cosparse vectors with coranks  $r_1$  and  $r_2$  the best estimation we can have for the corank of their sum is  $r_1 + r_2 - p$ .

Though linear dependencies allow  $\ell$  to be larger than  $d$  and be in the order of  $p$ , the value of the corank is always bounded by  $d$  and cannot be expected to be large enough for highly redundant analysis dictionaries. In addition, we will see hereafter that the number of measurements  $m$  required by the O-RIP is strongly dependent on  $\ell$  and less effected by the value of  $r$ . From the computational point of view we note also that using corank requires its computation in each iteration which increases the overall complexity of the algorithms. Thus, it is more reasonable to have conditions on  $\delta_{2\ell-p}$  and  $\delta_{4\ell-3p}$  than on  $\delta_{2r-p}^{\text{corank}}$  and  $\delta_{4r-3p}^{\text{corank}}$ , and our study will be focused on the cosparsity based algorithms.

#### 4.4.1 AIHT and AHTP Guarantees

A uniform guarantee for AIHT in the case that an optimal projection is given, is presented in [95]. The work in [95] dealt with a general union of subspaces,  $\mathcal{A}$ , and assumed that  $\mathbf{M}$  is bi-Lipschitz on the considered union of subspaces. In our case  $\mathcal{A} = \mathcal{A}_\ell$  and the bi-Lipschitz constants of  $\mathbf{M}$  are the largest  $B_L$  and smallest  $B_U$  where  $0 < B_L \leq B_U$  such that for all  $\ell$ -cosparsity vectors  $\mathbf{v}_1, \mathbf{v}_2$ :

$$B_L \|\mathbf{v}_1 + \mathbf{v}_2\|_2^2 \leq \|\mathbf{M}(\mathbf{v}_1 + \mathbf{v}_2)\|_2^2 \leq B_U \|\mathbf{v}_1 + \mathbf{v}_2\|_2^2. \quad (4.36)$$

Under this assumption, one can apply Theorem 2 from [95] to the idealized AIHT that has access to an optimal projection and uses a constant step size  $\mu^t = \mu$ . Relying on Table 4.1 we present this theorem and replace  $B_L$  and  $B_U$  with  $1 - \delta_{2\ell-p}$  and  $1 + \delta_{2\ell-p}$  respectively.

**Theorem 4.4.4 (Theorem 2 in [95])** *Consider the problem  $\mathcal{P}$ -Analysis with  $C_\ell = 1$  and apply AIHT with a constant step size  $\mu$ . If  $1 + \delta_{2\ell-p} \leq \frac{1}{\mu} < 1.5(1 - \delta_{2\ell-p})$  then after a finite number of iterations  $t^*$*

$$\|\mathbf{x} - \hat{\mathbf{x}}^{t^*}\|_2 \leq c_3 \|\mathbf{e}\|_2, \quad (4.37)$$

*implying that AIHT leads to a stable recovery. The constant  $c_3$  is a function of  $\delta_{2\ell-p}$  and  $\mu$ .*

In this chapter we extend the above in several ways: First, we refer to the case where optimal projection is not known, and show that the same flavor guarantees apply for a near-optimal projection<sup>4</sup>. The price we seemingly have to pay is that  $\sigma_{\mathbf{M}}$  enters the game. Second, we derive similar results for the AHTP method. Finally, we also consider the optimal step size and show that the same performance guarantees hold true in that case.

<sup>4</sup>Remark that we even improve the condition of the idealized case in [95] to be  $\delta_{2\ell-p} \leq \frac{1}{3}$  instead of  $\delta_{2\ell-p} \leq \frac{1}{5}$ .

**Theorem 4.4.5** Consider the problem  $\mathcal{P}$ -Analysis and apply either AIHT or AHTP with a constant step size  $\mu$  or an optimal changing step size. For a positive constant  $\eta > 0$ , let

$$b_1 := \frac{\eta}{1 + \eta} \quad \text{and} \quad b_2 := \frac{(C_\ell - 1)\sigma_{\mathbf{M}}^2 b_1^2}{C_\ell(1 - \delta_{2\ell-p})}.$$

Suppose  $\frac{b_2}{b_1^2} = \frac{(C_\ell - 1)\sigma_{\mathbf{M}}^2}{C_\ell(1 - \delta_{2\ell-p})} < 1$ ,  $1 + \delta_{2\ell-p} \leq \frac{1}{\mu} < \left(1 + \sqrt{1 - \frac{b_2}{b_1^2}}\right) b_1(1 - \delta_{2\ell-p})$  and  $\frac{1}{\mu} \leq \sigma_{\mathbf{M}}^2$ . Then for

$$t \geq t^* \triangleq \frac{\log\left(\frac{\eta\|\mathbf{e}\|_2^2}{\|\mathbf{y}\|_2^2}\right)}{\log\left(\left(1 + \frac{1}{\eta}\right)^2\left(\frac{1}{\mu(1 - \delta_{2\ell-p})} - 1\right)C_\ell + (C_\ell - 1)(\mu\sigma_{\mathbf{M}}^2 - 1) + \frac{C_\ell}{\eta^2}\right)}, \quad (4.38)$$

$$\|\mathbf{x} - \hat{\mathbf{x}}^t\|_2^2 \leq \frac{(1 + \eta)^2}{1 - \delta_{2\ell-p}} \|\mathbf{e}\|_2^2, \quad (4.39)$$

implying that AIHT and AHTP lead to a stable recovery. Note that for an optimal changing step-size we set  $\mu = \frac{1}{1 + \delta_{2\ell-p}}$  in  $t^*$  and the theorem conditions turn to be  $\frac{b_2}{b_1^2} < 1$  and  $1 + \delta_{2\ell-p} < \left(1 + \sqrt{1 - \frac{b_2}{b_1^2}}\right) b_1(1 - \delta_{2\ell-p})$ .

This theorem is the parallel to Theorems 2.1 in [102] for IHT. A few remarks are in order for the nature of the theorem, especially in regards to the constant  $\eta$ . One can view that  $\eta$  gives a trade-off between satisfying the theorem conditions and the amplification of the noise. In particular, one may consider that the above theorem proves the convergence result for the noiseless case by taking  $\eta$  to infinity; one can imagine solving the problem  $\mathcal{P}$ -Analysis where  $\mathbf{e} \rightarrow 0$ , and applying the theorem with appropriately chosen  $\eta$  which approaches infinity. It is indeed possible to show that the iterate solutions of AIHT and AHTP converges to  $\mathbf{x}$  when there is no noise. However, we will not give a separate proof since the basic idea of the arguments is the same for both cases.

As to the minimal number of iterations  $t^*$  given in (4.38), one may ask whether it can be negative. In order to answer this question it should be noted that according to the conditions of the Theorem the term inside the log in the denominator (4.38) is always greater than zero. Thus,  $t^*$  will be negative only if  $\|\mathbf{y}\|_2^2 < \eta\|\mathbf{e}\|_2^2$ . Indeed, in this case 0 iterations suffice for having the bound in (4.39).

The last remark is on the step-size selection. The advantage of the optimal changing step-size over the constant step-size is that we get the guarantee of the optimal constant step-size  $\mu = \frac{1}{1 + \delta_{2\ell-p}}$  without computing it. This is important since in practice we cannot evaluate the value of  $\delta_{2\ell-p}$ . However, the disadvantage of using the optimal changing step-size is its additional complexity for the algorithm. Thus, one option is to approximate the optimal selection

rule by replacing it with an adaptive one, for which we do not have a theoretical guarantee. Another option is to set  $\mu = 6/5$  which meets the theorem conditions for small enough  $\delta_{2\ell-p}$ , in the case where an optimal projection is at hand.

We will prove the theorem by proving two key lemmas first. The proof technique is based on ideas from [95] and [102]. Recall that the two iterative algorithms try to reduce the objective  $\|\mathbf{y} - \mathbf{M}\hat{\mathbf{x}}^t\|_2^2$  over iterations  $t$ . Thus, the progress of the algorithms can be indirectly measured by how much the objective  $\|\mathbf{y} - \mathbf{M}\hat{\mathbf{x}}^t\|_2^2$  is reduced at each iteration  $t$ . The two lemmas that we present capture this idea. The first lemma is similar to Lemma 3 in [95] and relates  $\|\mathbf{y} - \mathbf{M}\hat{\mathbf{x}}^t\|_2^2$  to  $\|\mathbf{y} - \mathbf{M}\hat{\mathbf{x}}^{t-1}\|_2^2$  and similar quantities at iteration  $t - 1$ . We remark that the constraint  $\frac{1}{\mu} \leq \sigma_{\mathbf{M}}^2$  in Theorem 4.4.5 may not be necessary and is added only for having a simpler derivation of the results in this theorem. Furthermore, this is a very mild condition compared to  $\frac{1}{\mu} < \left(1 + \sqrt{1 - \frac{b_2}{b_1}}\right) b_1(1 - \delta_{2\ell-p})$  and can only limit the range of values that can be used with the constant step size versions of the algorithms.

**Lemma 4.4.6** *Consider the problem  $\mathcal{P}$ -Analysis and apply either AIHT or AHTP with a constant step size  $\mu$  satisfying  $\frac{1}{\mu} \geq 1 + \delta_{2\ell-p}$  or an optimal step size. Then, at the  $t$ -th iteration, the following holds:*

$$\begin{aligned} \|\mathbf{y} - \mathbf{M}\hat{\mathbf{x}}^t\|_2^2 - \|\mathbf{y} - \mathbf{M}\hat{\mathbf{x}}^{t-1}\|_2^2 &\leq C_\ell \left( \|\mathbf{y} - \mathbf{M}\mathbf{x}\|_2^2 - \|\mathbf{y} - \mathbf{M}\hat{\mathbf{x}}^{t-1}\|_2^2 \right) \\ &+ C_\ell \left( \frac{1}{\mu(1 - \delta_{2\ell-p})} - 1 \right) \|\mathbf{M}(\mathbf{x} - \hat{\mathbf{x}}^{t-1})\|_2^2 + (C_\ell - 1)\mu\sigma_{\mathbf{M}}^2 \|\mathbf{y} - \mathbf{M}\hat{\mathbf{x}}^{t-1}\|_2^2. \end{aligned} \quad (4.40)$$

For the optimal step size the bound is achieved with the value  $\mu = \frac{1}{1 + \delta_{2\ell-p}}$ .

The proof of the above lemma appears in Appendix B.2. The second lemma is built on the result of Lemma 4.4.6. It shows that once the objective  $\|\mathbf{y} - \mathbf{M}\hat{\mathbf{x}}^{t-1}\|_2^2$  at iteration  $t - 1$  is small enough, then we are guaranteed to have small  $\|\mathbf{y} - \mathbf{M}\hat{\mathbf{x}}^t\|_2^2$  as well. Given the presence of noise, this is quite natural; one cannot expect it to approach 0 but may expect it not to become worse. Moreover, the lemma also shows that if  $\|\mathbf{y} - \mathbf{M}\hat{\mathbf{x}}^{t-1}\|_2^2$  is not small, then the objective in iteration  $t$  is necessarily reduced by a constant factor. Its proof appears also in Appendix B.3.

**Lemma 4.4.7** *Suppose that the same conditions of Theorem 4.4.5 hold true. If  $\|\mathbf{y} - \mathbf{M}\hat{\mathbf{x}}^{t-1}\|_2^2 \leq \eta^2 \|\mathbf{e}\|_2^2$ , then  $\|\mathbf{y} - \mathbf{M}\hat{\mathbf{x}}^t\|_2^2 \leq \eta^2 \|\mathbf{e}\|_2^2$ . Furthermore, if  $\|\mathbf{y} - \mathbf{M}\hat{\mathbf{x}}^{t-1}\|_2^2 > \eta^2 \|\mathbf{e}\|_2^2$ , then*

$$\|\mathbf{y} - \mathbf{M}\hat{\mathbf{x}}^t\|_2^2 \leq c_4 \|\mathbf{y} - \mathbf{M}\hat{\mathbf{x}}^{t-1}\|_2^2 \quad (4.41)$$

where

$$c_4 := \left(1 + \frac{1}{\eta}\right)^2 \left(\frac{1}{\mu(1 - \delta_{2\ell-p})} - 1\right) C_\ell + (C_\ell - 1)(\mu\sigma_{\mathbf{M}}^2 - 1) + \frac{C_\ell}{\eta^2} < 1.$$

Having the two lemmas above, the proof of the theorem is straightforward.

*Proof:*[Proof of Theorem 4.4.5] When we initialize  $\hat{\mathbf{x}}^0 = \mathbf{0}$ , we have  $\|\mathbf{y} - \mathbf{M}\hat{\mathbf{x}}^0\|_2^2 = \|\mathbf{y}\|_2^2$ .

Assuming that  $\|\mathbf{y}\|_2 > \eta \|\mathbf{e}\|_2$  and applying Lemma 4.4.7 repeatedly, we obtain

$$\|\mathbf{y} - \mathbf{M}\hat{\mathbf{x}}^t\|_2^2 \leq \max(c_4^t \|\mathbf{y}\|_2^2, \eta^2 \|\mathbf{e}\|_2^2).$$

Since  $c_4^t \|\mathbf{y}\|_2^2 \leq \eta^2 \|\mathbf{e}\|_2^2$  for  $t \geq t^*$ , we have simply

$$\|\mathbf{y} - \mathbf{M}\hat{\mathbf{x}}^t\|_2^2 \leq \eta^2 \|\mathbf{e}\|_2^2 \quad (4.42)$$

for  $t \geq t^*$ . If  $\|\mathbf{y} - \mathbf{M}\hat{\mathbf{x}}^0\|_2 = \|\mathbf{y}\|_2 \leq \eta \|\mathbf{e}\|_2$  then according to Lemma 4.4.7, (4.42) holds for every  $t > 0$ . Finally, we observe

$$\|\mathbf{x} - \hat{\mathbf{x}}^t\|_2^2 \leq \frac{1}{1 - \delta_{2\ell-p}} \|\mathbf{M}(\mathbf{x} - \hat{\mathbf{x}}^t)\|_2^2 \quad (4.43)$$

and, by the triangle inequality,

$$\|\mathbf{M}(\mathbf{x} - \hat{\mathbf{x}}^t)\|_2 \leq \|\mathbf{y} - \mathbf{M}\hat{\mathbf{x}}^t\|_2 + \|\mathbf{e}\|_2. \quad (4.44)$$

By plugging (4.42) into (4.44) and then the resulted inequality into (4.43), the result of the Theorem follows.  $\square$

As we have seen, the above AIHT and AHTP results hold for the cases of using a constant or an optimal changing step size. The advantage of using an optimal one is that we do not need to find  $\mu$  that satisfies the conditions of the theorem – the knowledge that such a  $\mu$  exists is enough. However, its disadvantage is the additional computational complexity it introduces. In Section 4.3 we have introduced a third option of using an approximated adaptive step size. In the next section we shall demonstrate this option in simulations, showing that it leads to the same reconstruction result as the optimal selection method. Note, however, that our theoretical guarantees do not cover this case.

#### 4.4.2 ACoSaMP Guarantees

Having the results for AIHT and AHTP we turn to ACoSaMP and ASP. We start with a theorem for ACoSaMP. Its proof is based on the proof for CoSaMP in [45].

**Theorem 4.4.8** Consider the problem  $\mathcal{P}$ -Analysis and apply ACoSaMP with  $a = \frac{2\ell-p}{\ell}$ . Let  $C_{\mathcal{S}} = \max(C_{\ell}, C_{2\ell-p})$  and suppose that there exists  $\gamma > 0$  such that

$$(1 + C_{\mathcal{S}}) \left( 1 - \left( \frac{C_{\mathcal{S}}}{(1 + \gamma)^2} - (C_{\mathcal{S}} - 1)\sigma_{\mathbf{M}}^2 \right) \right) < 1. \quad (4.45)$$

Then, there exists  $\delta_{\text{ACoSAMP}}(C_{\mathcal{S}}, \sigma_{\mathbf{M}}^2, \gamma) > 0$  such that, whenever  $\delta_{4\ell-3p} \leq \delta_{\text{ACoSAMP}}(C_{\mathcal{S}}, \sigma_{\mathbf{M}}^2, \gamma)$ , the  $t$ -th iteration of the algorithm satisfies

$$\|\mathbf{x} - \hat{\mathbf{x}}^t\|_2 \leq \rho_1 \rho_2 \|\mathbf{x} - \hat{\mathbf{x}}^{t-1}\|_2 + (\eta_1 + \rho_1 \eta_2) \|\mathbf{e}\|_2, \quad (4.46)$$

where

$$\begin{aligned} \eta_1 &\triangleq \frac{\sqrt{\frac{2+C_\ell}{1+C_\ell} + 2\sqrt{C_\ell} + C_\ell} \sqrt{1 + \delta_{3\ell-2p}}}{1 - \delta_{4\ell-3p}}, \\ \eta_2^2 &\triangleq \left( \frac{1 + \delta_{3\ell-2p}}{\gamma(1+\alpha)} + \frac{(1 + \delta_{2\ell-p})C_{2\ell-p}}{\gamma(1+\alpha)(1+\gamma)} + \frac{(C_{2\ell-p} - 1)(1+\gamma)\sigma_{\mathbf{M}}^2}{(1+\alpha)(1+\gamma)\gamma} \right), \\ \rho_1^2 &\triangleq \frac{1 + 2\delta_{4\ell-3p}\sqrt{C_\ell} + C_\ell}{1 - \delta_{4\ell-3p}^2}, \\ \rho_2^2 &\triangleq 1 - \left( \sqrt{\delta_{4\ell-3p}} - \sqrt{\frac{C_{2\ell-p}}{(1+\gamma)^2} (1 - \sqrt{\delta_{2\ell-p}})^2 - (C_{2\ell-p} - 1)(1 + \delta_{2\ell-p})\sigma_{\mathbf{M}}^2} \right)^2 \end{aligned}$$

and

$$\alpha = \frac{\sqrt{\delta_{4\ell-3p}}}{\sqrt{\frac{C_{2\ell-p}}{(1+\gamma)^2} (1 - \sqrt{\delta_{2\ell-p}})^2 - (C_{2\ell-p} - 1)(1 + \delta_{2\ell-p})\sigma_{\mathbf{M}}^2 - \delta_{4\ell-3p}}}.$$

Moreover,  $\rho_1^2 \rho_2^2 < 1$ , i.e., the iterates converges.

The constant  $\gamma$  plays a similar role to the constant  $\eta$  of Theorem 4.4.5. It gives a trade-off between satisfying the theorem conditions and the noise amplification. However, as opposed to  $\eta$ , the conditions for the noiseless case are achieved when  $\gamma$  tends to zero. An immediate corollary of the above theorem is the following.

**Corollary 4.4.9** Consider the problem  $\mathcal{P}$ -Analysis and apply ACoSaMP with  $a = \frac{2\ell-p}{\ell}$ . If (4.45) holds and  $\delta_{4\ell-3p} < \delta_{\text{ACoSAMP}}(C_{\mathcal{S}}, \sigma_{\mathbf{M}}^2, \gamma)$ , where  $C_{\mathcal{S}}$  and  $\gamma$  are as in Theorem 4.4.8 and  $\delta_{\text{ACoSAMP}}(C_{\mathcal{S}}, \sigma_{\mathbf{M}}^2, \gamma)$  is a constant guaranteed to be greater than zero whenever (4.34) is satisfied, then for any

$$t \geq t^* = \left\lceil \frac{\log(\|\mathbf{x}\|_2 / \|\mathbf{e}\|_2)}{\log(1/\rho_1 \rho_2)} \right\rceil,$$

$$\|\mathbf{x} - \hat{\mathbf{x}}_{\text{ACoSAMP}}^{t^*}\|_2 \leq \left( 1 + \frac{1 - (\rho_1 \rho_2)^{t^*}}{1 - \rho_1 \rho_2} (\eta_1 + \rho_1 \eta_2) \right) \|\mathbf{e}\|_2, \quad (4.47)$$

implying that ACoSaMP leads to a stable recovery. The constants  $\eta_1$ ,  $\eta_2$ ,  $\rho_1$  and  $\rho_2$  are the same as in Theorem 4.4.8.

*Proof:* By using (4.46) and recursion we have that

$$\begin{aligned} \left\| \mathbf{x} - \hat{\mathbf{x}}_{\text{ACoSAMP}}^{t^*} \right\|_2 &\leq (\rho_1 \rho_2)^{t^*} \left\| \mathbf{x} - \hat{\mathbf{x}}_{\text{ACoSAMP}}^0 \right\|_2 \\ &+ (1 + \rho_1 \rho_2 + (\rho_1 \rho_2)^2 + \dots + (\rho_1 \rho_2)^{t^*-1}) (\eta_1 + \rho_1 \eta_2) \|\mathbf{e}\|_2. \end{aligned} \quad (4.48)$$

Since  $\hat{\mathbf{x}}_{\text{ACoSAMP}}^0 = \mathbf{0}$ , after  $t^*$  iterations, one has

$$(\rho_1 \rho_2)^{t^*} \left\| \mathbf{x} - \hat{\mathbf{x}}_{\text{ACoSAMP}}^0 \right\|_2 = (\rho_1 \rho_2)^{t^*} \|\mathbf{x}\|_2 \leq \|\mathbf{e}\|_2. \quad (4.49)$$

By using the equation of geometric series with (4.48) and plugging (4.49) into it, we get (4.47).

□

We turn now to prove the theorem. Instead of presenting the proof directly, we divide the proof into several lemmas. The first lemma gives a bound for  $\|\mathbf{x} - \mathbf{w}\|_2$  as a function of  $\|\mathbf{e}\|_2$  and  $\|\mathbf{P}_{\tilde{\Lambda}^t}(\mathbf{x} - \mathbf{w})\|_2$ .

**Lemma 4.4.10** *Consider the problem  $\mathcal{P}$ -Analysis and apply ACoSaMP with  $a = \frac{2\ell-p}{\ell}$ . For each iteration we have*

$$\|\mathbf{x} - \mathbf{w}\|_2 \leq \frac{1}{\sqrt{1 - \delta_{4\ell-3p}^2}} \|\mathbf{P}_{\tilde{\Lambda}^t}(\mathbf{x} - \mathbf{w})\|_2 + \frac{\sqrt{1 + \delta_{3\ell-2p}}}{1 - \delta_{4\ell-3p}} \|\mathbf{e}\|_2. \quad (4.50)$$

The second lemma bounds  $\|\mathbf{x} - \hat{\mathbf{x}}_{\text{ACoSAMP}}^t\|_2$  in terms of  $\|\mathbf{P}_{\tilde{\Lambda}^t}(\mathbf{x} - \hat{\mathbf{x}}_{\text{ACoSAMP}}^t)\|_2$  and  $\|\mathbf{e}\|_2$  using the first lemma.

**Lemma 4.4.11** *Consider the problem  $\mathcal{P}$ -Analysis and apply ACoSaMP with  $a = \frac{2\ell-p}{\ell}$ . For each iteration we have*

$$\|\mathbf{x} - \hat{\mathbf{x}}^t\|_2 \leq \rho_1 \|\mathbf{P}_{\tilde{\Lambda}^t}(\mathbf{x} - \mathbf{w})\|_2 + \eta_1 \|\mathbf{e}\|_2, \quad (4.51)$$

where  $\eta_1$  and  $\rho_1$  are the same constants as in Theorem 4.4.8.

The last lemma bounds  $\|\mathbf{P}_{\tilde{\Lambda}^t}(\mathbf{x} - \mathbf{w})\|_2$  with  $\left\| \mathbf{x} - \hat{\mathbf{x}}_{\text{ACoSAMP}}^{t-1} \right\|_2$  and  $\|\mathbf{e}\|_2$ .

**Lemma 4.4.12** *Consider the problem  $\mathcal{P}$ -Analysis and apply ACoSaMP with  $a = \frac{2\ell-p}{\ell}$ . if*

$$C_{2\ell-p} < \frac{\sigma_{\mathbf{M}}^2(1 + \gamma)^2}{\sigma_{\mathbf{M}}^2(1 + \gamma)^2 - 1}, \quad (4.52)$$

then there exists  $\tilde{\delta}_{\text{ACoSAMP}}(C_{2\ell-p}, \sigma_{\mathbf{M}}^2, \gamma) > 0$  such that for any  $\delta_{2\ell-p} < \tilde{\delta}_{\text{ACoSAMP}}(C_{2\ell-p}, \sigma_{\mathbf{M}}^2, \gamma)$

$$\|\mathbf{P}_{\tilde{\Lambda}^t}(\mathbf{x} - \mathbf{w})\|_2 \leq \eta_2 \|\mathbf{e}\|_2 + \rho_2 \left\| \mathbf{x} - \hat{\mathbf{x}}^{t-1} \right\|_2. \quad (4.53)$$

The constants  $\eta_2$  and  $\rho_2$  are as defined in Theorem 4.4.8.

The proofs of Lemmas 4.4.10, 4.4.11 and 4.4.12 appear in Appendices B.4, B.5 and B.6 respectively. With the aid of the above three lemmas we turn to prove Theorem 4.4.8.

*Proof:*[Proof of Theorem 4.4.8] Remark that since  $1 + C_{\mathcal{S}} > 1$  we have that (4.45) implies  $\frac{C_{\mathcal{S}}}{(1+\gamma)^2} - (C_{\mathcal{S}} - 1)\sigma_{\mathbf{M}}^2 \geq 0$ . Because of that the condition in (4.52) in Lemma 4.4.12 holds. Substituting the inequality of Lemma 4.4.12 into the inequality of Lemma 4.4.11 gives (4.46). The iterates convergence if  $\rho_1^2 \rho_2^2 = \frac{1+2\delta_{4\ell-3p}\sqrt{C_{\ell}}+C_{\ell}}{1-\delta_{4\ell-3p}^2}\rho_2^2 < 1$ . By noticing that  $\rho_2^2 < 1$  it is enough to require  $\frac{1+C_{\ell}}{1-\delta_{4\ell-3p}^2}\rho_2^2 + \frac{2\delta_{4\ell-3p}\sqrt{C_{\ell}}}{1-\delta_{4\ell-3p}^2} < 1$ . The last is equivalent to

$$(1 + C_{\ell}) \left( 1 - \left( \sqrt{\delta_{4\ell-3p}} - \sqrt{\frac{C_{2\ell-p}}{(1+\gamma)^2} \left( 1 - \sqrt{\delta_{2\ell-p}} \right)^2 - (C_{2\ell-p} - 1)(1 + \delta_{2\ell-p})\sigma_{\mathbf{M}}^2} \right)^2 \right) + 2\delta_{4\ell-3p}\sqrt{C_{\ell}} - 1 + \delta_{4\ell-3p}^2 < 0. \quad (4.54)$$

It is easy to verify that  $\zeta(C, \delta) \triangleq \frac{C}{(1+\gamma)^2} \left( 1 - \sqrt{\delta} \right)^2 - (C - 1)(1 + \delta)\sigma_{\mathbf{M}}^2$  is a decreasing function of both  $\delta$  and  $C$  for  $0 \leq \delta \leq 1$  and  $C > 1$ . Since  $1 \leq C_{2\ell-p} \leq C_{\mathcal{S}}$ ,  $\delta_{2\ell-p} \leq \delta_{4\ell-3p}$  and  $\delta \geq 0$  we have that  $\zeta(C_{\mathcal{S}}, \delta_{4\ell-3p}) \leq \zeta(C_{2\ell-p}, \delta_{4\ell-3p}) \leq \zeta(C_{2\ell-p}, \delta_{2\ell-p}) \leq \zeta(1, 0) = \frac{1}{(1+\gamma)^2} \leq 1$ . Thus we have that  $-1 \leq -(\sqrt{\delta_{4\ell-3p}} - \zeta(C_{2\ell-p}, \delta_{2\ell-p}))^2 \leq -\delta_{4\ell-3p} + 2\sqrt{\delta_{4\ell-3p}} - \zeta(C_{\mathcal{S}}, \delta_{4\ell-3p})$ . Combining this with the fact that  $C_{\ell} \leq C_{\mathcal{S}}$  provides the following guarantee for  $\rho_1^2 \rho_2^2 < 1$ ,

$$(1 + C_{\mathcal{S}}) \left( 1 - \delta_{4\ell-3p} + 2\sqrt{\delta_{4\ell-3p}} - \frac{C_{\mathcal{S}}}{(1+\gamma)^2} \left( 1 - 2\sqrt{\delta_{4\ell-3p}} + \delta_{4\ell-3p} \right) \right) + (C_{\mathcal{S}} - 1)(1 + \delta_{4\ell-3p})\sigma_{\mathbf{M}}^2 + 2\delta_{4\ell-3p}\sqrt{C_{\mathcal{S}}} - 1 + \delta_{4\ell-3p}^2 < 0. \quad (4.55)$$

Let us now assume that  $\delta_{4\ell-3p} \leq \frac{1}{2}$ . This necessarily means that  $\delta_{\text{ACoSAMP}}(C_{\mathcal{S}}, \sigma_{\mathbf{M}}^2, \gamma) \leq \frac{1}{2}$  in the end. This assumption implies  $\delta_{4\ell-3p}^2 \leq \frac{1}{2}\delta_{4\ell-3p}$ . Using this and gathering coefficients, we now consider the condition

$$(1 + C_{\mathcal{S}}) \left( 1 - \frac{C_{\mathcal{S}}}{(1+\gamma)^2} + (C_{\mathcal{S}} - 1)\sigma_{\mathbf{M}}^2 \right) - 1 + 2(1 + C_{\mathcal{S}}) \left( 1 + \frac{C_{\mathcal{S}}}{(1+\gamma)^2} \right) \sqrt{\delta_{4\ell-3p}} + \left( (1 + C_{\mathcal{S}}) \left( -1 - \frac{C_{\mathcal{S}}}{(1+\gamma)^2} + (C_{\mathcal{S}} - 1)\sigma_{\mathbf{M}}^2 \right) + 2\sqrt{C_{\mathcal{S}}} + \frac{1}{2} \right) \delta_{4\ell-3p} < 0. \quad (4.56)$$

The expression on the LHS is a quadratic function of  $\sqrt{\delta_{4\ell-3p}}$ . Note that since (4.45) holds the constant term in the quadratic function is negative. This guarantees the existence of a range of values  $[0, \delta_{\text{ACoSAMP}}(C_{\mathcal{S}}, \sigma_{\mathbf{M}}^2, \gamma)]$  for  $\delta_{4\ell-3p}$  for which (4.56) holds, where  $\delta_{\text{ACoSAMP}}(C_{\mathcal{S}}, \sigma_{\mathbf{M}}^2, \gamma)$  is the square of the positive solution of the quadratic function. In case of two positive solutions we should take the smallest among them – in this case the coefficient of  $\delta_{4\ell-3p}$  in (4.56) will be positive.

Looking back at the proof of the theorem, we observe that the value of the constant  $\delta_{\text{ACoSAMP}}(\mathcal{C}_{\mathcal{S}}, \sigma_{\mathbf{M}}^2, \gamma)$  can potentially be improved: at the beginning of the proof, we have used  $\rho_2^2 \leq 1$ . By the end, we obtained  $\rho_2^2 \leq \rho_1^{-2} \leq 0.25$  since  $\rho_1 > 2$ . If we were to use this bound at the beginning, we would have obtained better constant  $\delta_{\text{ACoSAMP}}(\mathcal{C}_{\mathcal{S}}, \sigma_{\mathbf{M}}^2, \gamma)$ .  $\square$

### 4.4.3 ASP Guarantees

Having the result of ACoSaMP we turn to derive a similar result for ASP. The technique for deriving a result for ASP based on the result of ACoSaMP is similar to the one we used to derive a result for AHTP from the result of AIHT.

**Theorem 4.4.13** *Consider the problem  $\mathcal{P}$ -Analysis and apply ASP with  $a = \frac{2\ell-p}{\ell}$ . If (4.45) holds and  $\delta_{4\ell-3p} \leq \delta_{\text{ASP}}(\mathcal{C}_{\mathcal{S}}, \sigma_{\mathbf{M}}^2, \gamma)$ , where  $\mathcal{C}_{\mathcal{S}}$  and  $\gamma$  are as in Theorem 4.4.8, and  $\delta_{\text{ASP}}(\mathcal{C}_{\mathcal{S}}, \sigma_{\mathbf{M}}^2, \gamma)$  is a constant guaranteed to be greater than zero whenever (4.45) is satisfied, then the  $t$ -th iteration of the algorithm satisfies*

$$\|\mathbf{x} - \hat{\mathbf{x}}_{\text{ASP}}^t\|_2 \leq \frac{1 + \delta_{2\ell-p}}{1 - \delta_{2\ell-p}} \rho_1 \rho_2 \|\mathbf{x} - \hat{\mathbf{x}}_{\text{ASP}}^{t-1}\|_2 + \left( \frac{1 + \delta_{2\ell-p}}{1 - \delta_{2\ell-p}} (\eta_1 + \rho_1 \eta_2) + \frac{2}{1 - \delta_{2\ell-p}} \right) \|\mathbf{e}\|_2. \quad (4.57)$$

and the iterates converges, i.e.,  $\rho_1^2 \rho_2^2 < 1$ . The constants  $\eta_1$ ,  $\eta_2$ ,  $\rho_1$  and  $\rho_2$  are the same as in Theorem 4.4.8.

*Proof:* We first note that according to the selection rule of  $\hat{\mathbf{x}}_{\text{ASP}}$  we have that

$$\|\mathbf{y} - \mathbf{M}\hat{\mathbf{x}}_{\text{ASP}}^t\|_2 \leq \|\mathbf{y} - \mathbf{M}\mathbf{Q}_{\hat{\Lambda}^t}\mathbf{w}\|_2. \quad (4.58)$$

Using the triangle inequality and the fact that  $\mathbf{y} = \mathbf{M}\mathbf{x} + \mathbf{e}$  for both the LHS and the RHS we have

$$\|\mathbf{M}(\mathbf{x} - \hat{\mathbf{x}}_{\text{ASP}}^t)\|_2 - \|\mathbf{e}\|_2 \leq \|\mathbf{M}(\mathbf{x} - \mathbf{Q}_{\hat{\Lambda}^t}\mathbf{w})\|_2 + \|\mathbf{e}\|_2.$$

Using the O-RIP of  $\mathbf{M}$  with the fact that  $\mathbf{x}$ ,  $\hat{\mathbf{x}}_{\text{ASP}}$  and  $\mathbf{Q}_{\hat{\Lambda}^t}\mathbf{w}$  are  $\ell$ -cosparses we have

$$\|\mathbf{x} - \hat{\mathbf{x}}_{\text{ASP}}^t\|_2 \leq \frac{1 + \delta_{2\ell-p}}{1 - \delta_{2\ell-p}} \|\mathbf{x} - \mathbf{Q}_{\hat{\Lambda}^t}\mathbf{w}\|_2 + \frac{2}{1 - \delta_{2\ell-p}} \|\mathbf{e}\|_2.$$

Noticing that  $\mathbf{Q}_{\hat{\Lambda}^t}\mathbf{w}$  is the solution we get in one iteration of ACoSaMP with initialization of  $\hat{\mathbf{x}}_{\text{ASP}}^{t-1}$ , we can combine the above with the result of Theorem 4.4.8 getting (4.57). For  $\frac{1 + \delta_{2\ell-p}}{1 - \delta_{2\ell-p}} \rho_1 \rho_2 < 1$  to hold we need that

$$\frac{1 + 2\delta_{4\ell-3p}\sqrt{\tilde{C}_\ell} + C_\ell}{(1 - \delta_{4\ell-3p})^2} \left( 1 - \left( \left( \frac{\sqrt{\tilde{C}_{2\ell-p}}}{1 + \gamma} + 1 \right) \sqrt{\delta_{4\ell-3p}} - \frac{\sqrt{\tilde{C}_{2\ell-p}}}{1 + \gamma} \right)^2 \right) < 1. \quad (4.59)$$

Remark that the above differs from what we have for ACoSaMP only in the denominator of the first element in the LHS. In ACoSaMP  $1 - \delta_{4\ell-3p}^2$  appears instead of  $(1 - \delta_{4\ell-3p})^2$ . Thus, Using a similar process to the one in the proof of ACoSaMP we can show that (4.59) holds if the following holds

$$(1 + C_{\mathcal{S}}) \left( 1 - \frac{C_{\mathcal{S}}}{(1 + \gamma)^2} + (C_{\mathcal{S}} - 1)\sigma_{\mathbf{M}}^2 \right) - 1 + 2(1 + C_{\mathcal{S}}) \left( 1 + \frac{C_{\mathcal{S}}}{(1 + \gamma)^2} \right) \sqrt{\delta_{4\ell-3p}} \quad (4.60)$$

$$+ \left( (1 + C_{\mathcal{S}}) \left( -1 - \frac{C_{\mathcal{S}}}{(1 + \gamma)^2} + (C_{\mathcal{S}} - 1)\sigma_{\mathbf{M}}^2 \right) + 2\sqrt{C_{\mathcal{S}} + 2} \right) \delta_{4\ell-3p} < 0.$$

Notice that the only difference of the above compared to (4.56) is that we have +2 instead of +0.5 in the coefficient of  $\delta_{4\ell-3p}$  and this is due to the difference we mentioned before in the denominator in (4.59). The LHS of (4.60) is a quadratic function of  $\sqrt{\delta_{4\ell-3p}}$ . As before, we notice that if (4.45) holds then the constant term of the above is positive and thus  $\delta_{\text{ASP}}(C_{\mathcal{S}}, \sigma_{\mathbf{M}}^2, \gamma) \geq 0$  exists and is the square of the positive solution of the quadratic function.  $\square$

Having Theorem 4.4.13 we can immediately have the following corollary which is similar to the one we have for ACoSaMP. The proof resembles the one of Corollary 4.4.9 and omitted.

**Corollary 4.4.14** *Consider the problem  $\mathcal{P}$ -Analysis and apply ASP with  $a = \frac{2\ell-p}{\ell}$ . If (4.45) holds and  $\delta_{4\ell-3p} \leq \delta_{\text{ASP}}(C_{\mathcal{S}}, \sigma_{\mathbf{M}}^2, \gamma)$ , where  $C_{\mathcal{S}}$  and  $\gamma$  are as in Theorem 4.4.8, and  $\delta_{\text{ASP}}(C_{\mathcal{S}}, \sigma_{\mathbf{M}}^2, \gamma)$  is a constant guaranteed to be greater than zero whenever (4.34) is satisfied, then for any*

$$t \geq t^* = \left\lceil \frac{\log(\|\mathbf{x}\|_2 / \|\mathbf{e}\|_2)}{\log(1 / \frac{1+\delta_{2\ell-p}}{1-\delta_{2\ell-p}} \rho_1 \rho_2)} \right\rceil,$$

$$\|\mathbf{x}_{\text{ASP}}^t - \mathbf{x}\|_2 \leq \left( 1 + \frac{1 - \left( \frac{1+\delta_{2\ell-p}}{1-\delta_{2\ell-p}} \rho_1 \rho_2 \right)^t}{1 - \frac{1+\delta_{2\ell-p}}{1-\delta_{2\ell-p}} \rho_1 \rho_2} \cdot \left( \frac{1 + \delta_{2\ell-p}}{1 - \delta_{2\ell-p}} (\eta_1 + \rho_1 \eta_2) + \frac{2}{1 - \delta_{2\ell-p}} \right) \right) \|\mathbf{e}\|_2. \quad (4.61)$$

implying that ASP leads to a stable recovery. The constants  $\eta_1$ ,  $\eta_2$ ,  $\rho_1$  and  $\rho_2$  are the same as in Theorem 4.4.8.

#### 4.4.4 Non-Exact Cosparse Case

In the above guarantees we have assumed that the signal  $\mathbf{x}$  is  $\ell$ -cosparse. In many cases, it is not exactly  $\ell$ -cosparse but only nearly so. Denote by  $\mathbf{x}^\ell = \mathbf{Q}_{S_\ell^*(\mathbf{x})} \mathbf{x}$  the best  $\ell$ -cosparse approximation of  $\mathbf{x}$ , we have the following theorem that provides us with a guarantee also for this case. Similar result exists also in the synthesis case for the synthesis- $\ell_1$  minimization problem [72].

**Theorem 4.4.15** Consider a variation of problem  $\mathcal{P}$ -Analysis where  $\mathbf{x}$  is a general vector, and apply either AIHT or AHTP both with either constant or changing step size; or ACoSaMP or ASP with  $a = \frac{2\ell-p}{\ell}$ , and all are used with a zero initialization. Under the same conditions of Theorems 4.4.2 and 4.4.3 we have for any  $t \geq t^*$

$$\|\mathbf{x} - \hat{\mathbf{x}}\|_2 \leq \|\mathbf{x} - \mathbf{x}^\ell\|_2 + c \|\mathbf{M}(\mathbf{x} - \mathbf{x}^\ell)\|_2 + c \|\mathbf{e}\|_2, \quad (4.62)$$

where  $t^*$  and  $c$  are the constants from Theorems 4.4.2 and 4.4.3.

*Proof:* First we notice that we can rewrite  $\mathbf{y} = \mathbf{M}\mathbf{x}^\ell + \mathbf{M}(\mathbf{x} - \mathbf{x}^\ell) + \mathbf{e}$ . Denoting  $\mathbf{e}^\ell = \mathbf{M}(\mathbf{x} - \mathbf{x}^\ell) + \mathbf{e}$  we can use Theorems 4.4.2 and 4.4.3 to recover  $\mathbf{x}^\ell$  and have

$$\|\mathbf{x}^\ell - \hat{\mathbf{x}}\|_2 \leq c \|\mathbf{e}^\ell\|_2. \quad (4.63)$$

Using the triangle inequality for  $\|\mathbf{x} - \hat{\mathbf{x}}\|_2$  with the above gives

$$\|\mathbf{x} - \hat{\mathbf{x}}\|_2 \leq \|\mathbf{x} - \mathbf{x}^\ell\|_2 + \|\mathbf{x}^\ell - \hat{\mathbf{x}}\|_2 \leq \|\mathbf{x} - \mathbf{x}^\ell\|_2 + c \|\mathbf{e}^\ell\|_2. \quad (4.64)$$

Using again the triangle inequality for  $\|\mathbf{e}^\ell\|_2 \leq \|\mathbf{e}\|_2 + \|\mathbf{M}(\mathbf{x} - \mathbf{x}^\ell)\|_2$  provides us with the desired result.  $\square$

#### 4.4.5 Theorem Conditions

Having the results of the theorems we ask ourselves whether their conditions are feasible. As we have seen in Section 4.1, the requirement on the O-RIP holds for many non-trivial matrices. Another requirement by the theorems is that  $C_\ell$  and  $C_{2\ell-p}$  need to be one or close to one. Using the thresholding in (4.18) for cosupport selection with a unitary  $\mathbf{\Omega}$  satisfies the conditions in a trivial way since  $C_\ell = C_{2\ell-p} = 1$ . This case coincides with the synthesis model for which we already have theoretical guarantees. As shown in Section 4.2, optimal projection schemes exist for  $\mathbf{\Omega}_{\text{1D-DIF}}$  and  $\mathbf{\Omega}_{\text{FUS}}$  which do not belong to the the synthesis framework. For a general  $\mathbf{\Omega}$ , a general projection scheme is not known and if the thresholding method is used the constants in (4.18) do not equal one and are not even expected to be close to one [5]. It is interesting to ask whether there exists an efficient general projection scheme that guarantees small constants for any given operator  $\mathbf{\Omega}$ , or for specifically structured  $\mathbf{\Omega}$ . We leave these questions as subject for future work. Instead, we show empirically in the next section that a weaker projection scheme that does not fulfill all the requirements of the theorems leads to a good reconstruction result. This suggests that even in the absence of good near optimal projections we may still use the algorithms practically.

#### 4.4.6 Comparison to Other Works

Among the existing theoretical works that studied the performance of analysis algorithms [23, 25, 52], the result that resembles ours is the result for  $\ell_1$ -analysis in [24]. This work analyzed the  $\ell_1$ -analysis minimization problem with a synthesis perspective. The analysis dictionary  $\mathbf{\Omega}$  was replaced with the conjugate of a synthesis dictionary  $\mathbf{D}$  which is assumed to be a tight frame, resulting with the following minimization problem.

$$\hat{\mathbf{x}}_{A-\ell_1} = \underset{\mathbf{z}}{\operatorname{argmin}} \|\mathbf{D}^* \mathbf{z}\|_1 \quad \text{s.t.} \quad \|\mathbf{y} - \mathbf{Mz}\|_2 \leq \varepsilon, \quad (4.65)$$

where  $\varepsilon$  is a bound on the noise  $\ell_2$  norm. It was shown that if  $\mathbf{M}$  has the D-RIP (See definition 2.7.1) [24, 95] with  $\delta_{7k} < 0.6$  then

$$\|\hat{\mathbf{x}}_{A-\ell_1} - \mathbf{x}\|_2 \leq \tilde{C}_{\ell_1} \varepsilon + \frac{\|\mathbf{D}^* \mathbf{x} - [\mathbf{D}^* \mathbf{x}]_k\|_1}{\sqrt{k}}. \quad (4.66)$$

The authors in [24] presented this result as a synthesis result that allows linear dependencies in  $\mathbf{D}$  at the cost of limiting the family of signals to be those for which  $\|\mathbf{D}^* \mathbf{x} - [\mathbf{D}^* \mathbf{x}]_k\|_1$  is small. However, having the analysis perspective, we can realize that they provided a recovery guarantee for  $\ell_1$ -analysis under the new analysis model for the case that  $\mathbf{\Omega}$  is a tight frame. An easy way to see it is to observe that for an  $\ell$ -cospase signal  $\mathbf{x}$ , setting  $k = p - \ell$ , we have that  $\|\mathbf{\Omega} \mathbf{x} - [\mathbf{\Omega}^* \mathbf{x}]_{p-\ell}\|_1 = 0$  and thus in the case  $\varepsilon = 0$  we get that (4.66) guarantees the recovery of  $\mathbf{x}$  by using (4.65) with  $\mathbf{D}^* = \mathbf{\Omega}$ . Thus, though the result in [24] was presented as a reconstruction guarantee for the synthesis model, it is actually a guarantee for the analysis model.

Our main difference from [24] is that the proof technique relies on the analysis model and not on the synthesis one and that the results presented here are for general operators and not only for tight frames. For instance, the operators  $\mathbf{\Omega}_{1D-DIF}$  and  $\mathbf{\Omega}_{FUS}$  for which the guarantees hold are not tight frames where  $\mathbf{\Omega}_{1D-DIF}$  is not even a frame. However, the drawback of our approach compared to the work in [24] is that it is still not known how to perform an optimal or a near optimal projection for a tight frame.

In the non-exact sparse case our results differ from the one in (4.66) in the sense that it looks at the projection error and not at the values of  $\mathbf{\Omega} \mathbf{x}$ . It would be interesting to see if there is a connection between the two and whether one implies the other.

We mention that in [50, 51] the case of a general frame is studied, giving recovery conditions which depend on the frame constants. However, these results also do not support operators which are not frames like  $\mathbf{\Omega}_{1D-DIF}$ .

A recent work has studied the  $\ell_1$ -analysis minimization with the 2D-DIF operator, also known as anisotropic two dimensional total-variation (2D-TV) [27]. It would be interesting to see whether similar results can be achieved for the greedy-like techniques proposed here with 2D-DIF.

## 4.5 Experiments

In this section we repeat some of the experiments performed in [23] for the noiseless case ( $\mathbf{e} = 0$ ) and some of the experiments performed in [84] for the noisy case<sup>5</sup>.

### 4.5.1 Targeted Cosparsity

Just as in the synthesis counterpart of the proposed algorithms, where a target sparsity level  $k$  must be selected before running the algorithms, we have to choose the targeted cosparsity level which will dictate the projection steps. In the synthesis case it is known that it may be beneficial to over-estimate the sparsity  $k$ . Similarly in the analysis framework the question arises: In terms of recovery performance, does it help to under-estimate the cosparsity  $\ell$ ? A tentative positive answer comes from the following heuristic: Let  $\tilde{\Lambda}$  be a subset of the cosupport  $\Lambda$  of the signal  $\mathbf{x}$  with  $\tilde{\ell} := |\tilde{\Lambda}| < \ell = |\Lambda|$ . According to Proposition 3 in [23]

$$\kappa_{\Omega}(\tilde{\ell}) \leq \frac{m}{2} \quad (4.67)$$

is a sufficient condition to identify  $\tilde{\Lambda}$  in order to recover  $\mathbf{x}$  from the relations  $\mathbf{y} = \mathbf{M}\mathbf{x}$  and  $\mathbf{\Omega}_{\tilde{\Lambda}}\mathbf{x} = 0$ .  $\kappa_{\Omega}(\tilde{\ell}) = \max_{\tilde{\Lambda} \in \mathcal{L}_{\tilde{\ell}}} \dim(\mathcal{W}_{\tilde{\Lambda}})$  is a function of  $\tilde{\ell}$ . Therefore, we can replace  $\ell$  with the smallest  $\tilde{\ell}$  that satisfies (4.67) as the effective cosparsity in the algorithms. Since it is easier to identify a smaller cosupport set it is better to run the algorithm with the smallest possible value of  $\tilde{\ell}$ , in the absence of noise. In the presence of noise, larger values of  $\ell$  allows a better denoising. Note, that in some cases the smallest possible value of  $\tilde{\ell}$  will be larger than the actual cosparsity of  $\mathbf{x}$ . In this case we cannot replace  $\ell$  with  $\tilde{\ell}$ .

We take two examples for selecting  $\tilde{\ell}$ . The first is for  $\mathbf{\Omega}$  which is in general position and the second is for  $\mathbf{\Omega}_{2D-DIF}$ , the finite difference analysis operator that computes horizontal and vertical discrete derivatives of an image which is strongly connected to the total variation (TV) norm minimization as noted before. For  $\mathbf{\Omega}$  that is in general position  $\kappa_{\Omega}(\tilde{\ell}) = \max(d - \ell, 0)$

---

<sup>5</sup>A matlab package with code for the experiments performed in this chapter is available online as an open source distribution.

[23]. In this case we choose

$$\tilde{\ell} = \min\left(d - \frac{m}{2}, \ell\right). \quad (4.68)$$

For  $\Omega_{DIF}$  we have  $\kappa_{\Omega_{DIF}}(\tilde{\ell}) \geq d - \frac{\ell}{2} - \sqrt{\frac{\ell}{2}} - 1$  [23] and

$$\tilde{\ell} = \lceil \min((-1/\sqrt{2} + \sqrt{2d - m - 1.5})^2, \ell) \rceil. \quad (4.69)$$

Replacing  $\ell$  with  $\tilde{\ell}$  is more relevant to AIHT and AHTP than ACoSaMP and ASP since in the last we intersect cosupport sets and thus the estimated cosupport set need to be large enough to avoid empty intersections. Thus, for  $\Omega$  in general position we use the true cosparsity level for ACoSaMP and ASP. For  $\Omega_{DIF}$ , where linear dependencies occur, the corank does not equal the cosparsity and we use  $\tilde{\ell}$  instead of  $\ell$  since it will be favorable to run the algorithm targeting a cosparsity level in the middle. In this case  $\ell$  tends to be very large and it is more likely to have non-empty intersections .

#### 4.5.2 Phase Diagrams for Synthetic Signals in the Noiseless Case

We begin with with synthetic signals in the noiseless case. We test the performance of AIHT with a constant step-size, AIHT with an adaptive changing step-size, AHTP with a constant step-size, AHTP with an adaptive changing step-size, ACoSaMP with  $a = \frac{2\ell-p}{\ell}$ , ACoSaMP with  $a = 1$ , ASP with  $a = \frac{2\ell-p}{\ell}$  and ASP with  $a = 1$ . We compare the results to those of  $A$ - $\ell_1$ -minimization [22] and GAP [23]. We use a random matrix  $\mathbf{M}$  and a random tight frame with  $d = 120$  and  $p = 144$ , where each entry in the matrices is drawn independently from the Gaussian distribution.

We draw a phase transition diagram [104] for each of the algorithms. We test 20 different possible values of  $m$  and 20 different values of  $\ell$  and for each pair repeat the experiment 50 times. In each experiment we check whether we have a perfect reconstruction. White cells in the diagram denotes a perfect reconstruction in all the experiments of the pair and black cells denotes total failure in the reconstruction. The values of  $m$  and  $\ell$  are selected according to the following formula:

$$m = \delta d \quad \ell = d - \rho m, \quad (4.70)$$

where  $\delta$ , the sampling rate, is the x-axis of the phase diagram and  $\rho$ , the ratio between the cosparsity of the signal and the number of measurements, is the y-axis.

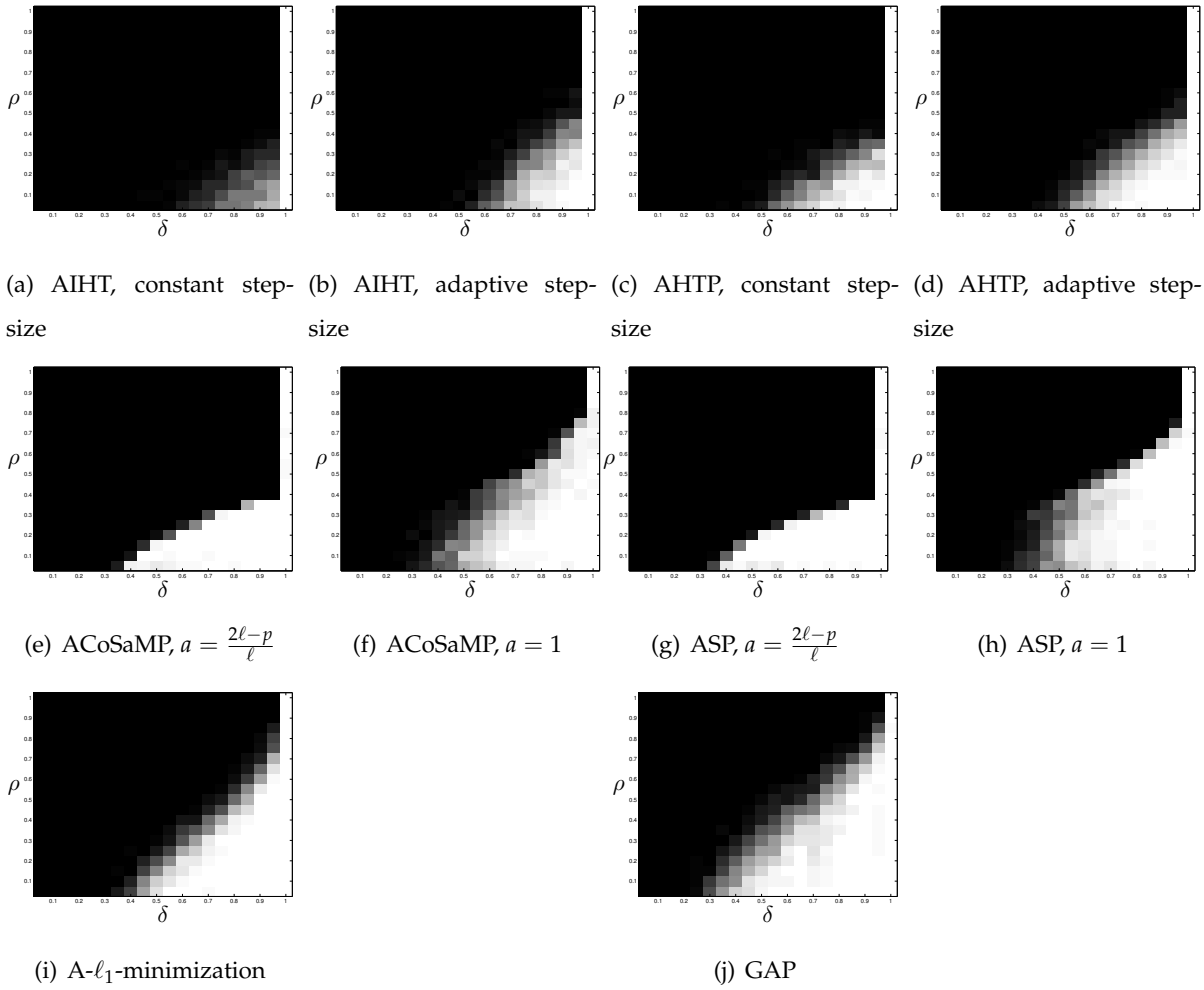


Figure 4.2: Recovery rate for a random tight frame with  $p = 144$  and  $d = 120$ . From left to right, up to bottom: AIHT with a constant step-size, AIHT with an adaptive changing step-size, AHTP with a constant step-size, AHTP with an adaptive changing step-size, ACoSaMP with  $a = \frac{2\ell-p}{\ell}$ , ACoSaMP with  $a = 1$ , ASP with  $a = \frac{2\ell-p}{\ell}$ , ASP with  $a = 1$ ,  $A\text{-}\ell_1\text{-minimization}$  and GAP.

Figure 4.2 presents the reconstruction results of the algorithms. It should be observed that AIHT and AHTP have better performance using the adaptive step-size than using the constant step-size. The optimal step-size has similar reconstruction result like the adaptive one and thus not presented. For ACoSaMP and ASP we observe that it is better to use  $a = 1$  instead of  $a = \frac{2\ell-p}{\ell}$ . Compared to each other we see that ACoSaMP and ASP achieve better recovery than AHTP and AIHT. Between the last two, AHTP is better. Though AIHT has inferior behavior, we should mention that with regards to running time AIHT is the most efficient. Afterwards we have AHTP and then ACoSaMP and ASP. Compared to  $\ell_1$  and GAP we observe that ACoSaMP

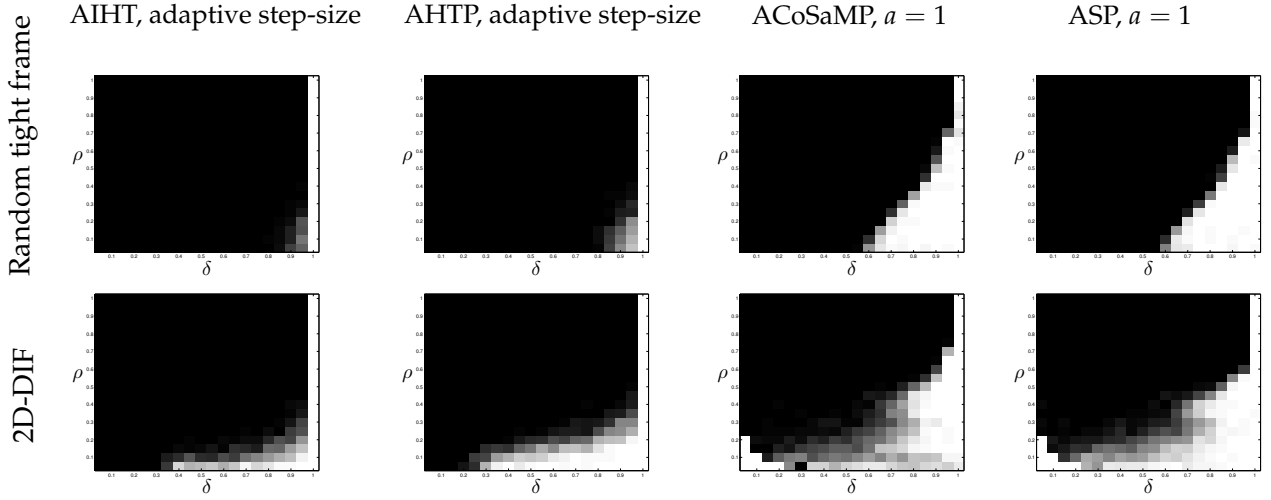


Figure 4.3: Recovery rate for a random tight frame with  $p = 240$  and  $d = 120$  (up) and a finite difference operator (bottom). From left to right: AIHT and AHTP with an adaptive changing step-size, and ACoSaMP and ASP with  $a = 1$ .

and ASP have competitive results.

With the above observations, we turn to test operators with higher redundancy and see the effect of linear dependencies in them. We test two operators. The first is a random tight frame as before but with redundancy factor of 2. The second is the two dimensional finite difference operator  $\Omega_{2D-DIF}$ . In Fig. 4.3 we present the phase diagrams for both operators using AIHT with an adaptive changing step-size, AHTP with an adaptive changing step-size, ACoSaMP with  $a = 1$ , and ASP with  $a = 1$ . As observed before, also in this case the ACoSaMP and ASP outperform AIHT and AHTP in both cases and AHTP outperform AIHT. We mention again that the better performance comes at the cost of higher complexity. In addition, as we expected, having redundancies in  $\Omega$  results with a better recovery.

### 4.5.3 Reconstruction of High Dimensional Images in the Noisy Case

We turn now to test the methods for high dimensional signals. We use RASP and RACoSaMP (relaxed versions of ASP and ACoSaMP defined in Section 4.3.3) for the reconstruction of the *Shepp-Logan phantom* from few number of measurements. The sampling operator is a two dimensional Fourier transform that measures only a certain number of radial lines from the Fourier transform. The cosparsity operator is  $\Omega_{2D-DIF}$  and the cosparsity used is the actual cosparsity of the signal under this operator ( $\ell = 128014$ ). The phantom image is presented in Fig. 4.4(a). Using the RACoSaMP and RASP we get a perfect reconstruction using only 15

radial lines, i.e., only  $m = 3782$  measurements out of  $d = 65536$  which is less than 6 percent of the data in the original image. The algorithm requires less than 20 iterations for having this perfect recovery. For AIHT and RAHTP we achieve a reconstruction which is only close to the original image using 35 radial lines. The reconstruction result of AIHT is presented in Fig 4.4(b). The advantage of the AIHT, though it has an inferior performance, over the other methods is its running time. While the others need several minutes for each reconstruction, for the AIHT it takes only few seconds to achieve a visually reasonable result.

Exploring the noisy case, we perform a reconstruction using RASP of a noisy measurement of the phantom with 22 radial lines and signal to noise ratio (SNR) of 20. Figure 4.4(c) presents the noisy image, the result of applying inverse Fourier transform on the measurements, and Fig. 4.4(d) presents its reconstruction result. Note that for the minimization process we solve conjugate gradients, in each iteration and take only the real part of the result and crop the values of the resulted image to be in the range of  $[0, 1]$ . We get a peak SNR (PSNR) of  $36dB$ . We get similar results using RACoSAMP but using more radial lines (25).

## 4.6 Discussion and Summary

In this chapter we presented new pursuit algorithms for the cosparse analysis model. A theoretical study of these algorithms was performed giving guarantees for stable recovery under the assumptions of the O-RIP and the existence of an optimal or a near optimal projection. We have shown that optimal projections exist for some non-trivial operators, i.e., operators that do not fall back to the synthesis case. In addition, we have demonstrated experimentally that using simpler kind of projections is possible in order to get good reconstruction results. We demonstrated both in the theoretical and the empirical results that linear dependencies within the analysis dictionary are favorable and enhance the recovery performance.

Note that the theoretical guarantees developed in this chapter do not cover frames as the analysis operators. A future work should explore this option for these techniques. In Chapter 6 we present another greedy-like technique with theoretical guarantees that do support frames as operators. In [105] we propose a new strategy that supports also the 2D-DIF operator.

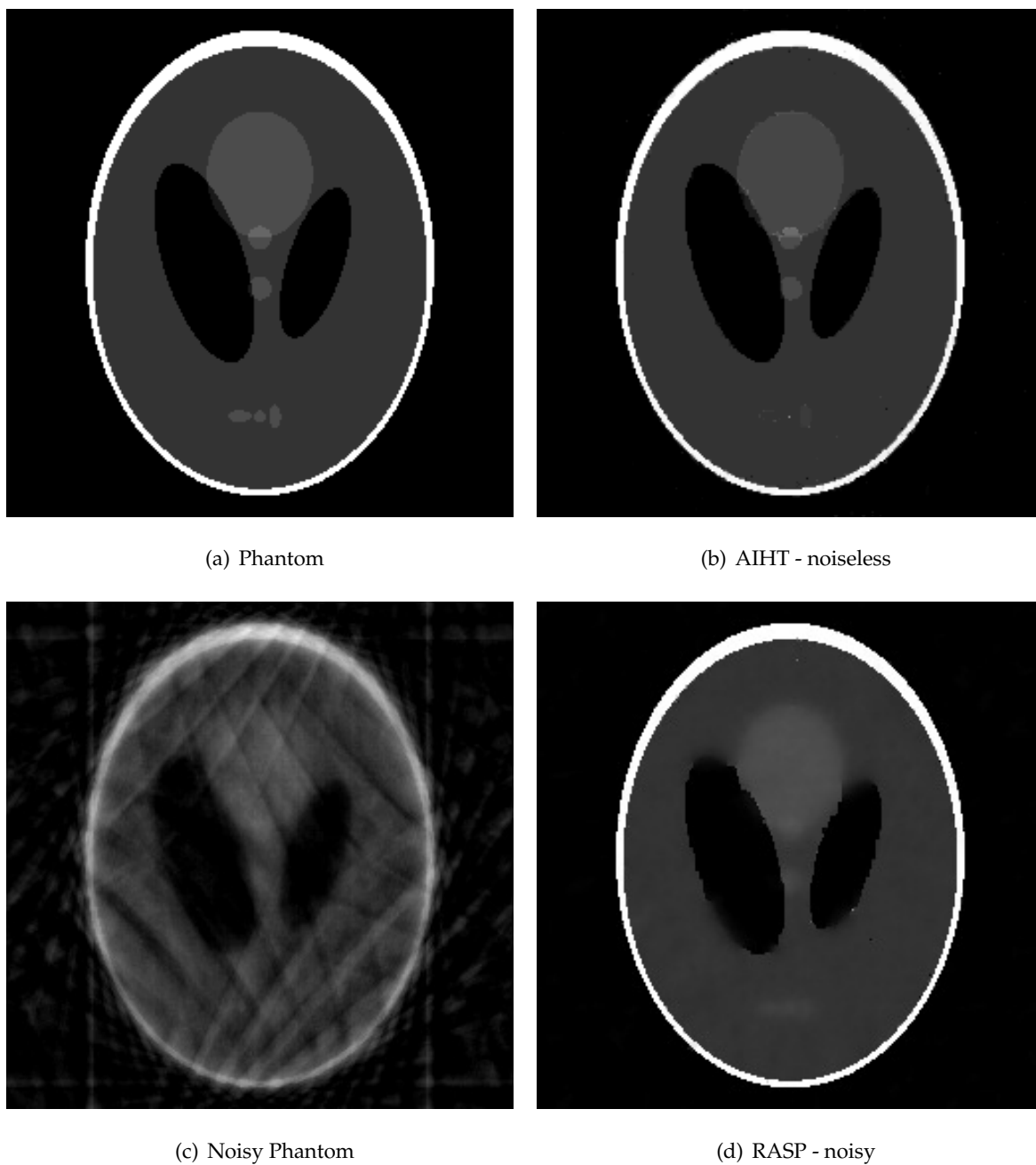


Figure 4.4: From left to right, to to bottom: Shepp Logan phantom image, AIHT reconstruction using 35 radial lines, noisy image with SNR of 20 and recovered image using RASP and only 22 radial lines. Note that for the noiseless case RASP and RACoSaMP get a perfect reconstruction using only 15 radial lines.



## Chapter 5

# The Signal Space Paradigm

The results shown in this chapter have been published and appeared in the following articles:

- R. Giryes and M. Elad, "Can we allow linear dependencies in the dictionary in the synthesis framework?," in *Proc. IEEE International Conference on Acoustics, Speech and Signal Processing (ICASSP)*, 26-31 May, 2013 [7].
- R. Giryes and M. Elad, "Iterative hard thresholding with near optimal projection for signal recovery," In *Proc. 10th International Conference on Sampling Theory and Applications (SAMPTA)*, 1-5, July, 2013 [8].
- R. Giryes and M. Elad, "OMP performance with highly coherent dictionaries," in *Proc. 10th International Conference on Sampling Theory and Applications (SAMPTA)*, 1-5, July, 2013 [9].
- R. Giryes and D. Needell, "Greedy signal space methods for incoherence and beyond," *Submitted*, 2013 [11].

In the previous chapter we have studied the analysis greedy-like algorithms, showing that linear dependencies can be allowed in the analysis dictionary and are even encouraged. Unlike the analysis model, which works in the signal domain and thus recovers the signal directly, the synthesis one operates in the representation domain and thus recovers the signal indirectly by recovering first its representation. For this reason, most of the efforts for developing theoretical guarantees for the synthesis framework provide bounds for the representation's reconstruction [28, 29, 35, 39, 40, 41, 42, 43], implying that the established error is also the signal's one only for

unitary dictionaries.

Results for more general dictionaries also exist [76, 106]. However, they require the dictionary to be highly incoherent and with no linear dependencies between small number of its columns. This requirement limits the types of dictionaries that may be used to model the signal. While this constraint is necessary for recovering the signal's representation, it is not clear that it is still required when our target is the signal. The goal of this chapter is to answer this very question. We aim at showing that highly-coherent and even linearly dependent atoms in  $\mathbf{D}$  still enable a reliable recovery of the signal from its measurements.

Since linear dependencies are shown to give profit in the analysis framework, it is conjectured that the requirement for an incoherent dictionary for the signal recovery in the synthesis framework is unnecessary as well. A clue for this very property is given in [24], where the reconstruction conditions are presented in terms of the D-RIP which is a property of the measurement matrix  $\mathbf{M}$  for the synthesis model. However, the results in [24] are derived for signals from the analysis model, thus leaving our question unresolved as of yet.

## 5.1 Preliminaries

In this chapter we focus on the synthesis model and ask: Is it possible to have a recovery guarantee for the synthesis model for a dictionary exhibiting linear dependencies within small groups of its columns? In order to answer this question, we start by studying the performance of the ideal  $\ell_0$ -minimization problem

$$\hat{\mathbf{a}} = \underset{\mathbf{w}}{\operatorname{argmin}} \|\mathbf{w}\|_0 \quad \text{s.t.} \quad \|\mathbf{y} - \mathbf{MD}\mathbf{w}\|_2 \leq \varepsilon. \quad (5.1)$$

This is the core approach for recovering a signal that is known to have the synthesis sparsity prior. The reconstructed signal in this technique is simply  $\hat{\mathbf{x}} = \mathbf{D}\hat{\mathbf{a}}$ . Recall that in the noiseless case, (5.1) turns to be simply

$$\hat{\mathbf{a}} = \underset{\mathbf{w}}{\operatorname{argmin}} \|\mathbf{w}\|_0 \quad \text{s.t.} \quad \mathbf{y} = \mathbf{MD}\mathbf{w}. \quad (5.2)$$

We first provide uniqueness conditions for the signal recovery in the noiseless case. Then we present stable reconstruction conditions for the noisy case, where the noise is adversarial, using the D-RIP. We recall its definition<sup>1</sup>, which enforces that the measurement matrix  $\mathbf{M}$  preserves the geometry of signals sparse with respect to  $\mathbf{D}$ :

<sup>1</sup>By abuse of notation we denote both the RIP and the D-RIP constants by  $\delta_k$ . It will be clear from the context to which one we refer at each point in this chapter.

**Definition 5.1.1 (D-RIP [24])** A matrix  $\mathbf{M}$  has the D-RIP with a dictionary  $\mathbf{D}$  and a constant  $\delta_k = \delta_{\mathbf{D},k}^D$ , if  $\delta_{\mathbf{D},k}^D$  is the smallest constant that satisfies

$$(1 - \delta_{\mathbf{D},k}^D) \|\mathbf{D}\mathbf{w}\|_2^2 \leq \|\mathbf{M}\mathbf{D}\mathbf{w}\|_2^2 \leq (1 + \delta_{\mathbf{D},k}^D) \|\mathbf{D}\mathbf{w}\|_2^2, \quad (5.3)$$

whenever  $\mathbf{w}$  is  $k$ -sparse.

The uniqueness and stability conditions that we present are generalization of previous results [28, 29, 32, 35, 43, 107] that assume  $\mathbf{D}$  to be incoherent. Our contribution is in providing reconstruction guarantees in the signal domain that do not pose incoherence requirement on the dictionary. Note that our stability result is a particular case of the result presented in [57, 95] in which a more general form of the D-RIP property has been proposed giving stable recovery guarantee for signals that come from a general union of subspaces model.

Having the results for the  $\ell_0$ -minimization problem, which is known to be NP-hard [61], we turn to approximation techniques and ask whether it is possible to extend the existing representation recovery guarantees to the signal case.

First steps in this direction have been taken for the CoSaMP algorithm in [108], presenting a variation for it, the Signal Space CoSaMP (SSCoSaMP) method, that targets the recovery of the signal directly. This technique has been studied under the assumption of the D-RIP [24]. It has been proven that under this assumption, if one has access to a support selection scheme  $\mathcal{S}_k$ , which defines a projection  $\mathbf{P}_{\mathcal{S}_k(\cdot)}$ , satisfying

$$\left\| \mathbf{P}_{\mathcal{S}_k(\mathbf{z})}\mathbf{z} - \mathbf{P}_{\mathcal{S}_k^{opt}(\mathbf{z})}\mathbf{z} \right\|_2 \leq \min \left( c_1 \left\| \mathbf{P}_{\mathcal{S}_k^{opt}(\mathbf{z})}\mathbf{z} \right\|_2, c_2 \left\| \mathbf{z} - \mathbf{P}_{\mathcal{S}_k^{opt}(\mathbf{z})}\mathbf{z} \right\|_2 \right), \quad (5.4)$$

where  $\mathcal{S}_k^{opt}$  denotes the optimal support selection scheme, then the method has a stable recovery for any  $k$ -sparse signal, i.e., its reconstructed signal  $\hat{\mathbf{x}}_{SSCoSaMP}$  satisfies

$$\|\mathbf{x} - \hat{\mathbf{x}}_{SSCoSaMP}\|_2 \leq C \cdot \varepsilon, \quad (5.5)$$

where  $C$  is a given constant. Although the other results for greedy methods in this setting also rely on similar assumptions regarding the optimality of the projection [4, 109] (See Chapter 4), it remains an open problem whether such projections can be obtained, even when the dictionary  $\mathbf{D}$  is incoherent or well-behaved on sparse signals. In this chapter, we remedy this issue by taking two different directions.

In the first direction explored we note that in [108] it is observed that OMP [37], though not backed up theoretically, achieves some success in recovering signals in the presence of high coherence in the dictionary. We provide the first steps to explain this behavior. We propose

a slightly modified version of OMP,  $\epsilon$ -OMP, and analyze its performance in the noiseless case ( $\mathbf{e} = 0$ ). Instead of using the D-RIP, we rely on a new property of  $\mathbf{M}$  and  $\mathbf{D}$ : The  $\epsilon$ -coherence  $\mu_\epsilon$ , which generalizes the definition of the regular coherence  $\mu$ . Using this definition we show that if  $k \leq \frac{1}{2}(1 + \frac{1}{\mu_\epsilon}) - O(\epsilon)$  then the signal recovery error of  $\epsilon$ -OMP is  $O(\epsilon)$ . This result implies that  $\epsilon$ -OMP achieves an almost exact reconstruction in the case of very high correlations within pairs of dictionary columns. We draw also the connection between OMP and  $\epsilon$ -OMP. Note that our conditions do not include the need for an efficient projection, as needed in [108].

In the second direction, we propose a variant of SSCoSAMP and an alternative proof technique that allows us to weaken the requirement on the projection. We provide similar guarantees to CoSaMP for incoherent dictionaries and show how these are extended for coherent ones.

The chapter is organized as follows. In Section 5.2 we introduce some properties of the D-RIP, which are similar to the ones shown for the O-RIP in Chapter 4. In Section 5.3 we present our new uniqueness and stability results for signal recovery for the  $\ell_0$ -minimization problem. Section 5.4 introduces the  $\epsilon$ -coherence along with other new definitions. In Section 5.5 a modified version of OMP is introduced to support high correlation between pairs of columns. In Section 5.6 the algorithm is analyzed using the  $\epsilon$ -coherence providing some performance guarantees for the noiseless case. Section 5.7 presents the signal space approach for greedy-like algorithms using near-optimal projections in the signal space. Section 5.8 provides an alternate study for signal space greedy methods which enforces assumptions on these projections which hold in several settings including those when the dictionary is incoherent or structurally coherent. In Section 5.9 we present some experimental results. Section 5.10 discusses related works and concludes the chapter.

## 5.2 D-RIP Properties

The D-RIP, like the standard RIP, inherits the following useful properties. The first two follow immediately from the definition and thus appear without a proof.

**Corollary 5.2.1** *If  $\mathbf{M}$  satisfies the D-RIP with a constant  $\delta_k$  then*

$$\|\mathbf{M}\mathbf{P}_T\|_2^2 \leq 1 + \delta_k \quad (5.6)$$

for every  $T$  such that  $|T| \leq k$ .

**Lemma 5.2.2** *For  $k \leq \tilde{k}$  it holds that  $\delta_k \leq \delta_{\tilde{k}}$ .*

**Lemma 5.2.3** *If  $\mathbf{M}$  satisfies the D-RIP then*

$$\|\mathbf{P}_T(\mathbf{I} - \mathbf{M}^*\mathbf{M})\mathbf{P}_T\|_2 \leq \delta_k \quad (5.7)$$

for any  $T$  such that  $|T| \leq k$ .

*Proof:* The proof is similar to the one of the standard RIP as appears in [45]. We first observe that the Definition (5.1.1) of the D-RIP is equivalent to requiring

$$\left| \|\mathbf{M}\mathbf{v}\|_2^2 - \|\mathbf{v}\|_2^2 \right| \leq \delta_k \|\mathbf{v}\|_2^2 \quad (5.8)$$

for any  $\mathbf{v} = \mathbf{D}\mathbf{w}$  such that  $\|\mathbf{w}\|_0 \leq k$ . From this it follows that

$$\left| \|\mathbf{M}\mathbf{P}_T\mathbf{z}\|_2^2 - \|\mathbf{P}_T\mathbf{z}\|_2^2 \right| \leq \delta_k \|\mathbf{P}_T\mathbf{z}\|_2^2 \leq \delta_k \|\mathbf{z}\|_2^2 \quad (5.9)$$

for any set  $T$  such that  $|T| \leq k$  and any  $\mathbf{z} \in \mathbb{R}^d$ . Next we notice that

$$\begin{aligned} \|\mathbf{M}\mathbf{P}_T\mathbf{z}\|_2^2 - \|\mathbf{P}_T\mathbf{z}\|_2^2 &= \mathbf{z}^*\mathbf{P}_T\mathbf{M}^*\mathbf{M}\mathbf{P}_T\mathbf{z} - \mathbf{z}^*\mathbf{P}_T\mathbf{z} \\ &= \mathbf{z}^*\mathbf{P}_T(\mathbf{M}^*\mathbf{M} - \mathbf{I})\mathbf{P}_T\mathbf{z} = \langle \mathbf{P}_T(\mathbf{M}^*\mathbf{M} - \mathbf{I})\mathbf{P}_T\mathbf{z}, \mathbf{z} \rangle. \end{aligned} \quad (5.10)$$

Since  $\mathbf{P}_T(\mathbf{M}^*\mathbf{M} - \mathbf{I})\mathbf{P}_T$  is Hermitian we have that

$$\max_{\mathbf{z}} \frac{\langle \mathbf{P}_T(\mathbf{M}^*\mathbf{M} - \mathbf{I})\mathbf{P}_T\mathbf{z}, \mathbf{z} \rangle}{\|\mathbf{z}\|_2} = \|\mathbf{P}_T(\mathbf{M}^*\mathbf{M} - \mathbf{I})\mathbf{P}_T\|_2. \quad (5.11)$$

Thus we have that the D-RIP implies (5.7) for any set  $T$  such that  $|T| \leq k$ .  $\square$

**Corollary 5.2.4** *If  $\mathbf{M}$  satisfies the D-RIP then*

$$\|\mathbf{P}_{T_1}(\mathbf{I} - \mathbf{M}^*\mathbf{M})\mathbf{P}_{T_2}\|_2 \leq \delta_k, \quad (5.12)$$

for any  $T_1$  and  $T_2$  with  $|T_1| \leq k_1$ ,  $|T_2| \leq k_2$ , and  $k_1 + k_2 \leq k$ .

*Proof:* Since  $T_1 \subset T_1 \cup T_2$  and  $T_2 \subset T_1 \cup T_2$ , we have from Lemma 5.2.3 that

$$\|\mathbf{P}_{T_1}(\mathbf{I} - \mathbf{M}^*\mathbf{M})\mathbf{P}_{T_2}\|_2 \leq \|\mathbf{P}_{T_2 \cup T_1}(\mathbf{I} - \mathbf{M}^*\mathbf{M})\mathbf{P}_{T_2 \cup T_1}\|_2 \leq \delta_k.$$

$\square$

### 5.3 Revisiting $\ell_0$ for Signal Recovery

In Sections 2.2.1 and 2.2.2 uniqueness and stability conditions for representation recovery, using the  $\ell_0$ -minimization, have been presented. Though these conditions are sharp for finding the representation, they are not sharp at all, in terms of finding the signal itself. This can be demonstrated using the following simple example. Let us assume that  $\mathbf{D} = [\mathbf{z}, \mathbf{z}, \dots, \mathbf{z}]$ , a dictionary with columns that are a duplicate of the same atom  $\mathbf{z}$ . Clearly, the signal  $\mathbf{x}=\mathbf{z}$  can be represented by any of the atoms of  $\mathbf{D}$ , which means that it has  $n$  different sparse representations, each with cardinality 1. Thus, for any measurement matrix  $\mathbf{M}$  there is no unique solution to (5.2). Indeed, in this case we have  $\text{spark}(\mathbf{MD}) = 2$  and the uniqueness condition (See Theorem 2.2.2) collapses to the trivial requirement  $\|\alpha\|_0 = 0$ . However, it is clear that if our goal is to recover the signal  $\mathbf{x}$  (i.e.  $\mathbf{D}\alpha$ ) and not its representation  $\alpha$ , then we can certainly have a uniqueness, as all the possible solutions to (5.2) lead to the same signal. Thus, we conclude that for the task of estimating the signal itself, the existing condition is not sharp and a better one should be explored. The same problem repeats also with respect to the stability condition  $\delta_{2k} < 1$  (here  $\delta_{2k}$  refers to the RIP, See Theorem 2.2.4), as it implies the same requirement we have had in the uniqueness case,  $2k < \text{spark}(\mathbf{MD})$ .

The reason that the Spark and RIP conditions for  $\mathbf{MD}$  are not sharp for the signal recovery task is that they are not designed for this purpose. In this section we use an extended Spark and RIP definitions that will serve better the signal recovery problem. The D-RIP [24] is used for having stable recovery conditions for the signal reconstruction. In a similar way, we propose a D-Spark property for the measurement matrix  $\mathbf{M}$ , introducing a new uniqueness condition for the signal recovery. Note that the results in this section are generalization of the ones presented in Sections 2.2.1 and 2.2.2 for the signal's representation. As a general guideline, by setting the measurement matrix to be  $\mathbf{MD}$  and the dictionary to be the identity, the results of this section coincide with the preceding ones.

#### 5.3.1 Uniqueness for Signal Recovery

As in the representation case, we are interested to know when we can guarantee that a signal  $\mathbf{x}$ , with a  $k$ -sparse representation under a matrix  $\mathbf{D}$ , is the unique solution of (5.2). In other words, whether there exists another signal  $\mathbf{x}_1 \neq \mathbf{x}$  with at most  $k$ -sparse representation under  $\mathbf{D}$  such that  $\mathbf{M}\mathbf{x} = \mathbf{M}\mathbf{x}_1$ . For this task we introduce the D-Spark, an extension of the Spark definition.

**Definition 5.3.1** *Given a matrix  $\mathbf{M}$  we define D-spark( $\mathbf{M}$ ) as the smallest possible number of columns*

from  $\mathbf{D}$ , marked as  $T$ , such that  $\text{range}(\mathbf{D}_T) \cap \mathbf{Null}(\mathbf{M}) \neq \{0\}$ .

In other words, for every set  $T$  with size  $|T| < \mathbf{D}\text{-spark}(\mathbf{M})$  we have  $\text{range}(\mathbf{D}_T) \cap \mathbf{Null}(\mathbf{M}) = \{0\}$ , implying that for any vector  $\mathbf{w} \in \mathbb{R}^{|T|}$ ,  $\mathbf{M}\mathbf{D}_T\mathbf{w} = 0$  if and only if  $\mathbf{D}_T\mathbf{w} = 0$ . Note that this definition coincides with the one of the Spark for  $\mathbf{D}=\mathbf{I}$ . This can be observed by noticing that in this case  $\mathbf{D}_T=\mathbf{I}_T$  and thus  $\mathbf{M}\mathbf{D}_T$  simply chooses  $T$  columns from  $\mathbf{M}$ . Thus, the above translates to the requirement that there is no subset of  $|T|$  columns in  $\mathbf{M}$  that are linearly dependent.

Having the  $\mathbf{D}$ -Spark definition, we propose a uniqueness condition for the signal recovery.

**Theorem 5.3.2** *Let  $\mathbf{y} = \mathbf{M}\mathbf{x}$  where  $\mathbf{x}$  has a  $k$ -sparse representation  $\boldsymbol{\alpha}$  under  $\mathbf{D}$ . If  $k < \mathbf{D}\text{-spark}(\mathbf{M})/2$  then  $\mathbf{x} = \mathbf{D}\hat{\boldsymbol{\alpha}}$  for  $\hat{\boldsymbol{\alpha}}$  the minimizer of (5.2), implying a perfect recovery.*

*Proof:* Let us assume the contrary, i.e., there exists a minimizer,  $\hat{\boldsymbol{\alpha}}_1$  for (5.2) such that  $\mathbf{D}\hat{\boldsymbol{\alpha}}_1 \neq \mathbf{D}\hat{\boldsymbol{\alpha}}$ . Let us denote the support sets of  $\hat{\boldsymbol{\alpha}}$  and  $\hat{\boldsymbol{\alpha}}_1$  by  $T$  and  $T_1$  respectively. Since  $\hat{\boldsymbol{\alpha}}$  is a feasible solution to (5.2) and  $\hat{\boldsymbol{\alpha}}_1$  is a minimizer, we have that  $|T_1| \leq |T| \leq k$ . Thus, by definition  $\mathbf{D}\hat{\boldsymbol{\alpha}}_1 - \mathbf{D}\hat{\boldsymbol{\alpha}} \in \text{range}(\mathbf{D}_{T_1 \cup T})$  where  $|T_1 \cup T| \leq 2k$ . Noticing that  $\mathbf{M}\mathbf{D}\hat{\boldsymbol{\alpha}}_1 = \mathbf{M}\mathbf{D}\hat{\boldsymbol{\alpha}}$ , by the constraint of (5.2), we have  $\mathbf{D}\hat{\boldsymbol{\alpha}}_1 - \mathbf{D}\hat{\boldsymbol{\alpha}} \in \mathbf{Null}(\mathbf{M})$ . This contradicts the assumption  $k < \mathbf{D}\text{-spark}(\mathbf{M})/2$  because we get that  $\mathbf{D}\hat{\boldsymbol{\alpha}}_1 - \mathbf{D}\hat{\boldsymbol{\alpha}} \in \text{range}(\mathbf{D}_{T_1 \cup T}) \cap \mathbf{Null}(\mathbf{M}) \neq \{0\}$ , which means that  $\mathbf{D}\text{-spark}(\mathbf{M}) < |T_1 \cup T| \leq 2k$ .  $\square$

Unlike the uniqueness condition of the regular Spark, the one of the  $\mathbf{D}$ -Spark allows linear dependencies within the dictionary  $\mathbf{D}$ . Returning to the example of the dictionary  $\mathbf{D} = [\mathbf{z}, \mathbf{z}, \dots, \mathbf{z}]$ , we have  $\text{range}(\mathbf{D}_T) = \{\beta\mathbf{z}, \beta \in \mathbb{R}\}$  for any non-empty support  $T$ . Thus, the uniqueness condition turns out to be  $\mathbf{z} \notin \mathbf{Null}(\mathbf{M})$ . This means that the matrices  $\mathbf{M}$  that guarantee uniqueness are the ones that have at least one row non-orthogonal to  $\mathbf{z}$ . This is far stronger compared to earlier condition as discussed above.

### 5.3.2 $\ell_0$ -Stability for Signal Recovery

Moving to the noisy case, we seek a generalization of the RIP that provides us with guarantees for the signal recovery. For this task we utilize the D-RIP [24]. As in the representation case, a connection between the D-RIP and the  $\mathbf{D}$ -Spark can be established.

**Proposition 5.3.3** *Given a matrix  $\mathbf{M}$  and sparsity  $k$ , if  $\delta_k < 1$  then  $k < \mathbf{D}\text{-spark}(\mathbf{M})$ .*

*Proof:* Requiring  $\delta_k < 1$  implies that for any vector  $\mathbf{x} \in \text{range}(\mathbf{D}_T)$  such that  $|T| \leq k$  it holds that  $\|\mathbf{M}\mathbf{x}\|_2 \geq (1 - \delta_k) \|\mathbf{x}\|_2 > 0$ , hence  $\mathbf{M}\mathbf{x} \neq 0$ . The last is equivalent to requiring  $\mathbf{Null}(\mathbf{M}) \cap$

$\text{range}(\mathbf{D}_T) = \{0\}$  for any support set  $T$  such that  $|T| \leq k$ , which is exactly equivalent to  $\mathbf{D}$ - $\text{spark}(\mathbf{M}) > k$ .  $\square$

Having the definition of the D-RIP we present a stability guarantee for the signal recovery, which is a particular case of the claims that appear in [57, 95].

**Theorem 5.3.4** *Let  $\mathbf{y} = \mathbf{M}\mathbf{x} + \mathbf{e}$  where  $\|\mathbf{e}\|_2 \leq \varepsilon$ ,  $\mathbf{x}$  has a  $k$ -sparse representation  $\boldsymbol{\alpha}$  under  $\mathbf{D}$ , and  $\mathbf{M}$  satisfies the D-RIP condition with  $\delta_{2k}$ . If  $\delta_{2k} < 1$  then recovering the signal using (5.1), where the recovered signal is  $\hat{\mathbf{x}} = \mathbf{D}\hat{\boldsymbol{\alpha}}$ , is stable:*

$$\|\mathbf{x} - \hat{\mathbf{x}}\|_2 \leq \frac{2\varepsilon}{\sqrt{1 - \delta_{2k}}}. \quad (5.13)$$

*Proof:* Since  $\boldsymbol{\alpha}$ , the representation of  $\mathbf{x}$ , is a feasible solution to (5.1) we have that  $\|\hat{\boldsymbol{\alpha}}\|_0 \leq \|\boldsymbol{\alpha}\|_0 \leq k$ . Thus,  $\mathbf{x} - \hat{\mathbf{x}}$  is a signal that has a  $2k$ -sparse representation. According to the constraint in (5.1) we also have  $\|\mathbf{y} - \mathbf{M}\hat{\mathbf{x}}\|_2 \leq \varepsilon$ . Using the D-RIP, the triangle inequality, and the fact that  $\|\mathbf{y} - \mathbf{M}\mathbf{x}\|_2 \leq \varepsilon$  as well, we get

$$\begin{aligned} \|\mathbf{x} - \hat{\mathbf{x}}\|_2 &\leq \frac{1}{\sqrt{1 - \delta_{2k}}} \|\mathbf{M}(\mathbf{x} - \hat{\mathbf{x}})\|_2 \\ &\leq \frac{1}{\sqrt{1 - \delta_{2k}}} (\|\mathbf{y} - \mathbf{M}\mathbf{x}\|_2 + \|\mathbf{y} - \mathbf{M}\hat{\mathbf{x}}\|_2) \leq \frac{2\varepsilon}{\sqrt{1 - \delta_{2k}}}, \end{aligned} \quad (5.14)$$

which is the stated result.  $\square$

## 5.4 New Coherence Definition

Having a result for the  $\ell_0$ -minimization problem, we turn to study approximation algorithms. The first tool used for treating the classical approximation techniques is the coherence [14]. Thus, we turn to present a generalization of the coherence together with other new related definitions that will aid us in our pursue for having improved guarantees for signal recovery. As in [14], also here the columns of  $\mathbf{M}\mathbf{D}$  are assumed to be normalized, as if this is not the case a simple scaling can be applied.

**Definition 5.4.1 ( $\varepsilon$ -coherence)** *Let  $0 \leq \varepsilon < 1$ ,  $\mathbf{M}$  be a fixed measurement matrix and  $\mathbf{D}$  be a fixed dictionary. The  $\varepsilon$ -coherence  $\mu_\varepsilon(\mathbf{M}, \mathbf{D})$  is defined as*

$$\mu_\varepsilon(\mathbf{M}, \mathbf{D}) = \max_{1 \leq i < j \leq n} |\langle \mathbf{M}\mathbf{d}_i, \mathbf{M}\mathbf{d}_j \rangle| \quad \text{s.t.} \quad \frac{|\langle \mathbf{d}_i, \mathbf{d}_j \rangle|^2}{\|\mathbf{d}_i\|_2^2 \|\mathbf{d}_j\|_2^2} < 1 - \varepsilon^2. \quad (5.15)$$

For calculating  $\mu_\epsilon(\mathbf{M}, \mathbf{D})$ , one may compute the Gram matrices  $\mathbf{G}_{\mathbf{MD}} = \mathbf{D}^* \mathbf{M}^* \mathbf{M} \mathbf{D}$  and  $\mathbf{G}_{\mathbf{D}} = \mathbf{W}_{\mathbf{D}}^{-1} \mathbf{D}^* \mathbf{D} \mathbf{W}_{\mathbf{D}}^{-1}$ , where  $\mathbf{W}_{\mathbf{D}}$  is a diagonal matrix that contains the norms of the columns of  $\mathbf{D}$  on its diagonal, i.e,  $\mathbf{W}_{i,i} = \|\mathbf{d}_i\|_2$ . The  $\epsilon$ -coherence is simply the value of the largest off-diagonal element in absolute value in  $\mathbf{G}_{\mathbf{MD}}$ , corresponding to an entry in  $\mathbf{G}_{\mathbf{D}}$  that is smaller in its absolute value than  $\sqrt{1 - \epsilon^2}$ . Note that for  $\mathbf{D} = \mathbf{I}$ , the  $\epsilon$ -coherence coincides with the regular coherence  $\mu(\mathbf{M})$  and we have  $\mu_\epsilon(\mathbf{M}, \mathbf{I}) = \mu(\mathbf{M})$ . When it is clear to which  $\mathbf{M}$  and  $\mathbf{D}$  we refer, we use simply  $\mu_\epsilon$ .

**Definition 5.4.2 ( $\epsilon$ -independent support set)** Let  $0 \leq \epsilon < 1$ ,  $\mathbf{D}$  be a fixed dictionary. A support set  $T$  is  $\epsilon$ -independent with respect to a dictionary  $\mathbf{D}$  if  $\forall i \neq j \in T, \frac{|\langle \mathbf{d}_i, \mathbf{d}_j \rangle|^2}{\|\mathbf{d}_i\|_2^2 \|\mathbf{d}_j\|_2^2} < 1 - \epsilon^2$ .

**Definition 5.4.3 ( $\epsilon$ -extension)<sup>2</sup>** Let  $0 \leq \epsilon < 1$  and  $\mathbf{D}$  be a fixed dictionary. The  $\epsilon$ -extension of a given support set  $T$  is defined as

$$\text{ext}_{\epsilon,2}(T) = \left\{ i : \exists j \in T, \frac{|\langle \mathbf{d}_i, \mathbf{d}_j \rangle|^2}{\|\mathbf{d}_i\|_2^2 \|\mathbf{d}_j\|_2^2} \geq 1 - \epsilon^2 \right\}.$$

The  $\epsilon$ -extension of a support  $T$  extends it to include each column in  $\mathbf{D}$  which is " $\epsilon$ -correlated" with elements included in  $T$ . Obviously,  $T \subseteq \text{ext}_{\epsilon,2}(T)$ . Note that the last two definitions are related to a given dictionary  $\mathbf{D}$ . If  $\mathbf{D}$  is clear from the context, it is omitted.

## 5.5 $\epsilon$ -Orthogonal Matching Pursuit

We use these new definitions to study the case of very high correlations within pairs of dictionary columns. For this scenario, we propose the  $\epsilon$ -orthogonal matching pursuit ( $\epsilon$ -OMP) presented in Algorithm 6, which is a modification of OMP [37].  $\epsilon$ -OMP is the same as the regular OMP but with the addition of an  $\epsilon$ -extension step in each iteration together with a post processing step at the end of the algorithm. The methods coincide if  $\epsilon = 0$  as OMP's orthogonality property guarantees not selecting the same vector twice and thus the  $\epsilon$ -extension step in  $\epsilon$ -OMP has no effect.

## 5.6 $\epsilon$ -OMP Recovery Guarantees

Turning to present the theoretical guarantee for  $\epsilon$ -OMP, we start with the following lemma.

<sup>2</sup>In [9] it is referred to as  $\epsilon$ -closure but since closure bears a different meaning in mathematics we use a different name here.

**Lemma 5.6.1** Let  $\mathbf{x} = \mathbf{D}\boldsymbol{\alpha}$ ,  $T$  be the support of  $\boldsymbol{\alpha}$ ,  $\tilde{T}$  be a support set such that  $T \subseteq \text{ext}_{\epsilon,2}(\tilde{T})$ ,  $\beta_i = \frac{\langle \mathbf{d}_i, \mathbf{d}_{F(i, \mathbf{D}_{\tilde{T}})} \rangle}{\|\mathbf{d}_{F(i, \mathbf{D}_{\tilde{T}})}\|_2}$  and  $\tilde{i} = F(i, \mathbf{D}_{\tilde{T}})$  is a function of  $i$  such that  $\tilde{i} \in \tilde{T}$  and  $\frac{|\langle \mathbf{d}_i, \mathbf{d}_{\tilde{i}} \rangle|^2}{\|\mathbf{d}_i\|_2^2 \|\mathbf{d}_{\tilde{i}}\|_2^2} \geq 1 - \epsilon^2$ . If there are several possible  $\tilde{i}$  for a given  $i$ , choose any one of those and proceed. For the construction

$$\tilde{\mathbf{x}} = \sum_{i \in T \cap \tilde{T}} \mathbf{d}_i \boldsymbol{\alpha}_i + \sum_{i \in T \setminus \tilde{T}} \beta_i \mathbf{d}_{F(i, \mathbf{D}_{\tilde{T}})} \boldsymbol{\alpha}_i, \quad (5.16)$$

we have

$$\|\mathbf{x} - \tilde{\mathbf{x}}\|_2^2 \leq \left\| \mathbf{W}_{\mathbf{D}_T} \boldsymbol{\alpha}_{T \setminus \tilde{T}} \right\|_1^2 \epsilon^2. \quad (5.17)$$

*Proof:* Note that  $\mathbf{x} - \tilde{\mathbf{x}} = \sum_{i \in T \setminus \tilde{T}} (\mathbf{d}_i - \beta_i \mathbf{d}_{F(i, \mathbf{D}_{\tilde{T}})}) \boldsymbol{\alpha}_i$  and  $\left\| \mathbf{d}_i - \beta_i \mathbf{d}_{F(i, \mathbf{D}_{\tilde{T}})} \right\|_2^2 = \|\mathbf{d}_i\|_2^2 \left( 1 - \frac{|\langle \mathbf{d}_i, \mathbf{d}_{\tilde{i}} \rangle|^2}{\|\mathbf{d}_i\|_2^2 \|\mathbf{d}_{\tilde{i}}\|_2^2} \right) \leq \|\mathbf{d}_i\|_2^2 \epsilon^2$ . The Cauchy-Schwartz inequality with some arithmetics gives

$$\begin{aligned} \|\mathbf{x} - \tilde{\mathbf{x}}\|_2^2 &= \left\| \sum_{i \in T \setminus \tilde{T}} (\mathbf{d}_i - \beta_i \mathbf{d}_{F(i, \mathbf{D}_{\tilde{T}})}) \boldsymbol{\alpha}_i \right\|_2^2 \\ &= \sum_{i, j \in T \setminus \tilde{T}} (\mathbf{d}_i - \beta_i \mathbf{d}_{F(i, \mathbf{D}_{\tilde{T}})})^* (\mathbf{d}_j - \beta_j \mathbf{d}_{F(j, \mathbf{D}_{\tilde{T}})}) \boldsymbol{\alpha}_i \boldsymbol{\alpha}_j \\ &\leq \sum_{i \in T \setminus \tilde{T}} \epsilon^2 \|\mathbf{d}_i\|_2^2 \boldsymbol{\alpha}_i^2 + \sum_{i \neq j \in T \setminus \tilde{T}} \epsilon^2 \|\mathbf{d}_i\|_2 \|\mathbf{d}_j\|_2 \boldsymbol{\alpha}_i \boldsymbol{\alpha}_j. \end{aligned} \quad (5.18)$$

By the definitions of the  $\ell_1$ -norm and  $\mathbf{W}_{\mathbf{D}_T}$  we have that the rhs (right-hand-side) of (5.18) is equal to the rhs of (5.17).  $\square$

**Theorem 5.6.2** Let  $0 \leq \epsilon < 1$ ,  $\mathbf{M}$  be a fixed measurement matrix,  $\mathbf{D}$  be a fixed dictionary with  $\epsilon$ -coherence  $\mu_\epsilon = \mu_\epsilon(\mathbf{M}, \mathbf{D})$  and  $\mathbf{y} = \mathbf{M}\mathbf{x}$  be a set of measurements of  $\mathbf{x} = \mathbf{D}\boldsymbol{\alpha}$  where  $\boldsymbol{\alpha}$  is supported on  $T$  and  $|T| = k$ . Let  $\tilde{T} \subseteq T$  be an  $\epsilon$ -independent set such that  $T \subseteq \text{ext}_{\epsilon,2}(\tilde{T})$  and  $\tilde{\mathbf{x}} = \mathbf{D}\tilde{\boldsymbol{\alpha}}$  is constructed according to (5.16) such that  $\tilde{\boldsymbol{\alpha}}$  is supported on  $\tilde{T}$ . If

$$k < \frac{1}{2} \left( 1 + \frac{1}{\mu_\epsilon} \right) - \frac{2 \|\mathbf{W}_{\mathbf{D}} \tilde{\boldsymbol{\alpha}}\|_1 + \left\| \mathbf{W}_{\mathbf{D}} \boldsymbol{\alpha}_{T \setminus \tilde{T}} \right\|_1}{|\tilde{\boldsymbol{\alpha}}_{\min}| \mu_\epsilon} \sigma_{\mathbf{M}} \epsilon, \quad (5.19)$$

where  $\tilde{\boldsymbol{\alpha}}_{\min}$  is the minimal non-zero entry in absolute value of  $\tilde{\boldsymbol{\alpha}}$ , then after  $k$  iterations at most,  $\hat{\mathbf{x}}_{\epsilon\text{-OMP}}$  satisfies

$$\|\hat{\mathbf{x}}_{\epsilon\text{-OMP}} - \mathbf{x}\|_2^2 \leq \left\| \mathbf{W}_{\mathbf{D}_{T \setminus \tilde{T}}} \boldsymbol{\alpha}_{T \setminus \tilde{T}} \right\|_1^2 \epsilon^2 + \|\mathbf{W}_{\mathbf{D}} \tilde{\boldsymbol{\alpha}}\|_1^2 \epsilon^2. \quad (5.20)$$

In particular, if  $T$  is an  $\epsilon$ -independent set then  $\boldsymbol{\alpha} = \tilde{\boldsymbol{\alpha}}$  and

$$\|\hat{\mathbf{x}}_{\epsilon\text{-OMP}} - \mathbf{x}\|_2^2 \leq \|\mathbf{W}_{\mathbf{D}} \boldsymbol{\alpha}\|_1^2 \epsilon^2. \quad (5.21)$$

**Algorithm 6**  $\epsilon$ -Orthogonal Matching Pursuit ( $\epsilon$ -OMP)

**Input:**  $k, \mathbf{M}, \mathbf{D}, \mathbf{y}$  where  $\mathbf{y} = \mathbf{M}\mathbf{x} + \mathbf{e}$ ,  $\mathbf{x} = \mathbf{D}\boldsymbol{\alpha}$ ,  $\|\boldsymbol{\alpha}\|_0 \leq k$  and  $\mathbf{e}$  is an additive noise.

**Output:**  $\hat{\mathbf{x}}_{\epsilon\text{-OMP}}$ :  $k$ -sparse approximation of  $\mathbf{x}$ .

Initialize estimate  $\hat{\mathbf{x}}^0 = \mathbf{0}$ , residual  $\mathbf{r}^0 = \mathbf{y}$ , support  $\hat{T}^0 = \check{T}^0 = \emptyset$  and set  $t = 0$ .

**while**  $t \leq k$  **do**

$t = t + 1$ .

    New support element:  $i^t = \operatorname{argmax}_{i \notin \check{T}^{t-1}} |\mathbf{d}_i^* \mathbf{M}^* (\mathbf{r}^{t-1})|$ .

    Extend support:  $\hat{T}^t = \hat{T}^{t-1} \cup \{i^t\}$ .

    Calculate a new estimate:  $\hat{\mathbf{x}}_{\epsilon\text{-OMP}}^t = \mathbf{D}_{\hat{T}^t} (\mathbf{M}_{\hat{T}^t})^\dagger \mathbf{y}$ .

    Calculate a new residual:  $\mathbf{r}^t = \mathbf{y} - \mathbf{M} \hat{\mathbf{x}}_{\epsilon\text{-OMP}}^t$ .

    Support  $\epsilon$ -extension:  $\check{T}^t = \operatorname{ext}_{\epsilon,2}(\hat{T}^t)$ .

**end while**

Form the final solution:  $\hat{\mathbf{x}}_{\epsilon\text{-OMP}} = \hat{\mathbf{x}}_{\epsilon\text{-OMP}}^k$ .

Set estimated extended support:  $\check{T} = \check{T}^k$ .

Form the extended final solution:  $\check{\mathbf{x}}_{\epsilon\text{-OMP}} = \mathbf{D}_{\check{T}} (\mathbf{M}_{\check{T}})^\dagger \mathbf{y}$ .

Before proceeding we comment on the role of  $\epsilon$  and  $\tilde{T}$  in the theorem. If two columns are  $\epsilon$ -correlated and we use the regular coherence  $\mu$ , the condition in (5.19) cannot be met. The use of  $\epsilon$ -coherence allows us to ignore these correlations and have a reduced coherence value. Thus, the value of  $\epsilon$  determines the level of correlations the algorithm can handle. Condition (5.19) bounds this level by  $\frac{\frac{1}{2}(\mu_\epsilon + 1) - k\mu_\epsilon}{2\|\mathbf{W}_{\mathbf{D}\tilde{\mathbf{a}}}\|_1 + \|\mathbf{W}_{\mathbf{D}\boldsymbol{\alpha}_{T \setminus \tilde{T}}}\|_1} \frac{|\tilde{\mathbf{a}}_{\min}|}{\sigma_{\mathbf{M}}}$ . Remark that as  $\epsilon$  approaches zero the value of  $\mu_\epsilon$  approaches  $\mu_0$ , a mutual coherence of  $\mathbf{D}$  that ignores the dependent columns.

The set  $\tilde{T}$  is needed in the theorem because the columns of  $\mathbf{D}_T$ , which span  $\mathbf{x}$ , might be  $\epsilon$ -correlated or even dependent. To avoid that, we select the maximal subset of  $T$  which is  $\epsilon$ -independent and still includes  $T$  in its  $\epsilon$ -extension. The construction of such a maximal subset is easy. We start by initializing  $\tilde{T} = T$ , and then sequentially for each index  $i \in \tilde{T}$  update  $\tilde{T} = \tilde{T} \setminus \operatorname{ext}_{\epsilon,2}(\{i\})$ . The resulting subset  $\tilde{T}$  is guaranteed to be  $\epsilon$ -independent and have  $T \subseteq \operatorname{ext}_{\epsilon,2}(\tilde{T})$ .

The following key Lemma is used in the Theorem's proof.

**Lemma 5.6.3** *Under the same setup of Theorem 5.6.2, we have*

$$\tilde{T} \subseteq \check{T}^k = \operatorname{ext}_{\epsilon,2}(\hat{T}^k). \quad (5.22)$$

*Proof:* We prove by induction on the iteration  $t \leq |\tilde{T}| = \tilde{k}$  that either  $\tilde{T} \subseteq \check{T}^t$  or  $\exists i \in \tilde{T}$  such that  $i \in \check{T}^t$  and  $i \notin \check{T}^{t-1}$ . Since the induction guarantees that in each iteration a new element from  $\tilde{T}$  is included in  $\check{T}^t$ , after  $k \geq \tilde{k}$  iterations (5.22) holds.

The basis of the induction is  $t = 1$ . Define  $\tilde{T} = \text{ext}_{\epsilon,2}(\tilde{T})$ . The basis holds if in the first iteration we select an element from  $\tilde{T}$ . This is true due to the fact that  $\forall i, j \in T, i \in \text{ext}_{\epsilon,2}(\{j\})$  iff  $j \in \text{ext}_{\epsilon,2}(\{i\})$ . Thus, we need to require

$$\max_{i \in \tilde{T}} |\mathbf{d}_i^* \mathbf{M}^* \mathbf{y}| > \max_{i \in \tilde{T}^c} |\mathbf{d}_i^* \mathbf{M}^* \mathbf{y}|. \quad (5.23)$$

First note that  $\mathbf{y} = \mathbf{M}\tilde{\mathbf{x}} + \mathbf{M}(\mathbf{x} - \tilde{\mathbf{x}})$ . Thus, using the triangle inequality, the Cauchy-Schwartz inequality and the facts that the  $\ell_2$ -norm is multiplicative and  $\|\mathbf{M}\mathbf{d}_i\|_2 = 1$ , (5.23) holds if

$$\max_{i \in \tilde{T}} |\mathbf{d}_i^* \mathbf{M}^* \mathbf{M}\tilde{\mathbf{x}}| > \max_{i \in \tilde{T}^c} |\mathbf{d}_i^* \mathbf{M}^* \mathbf{M}\tilde{\mathbf{x}}| + 2 \|\mathbf{M}(\mathbf{x} - \tilde{\mathbf{x}})\|_2. \quad (5.24)$$

In order to check when the last happens we shall bound its lhs (left-hand-side) from below and its rhs from above.

Assuming w.l.o.g that the index of the largest entry in  $\tilde{\mathbf{a}}$  is 1, we have for the lhs of (5.24)

$$\begin{aligned} \max_{i \in \tilde{T}} |\mathbf{d}_i^* \mathbf{M}^* \mathbf{M}\tilde{\mathbf{x}}| &\geq |\mathbf{d}_1^* \mathbf{M}^* \mathbf{M}\tilde{\mathbf{x}}| = \left| \sum_{l \in \tilde{T}} \mathbf{d}_1^* \mathbf{M}^* \mathbf{M}\mathbf{d}_l \tilde{\mathbf{a}}_l \right| \\ &\geq |\mathbf{d}_1^* \mathbf{M}^* \mathbf{M}\mathbf{d}_1 \tilde{\mathbf{a}}_1| - \sum_{l \in \tilde{T}, l \neq 1} |\mathbf{d}_1^* \mathbf{M}^* \mathbf{M}\mathbf{d}_l \tilde{\mathbf{a}}_l| \\ &\geq \tilde{\mathbf{a}}_1 - \mu_\epsilon \sum_{l \in \tilde{T}, l \neq 1} |\tilde{\mathbf{a}}_l| = (1 - (\tilde{k} - 1)\mu) |\tilde{\mathbf{a}}_1|, \end{aligned} \quad (5.25)$$

where the first inequality is due to the triangle inequality; the second is due to the fact that  $\|\mathbf{M}\mathbf{d}_i\|_2 = 1$ , the definition of  $\mu_\epsilon$  and the Cauchy-Schwartz inequality; and the last is because  $\tilde{\mathbf{a}}_1$  is the largest element in  $\tilde{\mathbf{a}}$  and  $|\tilde{T}| = \tilde{k}$ .

We turn now to bound the rhs of (5.24) from above. Using the same considerations, we have

$$\begin{aligned} \max_{i \in \tilde{T}^c} |\mathbf{d}_i^* \mathbf{M}^* \mathbf{M}\mathbf{x}| &= \max_{i \in \tilde{T}^c} \left| \sum_{l \in \tilde{T}} \mathbf{d}_i^* \mathbf{M}^* \mathbf{M}\mathbf{d}_l \tilde{\mathbf{a}}_l \right| \\ &\leq \max_{i \in \tilde{T}^c} \sum_{l \in \tilde{T}} |\mathbf{d}_i^* \mathbf{M}^* \mathbf{M}\mathbf{d}_l \tilde{\mathbf{a}}_l| \leq \sum_{l \in \tilde{T}} \mu_\epsilon |\tilde{\mathbf{a}}_l| \leq |\tilde{\mathbf{a}}_1| \tilde{k} \mu_\epsilon. \end{aligned} \quad (5.26)$$

Plugging (5.25) and (5.26) into (5.24) and then using Lemma 5.6.1 with the fact that  $\|\mathbf{M}\|_2 = \sigma_{\mathbf{M}}$  gives us the condition

$$\tilde{k} < \frac{1}{2} \left( 1 + \frac{1}{\mu_\epsilon} \right) - \frac{\sigma_{\mathbf{M}}}{\mu_\epsilon \tilde{\mathbf{a}}_1} \left\| \mathbf{W}_{\mathbf{D}_T} \boldsymbol{\alpha}_{T \setminus \tilde{T}} \right\|_1 \epsilon, \quad (5.27)$$

for selecting an element from  $\tilde{T}$  in the first iteration.

Having the induction basis proven, we turn to the induction step. Assume that the induction assumption holds till iteration  $t - 1$ . We need to prove that it holds also in the  $t$ -th iteration. Let  $\tilde{T}^t = \text{ext}_{\epsilon, 2}(\tilde{T} \setminus \check{T}^{t-1})$ . This set includes the  $\epsilon$ -extension of elements in  $\tilde{T}$  for which an element was not selected in the previous iterations. For proving the induction step it is enough to show that in the  $t$ -th iteration we select an index from  $\tilde{T}^t$ :

$$\max_{i \in \tilde{T}^t} |\mathbf{d}_i^* \mathbf{M}^* \mathbf{r}^{t-1}| > \max_{i \in (\tilde{T}^t)^c \setminus \check{T}^{t-1}} |\mathbf{d}_i^* \mathbf{M}^* \mathbf{r}^{t-1}|. \quad (5.28)$$

On the rhs we do not check the maximum over elements in  $\check{T}^{t-1}$  because  $\epsilon$ -OMP excludes these indices in the step of selecting a new element. As in the basis of the induction, in order to check when (5.28) holds we shall bound its lhs from below and its rhs from above. Let  $\tilde{\mathbf{x}}^{t-1} = \sum_{i \in \tilde{T} \setminus \check{T}^{t-1}} \mathbf{d}_i \tilde{\alpha}_i + \sum_{i \in \check{T}^{t-1}} \beta_i \mathbf{d}_{F(i, D_{\hat{T}^{t-1}})} \tilde{\alpha}_i$  be constructed as in (5.16) where we use the fact that  $\tilde{\alpha}$  is supported on  $\tilde{T}$ . Denoting  $\tilde{\mathbf{r}}^{t-1} = (\mathbf{I} - \mathbf{M} \mathbf{D}_{\hat{T}^{t-1}} (\mathbf{M} \mathbf{D}_{\hat{T}^{t-1}})^\dagger) \mathbf{M} \tilde{\mathbf{x}}^{t-1}$  and using a similar argument like in (5.24) we have that (5.28) holds if

$$\max_{i \in \tilde{T}^t} |\mathbf{d}_i^* \mathbf{M}^* \tilde{\mathbf{r}}^{t-1}| > \max_{i \in (\tilde{T}^t)^c \setminus \check{T}^{t-1}} |\mathbf{d}_i^* \mathbf{M}^* \tilde{\mathbf{r}}^{t-1}| + 2 \left\| \tilde{\mathbf{r}}^{t-1} - \mathbf{r}^{t-1} \right\|_2. \quad (5.29)$$

Notice that  $\tilde{\mathbf{r}}^{t-1}$  is supported on  $\hat{T}^{t-1} \cup (\tilde{T} \setminus \check{T}^{t-1})$ , i.e.,  $\tilde{\mathbf{r}}^{t-1} = \mathbf{M} \mathbf{D}_{\hat{T}^{t-1} \cup (\tilde{T} \setminus \check{T}^{t-1})} \tilde{\alpha}^{\hat{T}^{t-1}}$ , and  $\tilde{\alpha}_{\tilde{T} \setminus \check{T}^{t-1}}^{\hat{T}^{t-1}} = \tilde{\alpha}_{\tilde{T} \setminus \check{T}^{t-1}}$ .

We want to show that the index of the maximal coefficient (in absolute value) of  $\tilde{\mathbf{r}}^{t-1}$  belongs to  $\tilde{T} \setminus \check{T}^{t-1}$  and hence we will be able to use almost the same derivation of the basis of the induction. We prove it by contradiction. Assume that the maximum is achieved for  $i \in \hat{T}^{t-1}$ . By the orthogonality property of the residual it is easy to see that  $\mathbf{d}_i^* \mathbf{M}^* \tilde{\mathbf{r}}^{t-1} = 0$ . Using similar considerations as in (5.25) we have  $0 = |\mathbf{d}_i^* \mathbf{M}^* \tilde{\mathbf{r}}^{t-1}| \geq (1 - (\tilde{k} - 1)\mu_\epsilon) \left| \tilde{\alpha}_i^{\hat{T}^{t-1}} \right|$  which implies  $\tilde{k} \geq 1 + \frac{1}{\mu_\epsilon}$  and we get a contradiction to (5.19).

Let w.l.o.g.  $t$  be the maximal coefficient in  $\tilde{\alpha}_{i_t}^{\hat{T}^{t-1}}$ . By the above observations  $t \in \tilde{T} \setminus \check{T}^{t-1}$  and  $\tilde{\alpha}_i^{\hat{T}^{t-1}} = \tilde{\alpha}_i$ . Applying the same steps as in (5.25) and (5.26), we have

$$\begin{aligned} \max_{i \in \tilde{T}^t} |\mathbf{d}_i^* \mathbf{M}^* \tilde{\mathbf{r}}^{t-1}| &\geq (1 - \mu_\epsilon(\tilde{k} - 1)) |\tilde{\alpha}_t|, \\ \max_{i \in (\tilde{T}^t)^c \setminus \check{T}^{t-1}} |\mathbf{d}_i^* \mathbf{M}^* \tilde{\mathbf{r}}^{t-1}| &\leq \mu_\epsilon \tilde{k} |\tilde{\alpha}_t|. \end{aligned} \quad (5.30)$$

Using norm inequalities and the projection property that implies  $\|\mathbf{I} - \mathbf{M} \mathbf{D}_{\hat{T}^{t-1}} (\mathbf{M} \mathbf{D}_{\hat{T}^{t-1}})^\dagger\|_2 \leq 1$ , we have

$$\left\| \tilde{\mathbf{r}}^{t-1} - \mathbf{r}^{t-1} \right\|_2 \leq \left\| \mathbf{M}(\tilde{\mathbf{x}}^{t-1} - \mathbf{x}) \right\|_2 \leq \sigma_{\mathbf{M}} \left\| \tilde{\mathbf{x}}^{t-1} - \mathbf{x} \right\|_2 \leq \sigma_{\mathbf{M}} \left\| \tilde{\mathbf{x}}^{t-1} - \tilde{\mathbf{x}} \right\|_2 + \sigma_{\mathbf{M}} \left\| \tilde{\mathbf{x}} - \mathbf{x} \right\|_2. \quad (5.31)$$

Using Lemma 5.6.1 with (5.31) and then combining it with (5.29) and (5.30) results with the condition

$$\tilde{k} < \frac{1}{2} + \frac{1}{2\mu_\epsilon} - \frac{\sigma_{\mathbf{M}}\epsilon}{|\tilde{\mathbf{a}}_t|\mu_\epsilon} (\|\mathbf{W}_{\mathbf{D}}\tilde{\mathbf{a}}_{\hat{T}^{t-1}}\|_1 + \|\mathbf{W}_{\mathbf{D}}\boldsymbol{\alpha}_{T\setminus\hat{T}}\|_1). \quad (5.32)$$

The proof ends by noticing that (5.32) is implied by (5.19).  $\square$

*Proof of Theorem 5.6.2:* Note that  $\hat{\mathbf{x}}_{\epsilon\text{-OMP}} = \mathbf{D}_{\hat{T}^k}(\mathbf{M}\mathbf{D}_{\hat{T}^k})^\dagger \mathbf{y}$  and  $\mathbf{y} = \mathbf{M}\mathbf{x}$ . Using some basic algebraic steps we have

$$\begin{aligned} \|\hat{\mathbf{x}}_{\epsilon\text{-OMP}} - \mathbf{x}\|_2 &= \left\| \mathbf{D}_{\hat{T}^k}(\mathbf{M}\mathbf{D}_{\hat{T}^k})^\dagger \mathbf{M}\mathbf{x} - \mathbf{x} \right\|_2 \\ &= \left\| (\mathbf{D}_{\hat{T}^k}(\mathbf{M}\mathbf{D}_{\hat{T}^k})^\dagger \mathbf{M} - \mathbf{I})(\mathbf{I} - \mathbf{D}_{\hat{T}^k}\mathbf{D}_{\hat{T}^k}^\dagger)\mathbf{x} \right\|_2 \\ &\leq \left\| (\mathbf{I} - \mathbf{D}_{\hat{T}^k}\mathbf{D}_{\hat{T}^k}^\dagger)\mathbf{x} \right\|_2, \end{aligned} \quad (5.33)$$

where the last inequality is due to the fact that  $\mathbf{D}_{\hat{T}^k}(\mathbf{M}\mathbf{D}_{\hat{T}^k})^\dagger \mathbf{M} - \mathbf{I}$  is a projection operator and thus its operator norm is smaller or equal to 1. Splitting  $\mathbf{x}$  into  $\tilde{\mathbf{x}}$  and  $\mathbf{x} - \tilde{\mathbf{x}}$ , and then using the triangle inequality and the fact that  $\mathbf{I} - \mathbf{D}_{\hat{T}^k}\mathbf{D}_{\hat{T}^k}^\dagger$  is a projection with (5.33) give

$$\|\hat{\mathbf{x}}_{\text{OMP}} - \mathbf{x}\|_2 \leq \left\| (\mathbf{I} - \mathbf{D}_{\hat{T}^k}\mathbf{D}_{\hat{T}^k}^\dagger)\tilde{\mathbf{x}} \right\|_2 + \|\mathbf{x} - \tilde{\mathbf{x}}\|_2. \quad (5.34)$$

By Lemma 5.6.3, after  $k$  iterations (5.22) holds. Thus, Lemma 5.6.1 implies the existence of a vector  $\hat{\mathbf{z}}^k$ , with a representation supported on  $\hat{T}^k$ , satisfying  $\|\tilde{\mathbf{x}} - \hat{\mathbf{z}}^k\|_2 \leq \|\mathbf{W}_{\mathbf{D}_{\hat{T}^k}}\tilde{\mathbf{a}}\|_1 \epsilon$ . This and projection properties yield for the first element in the rhs

$$\left\| (\mathbf{I} - \mathbf{D}_{\hat{T}^k}\mathbf{D}_{\hat{T}^k}^\dagger)\tilde{\mathbf{x}} \right\|_2 \leq \|\tilde{\mathbf{x}} - \hat{\mathbf{z}}^k\|_2 \leq \|\mathbf{W}_{\mathbf{D}_{\hat{T}^k}}\tilde{\mathbf{a}}\|_1 \epsilon. \quad (5.35)$$

For the second element we have using Lemma 5.6.1

$$\|\mathbf{x} - \tilde{\mathbf{x}}\|_2 \leq \left\| \mathbf{W}_{\mathbf{D}_{T\setminus\hat{T}^k}}\boldsymbol{\alpha}_{T\setminus\hat{T}^k} \right\|_1 \epsilon. \quad (5.36)$$

Plugging (5.36) and (5.35) in (5.34) results with (5.20). Notice that if  $T$  is an  $\epsilon$ -independent set then  $T = \hat{T}$  and (5.21) follows immediately from (5.20) because the first term in its rhs vanishes and in the second one  $\mathbf{W}_{\mathbf{D}_T}\boldsymbol{\alpha}_T = \mathbf{W}_{\mathbf{D}}\boldsymbol{\alpha}$  since  $\boldsymbol{\alpha}_{T^c} = 0$ .  $\square$

**Remark 5.6.4** *Theorem 5.6.2 can be easily extended to the noisy case using the proof technique in [14].*

**Remark 5.6.5** *If for a certain vector  $\mathbf{x}$  supported on  $T$ , we get  $|\hat{T}^k| \leq d$  then the condition in (5.19) in Theorem 5.6.2 implies a perfect recovery for the extended final solution of  $\epsilon$ -OMP,  $\hat{\mathbf{x}}_{\epsilon\text{-OMP}}$ . Due to uniqueness conditions, in this case  $\hat{\mathbf{x}}_{\epsilon\text{-OMP}} = \mathbf{x}$ . It can be easily shown that  $|\text{ext}_{2\epsilon,2}(T)| \leq d$  is a sufficient condition for this to happen.*

**Algorithm 7** Signal Space CoSaMP (SSCoSaMP)

**Input:**  $k, \mathbf{M}, \mathbf{D}, \mathbf{y}, a$  where  $\mathbf{y} = \mathbf{M}\mathbf{x} + \mathbf{e}$ ,  $k$  is the sparsity of  $\mathbf{x}$  under  $\mathbf{D}$  and  $\mathbf{e}$  is the additive noise.

$\mathcal{S}_{ak,1}$  and  $\mathcal{S}_{k,2}$  are two near optimal support selection schemes.

**Output:**  $\hat{\mathbf{x}}$ :  $k$ -sparse approximation of  $\mathbf{x}$ .

Initialize the support  $T^0 = \emptyset$ , the residual  $\mathbf{y}_r^0 = \mathbf{y}$  and set  $t = 0$ .

**while** halting criterion is not satisfied **do**

$t = t + 1$ .

Find new support elements:  $T_\Delta = \mathcal{S}_{ak,1}(\mathbf{M}^* \mathbf{y}_r^{t-1})$ .

Update the support:  $\tilde{T}^t = T^{t-1} \cup T_\Delta$ .

Compute the representation:

$$\mathbf{x}_p = \mathbf{D}(\mathbf{M}\mathbf{D}_{\tilde{T}^t})^\dagger \mathbf{y} = \mathbf{D} \left( \operatorname{argmin}_{\mathbf{w}} \|\mathbf{y} - \mathbf{M}\mathbf{D}\mathbf{w}\|_2^2 \text{ s.t. } \mathbf{w}_{(\tilde{T}^t)^c} = 0 \right).$$

Shrink support:  $T^t = \mathcal{S}_{k,2}(\mathbf{x}_p)$ .

Calculate new representation:  $\mathbf{x}^t = \mathbf{P}_{T^t} \mathbf{x}_p$ .

Update the residual:  $\mathbf{y}_r^t = \mathbf{y} - \mathbf{M}\mathbf{x}^t$ .

**end while**

Form final solution  $\hat{\mathbf{x}} = \mathbf{x}^t$ .

**Remark 5.6.6** From the previous remark we conclude that if for any  $T$  such that  $|T| \leq k$  we have  $|\operatorname{ext}_{2\epsilon,2}(T)| \leq d$  then the algorithm provides us always with a perfect recovery.

**Remark 5.6.7** Theorem 5.6.2 applies also to the regular OMP if  $\frac{|\langle \mathbf{d}_i, \mathbf{d}_j \rangle|^2}{\|\mathbf{d}_i\|_2^2 \|\mathbf{d}_j\|_2^2} < 1 - \epsilon^2$  implies  $|\langle \mathbf{M}\mathbf{d}_i, \mathbf{M}\mathbf{d}_j \rangle|^2 < 1 - \epsilon^2$ . The latter property guarantees that in the step of selecting a new element, OMP does not choose an index from  $\tilde{T}^t$ . For a formal proof, the induction step in Lemma 5.6.3 needs to be modified showing that an element from  $\tilde{T}^t$  is not chosen.

## 5.7 Signal Space Algorithms

Having a result for an OMP variant for the noiseless case using a modified coherence definition, we turn to variants of the greedy-like algorithms. In [108] the *Signal Space CoSaMP* has been proposed. It is shown in Algorithm 7. In the algorithm, the function  $\mathcal{S}_k(\mathbf{y})$  returns the support of the best  $k$ -sparse representation of  $\mathbf{y}$  in the dictionary  $\mathbf{D}$ , and  $\mathbf{P}_T$  denotes the projection onto that support. Note that in [108] only one support selection method has been used within the algorithm, i.e.,  $\mathcal{S}_{k,1} = \mathcal{S}_{k,2}$ . Using two different schemes is a generalization we propose that will aid us later in the theoretical study of SSCOsaMP.

**Algorithm 8** Signal Space Iterative Hard Thresholding (SSIHT)

**Input:**  $k, \mathbf{M}, \mathbf{D}, \mathbf{y}$  where  $\mathbf{y} = \mathbf{MD}\boldsymbol{\alpha} + \mathbf{e}$ ,  $k$  is the cardinality of  $\boldsymbol{\alpha}_0$  and  $\mathbf{e}$  is an additive noise.

**Output:**  $\hat{\mathbf{x}}_{\text{SSIHT}}$ :  $k$ -sparse approximation of  $\mathbf{x}$ .

Initialize estimate  $\mathbf{x}^0 = \mathbf{0}$  and set  $t = 0$ .

**while** halting criterion is not satisfied **do**

$t = t + 1$ .

Perform a gradient step:  $\mathbf{x}_g = \mathbf{x}^{t-1} + \mu^t \mathbf{M}^*(\mathbf{y} - \mathbf{M}\mathbf{x}^{t-1})$

Find a new support:  $T^t = \hat{\mathcal{S}}_k(\mathbf{x}_g)$

Project to get a new estimate:  $\mathbf{x}^t = \mathbf{D}_{T^t} \mathbf{D}_{T^t}^\dagger \mathbf{x}_g$ .

**end while**

Form the final solution  $\hat{\mathbf{x}}_{\text{SSIHT}} = \mathbf{x}^t$ .

Noticing that SSCoSaMP is a variant of ACoSaMP, with the difference that instead of applying the projections in the analysis signal space they are applied in the synthesis signal space, we propose a signal space variant for IHT presented in Algorithm 8. The signal space IHT (SSIHT) emerges from IHT as SSCoSaMP emerges from CoSaMP. We have shown in [8] that SSIHT inherits very similar guarantees to AIHT under the same near-optimality assumptions on the projections used in Chapter 4 for AIHT. Note that the proof technique used in [8] can be adopted to develop new theoretical results for SSCoSaMP that differ from those in [108] and resemble those of ACoSaMP in Chapter 4. However, in this chapter we take a different route.

## 5.8 SSCoSaMP Guarantees

As is evident by Algorithms 7 and 8, we need access to a projection which, given a general vector, finds the closest (in the  $\ell_2$  sense)  $k$ -sparse vector. Recall that in the representation case (when  $\mathbf{D} = \mathbf{I}$ ), simple hard thresholding gives the desired result. However, in the signal space we need to solve

$$\mathcal{S}_k^*(\mathbf{z}) = \underset{|T| \leq k}{\operatorname{argmin}} \|\mathbf{z} - \mathbf{P}_T \mathbf{z}\|_2^2. \quad (5.37)$$

This problem seems to be NP-hard in general, as is the case in the analysis framework [99], so an approximation is needed. Unlike the analysis case, in the signal space setup we are not aware of any non-trivial dictionary (which is not unitary) for which an optimal projection exists. Moreover, the same holds true also with respect to the near-optimal projections used with SSCoSaMP in [108] and SSIHT in [8].

For this reason we propose a new near-optimal projection definition which is an extension of the one given in Section 4.2 and is similar to the one in (5.4) [108].

**Definition 5.8.1** A procedure  $\hat{\mathcal{S}}_{\zeta k}$  implies a near-optimal projection  $\mathbf{P}_{\hat{\mathcal{S}}_{\zeta k}(\cdot)}$  with constants  $C_k$  and  $\tilde{C}_k$  if for any  $\mathbf{z} \in \mathbb{R}^d$ ,  $|\hat{\mathcal{S}}_{\zeta k}(\mathbf{z})| \leq \zeta k$ , with  $\zeta \geq 1$ , and

$$\left\| \mathbf{z} - \mathbf{P}_{\hat{\mathcal{S}}_{\zeta k}(\mathbf{z})} \mathbf{z} \right\|_2^2 \leq C_k \left\| \mathbf{z} - \mathbf{P}_{\mathcal{S}_k^*(\mathbf{z})} \mathbf{z} \right\|_2^2 \quad \text{as well as} \quad \left\| \mathbf{P}_{\hat{\mathcal{S}}_{\zeta k}(\mathbf{z})} \mathbf{z} \right\|_2^2 \geq \tilde{C}_k \left\| \mathbf{P}_{\mathcal{S}_k^*(\mathbf{z})} \mathbf{z} \right\|_2^2, \quad (5.38)$$

where  $\mathbf{P}_{\mathcal{S}_k^*}$  denotes the optimal projection as in (5.37).

We point out some consequences of the definition of near-optimal projections, as in Definition 5.8.1. A clear implication of this definition is that for any vector  $\mathbf{v} \in \mathbb{R}^d$  that has a  $k$ -sparse representation and a support set  $T$  such that  $|T| \leq k$ , and for any  $\mathbf{z} \in \mathbb{R}^d$  we have that

$$\left\| \mathbf{z} - \mathbf{P}_{\hat{\mathcal{S}}_{\gamma k}(\mathbf{z})} \mathbf{z} \right\|_2^2 \leq C_k \|\mathbf{v} - \mathbf{z}\|_2^2, \quad \text{and} \quad (5.39)$$

$$\left\| \mathbf{P}_{\hat{\mathcal{S}}_{\gamma k}(\mathbf{z})} \mathbf{z} \right\|_2^2 \geq \tilde{C}_k \|\mathbf{P}_T \mathbf{z}\|_2^2. \quad (5.40)$$

The constants  $C_k$  and  $\tilde{C}_{2k}$  will play a role in the convergence guarantees we develop for SSCoSAMP. Requirements on the allowed values and the type of dictionaries that has near optimal support selection schemes will be discussed later in Section 5.8.3.

Our main result can now be summarized as follows.

**Theorem 5.8.2** Let  $\mathbf{M}$  satisfy the D-RIP (5.1.1) with a constant  $\delta_{(3\zeta+1)k}$  ( $\zeta \geq 1$ ). Suppose that  $\mathcal{S}_{\zeta k,1}$  and  $\mathcal{S}_{2\zeta k,2}$  are near optimal projections (as in Definition 5.8.1) with constants  $C_k, \tilde{C}_k$  and  $C_{2k}, \tilde{C}_{2k}$  respectively. Apply SSCoSAMP (with  $a = 2$ ) and let  $\mathbf{x}^t$  denote the approximation after  $t$  iterations. If  $\delta_{(3\zeta+1)k} < \epsilon_{C_k, \tilde{C}_{2k}, \gamma}^2$  and

$$(1 + C_k) \left( 1 - \frac{\tilde{C}_{2k}}{(1 + \gamma)^2} \right) < 1, \quad (5.41)$$

then after a constant number of iterations  $t^*$  it holds that

$$\left\| \mathbf{x}^{t^*} - \mathbf{x} \right\|_2 \leq \eta_0 \|\mathbf{e}\|_2, \quad (5.42)$$

where  $\gamma$  is an arbitrary constant, and  $\eta_0$  is a constant depending on  $\delta_{(3\zeta+1)k}$ ,  $C_k$ ,  $\tilde{C}_{2k}$  and  $\gamma$ . The constant  $\epsilon_{C_k, \tilde{C}_{2k}, \gamma}$  is greater than zero if and only if (5.41) holds.

Unlike previous results in the signal space setting, the requirement (5.41) on the near-optimal projections holds in many common sparse approximation settings such as those when the dictionary  $\mathbf{D}$  is incoherent or satisfies the RIP. In those settings, classical recovery methods

may be utilized for the projections. We thus offer an improvement over the existing signal space theoretical guarantees which enforce requirements on the projections which do not even hold when the dictionary is highly incoherent.

In this section we provide theoretical guarantees for the reconstruction performance of SS-CoSaMP. The results here are for the choice of  $a = 2$  in the algorithm, however, analogous results for other values follow similarly. We will prove the main result, Theorem 5.8.2, via Corollary 5.8.4. The proof and discussion of this corollary occupy the remainder of this section.

### 5.8.1 Theorem Conditions

Before we begin the proof of the theorem we first ask under what conditions the assumptions of the theorem hold. One condition of Theorem 5.8.2 is that  $\delta_{2(1+\zeta)k} \leq \epsilon_{C_k, \tilde{C}_{2k}, \gamma}^2$  for a constant  $\epsilon_{C_k, \tilde{C}_{2k}, \gamma}^2 > 0$ . When the dictionary  $\mathbf{D}$  is unitary, it was shown for many families of random matrices that for any value of  $\epsilon_k$ , if  $m \geq \frac{C_{\epsilon_k}}{\epsilon_k^2} k \log(\frac{m}{k\epsilon_k})$  then  $\delta_k \leq \epsilon_k$  [28, 76, 96]. A similar result for the same family of random matrices holds for the D-RIP [24]. Thus, the critical part in the conditions of the Theorem is condition (5.41), that impose a requirement on  $C_k$  and  $\tilde{C}_{2k}$  to be close to 1. We have an access to projection operators that satisfy this condition in many practical settings which are not supported by the guarantees provided in previous papers that used near optimal projections [4, 108, 109]. This is due to the near-optimality definition and the proof technique used in this chapter; A detailed discussion of this subject is left to Section 5.8.3 below.

### 5.8.2 SSCoSaMP Theorem

Analogously to that of CoSaMP in [45], our proof relies on iteration invariant which shows that each iteration substantially reduces the recovery error.

**Theorem 5.8.3** *Let  $\mathbf{M}$  satisfy the D-RIP (5.1.1) with constants  $\delta_{(\zeta+1)k}, \delta_{3\zeta k}, \delta_{(3\zeta+1)k}$  and let  $S_{\zeta k, 1}$  and  $S_{2\zeta k, 2}$  be near optimal projections as in Definition 5.8.1 with constants  $C_k, \tilde{C}_k$  and  $C_{2k}, \tilde{C}_{2k}$  respectively. Then*

$$\|\mathbf{x}^t - \mathbf{x}\|_2 \leq \rho \|\mathbf{x}^{t-1} - \mathbf{x}\|_2 + \eta \|\mathbf{e}\|_2, \quad (5.43)$$

for constants  $\rho$  and  $\eta$ . The iterates converge, i.e.  $\rho < 1$ , if  $\delta_{(3\zeta+1)k} < \epsilon_{C_k, \tilde{C}_{2k}, \gamma}^2$ , for some positive constant  $\epsilon_{C_k, \tilde{C}_{2k}, \gamma}^2$ , and (5.41) holds.

An immediate corollary of the above theorem is the following

**Corollary 5.8.4** *Assume the conditions of Theorem 5.8.3. Then after a constant number of iterations*

$t^* = \left\lceil \frac{\log(\|\mathbf{x}\|_2/\|\mathbf{e}\|_2)}{\log(1/\rho)} \right\rceil$  *it holds that*

$$\|\mathbf{x}^{t^*} - \mathbf{x}\|_2 \leq \left(1 + \frac{1 - \rho^{t^*}}{1 - \rho}\right) \eta \|\mathbf{e}\|_2. \quad (5.44)$$

*Proof:* By using (5.43) and recursion we have that after  $t^*$  iterations

$$\|\mathbf{x}^{t^*} - \mathbf{x}\|_2 \leq \rho^{t^*} \|\mathbf{x} - \mathbf{x}^0\|_2 + (1 + \rho + \rho^2 + \dots + \rho^{t^*-1}) \eta \|\mathbf{e}\|_2 \leq \left(1 + \frac{1 - \rho^{t^*}}{1 - \rho}\right) \eta \|\mathbf{e}\|_2, \quad (5.45)$$

where the last inequality is due to the equation of the geometric series, the choice of  $t^*$ , and the fact that  $\mathbf{x}^0 = \mathbf{0}$ .  $\square$

Note that Corollary 5.8.4 implies our main result, Theorem 5.8.2, with  $\eta_0 = \left(1 + \frac{1 - \rho^{t^*}}{1 - \rho}\right) \eta$ .

We turn now to prove the iteration invariant, Theorem 5.8.3. Instead of presenting the proof directly, we divide the proof into several lemmas. The first lemma gives a bound for  $\|\mathbf{x}_p - \mathbf{x}\|_2$  as a function of  $\|\mathbf{e}\|_2$  and  $\|\mathbf{Q}_{\tilde{T}^t}(\mathbf{x}_p - \mathbf{x})\|_2$ .

**Lemma 5.8.5** *If  $\mathbf{M}$  has the D-RIP with a constant  $\delta_{3\zeta k}$ , then with the notation of Algorithm 7, we have*

$$\|\mathbf{x}_p - \mathbf{x}\|_2 \leq \frac{1}{\sqrt{1 - \delta_{(3\zeta+1)k}^2}} \|\mathbf{Q}_{\tilde{T}^t}(\mathbf{x}_p - \mathbf{x})\|_2 + \frac{\sqrt{1 + \delta_{3\zeta k}}}{1 - \delta_{(3\zeta+1)k}} \|\mathbf{e}\|_2 \quad (5.46)$$

The second lemma bounds  $\|\mathbf{x}^t - \mathbf{x}\|_2$  in terms of  $\|\mathbf{Q}_{\tilde{T}^t}(\mathbf{x}_p - \mathbf{x})\|_2$  and  $\|\mathbf{e}\|_2$  using the first lemma.

**Lemma 5.8.6** *Given that  $\mathcal{S}_{\zeta k, 2}$  is a near support selection scheme with a constant  $C_k$ , if  $\mathbf{M}$  has the D-RIP with a constant  $\delta_{(3\zeta+1)k}$ , then*

$$\|\mathbf{x}^t - \mathbf{x}\|_2 \leq \rho_1 \|\mathbf{Q}_{\tilde{T}^t}(\mathbf{x}_p - \mathbf{x})\|_2 + \eta_1 \|\mathbf{e}\|_2 \quad (5.47)$$

The last lemma bounds  $\|\mathbf{Q}_{\tilde{T}^t}(\mathbf{x}_p - \mathbf{x})\|_2$  with  $\|\mathbf{x}^{t-1} - \mathbf{x}\|_2$  and  $\|\mathbf{e}\|_2$ .

**Lemma 5.8.7** *Given that  $\mathcal{S}_{2\zeta k, 1}$  is a near optimal support selection scheme with a constant  $\tilde{C}_{2k}$ , if  $\mathbf{M}$  has the D-RIP with constants  $\delta_{(3\zeta+1)k}$  and  $\delta_{2\zeta k}$  then*

$$\|\mathbf{Q}_{\tilde{T}^t}(\mathbf{x}_p - \mathbf{x})\|_2 \leq \eta_2 \|\mathbf{e}\|_2 + \rho_2 \|\mathbf{x} - \mathbf{x}^{t-1}\|_2. \quad (5.48)$$

The proofs of Lemmas 5.8.5, 5.8.6 and 5.8.7 appear in Appendices C.1, C.2 and C.3, respectively. With the aid of the above three lemmas we turn to the proof of the iteration invariant, Theorem 5.8.3.

*Proof of Theorem 5.8.3:* Substituting the inequality of Lemma 5.8.7 into the inequality of Lemma 5.8.6 gives (5.43) with  $\rho = \rho_1\rho_2$  and  $\eta = \eta_1 + \rho_1\eta_2$ . The iterates converge if  $\rho_1^2\rho_2^2 < 1$ . Since  $\delta_{(\zeta+1)k} \leq \delta_{3\zeta k} \leq \delta_{(3\zeta+1)k}$  this holds if

$$\left( \frac{1 + 2\delta_{(3\zeta+1)k}\sqrt{C_k} + C_k}{1 - \delta_{(3\zeta+1)k}^2} \right) \cdot \left( 1 - \left( \left( \frac{\sqrt{\tilde{C}_{2k}}}{1 + \gamma} + 1 \right) \sqrt{\delta_{(3\zeta+1)k}} - \frac{\sqrt{\tilde{C}_{2k}}}{1 + \gamma} \right)^2 \right) < 1. \quad (5.49)$$

Since  $\delta_{(3\zeta+1)k} < 1$ , we have  $\delta_{(3\zeta+1)k}^2 < \delta_{(3\zeta+1)k} < \sqrt{\delta_{(3\zeta+1)k}}$ . Using this fact and expanding (5.49) yields the stricter condition

$$\begin{aligned} & \left( (1 + C_k) \left( 1 - \left( \frac{\sqrt{\tilde{C}_{2k}}}{1 + \gamma} \right)^2 \right) - 1 \right) + 2(1 + C_l) \left( \frac{\sqrt{\tilde{C}_{2k}}}{1 + \gamma} \right) \left( \frac{\sqrt{\tilde{C}_{2k}}}{1 + \gamma} + 1 \right) \sqrt{\delta_{(3\zeta+1)k}} \\ & + \left( 2\sqrt{C_k} \left( 1 - \left( \frac{\sqrt{\tilde{C}_{2l-p}}}{1 + \gamma} \right)^2 \right) - (1 + C_l) \left( 1 + \frac{\sqrt{\tilde{C}_{2k}}}{1 + \gamma} \right)^2 \right. \\ & \quad \left. + 4\sqrt{C_k} \left( \frac{\sqrt{\tilde{C}_{2k}}}{1 + \gamma} \right) \left( \frac{\sqrt{\tilde{C}_{2k}}}{1 + \gamma} + 1 \right) + 2 \right) \delta_{(3\zeta+1)k} < 0. \end{aligned} \quad (5.50)$$

The above equation has a positive solution if and only if (5.41) holds. Denoting its positive solution by  $\epsilon_{C_k, \tilde{C}_{2k}, \gamma}$  we have that the expression holds when  $\delta_{(3\zeta+1)k} \leq \epsilon_{C_k, \tilde{C}_{2k}, \gamma}^2$ , which completes the proof. Note that in the proof we have

$$\begin{aligned} \eta_1 &= \frac{\sqrt{\frac{2+C_k}{1+C_k}} + 2\sqrt{C_k} + C_k\sqrt{1 + \delta_{3\zeta k}}}{1 - \delta_{(3\zeta+1)k}}, & \eta_2 &= \left( \frac{1 + \delta_{3\zeta k}}{\gamma(1 + \alpha)} + \frac{(1 + \delta_{(\zeta+1)k})\tilde{C}_{2k}}{\gamma(1 + \alpha)(1 + \gamma)} \right), \\ \rho_1^2 &= \frac{1 + 2\delta_{(3\zeta+1)k}\sqrt{C_k} + C_k}{1 - \delta_{(3\zeta+1)k}^2}, & \rho_2^2 &= 1 - \left( \sqrt{\delta_{(3\zeta+1)k}} - \frac{\sqrt{\tilde{C}_{2k}}}{1 + \gamma} \left( 1 - \sqrt{\delta_{(\zeta+1)k}} \right) \right)^2, \\ \alpha &= \frac{\sqrt{\delta_{(3\zeta+1)k}}}{\sqrt{\frac{\tilde{C}_{2k}}{(1+\gamma_1)(1+\gamma_2)} \left( 1 - \sqrt{\delta_{(\zeta+1)k}} \right) - \sqrt{\delta_{(3\zeta+1)k}}}} \end{aligned}$$

and  $\gamma > 0$  is an arbitrary constant. □

### 5.8.3 Near Optimal Projection Examples

In this part we give several examples for which condition (5.41),

$$(1 + C_k) \left( 1 - \frac{\tilde{C}_{2k}}{(1 + \gamma)^2} \right) < 1,$$

can be satisfied with accessible projection methods.

### Unitary Dictionaries

For unitary  $\mathbf{D}$  the conditions hold trivially since  $C_k = \tilde{C}_{2k} = 1$  using simple thresholding. In this case our results coincide with the standard representation model for which we already have theoretical guarantees [39]. However, for a general dictionary  $\mathbf{D}$  simple thresholding is not expected to have this property.

### RIP Dictionaries

We next consider the setting in which the dictionary  $\mathbf{D}$  itself satisfies the RIP. In this case we may use a standard method like IHT or CoSaMP for  $\mathcal{S}_{k,1}$  and simple thresholding for  $\mathcal{S}_{2k,1}$ . Note that  $\zeta = 1$  in this case. For dictionaries that satisfy the RIP, it is easy to use existing results in order to derive bounds on the constant  $C_k$ .

In order to see how such bounds can be achieved, notice that standard bounds exists for these techniques in terms of the representation error rather than the signal error. That is, for a given vector  $\mathbf{v} = \mathbf{D}\boldsymbol{\alpha} + \mathbf{e}$  and any support set  $T^*$  of size  $k$ , it is guaranteed that if  $\delta_{4k} \leq 0.1$  (or  $\delta_{3k} \leq \frac{1}{\sqrt{32}}$ ) then  $\hat{\boldsymbol{\alpha}}$ , the recovered representation of CoSaMP (or IHT), satisfies

$$\|\boldsymbol{\alpha} - \hat{\boldsymbol{\alpha}}\|_2 \leq C_e \|\mathbf{v} - \mathbf{P}_{T^*}\mathbf{v}\|_2, \quad (5.51)$$

where  $C_e \simeq 5.6686$  (or  $C_e \simeq 3.3562$ ) [45, 39, 41].

We use this result to bound  $C_k$  as follows. For a general vector  $\mathbf{v}$  we may write its optimal projection as  $\mathbf{P}_{T^*}\mathbf{v} = \mathbf{D}\boldsymbol{\alpha}$  with  $\text{supp}(\boldsymbol{\alpha}) = T^*$ . Applying the bound in (5.51) with  $\mathbf{e} = \mathbf{v} - \mathbf{P}_{T^*}\mathbf{v}$  and  $\mathbf{P}_{\hat{T}}\mathbf{v} = \mathbf{D}\hat{\boldsymbol{\alpha}}$  along with the RIP yields

$$\begin{aligned} \|\mathbf{v} - \mathbf{P}_{\hat{T}}\mathbf{v}\|_2 &\leq \|\mathbf{v} - \mathbf{P}_{T^*}\mathbf{v}\|_2 + \|\mathbf{P}_{T^*}\mathbf{v} - \mathbf{P}_{\hat{T}}\mathbf{v}\|_2 \\ &= \|\mathbf{v} - \mathbf{P}_{T^*}\mathbf{v}\|_2 + \|\mathbf{D}\boldsymbol{\alpha} - \mathbf{D}\hat{\boldsymbol{\alpha}}\|_2 \\ &\leq \|\mathbf{v} - \mathbf{P}_{T^*}\mathbf{v}\|_2 + \sqrt{1 + \delta_{2k}} \|\boldsymbol{\alpha} - \hat{\boldsymbol{\alpha}}\|_2 \\ &\leq \|\mathbf{v} - \mathbf{P}_{T^*}\mathbf{v}\|_2 + C_e \sqrt{1 + \delta_{2k}} \|\mathbf{v} - \mathbf{P}_{T^*}\mathbf{v}\|_2. \end{aligned} \quad (5.52)$$

This implies that

$$C_k \leq 1 + C_e \sqrt{1 + \delta_{2k}}. \quad (5.53)$$

For example, if  $\delta_{4k} \leq 0.1$  then  $C_k \leq 6.9453$  for CoSaMP and if  $\delta_{3k} \leq \frac{1}{\sqrt{32}}$  then  $C_k \leq 4.6408$  for IHT. The inequality in (5.53) holds true not only for CoSaMP and IHT but for any algorithm that provides a  $k$ -sparse representation that obeys the bound in (5.51). Note that many

greedy algorithms have these properties (e.g. [42, 40, 44]), but relaxation techniques such as  $\ell_1$ -minimization [29] or the Dantzig selector [30] are not guaranteed to give a  $k$ -sparse result.

Having a bound for  $C_k$ , we realize that in order to satisfy (5.41) we now have a condition on the second constant,

$$\tilde{C}_{2k} \geq \left(1 - \frac{1}{1 + C_k}\right) (1 + \gamma)^2. \quad (5.54)$$

In order to show that this condition can be satisfied we provide an upper bound for  $\tilde{C}_{2k}$  which is a function of the RIP constants of  $\mathbf{D}$ . The near-optimal projection can be obtained by simple thresholding under the image of  $\mathbf{D}^*$ :

$$\mathcal{S}_{k,2}(\mathbf{v}) = \underset{|T|=k}{\operatorname{argmin}} \|\mathbf{D}_T^* \mathbf{v}\|_2. \quad (5.55)$$

**Lemma 5.8.8 (Thresholding Projection RIP bound)** *If  $\mathbf{D}$  is a dictionary that satisfies the RIP with a constant  $\delta_k$ , then using (5.55) as the thresholding projector yields*

$$\tilde{C}_k \geq \frac{1 - \delta_k}{1 + \delta_k}.$$

*Proof:* Let  $\mathbf{v}$  be a general vector. Let  $\hat{T}$  be the indices of the largest  $k$  entries of  $\mathbf{D}^* \mathbf{v}$  and  $T^*$  the support selected by the optimal support selection scheme as in (5.37). By definition we have that

$$\|\mathbf{D}_{\hat{T}}^* \mathbf{v}\|_2^2 \geq \|\mathbf{D}_{T^*}^* \mathbf{v}\|_2^2. \quad (5.56)$$

Since  $\frac{1}{1 + \delta_k} \leq \|(\mathbf{D}_{\hat{T}}^*)^\dagger\|_2^2 \leq \frac{1}{1 - \delta_k}$  for  $|T| \leq k$  (see Prop. 3.1 of [39]), we have that

$$(1 + \delta_k) \left\| (\mathbf{D}_{\hat{T}}^*)^\dagger \mathbf{D}_{\hat{T}}^* \mathbf{v} \right\|_2^2 \geq (1 - \delta_k) \left\| (\mathbf{D}_{T^*}^*)^\dagger \mathbf{D}_{T^*}^* \mathbf{v} \right\|_2^2. \quad (5.57)$$

Since  $\mathbf{P}_{\hat{T}} = (\mathbf{D}_{\hat{T}}^*)^\dagger \mathbf{D}_{\hat{T}}^*$  we get that

$$\|\mathbf{P}_{\hat{T}} \mathbf{v}\|_2^2 \geq \frac{1 - \delta_k}{1 + \delta_k} \|\mathbf{P}_{T^*} \mathbf{v}\|_2^2. \quad (5.58)$$

Thus  $\tilde{C}_k \geq \frac{1 - \delta_k(\mathbf{D})}{1 + \delta_k(\mathbf{D})}$ . □

Hence, the condition on the RIP of  $\mathbf{D}$  for satisfying (5.41) turns to be

$$\frac{1 - \delta_{2k}}{1 + \delta_{2k}} \geq \left(1 - \frac{1}{1 + C_k}\right) (1 + \gamma)^2. \quad (5.59)$$

By using the exact expression for  $C_k$  in terms of RIP constants, one can obtain guarantees in terms of the RIP constants only. For example, from [39], for CoSaMP one has more precisely that for any vector  $\boldsymbol{\alpha}$ , the reconstructed vector  $\hat{\boldsymbol{\alpha}}$  from measurements  $\mathbf{z} = \mathbf{D}\boldsymbol{\alpha} + \mathbf{e}$  satisfies

$$\|\boldsymbol{\alpha} - \hat{\boldsymbol{\alpha}}\|_2 \leq \left[ \frac{2}{\sqrt{1 - \delta_{3k}}} + 4 \left(1 + \frac{\delta_{4k}}{1 - \delta_{3k}}\right) \cdot \frac{1}{\sqrt{1 - \delta_{2k}}} \right] \|\mathbf{e}\|_2.$$

Using (5.53) we have

$$C_k \leq 1 + \sqrt{1 + \delta_{2k}} \left[ \frac{2}{\sqrt{1 - \delta_{3k}}} + 4 \left( 1 + \frac{\delta_{4k}}{1 - \delta_{3k}} \right) \cdot \frac{1}{\sqrt{1 - \delta_{2k}}} \right]. \quad (5.60)$$

Substituting this into the expression (5.59) gives a bound on the RIP constants alone. For example, setting  $\gamma = 0.01$ , one finds that the requirement  $\delta_{4k} \leq 0.052$  is enough to guarantee (5.41) holds using CoSaMP.

### Incoherent Dictionaries

Given that a dictionary  $\mathbf{D}$  has a coherence  $\mu$ , it is known that the RIP constant can be upper bounded by  $\mu$  in the following way [110]

$$\delta_k \leq (k - 1)\mu. \quad (5.61)$$

Hence, using this relation one may get recovery conditions based on the coherence value using the conditions from the previous subsection. For example, if we use CoSaMP for the first projection and thresholding for the second one, one may have the following condition in terms of the coherence (instead of the RIP):  $\mu \leq \frac{0.052}{4k-1}$ .

### Support Selection using Highly Correlated Dictionaries

In all the above cases, the dictionary is required to be incoherent. This follows from the simple fact that decoding under a coherent dictionary is a hard problem in general. However, in some cases we have a coherent dictionary in which each atom has a high correlation with a small number of other atoms and very small correlation with all the rest. In this case, the high coherence is due to these rare high correlations and pursuit algorithms may fail to select the right atoms in their support estimate as they may be confused between the right atom and its highly correlated columns. Hence, one may update the pursuit strategies to add in each of their steps only atoms which are not highly correlated with the current selected atoms and as a final stage extend the estimated support to include all the atoms which have high coherence with the selected support set.

This idea is related to the recent literature of super-resolution (see e.g. [111, 112, 113, 114, 115] and references therein) and to the  $\epsilon$ -OMP algorithm presented above in Section 5.5. We employ  $\epsilon$ -OMP with  $\mathbf{M} = \mathbf{I}$  as a support selection procedure (we use its extended estimated support  $\check{T}$ ). We also propose a similar extension for thresholding,  $\epsilon$ -thresholding, for the case  $\mathbf{M} = \mathbf{I}$  that for a given signal  $\mathbf{z}$ , selects the support in the following way. It picks the indices

**Algorithm 9**  $\epsilon$ -thresholding

**Input:**  $k, \mathbf{D}, \mathbf{z}$  where  $\mathbf{z} = \mathbf{x} + \mathbf{e}$ ,  $\mathbf{x} = \mathbf{D}\boldsymbol{\alpha}$ ,  $\|\boldsymbol{\alpha}\|_0 \leq k$  and  $\mathbf{e}$  is an additive noise.

**Output:**  $\hat{\mathbf{x}}$ : a  $k$ -sparse approximation of  $\mathbf{x}$  supported on  $\hat{T}$ .

Initialize support  $\hat{T}^0 = \check{T}^0 = \emptyset$  and set  $t = 0$ .

Calculate correlation between dictionary and measurements:  $\mathbf{v} = \mathbf{D}^*\mathbf{z}$ .

**while**  $t \leq k$  **do**

$t = t + 1$ .

New support element:  $i^t = \operatorname{argmax}_{i \notin \hat{T}^{t-1}} |\mathbf{v}_i|$ .

Extend support:  $\hat{T}^t = \hat{T}^{t-1} \cup \{i^t\}$ .

Support  $\epsilon$ -extension:  $\check{T}^t = \operatorname{ext}_{\epsilon,2}(\hat{T}^t)$ .

**end while**

Set estimated support  $\hat{T} = \check{T}^t$ .

Form the final solution  $\hat{\mathbf{x}} = \mathbf{D}_{\hat{T}}\mathbf{D}_{\hat{T}}^\dagger\mathbf{z}$ .

of the largest elements of  $\mathbf{D}^*\mathbf{z}$  one at a time, where at each time it adds the atom with highest correlation to  $\mathbf{z}$  excluding the already selected ones. Each atom is added together with its highly correlated columns. We present the  $\epsilon$ -Thresholding technique in Algorithm 9.

Note that the size of the group of atoms which are highly correlated with one atom of  $\mathbf{D}$  is bounded. The size of the largest group is an upper bound for the near-optimality constant  $\zeta$ . More precisely, if the allowed high correlations are greater than  $1 - \epsilon^2$  then we have the upper bound

$$\zeta \leq \max_{T:|T| \leq k} |\operatorname{ext}_{\epsilon,2}(T)| \leq \max_{1 \leq i \leq n} k |\operatorname{ext}_{\epsilon,2}(\{i\})|.$$

We have a trade-off between the size of the correlation which we can allow and the size of the estimated support which we get. The smaller the correlation between columns we allow, the larger  $\zeta$  is and thus also the estimated support. On the one hand, this attribute is positive; the larger the support, the higher the probability that our near-optimality constants  $C_k$  and  $\tilde{C}_k$  are close to 1. On the other hand, for large  $\zeta$ ,  $\delta_{(3\zeta+1)k}$  is larger and it is harder to satisfy the RIP requirements. Hence we expect that if the number of measurements is small, the size of  $\zeta$  would be more critical as it would be harder to satisfy the RIP condition. When the number of measurements gets higher, the RIP requirement is easier to satisfy and can handle higher values of  $\zeta$ .

One trivial example, in which the above projections have known near-optimality constants is when  $\mathbf{D}$  is an incoherent dictionary with one or more repeated columns. In this case, the

projection constants of  $\mathbf{D}$  are simply the ones of the underlying incoherent dictionary.

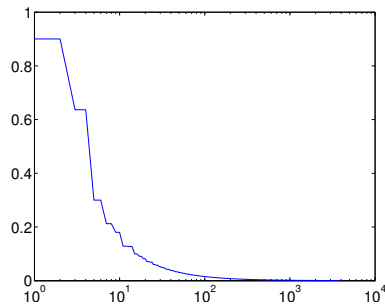


Figure 5.1: Correlation size (inner product) in a sorted order of one atom of the 4 times redundant-DFT dictionary with the other atoms. Note that the x-axis is in a log-scale.

In other cases we still do not have guarantees for these constants. Though we have guarantees for  $\epsilon$ -OMP in the case of high correlations in the dictionary  $\mathbf{D}$ , these impose requirements on the magnitude of the signal coefficients which we do not have control of in the projection problem. Hence, the existing recovery guarantees for  $\epsilon$ -OMP cannot be used for developing bounds for the near-optimal projection constants.

Though theoretical statements are not at hand yet, we shall see that these methods give good recovery in practice. Clearly, we need each atom in  $\mathbf{D}$  to be highly correlated only with a small group of other columns and incoherent with all the rest. An example of such a dictionary is the overcomplete-DFT which is a highly coherent dictionary. The correlations between each atom in this dictionary and its neighboring atoms are the same, i.e., each of the diagonals of its Gram matrix have the same value. A plot of the coherence value of a given atom with its neighbors in a sorted order appears in Fig. 5.1 for a four times overcomplete DFT and signal dimension  $d = 1024$ .

Note that when we determine a correlation to be high, if the inner product (atoms are normalized) between two atoms is greater than 0.9 ( $\epsilon = \sqrt{0.1}$ ), we get that each atom has two other highly correlated columns with correlation of size 0.9. The correlation with the rest is below 0.64, where the largest portion has inner products smaller than 0.1.

## 5.9 Experimental Results

We repeat the experiments from [108] for the overcomplete-DFT with redundancy factor 4 and check the effect of the new support selection methods both for the case where the signal coefficients are clustered and the case where they are well separated. We compare the performance

of OMP,  $\epsilon$ -OMP (we use its extended estimate  $\check{\mathbf{x}}_{\epsilon\text{-OMP}}$ , see Algorithm 6) and  $\epsilon$ -thresholding for the approximate projections. We do not include other methods since a thorough comparison has been already performed in [108], and the goal here is to check the effect of the  $\epsilon$ -extension step.

The recovery results appear in Figures 5.2–5.4. As seen from Figure 5.2, in the separated case SSCoSaMP-OMP works better for small values of  $m$ . This is likely because it uses a smaller support set for which it is easier to satisfy the RIP condition. As separated atoms are very uncorrelated it is likely that OMP will not be confused between them. When the atoms are clustered, the high correlations take more effect and OMP is not able to recovery the right support because of the high coherence between close atoms in the cluster and around it. This is overcome by using  $\epsilon$ -OMP which uses larger support sets and thus resolves the confusion. Note that even  $\epsilon$ -thresholding gets better recovery in this case, though it is a much simpler technique, and this shows that indeed the improvement is due to the extended support selection strategy. As expected, using larger support estimates for the projection is more effective when the number of measurements  $m$  is large.

We may say that the support extension step leads to a better recovery rate overall as it gets a good recovery on both the separated and clustered coefficient cases. In [108] it is shown that all the projection algorithms either perform well on the first case and very bad on the other or vice versa. Using SSCoSaMP with  $\epsilon$ -OMP we have, at the cost of getting slightly inferior behavior in the separated case compared to SSCoSaMP with OMP, much improved behavior for the clustered case where the latter gets no recovery at all.

Figures 5.3–5.4 demonstrate the sensitivity of the approximation algorithms to the choice of  $\epsilon$  (note that  $\epsilon = 0$  reverts to the Thresholding/OMP algorithm). While it is clear that  $\epsilon$  cannot be too large (or far too many atoms will be included), the optimum choice of  $\epsilon$  may not always be easy to identify since it depends on the dictionary  $\mathbf{D}$ .

## 5.10 Discussion and Summary

In this chapter we have studied the  $\ell_0$ -synthesis problem for signal recovery in the case of a general dictionary  $\mathbf{D}$ . We have shown that in the case where  $\mathbf{D}$  contains linear dependencies signal recovery is still theoretically plausible if the signal is the target and not its representation. We derived theoretical conditions for uniqueness of the solution in the noiseless case and stability for the noisy case.

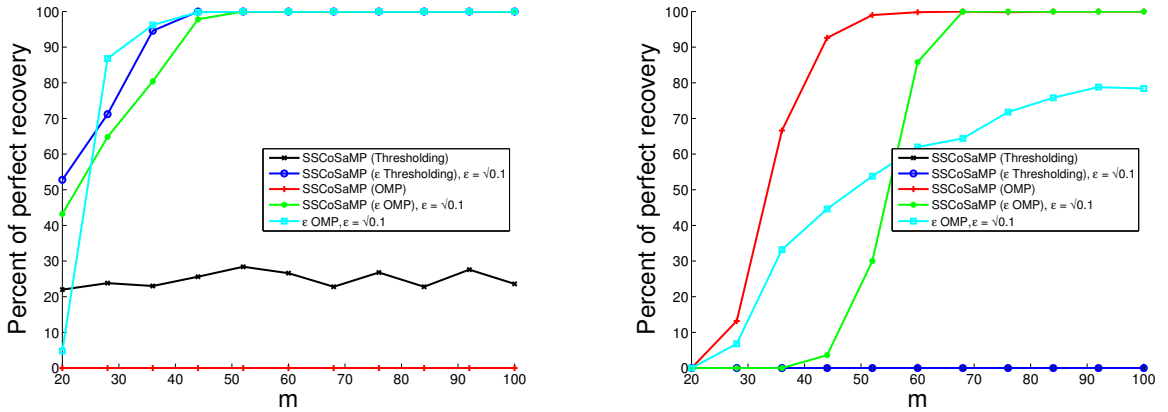


Figure 5.2: Recovery rate for SSSCoSaMP (Thresholding), SSSCoSaMP ( $\epsilon$ -Thresholding) with  $\epsilon = \sqrt{0.1}$ , SSSCoSaMP (OMP), SSSCoSaMP ( $\epsilon$ -OMP) with  $\epsilon = \sqrt{0.1}$  and  $\epsilon$ -OMP with  $\epsilon = \sqrt{0.1}$  for a random  $m \times 1024$  Gaussian matrix  $\mathbf{M}$  and a 4 times overcomplete DFT matrix  $\mathbf{D}$ . The signal is 8-sparse and on the left the coefficients of the original signal are clustered whereas on the right they are separated.

Since the  $\ell_0$ -problem is non-feasible in most applications, approximation techniques are of vital importance. For this purpose we have adapted representation based greedy and greedy-like methods to signal recovery.

We have proposed a variant of the OMP algorithm – the  $\epsilon$ -OMP method – for recovering signals with sparse representations under dictionaries with pairs of highly correlated columns. We have shown, both theoretically and empirically, that  $\epsilon$ -OMP succeeds in recovering such signals and that the same holds for OMP. These results are a first step for explaining its success for coherent dictionaries.

Then, we have turned to the greedy-like methods and extended SSSCoSaMP and proposed SSIHT. These methods rely on approximate projections, which are their computational bottleneck in the case that the used dictionary is not orthonormal. Focusing on SSSCoSaMP, we have extended the idea of a *near-optimal projection*, and have considered two possibly different near-optimal projections in the SSSCoSaMP method. Our new analysis enforces weaker assumptions on these projections, which hold when the dictionary  $\mathbf{D}$  is incoherent or satisfies the RIP, unlike previous results whose assumptions do not hold in this setting. Above, we have discussed several important settings and have described algorithms that can be used for the approximate projections which satisfy our requirements for accurate signal recovery. This includes even the case when the dictionary is highly coherent but each atom is only highly correlated with a small number of atoms, an important example in applications like super-resolution.

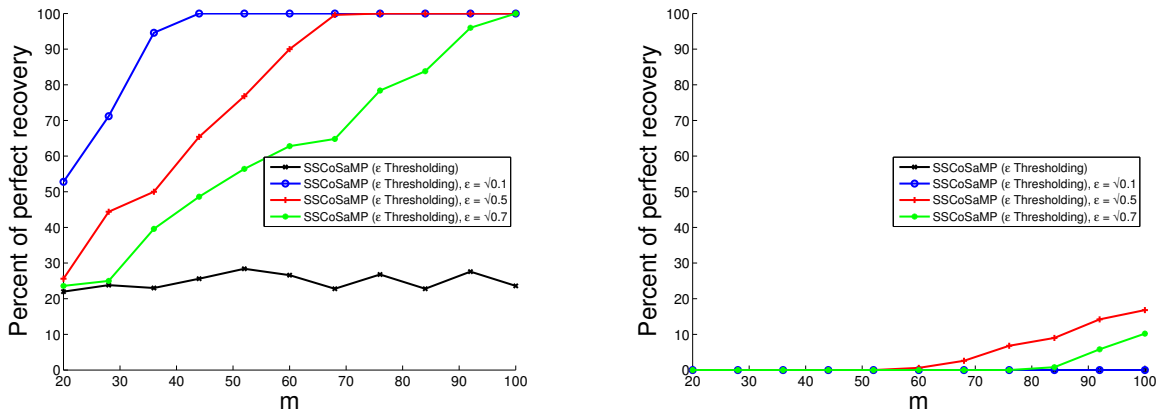


Figure 5.3: Recovery rate for SSSoSaMP ( $\epsilon$ -Thresholding) with different values of  $\epsilon$  for a random  $m \times 1024$  Gaussian matrix  $\mathbf{M}$  and a 4 times overcomplete DFT matrix  $\mathbf{D}$ . The signal is 8-sparse and on the left the coefficients of the original signal are clustered whereas on the right they are separated.

Our work for SSSoSaMP extends the work of Davenport, Needell, and Wakin [108] who develop and analyze the Signal Space CoSaMP algorithm. In that work, the D-RIP is enforced, as well as access to projections which satisfy (5.4). It is currently unknown whether there exist efficient projections which satisfy these requirements, even for well-behaved dictionaries like those that satisfy the RIP or have an incoherence property. That being said, other results on signal space methods rely on such assumptions. For example, a related work by Blumensath analyzes an algorithm which is a signal space extension of the Iterative Hard Thresholding (IHT) method [109]. The model in that work utilizes a union-of-subspaces model and also assumes the D-RIP and projections with even stronger requirements than those in (5.4).

These types of projections also appear in *model-based* compressive sensing, where such operators project onto a specified model set. The model may describe structured sparsity patterns like tree-like or block sparsity, or may be a more general mode. In this setting, signal recovery is performed by first reconstructing the coefficient vector, and then mapping to the signal space. When the dictionary  $\mathbf{D}$  is an orthonormal basis, greedy methods have been adapted to structured sparsity models [116]. The assumptions, however, nearly require the product  $\mathbf{MD}$  to satisfy the traditional RIP, and so extensions to non-orthonormal dictionaries serve to be difficult. Although our work differs in its assumptions and domain model, model-based methods inspired the development of signal space CoSaMP [108, 117].

Finally, a related but significantly different path of work also exists that studies signals from *analysis* space rather than synthesis signal space. Indeed, it was in this context that the D-RIP

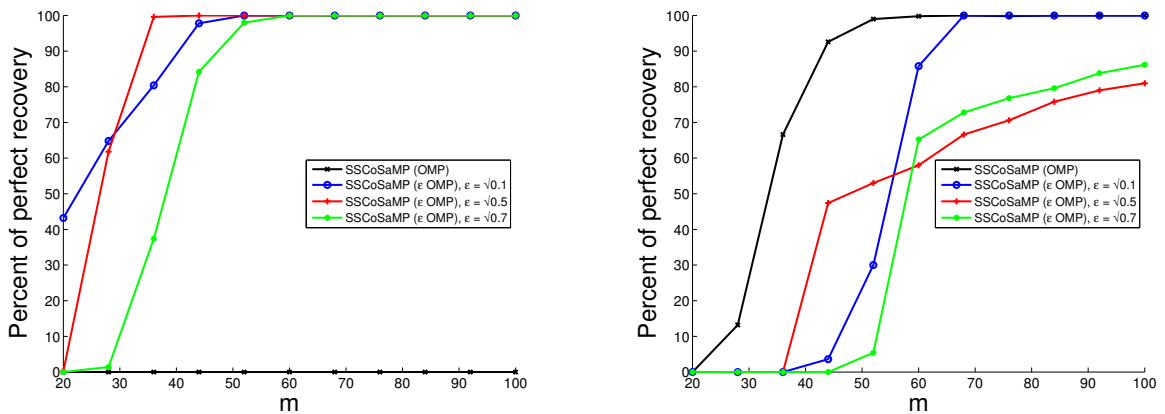


Figure 5.4: Recovery rate for SSCoSaMP ( $\epsilon$ -OMP) with different values of  $\epsilon$  for a random  $m \times 1024$  Gaussian matrix  $\mathbf{M}$  and a 4 times overcomplete DFT matrix  $\mathbf{D}$ . The signal is 8-sparse and on the left the coefficients of the original signal are clustered whereas on the right they are separated.

was first proposed and enforced for reconstruction [24]. In this setting, one requires that the analysis coefficients  $\mathbf{D}^* \mathbf{x}$  are sparse or compressible, and reconstruction is performed in that domain. Standard optimization based and greedy methods for sparse approximation have been extended and studied in this setting as well. In particular,  $\ell_1$ -minimization [22, 24, 23, 25, 27], and greedy methods like CoSaMP and IHT have all been adapted to account for analysis (co)sparsity [4, 52, 5, 6], like we have seen in Chapter 4.



## Chapter 6

# The Analysis Transform Domain

## Strategy

The results shown in this chapter have appeared in the following article:

- R. Giryes, "Greedy algorithm for the analysis transform domain," Submitted, 2013 [12].

In Chapter 4 we have considered the analysis greedy-like techniques and shown that linear dependencies can be allowed within the analysis dictionary as the focus of these algorithms is directly the signal. Then we have used the same idea in Chapter 5 for the synthesis framework, turning the focus from the representation to the signal, showing that with this new perspective, high correlations within the dictionary may be allowed also in the synthesis model.

One main disadvantage in the recovery conditions we have developed in Chapter 4 for the analysis greedy-like pursuit methods is the requirement on the near-optimality constant  $C_\ell$  to be close to 1. As mentioned before, having a general projection scheme with  $C_\ell = 1$  is NP-hard [99]. The existence of a program with a constant close to one for a general operator is still an open problem. In particular, it is not known whether there exists a procedure that gives a small constant for frames. Thus, there is a gap between the results for the greedy techniques and the ones for the  $\ell_1$ -minimization.

In this chapter we aim to close this gap for frames. We take the opposite direction to the one taken in the synthesis signal-space paradigm. We turn from operating in the analysis signal domain to the analysis transform domain. We propose a new greedy program, the transform domain IHT (TDIHT), which is an extension of IHT for the analysis transform domain. We show that it inherits guarantees similar to the ones of analysis  $\ell_1$ -minimization for frames.

Another gap that exists between synthesis and analysis is treated in this chapter. To the best of our knowledge, no denoising guarantees have been proposed for analysis strategies apart from the one in [52] that treats analysis thresholding in the case  $\mathbf{M} = \mathbf{I}$ . Our developed results handle both the Gaussian and the adversarial noise cases. For the Gaussian case we show that it is possible to have a denoising effect using the analysis model also when  $\mathbf{M} \neq \mathbf{I}$ .

Our contribution in this chapter can be summarized by the following theorem:

**Theorem 6.0.1 (Recovery Guarantees for TDIHT with Frames)** *Let  $\mathbf{y} = \mathbf{M}\mathbf{x} + \mathbf{e}$  where  $\|\mathbf{\Omega}\mathbf{x}\|_0 \leq k$  and  $\mathbf{\Omega}$  is a tight frame with frame constants  $A$  and  $B$ , i.e.,  $\|\mathbf{\Omega}\|_2 \leq B$  and  $\|\mathbf{\Omega}^\dagger\|_2 \leq \frac{1}{A}$ . For certain selections of  $\mathbf{M}$  and using only  $m = O(\frac{B}{A}k \log(p/k))$  measurements, the recovery result  $\hat{\mathbf{x}}$  of TDIHT satisfies*

$$\|\mathbf{x} - \hat{\mathbf{x}}\|_2 \leq O\left(\frac{B}{A} \|\mathbf{e}\|_2\right) + O\left(\frac{1+A}{A^2} \|\mathbf{\Omega}_{T^c}\mathbf{x}\|_2 + \frac{1}{A^2\sqrt{k}} \|\mathbf{\Omega}_{T^c}\mathbf{x}\|_1\right), \quad (6.1)$$

for the case where  $\mathbf{e}$  is an adversarial noise, implying that TDIHT leads to a stable recovery. For the case that  $\mathbf{e}$  is random i.i.d zero-mean Gaussian distributed noise with a known variance  $\sigma^2$  we have

$$E \|\mathbf{x} - \hat{\mathbf{x}}\|_2^2 \leq O\left(\frac{B^2}{A^2} k \log(p) \sigma^2\right) + O\left(\frac{1+A}{A^2} \|\mathbf{\Omega}_{T^c}\mathbf{x}\|_2 + \frac{1}{A^2\sqrt{k}} \|\mathbf{\Omega}_{T^c}\mathbf{x}\|_1\right)^2, \quad (6.2)$$

implying that TDIHT achieves a denoising effect.

**Remark 6.0.2** Note that  $\mathbf{\Omega}_{T^c}\mathbf{x} = \mathbf{\Omega}\mathbf{x} - [\mathbf{\Omega}\mathbf{x}]_k$ .

**Remark 6.0.3** Using Remark 2.3 in [39], we can convert the  $\ell_2$  norm into an  $\ell_1$  norm in the model mismatch terms in (6.1) and (6.2), turning it to be more similar to what we have in the bound for analysis  $\ell_1$ -minimization in (2.29).

**Remark 6.0.4** Theorem 6.0.1 is a combination of Theorems 6.3.1 and 6.3.4, plugging the minimal number of measurements implied by the D-RIP conditions of these theorems. Measurement matrices with sub-Gaussian entries are examples for matrices that satisfy this number of measurements [24].

This chapter is organized as follows. Section 6.1 includes a preliminary lemma for the D-RIP. Section 6.2 presents the transform domain IHT (TDIHT) and Section 6.3 provides theoretical guarantees for this method and proves Theorem 6.0.1. Section 6.4 discusses the developed results and summarizes the chapter.

---

<sup>1</sup>Since  $A$  is the smallest singular value of  $\mathbf{\Omega}$  it is also the largest singular value of  $\mathbf{\Omega}^\dagger$ .

## 6.1 Preliminary Lemma

In the work in this chapter we rely on the D-RIP properties proposed in Section 5.2. In addition, we use the following lemma which is a generalization of Proposition 3.5 in [39].

**Lemma 6.1.1** *Suppose that  $\mathbf{M}$  satisfies the upper inequality of the D-RIP, i.e.,*

$$\|\mathbf{M}\mathbf{D}\mathbf{w}\|_2 \leq \sqrt{1 + \delta_k} \|\mathbf{D}\mathbf{w}\|_2 \quad \forall \mathbf{w}, \|\mathbf{w}\|_0 \leq k, \quad (6.3)$$

and that  $\|\mathbf{D}\|_2 \leq \frac{1}{A}$ . Then for any representation  $\mathbf{w}$  we have

$$\|\mathbf{M}\mathbf{D}\mathbf{w}\|_2 \leq \frac{\sqrt{1 + \delta_k}}{A} \left( \|\mathbf{w}\|_2 + \frac{1}{\sqrt{k}} \|\mathbf{w}\|_1 \right). \quad (6.4)$$

*Proof:* We follow the proof of Proposition 3.5 in [39]. We define the following two convex bodies

$$S = \text{conv} \{ \mathbf{D}\mathbf{w} : \mathbf{w}_{T^c} = 0, |T| \leq k, \|\mathbf{D}\mathbf{w}\|_2 \leq 1 \}, \quad (6.5)$$

$$K = \left\{ \mathbf{D}\mathbf{w} : \frac{1}{A} \left( \|\mathbf{w}\|_2 + \frac{1}{\sqrt{k}} \|\mathbf{w}\|_1 \right) \leq 1 \right\}. \quad (6.6)$$

Since

$$\|\mathbf{M}\|_{S \rightarrow 2} = \max_{\mathbf{v} \in S} \|\mathbf{M}\mathbf{v}\|_2 \leq \sqrt{1 + \delta_k}, \quad (6.7)$$

it is sufficient to show that  $\|\mathbf{M}\|_{K \rightarrow 2} = \max_{\mathbf{v} \in K} \|\mathbf{M}\mathbf{v}\|_2 \leq \|\mathbf{M}\|_{S \rightarrow 2}$  which holds if  $K \subset S$ . For proving the latter, let  $\mathbf{D}\mathbf{w} \in K$  and  $\{T_0, T_1, \dots, T_J\}$  be a set of distinct sets such that  $T_0$  is composed of the indexes of the  $k$ -largest entries in  $\mathbf{w}$ ,  $T_1$  of the next  $k$ -largest entries, and so on. Thus, we can rewrite  $\mathbf{D}\mathbf{w} = \sum_{i=0}^J \mathbf{D}\mathbf{w}_{T_i} = \sum_{i=0}^J \lambda_i \mathbf{D}\tilde{\mathbf{w}}_{T_i}$ , where  $\lambda_i = \|\mathbf{D}\mathbf{w}_{T_i}\|_2$  and  $\tilde{\mathbf{w}}_{T_i} = \mathbf{w}_{T_i} / \lambda_i$ . Notice that by definition  $\mathbf{D}\tilde{\mathbf{w}}_{T_i} \in S$ . It remains to show that  $\sum_{i=0}^J \lambda_i \leq 1$  in order to show that  $\mathbf{D}\mathbf{w} \in S$ . It is easy to show that  $\|\mathbf{w}_{T_i}\|_2 \leq \frac{\|\mathbf{w}_{T_{i-1}}\|_1}{\sqrt{k}}$ . Combining this with the fact that  $\|\mathbf{D}\|_2 \leq \frac{1}{A}$  leads to

$$\sum_{i=1}^J \lambda_i = \sum_{i=1}^J \|\mathbf{D}\mathbf{w}_{T_i}\|_2 \leq \frac{1}{A} \sum_{i=1}^J \|\mathbf{w}_{T_i}\|_2 \leq \frac{1}{A\sqrt{k}} \sum_{i=0}^{J-1} \|\mathbf{w}_{T_i}\|_1 \leq \frac{1}{A\sqrt{k}} \|\mathbf{w}\|_1. \quad (6.8)$$

Using the fact that  $\lambda_0 = \|\mathbf{D}\mathbf{w}_{T_0}\|_2 \leq \frac{1}{A} \|\mathbf{w}_{T_0}\|_2 \leq \frac{1}{A} \|\mathbf{w}\|_2$ , we have

$$\sum_{i=0}^J \lambda_i \leq \frac{1}{A} \left( \|\mathbf{w}\|_2 + \frac{1}{\sqrt{k}} \|\mathbf{w}\|_1 \right) \leq 1, \quad (6.9)$$

where the last inequality is due to the fact that  $\mathbf{D}\mathbf{w} \in K$ .  $\square$

Before we proceed we recall the problem we aim at solving:

**Definition 6.1.2 (Problem  $\mathcal{P}$ )** Consider a measurement vector  $\mathbf{y} \in \mathbb{R}^m$  such that  $\mathbf{y} = \mathbf{M}\mathbf{x} + \mathbf{e}$ , where  $\mathbf{x} \in \mathbb{R}^d$  is either  $\ell$ -cosparsely under a given and fixed analysis operator  $\mathbf{\Omega} \in \mathbb{R}^{p \times d}$  or almost  $\ell$ -cosparsely, i.e.  $\mathbf{\Omega}\mathbf{x}$  has  $k = p - \ell$  leading elements. The non-zero locations of the  $k$  leading elements is denoted by  $T$ .  $\mathbf{M} \in \mathbb{R}^{m \times d}$  is a degradation operator and  $\mathbf{e} \in \mathbb{R}^m$  is an additive noise. Our task is to recover  $\mathbf{x}$  from  $\mathbf{y}$ . The recovery result is denoted by  $\hat{\mathbf{x}}$ .

## 6.2 Transform Domain Iterative Hard Thresholding

Our goal in this section is to provide a greedy-like approach that provides guarantees similar to the ones of analysis  $\ell_1$ -minimization. By analyzing the latter we notice that though it operates directly on the signal, it actually minimizes the coefficients in the transform domain. In fact, all the proof techniques utilized for this recovery strategy use the fact that nearness in the analysis dictionary domain implies a nearness in the signal domain [24, 27, 50]. Using this fact, recovery guarantees have been developed for tight frames [24], general frames [50] and the 2D-DIF operator which corresponds to total variation (TV) [27]. Working in the transform domain is not a new idea and was used before, especially in the context of dictionary learning [118, 119, 120].

Henceforth, our strategy for extending the results of the  $\ell_1$ -relaxation is to modify the greedy-like approaches to operate in the transform domain. In this chapter we concentrate on iterative hard thresholding (IHT) to demonstrate this line of reasoning.

The drawback of AIHT for handling analysis signals is that it assumes the existence of a near optimal cosupport selection scheme  $\mathcal{S}_\ell$ . The type of analysis dictionaries for which a known feasible cosupport selection technique exists is very limited [4, 99] (See Section 4.2). Note that this limit is not unique only to the analysis framework [8, 108, 109] (See Section 5.8.3). Of course, it is possible to use a cosupport selection strategy with no guarantees on its near-optimality constant and it might work well in practice. For instance, simple hard thresholding has been shown to operate reasonably well in several instances where no practical projection is at hand [4]. However, the theoretical performance guarantees depend heavily on the near-optimality constant. Since for many operators there are no known selection schemes with small constants, the existing guarantees for AIHT, as well as the ones of the other greedy-like algorithms, are very limited. In particular, to date, they do not cover frames and the 2D-DIF operator as the analysis dictionary.

To bypass this problem we propose an alternative greedy approach for the analysis frame-

work that operates in the transform domain instead of the signal domain. This strategy aims at finding the closest approximation to  $\Omega\mathbf{x}$  and not to  $\mathbf{x}$  using the fact that for many analysis operators proximity in the transform domain implies the same in the signal domain. In some sense, this approach imitates the classical synthesis techniques that recover the signal by putting the representation as the target.

In Algorithm 10 an extension for IHT for the transform domain is proposed. This algorithm makes use of  $k$ , the number of non-zeros in  $\Omega\mathbf{x}$ , and  $\mathbf{D}$ , a dictionary satisfying  $\mathbf{D}\Omega = \mathbf{I}$ . One option for  $\mathbf{D}$  is  $\mathbf{D} = \Omega^\dagger$ . If  $\Omega$  does not have a full row rank, we may compute  $\mathbf{D}$  by adding to  $\Omega$  rows that resides in its rows' null space and then applying the pseudo-inverse. For example, for the 2D-DIF operator we may calculate  $\mathbf{D}$  by computing the pseudo inverse of  $\Omega_{2D-DIF}$  with an additional row composed of ones divided by  $\sqrt{d}$ . However, this option is not likely to provide good guarantees. As the 2D-DIF operator is beyond the scope of the work in this chapter, we refer the reader to [27] for more details on this subject.

---

**Algorithm 10** Transform Domain Iterative hard thresholding (TDIHT)

---

**Input:**  $k, \mathbf{M} \in \mathbb{R}^{m \times d}, \Omega \in \mathbb{R}^{p \times d}, \mathbf{D} \in \mathbb{R}^{d \times p}, \mathbf{y}$ , where  $\mathbf{y} = \mathbf{M}\mathbf{x} + \mathbf{e}$ ,  $\mathbf{D}$  satisfies  $\mathbf{D}\Omega = \mathbf{I}$ ,  $\mathbf{x}$  is  $p - k$  cosparse under  $\Omega$  which implies that it has a  $k$ -sparse representation under  $\mathbf{D}$ , and  $\mathbf{e}$  is an additive noise.

**Output:**  $\hat{\mathbf{x}}_{\text{TDIHT}}$ : Approximation of  $\mathbf{x}$ .

Initialize estimate  $\hat{\mathbf{w}}^0 = \mathbf{0}$  and set  $t = 0$ .

**while** halting criterion is not satisfied **do**

$t = t + 1$ .

Perform a gradient step:  $\mathbf{w}_g^t = \Omega\mathbf{D}\hat{\mathbf{w}}^{t-1} + \mu^t\Omega\mathbf{M}^*(\mathbf{y} - \mathbf{M}\mathbf{D}\hat{\mathbf{w}}^{t-1})$

Find a new transform domain support:  $\hat{T}^t = \text{supp}(\mathbf{w}_g^t, k)$

Calculate a new estimate:  $\hat{\mathbf{w}}^t = (\mathbf{w}_g^t)_{\hat{T}^t}$ .

**end while**

Form the final solution  $\hat{\mathbf{x}}_{\text{TDIHT}} = \mathbf{D}\hat{\mathbf{w}}^t$ .

---

### 6.3 Frame Guarantees

We provide theoretical guarantees for the reconstruction performance of the transform domain analysis IHT (TDIHT), with a constant step size  $\mu = 1$ , for frames. These can be easily extended also to other step-size selection options using the proof technique in [4, 64]. We start with the

case that the noise is bounded and adversarial.

**Theorem 6.3.1 (Stable Recovery of TDIHT with Frames)** Consider the problem  $\mathcal{P}$  and apply TDIHT with a constant step-size  $\mu = 1$  and  $\mathbf{D} = \mathbf{\Omega}^\dagger$ . Suppose that  $\mathbf{e}$  is a bounded adversarial noise,  $\mathbf{\Omega}$  is a frame with frame constants  $0 < A, B < \infty$  such that  $\|\mathbf{\Omega}\|_2 \leq B$  and  $\|\mathbf{D}\|_2 \leq \frac{1}{A}$ , and  $\mathbf{M}$  has the D-RIP with the dictionary  $[\mathbf{D}, \mathbf{\Omega}^*]$  and a constant  $\delta_{\bar{k}} = \delta_{[\mathbf{D}, \mathbf{\Omega}^*], \bar{k}}^D$ . If  $\rho \triangleq \frac{2\delta_{ak}B}{A} < 1$  (i.e.  $\delta_{ak} \leq \frac{A}{2B}$ ), then after a finite number of iterations  $t \geq t^* = \frac{\log((\sqrt{1+\delta_{2k}B}\|\mathbf{e}\|_2 + \eta) / \|\mathbf{\Omega}_T \mathbf{x}\|_2)}{\log(\rho)}$

$$\begin{aligned} \|\mathbf{x} - \hat{\mathbf{x}}^t\|_2 &\leq \frac{2\eta}{A} + \frac{2B\sqrt{1+\delta_{2k}}}{A} \left(1 + \frac{1-\rho^t}{1-\rho}\right) \|\mathbf{e}\|_2 \\ &\quad + \frac{2(1+\delta_{2k})}{A^2} \frac{1-\rho^t}{1-\rho} \left( \left(1 + A + \frac{A^2}{2}\right) \|\mathbf{\Omega}_{T^c} \mathbf{x}\|_2 + \frac{1}{\sqrt{k}} \|\mathbf{\Omega}_{T^c} \mathbf{x}\|_1 \right), \end{aligned} \quad (6.10)$$

implying that TDIHT leads to a stable recovery. For tight frames  $a = 3$  and for other frames  $a = 4$ .

The result of this theorem is a generalization of the one presented in [45] for IHT. Its proof follows from the following lemma.

**Lemma 6.3.2** Consider the same setup of Theorem 6.3.1. Then the  $t$ -th iteration of TDIHT satisfies

$$\begin{aligned} \left\| \left( \mathbf{\Omega} \mathbf{x} - \mathbf{w}_g^t \right)_{T \cup \hat{T}^t} \right\|_2 &\leq 2\delta_{ak} \frac{B}{A} \left\| \left( \mathbf{\Omega} \mathbf{x} - \mathbf{w}_g^{t-1} \right)_{T \cup \hat{T}^{t-1}} \right\|_2 \\ &\quad + \frac{1+\delta_{2k}}{A} \left( \left(1 + A + \frac{A^2}{2}\right) \|\mathbf{\Omega}_{T^c} \mathbf{x}\|_2 + \frac{1}{\sqrt{k}} \|\mathbf{\Omega}_{T^c} \mathbf{x}\|_1 \right) + \|\mathbf{\Omega}_{T \cup \hat{T}^t} \mathbf{M}^* \mathbf{e}\|_2. \end{aligned} \quad (6.11)$$

*Proof:* Our proof technique is based on the one of IHT in [45], utilizing the properties of  $\mathbf{\Omega}$  and  $\mathbf{D}$ . Denoting  $\mathbf{w} = \mathbf{\Omega} \mathbf{x}$  and using the fact that  $\mathbf{w}_g^t = \mathbf{\Omega} \mathbf{D} \hat{\mathbf{w}}^{t-1} - \mathbf{\Omega} \mathbf{M}^* (\mathbf{y} - \mathbf{M} \mathbf{D} \hat{\mathbf{w}}^{t-1})$  we have

$$\left\| \left( \mathbf{w} - \mathbf{w}_g^t \right)_{T \cup \hat{T}^t} \right\|_2 = \left\| \left( \mathbf{w} - \mathbf{\Omega} \mathbf{D} \hat{\mathbf{w}}^{t-1} \right)_{T \cup \hat{T}^t} - \left( \mathbf{\Omega} \mathbf{M}^* (\mathbf{y} - \mathbf{M} \mathbf{D} \hat{\mathbf{w}}^{t-1}) \right)_{T \cup \hat{T}^t} \right\|_2. \quad (6.12)$$

By definition  $\mathbf{w} = \mathbf{\Omega} \mathbf{D} \mathbf{w}$  and  $\mathbf{y} = \mathbf{M} \mathbf{D} \mathbf{w} + \mathbf{e}$ . Henceforth

$$\begin{aligned} \left\| \left( \mathbf{w} - \mathbf{w}_g^t \right)_{T \cup \hat{T}^t} \right\|_2 &= \left\| \mathbf{\Omega}_{T \cup \hat{T}^t} \mathbf{D} \left( \mathbf{w} - \hat{\mathbf{w}}^{t-1} \right) - \mathbf{\Omega}_{T \cup \hat{T}^t} \mathbf{M}^* (\mathbf{y} - \mathbf{M} \mathbf{D} \hat{\mathbf{w}}^{t-1}) \right\|_2 \\ &= \left\| \mathbf{\Omega}_{T \cup \hat{T}^t} (\mathbf{I} - \mathbf{M}^* \mathbf{M}) \mathbf{D} \left( \mathbf{w} - \hat{\mathbf{w}}^{t-1} \right) - \mathbf{\Omega}_{T \cup \hat{T}^t} \mathbf{M}^* \mathbf{e} \right\|_2 \\ &\leq \left\| \mathbf{\Omega}_{T \cup \hat{T}^t} (\mathbf{I} - \mathbf{M}^* \mathbf{M}) \mathbf{D} \left( \mathbf{w}_T - \hat{\mathbf{w}}^{t-1} \right) \right\|_2 + \|\mathbf{\Omega}_{T \cup \hat{T}^t} (\mathbf{I} - \mathbf{M}^* \mathbf{M}) \mathbf{D} \mathbf{w}_{T^c}\|_2 + \|\mathbf{\Omega}_{T \cup \hat{T}^t} \mathbf{M}^* \mathbf{e}\|_2, \end{aligned} \quad (6.13)$$

where the last step is due to the triangle inequality. Denote by  $\mathbf{P}$  the projection onto  $\text{range}([\mathbf{\Omega}_{T \cup \hat{T}^t}^*, \mathbf{D}_{T \cup \hat{T}^{t-1}}])$  which is a subspace of vectors with  $4k$ -sparse representations. As

$\mathbf{w}_T - \hat{\mathbf{w}}^{t-1}$  is supported on  $T \cup T^{t-1}$  and  $\mathbf{M}$  satisfies the D-RIP for  $[\mathbf{\Omega}^*, \mathbf{D}]$ , we have using norm inequalities and Lemma 5.2.3 that

$$\begin{aligned} \left\| \mathbf{\Omega}_{T \cup \hat{T}^t} (\mathbf{I} - \mathbf{M}^* \mathbf{M}) \mathbf{D} (\mathbf{w}_T - \hat{\mathbf{w}}^{t-1}) \right\|_2 &= \left\| \mathbf{\Omega}_{T \cup \hat{T}^t} \mathbf{P} (\mathbf{I} - \mathbf{M}^* \mathbf{M}) \mathbf{P} \mathbf{D} (\mathbf{w}_T - \hat{\mathbf{w}}^{t-1}) \right\|_2 \\ &\leq \left\| \mathbf{\Omega}_{T \cup \hat{T}^t} \right\|_2 \left\| \mathbf{P} (\mathbf{I} - \mathbf{M}^* \mathbf{M}) \mathbf{P} \right\|_2 \left\| \mathbf{D} \right\|_2 \left\| \mathbf{w}_T - \hat{\mathbf{w}}^{t-1} \right\|_2 \leq \delta_{4k} \frac{B}{A} \left\| \mathbf{w}_T - \hat{\mathbf{w}}^{t-1} \right\|_2, \end{aligned} \quad (6.14)$$

where  $A$  and  $B$  are the frame constants and we use the fact that  $\|\mathbf{D}\|_2 \leq \frac{1}{A}$  and that  $\|\mathbf{\Omega}_{T \cup \hat{T}^t}\|_2 \leq \|\mathbf{\Omega}\|_2 \leq B$ . Notice that when  $\mathbf{\Omega}$  is tight frame,  $\mathbf{\Omega}^* = \mathbf{D}$  and thus  $\mathbf{\Omega}_T^* = \mathbf{D}_T$ . Hence, we have  $\delta_{3k}$  instead of  $\delta_{4k}$  since  $\text{range}([\mathbf{\Omega}_{T \cup \hat{T}^t}^*, \mathbf{D}_{T \cup \hat{T}^t-1}])$  is a subspace of vectors with  $3k$ -sparse representations.

For completing the proof we first notice that  $\mathbf{w}_T - \hat{\mathbf{w}}^{t-1} = (\mathbf{w} - \hat{\mathbf{w}}^{t-1})_{T \cup \hat{T}^{t-1}}$  and that  $\hat{\mathbf{w}}^{t-1}$  is the best  $k$ -term approximation of  $\mathbf{w}_g^{t-1}$  in the  $\ell_2$  norm sense. In particular it is also the best  $k$ -term approximation of  $(\mathbf{w}_g^{t-1})_{T \cup \hat{T}^{t-1}}$  and therefore  $\left\| (\hat{\mathbf{w}}^{t-1} - \mathbf{w}_g^{t-1})_{T \cup \hat{T}^{t-1}} \right\|_2 \leq \left\| (\mathbf{w} - \mathbf{w}_g^{t-1})_{T \cup \hat{T}^{t-1}} \right\|_2$ . Starting with the triangle inequality and then applying this fact we have

$$\begin{aligned} \left\| \mathbf{w}_T - \hat{\mathbf{w}}^{t-1} \right\|_2 &= \left\| (\mathbf{w} - \mathbf{w}_g^{t-1} + \mathbf{w}_g^{t-1} - \hat{\mathbf{w}}^{t-1})_{T \cup \hat{T}^{t-1}} \right\|_2 \\ &\leq \left\| (\mathbf{w} - \mathbf{w}_g^{t-1})_{T \cup \hat{T}^{t-1}} \right\|_2 + \left\| (\hat{\mathbf{w}}^{t-1} - \mathbf{w}_g^{t-1})_{T \cup \hat{T}^{t-1}} \right\|_2 \leq 2 \left\| (\mathbf{w} - \mathbf{w}_g^{t-1})_{T \cup \hat{T}^{t-1}} \right\|_2. \end{aligned} \quad (6.15)$$

Combining (6.15) and (6.14) with (6.13) leads to

$$\begin{aligned} \left\| (\mathbf{w} - \mathbf{w}_g^t)_{T \cup \hat{T}^t} \right\|_2 &\leq 2\delta_{4k} \frac{B}{A} \left\| (\mathbf{w} - \mathbf{w}_g^{t-1})_{T \cup \hat{T}^{t-1}} \right\|_2 \\ &\quad + \left\| \mathbf{\Omega}_{T \cup \hat{T}^t} (\mathbf{I} - \mathbf{M}^* \mathbf{M}) \mathbf{D} \mathbf{w}_{T^c} \right\|_2 + \left\| \mathbf{\Omega}_{T \cup \hat{T}^t} \mathbf{M}^* \mathbf{e} \right\|_2. \end{aligned} \quad (6.16)$$

It remains to bound the second term of the rhs. By using the triangle inequality and then the D-RIP with the fact that  $\|\mathbf{\Omega}_{T \cup \hat{T}^t} \mathbf{D}\|_2 \leq \|\mathbf{\Omega} \mathbf{D}\|_2 \leq 1$  we have

$$\begin{aligned} \left\| \mathbf{\Omega}_{T \cup \hat{T}^t} (\mathbf{I} - \mathbf{M}^* \mathbf{M}) \mathbf{D} \mathbf{w}_{T^c} \right\|_2 &\leq \left\| \mathbf{\Omega}_{T \cup \hat{T}^t} \mathbf{D} \mathbf{w}_{T^c} \right\|_2 + \left\| \mathbf{\Omega}_{T \cup \hat{T}^t} \mathbf{M}^* \mathbf{M} \mathbf{D} \mathbf{w}_{T^c} \right\|_2 \\ &\leq \left\| \mathbf{w}_{T^c} \right\|_2 + \sqrt{1 + \delta_{2k}} \left\| \mathbf{M} \mathbf{D} \mathbf{w}_{T^c} \right\|_2 \\ &\leq \left\| \mathbf{w}_{T^c} \right\|_2 + \frac{1 + \delta_{2k}}{A} \left( \left\| \mathbf{w}_{T^c} \right\|_2 + \frac{1}{\sqrt{k}} \left\| \mathbf{w}_{T^c} \right\|_1 \right), \end{aligned} \quad (6.17)$$

where the last inequality is due to Lemmas 6.1.1 and 5.2.2. The desired result is achieved by plugging (6.17) into (6.16) and using the fact that  $1 + \frac{1 + \delta_{2k}}{A} \leq \frac{(1 + \delta_{2k})(1 + A)}{A}$ .  $\square$

Having Lemma 6.3.2 proven, we turn now to prove Theorem 6.3.1.

*Proof:*[Proof of Theorem 6.3.1] First notice that  $\hat{\mathbf{w}}^0 = 0$  implies that  $\mathbf{w}_g^0 = 0$ . Using Lemma 6.3.2, recursion and the definitions of  $\rho$  and  $T_e \triangleq \text{argmax}_{\tilde{T}: |\tilde{T}| \leq k} \left\| \mathbf{\Omega}_{T \cup \tilde{T}} \mathbf{M}^* \mathbf{e} \right\|_2$ , we have

that after  $t$  iterations

$$\begin{aligned} \left\| \left( \mathbf{\Omega} \mathbf{x} - \mathbf{w}_g^t \right)_{T \cup \hat{T}^t} \right\|_2 &\leq \rho^t \left\| \left( \mathbf{\Omega} \mathbf{x} - \mathbf{w}_g^{t-1} \right)_{T \cup \hat{T}^{t-1}} \right\|_2 \\ &+ (1 + \rho + \rho^2 + \dots + \rho^{t-1}) \left( \left\| \mathbf{\Omega}_{T \cup T_e} \mathbf{M}^* \mathbf{e} \right\|_2 + \frac{1 + \delta_{2k}}{A} \left( (1 + A) \left\| \mathbf{\Omega}_{T^c} \mathbf{x} \right\|_2 + \frac{1}{\sqrt{k}} \left\| \mathbf{\Omega}_{T^c} \mathbf{x} \right\|_1 \right) \right) \\ &= \rho^t \left\| \mathbf{\Omega}_{T^c} \mathbf{x} \right\|_2 + \frac{1 - \rho^t}{1 - \rho} \left( \left\| \mathbf{\Omega}_{T \cup T_e} \mathbf{M}^* \mathbf{e} \right\|_2 + \frac{1 + \delta_{2k}}{A} \left( (1 + A) \left\| \mathbf{\Omega}_{T^c} \mathbf{x} \right\|_2 + \frac{1}{\sqrt{k}} \left\| \mathbf{\Omega}_{T^c} \mathbf{x} \right\|_1 \right) \right), \end{aligned} \quad (6.18)$$

where the last equality is due to the equation of geometric series ( $\rho < 1$ ) and the facts that  $\mathbf{w}_g^0 = \mathbf{0}$  and  $T^0 = \emptyset$ . For a given precision factor  $\eta$  we have that if  $t \geq t^* = \frac{\log((\left\| \mathbf{\Omega}_{T \cup T_e} \mathbf{M}^* \mathbf{e} \right\|_2 + \eta) / \left\| \mathbf{\Omega}_{T^c} \mathbf{x} \right\|_2)}{\log(\rho)}$  then

$$\rho^t \left\| \mathbf{\Omega}_{T^c} \mathbf{x} \right\|_2 \leq \eta + \left\| \mathbf{\Omega}_{T \cup T_e} \mathbf{M}^* \mathbf{e} \right\|_2. \quad (6.19)$$

As  $\mathbf{x} = \mathbf{D} \mathbf{\Omega} \mathbf{x}$  and  $\hat{\mathbf{x}}^t = \mathbf{D} \hat{\mathbf{w}}^t$ , we have using matrix norm inequality that

$$\left\| \mathbf{x} - \hat{\mathbf{x}}^t \right\|_2 = \left\| \mathbf{D} (\mathbf{\Omega} \mathbf{x} - \hat{\mathbf{w}}^t) \right\|_2 \leq \frac{1}{A} \left\| \mathbf{\Omega} \mathbf{x} - \hat{\mathbf{w}}^t \right\|_2. \quad (6.20)$$

Using the triangle inequality and the facts that  $\hat{\mathbf{w}}^t$  is supported on  $\hat{T}^t$  and  $\left\| \mathbf{\Omega}_{(T \cup \hat{T}^t)^c} \mathbf{x} \right\|_2 \leq \left\| \mathbf{\Omega}_{T^c} \mathbf{x} \right\|_2$ , we have

$$\left\| \mathbf{x} - \hat{\mathbf{x}}^t \right\|_2 \leq \frac{1}{A} \left\| \mathbf{\Omega}_{T^c} \mathbf{x} \right\|_2 + \frac{1}{A} \left\| (\mathbf{\Omega} \mathbf{x} - \hat{\mathbf{w}}^t)_{T \cup \hat{T}^t} \right\|_2. \quad (6.21)$$

By using again the triangle inequality and the fact that  $\hat{\mathbf{w}}^t$  is the best  $k$ -term approximation for  $\mathbf{w}_g^t$  we get

$$\begin{aligned} \left\| \mathbf{x} - \hat{\mathbf{x}}^t \right\|_2 &\leq \frac{1}{A} \left\| \mathbf{\Omega}_{T^c} \mathbf{x} \right\|_2 + \frac{1}{A} \left\| (\mathbf{\Omega} \mathbf{x} - \mathbf{w}_g^t)_{T \cup \hat{T}^t} \right\|_2 + \frac{1}{A} \left\| (\mathbf{w}_g^t - \hat{\mathbf{w}}^t)_{T \cup \hat{T}^t} \right\|_2 \\ &\leq \frac{1}{A} \left\| \mathbf{\Omega}_{T^c} \mathbf{x} \right\|_2 + \frac{2}{A} \left\| (\mathbf{\Omega} \mathbf{x} - \mathbf{w}_g^t)_{T \cup \hat{T}^t} \right\|_2. \end{aligned} \quad (6.22)$$

Plugging (6.19) and (6.18) in (6.22) yields

$$\begin{aligned} \left\| \mathbf{x} - \hat{\mathbf{x}}^t \right\|_2 &\leq \frac{2\eta}{A} + \frac{2}{A} \left( 1 + \frac{1 - \rho^t}{1 - \rho} \right) \left\| \mathbf{\Omega}_{T \cup T_e} \mathbf{M}^* \mathbf{e} \right\|_2 \\ &+ \frac{2(1 + \delta_{2k})}{A^2} \frac{1 - \rho^t}{1 - \rho} \left( \left( 1 + A + \frac{A^2}{2} \right) \left\| \mathbf{\Omega}_{T^c} \mathbf{x} \right\|_2 + \frac{1}{\sqrt{k}} \left\| \mathbf{\Omega}_{T^c} \mathbf{x} \right\|_1 \right). \end{aligned} \quad (6.23)$$

Using the D-RIP and the fact that  $\mathbf{\Omega}$  is a frame we have that  $\left\| \mathbf{\Omega}_{T \cup T_e} \mathbf{M}^* \mathbf{e} \right\|_2 \leq B \sqrt{1 + \delta_{2k}} \left\| \mathbf{e} \right\|_2$  and this completes the proof.  $\square$

Having a results for the adversarial noise case we turn to give a bound for the case where a distribution of the noise is given. We dwell on the white Gaussian noise case. For this type of noise we make use of the following lemma.

**Lemma 6.3.3** *If  $\mathbf{e}$  is a zero-mean white Gaussian noise with a variance  $\sigma^2$  then*

$$E[\max_{|T| \leq k} \|\mathbf{\Omega}_T \mathbf{M}^* \mathbf{e}\|_2^2] \leq 4 \max_i \|\mathbf{\Omega}_i^*\|_2^2 (1 + \delta_1) k \log(p) \sigma^2. \quad (6.24)$$

*Proof:* First notice that the  $i$ -th entry in  $\mathbf{\Omega}_T \mathbf{M}^* \mathbf{e}$  is Gaussian distributed random variable with zero-mean and variance  $\|\mathbf{M} \mathbf{\Omega}_i^*\|_2^2 \sigma^2$ . Denoting by  $\mathbf{W}$  a diagonal matrix such that  $\mathbf{W}_{i,i} = \|\mathbf{M} \mathbf{\Omega}_i^*\|_2$ , we have that each entry in  $\mathbf{W}^{-1} \mathbf{\Omega}_T \mathbf{M}^* \mathbf{e}$  is Gaussian distributed with variance  $\sigma^2$ . Therefore, using Theorem 3.2.10 we have  $E[\max_{|T| \leq k} \|\mathbf{W}^{-1} \mathbf{\Omega}_T \mathbf{M}^* \mathbf{e}\|_2^2] \leq 4k \log(p) \sigma^2$ . Using the D-RIP we have that  $\|\mathbf{M} \mathbf{\Omega}_i^*\|_2^2 \leq (1 + \delta_1) \|\mathbf{\Omega}_i^*\|_2^2$ . Since the  $\ell_2$  matrix norm of a diagonal matrix is the maximal diagonal element we have that  $\|\mathbf{W}\|_2^2 \leq \max_i (1 + \delta_1) \|\mathbf{\Omega}_i^*\|_2^2$  and this provides the desired result.  $\square$

**Theorem 6.3.4 (Denoising Performance of TDIHT with Frames)** *Consider the problem  $\mathcal{P}$  and apply TDIHT with a constant step-size  $\mu = 1$ . Suppose that  $\mathbf{e}$  is an additive white Gaussian noise with a known variance  $\sigma^2$  (i.e. for each element  $\mathbf{e}_i \sim N(0, \sigma^2)$ ),  $\mathbf{\Omega}$  is a frame with frame constants  $0 < A, B < \infty$  such that  $\|\mathbf{\Omega}\|_2 \leq B$  and  $\|\mathbf{D}\|_2 \leq \frac{1}{A}$ , and  $\mathbf{M}$  has the D-RIP with the dictionary  $[\mathbf{D}, \mathbf{\Omega}^*]$  and a constant  $\delta_{\tilde{k}} = \delta_{[\mathbf{D}, \mathbf{\Omega}^*], \tilde{k}}^D$ . If  $\rho \triangleq \frac{2\delta_{ak}B}{A} < 1$  (i.e.  $\delta_{ak} \leq \frac{A}{2B}$ ), then after a finite number of iterations  $t \geq t^* = \frac{\log((\|\mathbf{\Omega}_{T \cup T_e} \mathbf{M}^* \mathbf{e}\|_2 + \eta) / \|\mathbf{\Omega}_T \mathbf{x}\|_2)}{\log(\rho)}$*

$$E \|\mathbf{x} - \hat{\mathbf{x}}^t\|_2^2 \leq \frac{32(1 + \delta_1)B^2}{A^2} \left(1 + \frac{1 - \rho^t}{1 - \rho}\right)^2 k \log(p) \sigma^2 \quad (6.25)$$

$$+ \frac{8(1 + \delta_{2k})^2}{A^4} \left(\frac{1 - \rho^t}{1 - \rho}\right)^2 \left( \left(1 + A + \frac{A^2}{2}\right) \|\mathbf{\Omega}_{T^c} \mathbf{x}\|_2 + \frac{1}{\sqrt{k}} \|\mathbf{\Omega}_{T^c} \mathbf{x}\|_1 \right)^2,$$

implying that TDIHT has a denoising effect. For tight frames  $a = 3$  and for other frames  $a = 4$ .

*Proof:* Using the fact that for tight frames  $\max_i \|\mathbf{\Omega}_i^*\|_2^2 \leq B$ , we have using Lemma 6.3.3 that

$$E \|\mathbf{\Omega}_{T \cup T_e} \mathbf{M}^* \mathbf{e}\|_2^2 \leq 4B^2 (1 + \delta_1) k \log(p) \sigma^2. \quad (6.26)$$

Plugging this in a squared version of (6.23) (with  $\eta = 0$ ), using the fact that for any two constants  $a, b$  we have  $(a + b)^2 \leq 2a^2 + 2b^2$ , leads to the desired result.  $\square$

## 6.4 Discussion and Summary

Notice that in all the conditions posed above, the number of measurements we need is  $O((p - \ell) \log(p))$  and it is not dependent explicitly on the intrinsic dimension of the signal. Intuitively,

we would expect the minimal number of measurements to be rather a function of  $d - r$ , where  $r = \text{rank}(\mathbf{\Omega}_\Lambda)$  is the corank of the cospase subspace defined by  $\mathbf{\Omega}_\Lambda$  [23], and henceforth our recovery conditions seems to be sub-optimal.

Indeed, this is the case with the analysis  $\ell_0$ -minimization problem [23]. However, all the guarantees developed for feasible programs [24, 4, 27, 50, 51] require at least  $O((p - \ell) \log(p/(p - \ell)))$  measurements. Apparently, such conditions are too demanding because the corank, which can be much smaller than  $p - \ell$ , does not play any role in them. However, it seems that it is impossible to robustly reconstruct the signal with fewer measurements [121].

The same argument can be used for the denoising bound we have for TDIHT which is  $O((p - \ell) \log(p)\sigma^2)$ , saying that we would expect it to be  $O((d - r) \log(p)\sigma^2)$ . Interestingly, even the  $\ell_0$  solution can not achieve the latter bound but it can achieve the first which is a function of the cosparsity [121].

In this chapter we developed recovery guarantees for TDIHT with frames. These close a gap between relaxation based techniques and greedy algorithms in the analysis framework and extends the denoising guarantees of synthesis methods to analysis. It is interesting to ask whether these can be extended to other operators such as the 2D-DIF or to other methods such as AIHT or an analysis version of the Dantzig selector. The core idea in this chapter is the connection between the signal domain and the transform domain. We believe that the relationships used in this chapter can be developed further, leading to other new results and improving existing techniques. In [105] we have taken some steps in this direction, suggesting a new sampling strategy with new theoretical guarantees that cover also the 2D-DIF operator.

## Chapter 7

# Poisson Noise Model

The results shown in this chapter have been published and appeared in the following articles:

- R. Giryes and M. Elad, "Sparsity based Poisson denoising," in *Proc. IEEE 27-th Convention of Electronics and Electrical Engineers in Israel (IEEEI'12), Eilat, Israel, Nov. 2012* [10].
- R. Giryes and M. Elad, "Sparsity based Poisson denoising with dictionary learning," *Submitted, 2013* [13].

In this chapter we turn to deal with the Poisson denoising problem. Its formulation differs from the previous chapters, where we had a measurements matrix  $\mathbf{M}$  and an additive noise  $\mathbf{e}$ , because in the Poisson denoising formulation we have no measurement matrix and the noise is not additive. One option for treating the Poisson denoising problem is to use a transformation that approximately converts the noise statistics to be additive, ending up with our "standard formulation", and then using the standard denoising methods for additive noise. Among these transformations we mention the Anscombe [90] and the Fitz [91] transforms.

One of the problems with the Anscombe transformation and the like is the need to compute their inverse. In [88] a refined inverse Anscombe transform has been proposed, leading to better recovery performance. However, as said above, even with this method the recovery error dramatically increases for  $\text{peak} < 4$  (this term and its importance will be explained in details shortly). In order to deal with this deficiency, a strategy that relies directly on the Poisson statistics is required. This direction has been taken in [20, 53], providing a Gaussian mixture model (GMM) [55] based approach that relies directly on the Poisson noise properties. By dividing the image into overlapping patches, dividing them to few large clusters and then

performing a projection onto the largest components of a PCA-like basis for each group, state-of-the-art results have been reported for small peak values. This approach has two versions. In the first, the non-local PCA (NLPCA), the projection is computed by a simple  $\ell_2$ -minimization process, while in the second, the non-local sparse PCA (NLSPCA), the SPIRAL method [122] that adds an  $\ell_1$  regularization term to the minimized objective is used resulting with a better recovery performance.

In this chapter we take a similar path as [20] and use image patches modeling for the recovery process. However, we take a different route and propose a sparse representation modeling and a dictionary learning based denoising strategy [93] instead of the GMM. We employ a greedy OMP-like method for sparse coding of the patches and use a smart boot-strapped stopping criterion. We demonstrate the superiority of the proposed scheme in various experiments.

We have presented a preliminary version of the proposed OMP-like technique that achieves a relatively poor recovery performance in a local conference [10]. In this chapter, both the algorithmic and the experimental parts have been remarkably improved.

The main contributions of this chapter are:

- We introduce a greedy technique for the Poisson sparse model. Such pursuit methods for a Gaussian noise are commonly used, and extensive work has been devoted in the past two decades to their construction and analysis. Thus, a proposal of a greedy strategy for the Poisson model is of importance and may open the door for many other variants and theoretical study, similar to what exists in the Gaussian regime. We mention that in some low light Poisson denoising applications the dictionary is already known. One example is Fluorescence microscopy where the cells are sparse by themselves and the dictionary is a known measurement matrix. Hence, in such cases the introduction of a new recovery method by itself is important.
- We introduce a novel stopping criteria for iterative algorithm, and its incorporation into the pursuit leads to much improved results. To the best of our knowledge, this boosting based stopping criterion first appears in our chapter.
- The interplay between GMM and dictionary learning based models has significance of its own, as seen in the treatment of the simpler Gaussian image denoising problem. The migration from GMM to dictionary learning poses series of difficulties that our chapter describes and solves.

- The integration of the above leads to state-of-the-art results, especially for the very low SNR case.

The organization of this chapter is as follows. Section 7.1 describes the Poisson denoising problem with more details, and presents the previous contributions. Section 7.2 introduces the proposed denoising algorithm, starting with the pursuit task, moving to the clustering that we employ for achieving non-locality in the denoising process, discussing the role of learning the dictionary, and concluding with the overall scheme. Section 7.3 presents various tests and comparisons that demonstrate the denoising performance and superiority of the proposed scheme. Section 7.4 discusses future work directions and summary.

## 7.1 Poisson Sparsity Model

Various image processing applications use the fact that image patches can be represented sparsely with a given dictionary  $\mathbf{D} \in \mathbb{R}^{d \times n}$  [110]. Under this assumption each patch  $\mathbf{p}_i \in \mathbb{R}^d$  from  $\mathbf{x}$  can be represented as  $\mathbf{p}_i = \mathbf{D}\boldsymbol{\alpha}_i$ , where  $\boldsymbol{\alpha}_i \in \mathbb{R}^n$  is  $k$ -sparse, i.e., it has only  $k$  non-zero entries, where  $k \ll d$ . This model leads to state-of-the-art results in Gaussian denoising [92, 110, 93]. In order to use this sparsity-inspired model for the Poisson noise case one has two options: (i) convert the Poisson noise into a Gaussian one, as done in [88]; or (ii) adapt the Gaussian denoising tools to the Poisson statistics. As explained above, the later is important for cases where the Anscombe is non-effective, and this approach is indeed practiced in [20, 53, 122]. Maximizing of the log-likelihood of the Poisson distribution

$$P(\mathbf{y}[i]|\mathbf{x}[i]) = \begin{cases} \frac{(\mathbf{x}[i])^{y[i]}}{y[i]!} \exp(-\mathbf{x}[i]) & \mathbf{x}[i] > 0 \\ \delta_0(\mathbf{y}[i]) & \mathbf{x}[i] = 0, \end{cases} \quad (7.1)$$

provides us with the following minimization problem for recovering the  $i$ -th patch  $\mathbf{p}_i$  from its corresponding Poisson noisy patch  $\mathbf{q}_i$ ,

$$\min_{\mathbf{p}_i} \mathbf{1}^* \mathbf{p}_i - \mathbf{q}_i^* \log(\mathbf{p}_i), \quad (7.2)$$

where  $\mathbf{1}$  is a vector composed of ones and the  $\log(\cdot)$  operation is applied element-wise. Note that this minimization problem allows zero entries in  $\mathbf{p}_i$  only if the corresponding entries in  $\mathbf{q}_i$  are zeros as well. The minimizer of (7.2) is the noisy patch  $\mathbf{q}_i$  itself, and thus using only (7.2) is not enough and a prior is needed. By using the standard sparsity prior for patches as practiced

in [93] and elsewhere,  $\mathbf{p}_i = \mathbf{D}\boldsymbol{\alpha}_i$ , we end up with the following minimization problem:

$$\begin{aligned} \min_{\boldsymbol{\alpha}_i} \mathbf{1}^* \mathbf{D}\boldsymbol{\alpha}_i - \mathbf{q}_i^* \log(\mathbf{D}\boldsymbol{\alpha}_i), \\ \text{s.t. } \|\boldsymbol{\alpha}_i\|_0 \leq k, \mathbf{D}\boldsymbol{\alpha}_i > 0, \end{aligned} \quad (7.3)$$

where  $\|\cdot\|_0$  is the  $\ell_0$  semi-norm which counts the number of non-zeros in a vector. Besides the fact that (7.3) is a combinatorial problem, it also imposes a non-negativity constraint on the recovered patch, which further complicates the numerical task at hand. In order to resolve the latter issue we follow [20] and set  $\mathbf{p}_i = \exp(\mathbf{D}\boldsymbol{\alpha}_i)$  where  $\exp(\cdot)$  is applied element-wise and  $\boldsymbol{\alpha}_i$  is still a  $k$ -sparse vector. This leads to the following minimization problem,

$$\min_{\boldsymbol{\alpha}_i} \mathbf{1}^* \exp(\mathbf{D}\boldsymbol{\alpha}_i) - \mathbf{q}_i^* \mathbf{D}\boldsymbol{\alpha}_i \quad \text{s.t. } \|\boldsymbol{\alpha}_i\|_0 \leq k. \quad (7.4)$$

Having the non-negativity constraint removed, we still need to have an approximation algorithm for solving (7.4) as it is likely to be NP-hard. One option is to use an  $\ell_1$  relaxation, which leads to the SPIRAL method [122]. Another, simpler option is to reduce the dictionary  $\mathbf{D}$  to have only  $k$  columns and thus (7.4) can be minimized with any standard optimization toolbox for convex optimization<sup>1</sup>. This approach is taken in the NLPCA technique [53] where the patches of  $\mathbf{y}$  are clustered into a small number of disjoint groups and each group has its own narrow dictionary. Denoting by  $j$ ,  $\{\mathbf{q}_{j,1}, \dots, \mathbf{q}_{j,N_j}\}$ ,  $\{\boldsymbol{\alpha}_{j,1}, \dots, \boldsymbol{\alpha}_{j,N_j}\}$  and  $\mathbf{D}_j \in \mathbb{R}^{d \times k}$  the group number, its noisy patches, the representations of the patches and their dictionary, the minimization problem NLPCA aims at solving for the  $j$ -th group is

$$\min_{\mathbf{D}_j, \boldsymbol{\alpha}_{j,1}, \dots, \boldsymbol{\alpha}_{j,N_j}} \sum_{i=1}^{N_j} \mathbf{1}^* \exp(\mathbf{D}_j \boldsymbol{\alpha}_{j,i}) - \mathbf{q}_{j,i}^* \mathbf{D}_j \boldsymbol{\alpha}_{j,i}. \quad (7.5)$$

Notice that  $\mathbf{D}_j$  is calculated also as part of the minimization process as each group has its own dictionary that should be optimized. The typical sparsity  $k$  and number of clusters used in NLPCA are 4 and 14 respectively. As it is hard to minimize (7.5) both with respect to the dictionary and to the representations, an alternating minimization process is used by applying Newton steps updating the dictionary and the representations alternately. Having the recovered patches, we return each to its corresponding location in the recovered image and average pixels that are mapped to the same place (since overlapping patches are used). The authors in [53] suggest to repeat the whole process, using the output of the algorithm as an input for the clustering process and then applying the algorithm again with the new division. An improved version of NLPCA, the NLSPCA, is proposed in [20], replacing the Newton step with the SPIRAL algorithm [122] for calculating the patches' representations.

<sup>1</sup>For a given support (location of the non-zeros in  $\boldsymbol{\alpha}$ ), the problem posed in (7.4) is convex.

The NLPCA for Poisson denoising is based on ideas related to the GMM model developed for the Gaussian denoising case [55]. Of course, this method can be used for the Poisson noise by applying an Anscombe transform. However, such an approach is shown in [20] to be inferior to the Poisson model based strategy in the low-photon count case.

Like [20, 53], in this work we do not use the Anscombe and rely on the Poisson based model. However, as opposed to [20, 53], we use one global dictionary for all patches and propose a greedy algorithm for finding the representation of each patch. In an approach similar to the one advocated in [93], we treat similar patches jointly by forcing them to share the same atoms in their representations. This introduces a non-local force and sharing of information between different regions in the image. A dictionary learning process is utilized in our scheme as well, in order to improve the initial dictionary used for the data, as the initial dictionary we embark from is global for all images.

Before moving to the next section we mention a technique proposed in [20] to enhance the SNR in noisy images. This method is effective especially in very low SNR scenarios such as peak smaller than 0.5. Instead of denoising the given image directly, one can downsample the image by applying a low-pass filter followed by down-sampling. This provides us with a smaller image but with a higher SNR. For example, if our low-pass filter is a kernel of size  $3 \times 3$  containing ones, and we sample every third row and every third column, we end up with a nine times smaller image that has a nine times larger peak value. Having the low-res noisy image, one may apply on it any Poisson denoising algorithm and then perform an upscaling interpolation on the recovered small image in order to return to the original dimensions. This method is referred to as binning in [20] and related to multi-scale programs [123]. Note that this technique is especially effective for the Anscombe based techniques as the peak value of the processed image is larger than the initial value.

## 7.2 Sparse Poisson Denoising Algorithm (SPDA)

Our denoising strategy is based on a dictionary learning based approach. We start by extracting a set of overlapping patches  $\{\mathbf{q}_i | 1 \leq i \leq (m_1 - \sqrt{d} + 1)(m_2 - \sqrt{d} + 1)\}$  ( $m_1$  and  $m_2$  are the vertical and horizontal dimensions of the noisy image  $\mathbf{y}$  respectively) of size  $\sqrt{d} \times \sqrt{d}$  from the noisy image  $\mathbf{y}$ . The goal is to find the dictionary  $\mathbf{D}$  that leads to the sparsest representation of this set of patches under the exponential formulation. In other words our target is to

**Algorithm 11** Patch Grouping Algorithm

**Input:**  $\mathbf{y}$  is a given image,  $\sqrt{d} \times \sqrt{d}$  is the patch size to use,  $l$  is a target group size,  $h$  is a given convolution kernel (typically a wide Gaussian) and  $\epsilon$  is a tolerance factor.

**Output:** Division to disjoint groups of patches  $Q_j = \{\mathbf{q}_{j,1}, \dots, \mathbf{q}_{j,N_j}\}$  of size  $N_j$  where  $N_j \geq l$ .

Begin Algorithm:

-Convolve the image with the kernel:  $\tilde{\mathbf{y}} = \mathbf{y} * h$ . We take  $\tilde{\mathbf{y}}$  to be of the same size of  $\mathbf{y}$ .

-Extract all overlapping patches  $Q = \{\mathbf{q}_1, \dots, \mathbf{q}_N\}$  of size  $\sqrt{d} \times \sqrt{d}$  from  $\mathbf{y}$  and their corresponding overlapping patches  $\{\tilde{\mathbf{q}}_1, \dots, \tilde{\mathbf{q}}_N\}$  of size  $\sqrt{d} \times \sqrt{d}$  from  $\tilde{\mathbf{y}}$ .

-Set first group pivot index:  $s_0 = \operatorname{argmin}_{1 \leq i \leq N} \|\tilde{\mathbf{q}}_i\|_2^2$ .

-Initialize  $j = 0$  and  $i_j^{\text{prev}} = 0$ .

**while**  $Q \neq \emptyset$  **do**

-Initialize group  $j$ :  $Q_j = \emptyset$  and  $l_j = 0$ .

-Select first candidate:  $i_j = \operatorname{argmin}_i \|\tilde{\mathbf{q}}_{s_j} - \tilde{\mathbf{q}}_i\|_2^2$

**while**  $(l_j \leq l \text{ or } \left| \|\tilde{\mathbf{q}}_{s_j} - \tilde{\mathbf{q}}_{i_j}\|_2^2 - \|\tilde{\mathbf{q}}_{s_j} - \tilde{\mathbf{q}}_{i_j^{\text{prev}}}\|_2^2 \right| \leq \epsilon^2)$  and  $Q \neq \emptyset$  **do**

-Add patch to group  $j$ :  $Q_j = Q_j \cup \{\mathbf{q}_{i_j}\}$ ,  $l_j = l_j + 1$ .

-Exclude patch from search:  $Q = Q \setminus \{\mathbf{q}_{i_j}\}$ .

-Save previous selection:  $i_j^{\text{prev}} = i_j$ .

-Select new candidate:  $i_j = \operatorname{argmin}_i \|\tilde{\mathbf{q}}_{s_j} - \tilde{\mathbf{q}}_i\|_2^2$ .

**end while**

-Set pivot index for next group:  $j = j + 1$ ,  $s_j = i_{j-1}$ .

**end while**

-Merge the last group with the previous one to ensure its size to be bigger than  $l$ .

minimize

$$\min_{\mathbf{D}, \boldsymbol{\alpha}_1, \dots, \boldsymbol{\alpha}_N} \sum_{i=1}^N \mathbf{1}^* \exp(\mathbf{D}\boldsymbol{\alpha}_i) - \mathbf{q}_i^* \mathbf{D}\boldsymbol{\alpha}_i \quad (7.6)$$

$$\text{s.t. } \|\boldsymbol{\alpha}_i\|_0 \leq k, 1 \leq i \leq N.$$

As in [20, 53], since minimizing both with respect to the dictionary and the representations at the same time is a hard problem, we minimize this function alternately. The dictionary update is done using a Newton step in a similar way to [20], with an addition of an Armijio rule. The pursuit (updating the representations) is performed using a greedy technique which returns a  $k$ -sparse representation for each patch, unlike the global Newton step or SPIRAL which is not guaranteed to have a sparse output.

In order to further boost the performance of our algorithm and exploit the fact that similar patches in the image domain may support each other, the patches are clustered into a large number of small disjoint groups of similar patches. A typical number of clusters for an image of size  $256 \times 256$  is 1000. Ideally, as Poisson noisy images with very low SNR are almost binary images, a good criterion for measuring the similarity between patches would be the earth mover's distance (EMD). We approximate this measure by setting the distance between patches to be their Euclidean distance in the image after it passes through a Gaussian filter. The grouping algorithm is described in details in Algorithm 11. It creates disjoint groups of size (at least)  $l$  in a sequential way, adding elements one by one. Once a group gets to the destination size, the algorithm continues to add elements whose distance from the first element in the group (the pivot) is up to  $\epsilon$  away from the distance of the last added element (See Algorithm 11).

For calculating the representations we use a joint sparsity assumption for each group of patches with a greedy algorithm that finds the representations of each group together. This algorithm is iterative and in each iteration it adds the atom that reduces the most the cost function (7.4) for all the representations that belong to the same group.

An important aspect in our pursuit algorithm is to decide how many atoms to associate with each patch, i.e., what should be the stopping criterion of the algorithm. We employ two options. The first is to run the algorithm with a constant number of iterations. However, this choice leads to a suboptimal denoising effect as different patches contain different content-complexity and thus require different sparsity levels. Another option is to set a different cardinality for each group. In order to do so we need a way to evaluate the error in each iteration with respect to the true image and then stop the iterations once the error starts increasing. One option for estimating the error is using the Stein unbiased risk (SURE) estimator as done in [124] for the NL-means algorithm. However, in our context the computation of the SURE is too demanding. Instead, we use boot-strapping – we rely on the fact that our scheme is iterative and after each step of representation decoding and dictionary update we have a new estimate of the original image. We use the patches of the reconstructed image from the previous iteration as a proxy for the patches of the true image and compute the error with respect to them. Note that since we update the dictionary between iterations and average the patches in the recovered image, we do not get stuck on the same patch again by using this stopping criteria. In practice, this condition improves the recovery performance significantly as each group of patches is represented with a cardinality that suits its content better.

The greedy Poisson algorithm is summarized in Algorithm 12. In the first time we apply the

decoding algorithm we use a constant  $k$  as we do not have a previous estimate. In subsequent iterations the recovered image from the previous stage is used as an input. Finding a new representation in the algorithm requires solving (7.4) for a fixed given support. As mentioned before, this is a convex problem which appears also in the NLPCA technique and can be solved by the Newton method or any convex optimization toolbox.

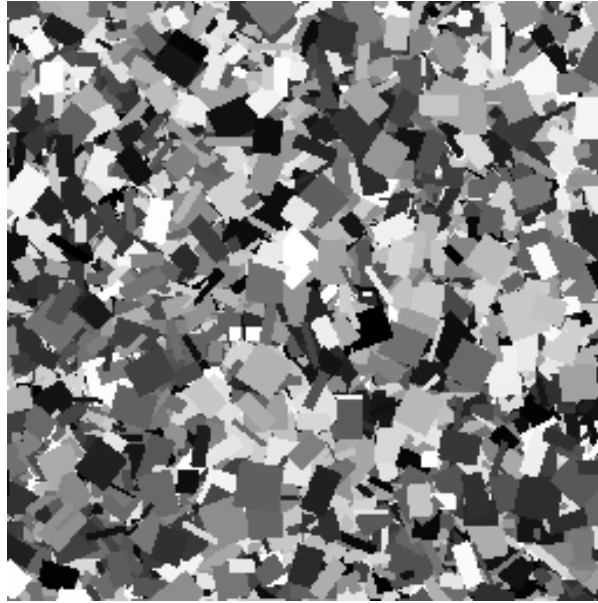


Figure 7.1: The piecewise constant image used for the offline training of the initial dictionary. For each range of peak values the image is scaled appropriately.

Having updated the representations, we perform a single Newton step for updating the dictionary as in the NLPCA. If we find that some atoms are not participating in any of the representations, we remove them from the dictionary resulting with a narrower dictionary (we do so until a certain limit on the dictionary size where we stop removing columns). The initial dictionary we use is a dictionary trained off-line on patches of a clean piecewise constant image shown in Fig. 7.1. This training process for an initial dictionary is needed since, unlike the standard sparsity model where many good dictionaries are present, for the exponential sparsity model no such dictionary is intuitively known. Notice also that the representation in the new model is sensitive to the scale of the image, unlike the standard one which is scale invariant. Thus, we train different initialization dictionaries for different peak values. However, we should mention that this training is done once and off-line.

Iterating over the pursuit and dictionary learning stages we get an estimate for the image patches. For recovering the whole image we reproject each patch to its corresponding location

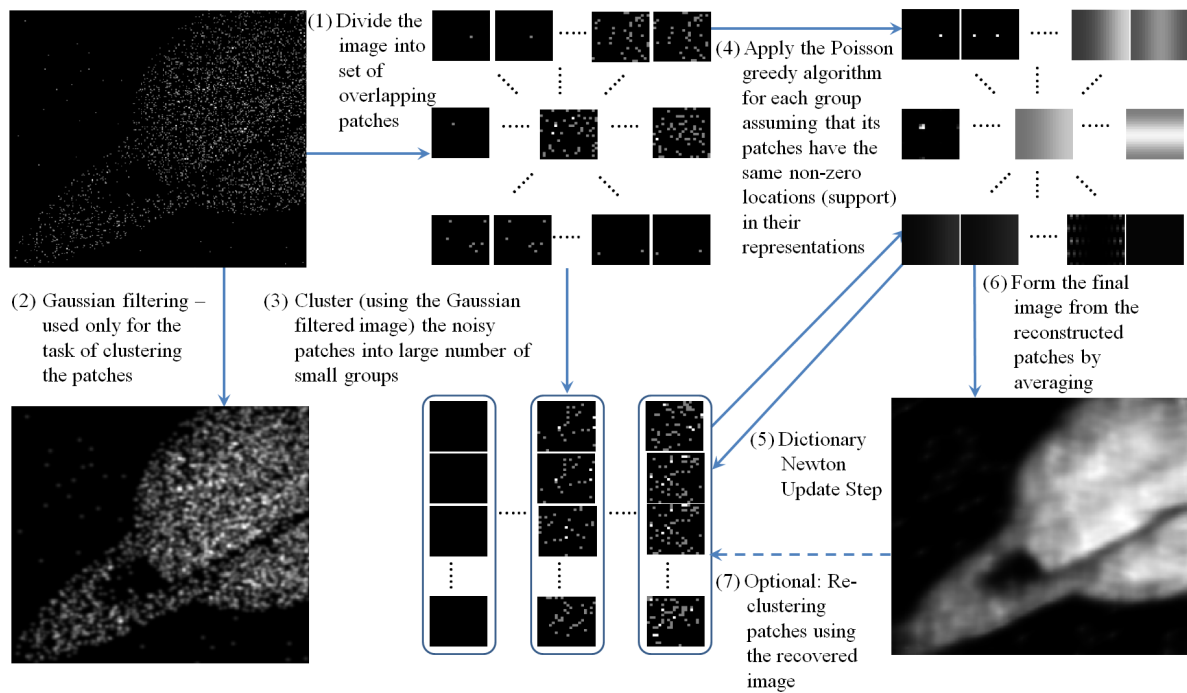


Figure 7.2: The proposed sparse Poisson denoising algorithm (SPDA).

with averaging. At this point it is possible to re-cluster the patches according to the new recovered image and repeat all the process. Our proposed sparse Poisson denoising algorithm (SPDA) is summarized in Fig. 7.2.

The main difference between our proposed algorithm and the NLPCA and NLSPCA is reminiscent of the difference between the K-SVD image denoising algorithm [93] and the GMM alternative approach [55], both developed for the Gaussian denoising problem. Furthermore, when it comes to the clustering of patches, NLPCA and NLSPCA use a small number of large clusters obtained using a k-means like algorithm. In our scheme the notion of joint sparsity is used which implies a large number of disjoint small groups that are divided using a simple algorithm. In NLPCA and NLSPCA, a different set of basis vectors is used for each cluster while we use one (thicker) dictionary for all patches together, from which subspaces are created by different choices of small groups of atoms. Unlike NLPCA and NLSPCA, our dictionary can change its size during the learning steps, and the cardinalities allocated to different patches are dynamic. As a last point we mention that NLPCA uses a Newton step and NLSPCA uses the SPIRAL algorithm for the representation decoding while we propose a new greedy pursuit for this task which guarantees a destination cardinality or reconstruction error.

### 7.3 Experiments



Figure 7.3: Test images used in this chapter. From left to right: Saturn, Flag, Cameraman, House, Swoosh, Peppers, Bridge and Ridges.

In order to evaluate the SPDA (with and without binning) performance we repeat the denoising experiment performed in [20]. We test the recovery error for various images with different peak values ranging from 0.1 to 4. The tested images appear in Fig. 7.3. The methods we compare to are the NLSPCA [20] and the BM3D with the refined inverse Anscombe [88] (both with and without binning) as those are the best-performing methods up to date. The code for these techniques is available online and we use the same parameter settings as appears in the code. For the binning we follow [20] and use a  $3 \times 3$  ones kernel that increases the peak value to be 9 times higher, and a bilinear interpolation for the upscaling of the low-resolution recovered image.

For SPDA we use the following parameter setting: the number of groups is of the order of 1000. As our images are of size  $256 \times 256$ , we set the group size  $l = 50$  if binning is not used and  $l = 6$  if it is used. The size of each patch is set to be  $20 \times 20$  pixels. In the first iteration we set  $k = 2$ . The initial dictionary is square ( $400 \times 400$ ) and dependent on the peak value. For  $\text{peak} \leq 0.2$  we use a dictionary trained on the squares image with peak 0.2, for  $0.2 < \text{peak} \leq 4$  we train for  $\text{peak} = 2$  and for  $\text{peak} > 4$  we train for  $\text{peak} = 18$  (this is relevant for SPDA with binning when the original peak is greater than  $4/9$ ). Note that since in Poisson noise the mean is

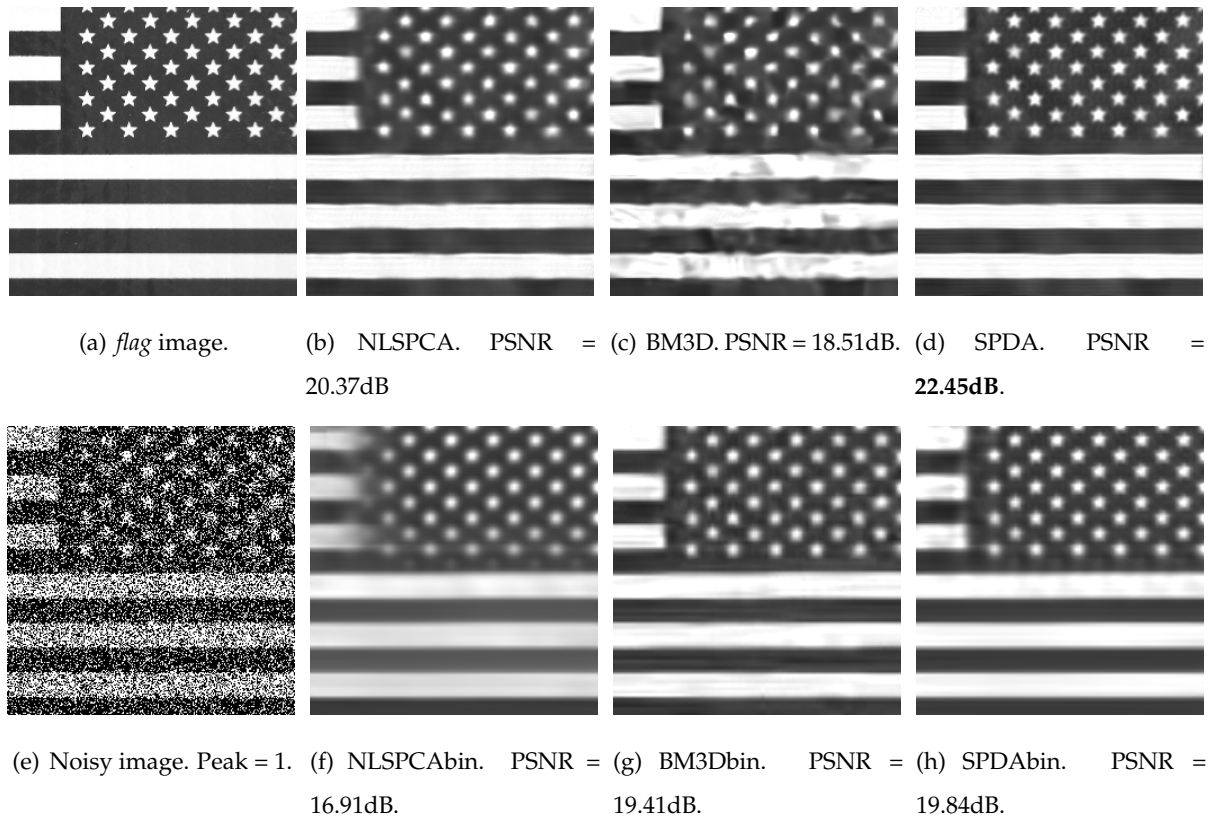


Figure 7.4: Denoising of *flag* with peak = 1. The PSNR is of the presented recovered images.

equal to the original signal, a rough estimation for the peak is an easy task. In addition, we note that our algorithm is not sensitive to the initial dictionary selection and a wrong selection of the dictionary does not affect the recovery significantly. Setting the number of iterations is also dependent on the peak value. For  $\text{peak} \leq 0.2$  we use 120 learning iterations and for  $\text{peak} > 0.2$  we use 20 iterations as the first stage, then re-cluster and apply additional 20 iterations<sup>2</sup>.

A comparison between the recovery of the *flag* image with peak = 1 is presented in Fig 7.4. It can be observed that this image is recovered very accurately while in the other methods there are many artifacts. Samples from the dictionary atoms learned by SPDA are presented in Fig. 7.5. It can be observed that the dictionary learning process captures the shape of the stars and the lines in the flag. Figures 7.6, 7.7 and 7.8 present the recovery of *ridges*, *Saturn* and *house* for peak = 0.2 and peak = 2 respectively. It can be seen that for the low peak value the binning methods capture the structure of the image better and provide lower error. However, when the peak is higher the binning provides degraded performance compared to the reconstruction using the original image. In all images the SPDA recovers the images' details better.

<sup>2</sup>We plan to release a package with the code to make the results reproducible.

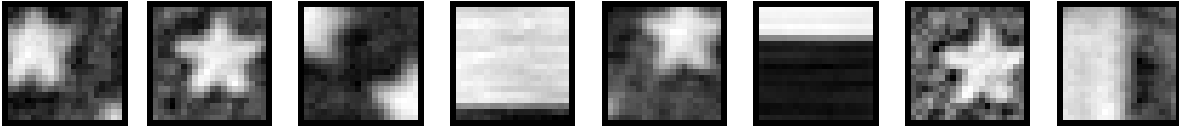
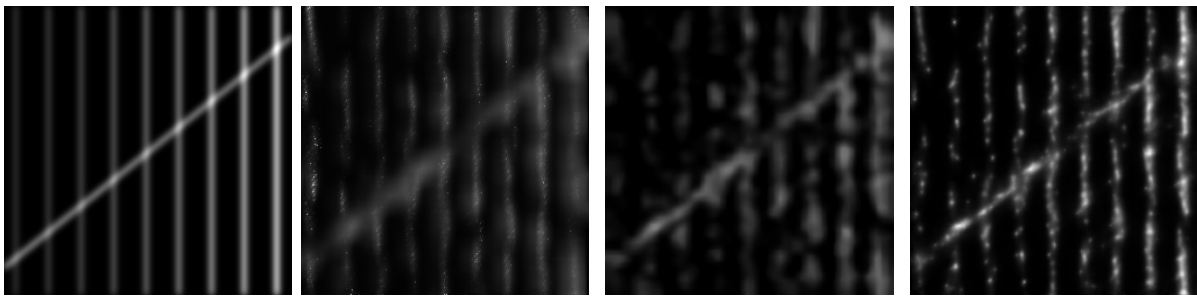
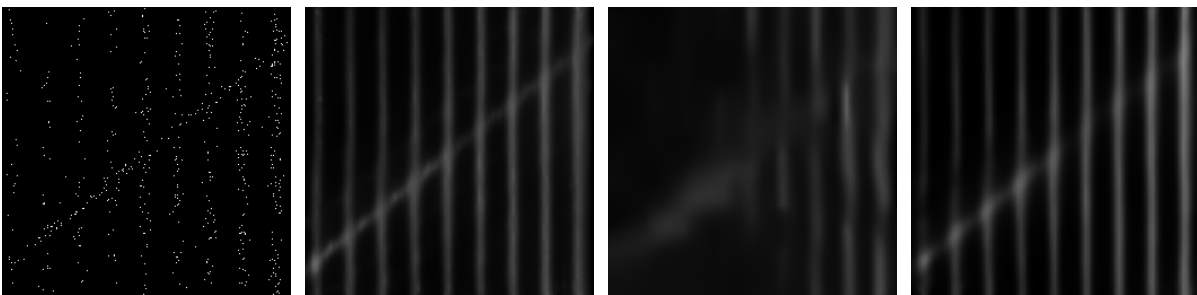


Figure 7.5: Samples of atoms from the dictionary  $D$  learned using SPDA for *flag* with  $\text{peak} = 1$ .



(a) *ridges* image. (b) NLSPCA. PSNR = 19.57dB. (c) BM3D. PSNR = 19.66dB. (d) SPDA. PSNR = 20.94dB.



(e) Noisy image. Peak = 0.1. (f) NLSPCAbin. PSNR = 21.84dB. (g) BM3Dbin. PSNR = 18.98dB. (h) SPDAbin. PSNR = 23.77dB.

Figure 7.6: Denoising of *ridges* with  $\text{peak} = 0.1$ . The PSNR is of the presented recovered images.

---

**Algorithm 12** Poisson Greedy Algorithm

---

**Input:**  $k, \mathbf{D} \in \mathbb{R}^{d \times n}, \{\mathbf{q}_1, \dots, \mathbf{q}_l\}$  where  $\mathbf{q}_i \in \mathbb{R}^d$  is a Poisson distributed vector with mean and variance  $\exp(\mathbf{D}\boldsymbol{\alpha}_i)$ , and  $k$  is the maximal cardinality of  $\boldsymbol{\alpha}_i$ . All representations  $\boldsymbol{\alpha}_i$  are assumed to have the same support. Optional parameter: Estimates of the true image patches  $\{\mathbf{p}_1, \dots, \mathbf{p}_l\}$ .

**Output:**  $\hat{\mathbf{p}}_i = \exp(\mathbf{D}\hat{\boldsymbol{\alpha}}_i)$  an estimate for  $\exp(\mathbf{D}\boldsymbol{\alpha}_i)$ .

Begin Algorithm:

-Initialize the support  $T^0 = \emptyset$  and set  $t = 0$ .

**while**  $t < k$  **do**

-Update iteration counter:  $t = t + 1$ .

-Set initial objective value:  $v_o = \text{inf}$ .

**for**  $j = 1 : n$  **do**

-Check atom  $j$ :  $\tilde{T}^t = T^{t-1} \cup \{j\}$ .

-Calculate current objective value:  $v_c = \min_{\boldsymbol{\alpha}_1, \dots, \boldsymbol{\alpha}_l} \sum_{i=1}^l \mathbf{1}^* \exp(\mathbf{D}_{\tilde{T}^t} \boldsymbol{\alpha}_i) - \mathbf{q}_i^* \mathbf{D}_{\tilde{T}^t} \boldsymbol{\alpha}_i$

**if**  $v_o > v_c$  **then**

-Update selection:  $j^t = j$  and  $v_o = v_c$ .

**end if**

**end for**

-Update the support:  $T^t = T^{t-1} \cup \{j^t\}$ .

-Update representation estimate:  $[\hat{\boldsymbol{\alpha}}_1^t, \dots, \hat{\boldsymbol{\alpha}}_l^t] =$

$\text{argmin}_{\boldsymbol{\alpha}_1, \dots, \boldsymbol{\alpha}_l} \sum_{i=1}^l \mathbf{1}^* \exp(\mathbf{D}_{T^t} \boldsymbol{\alpha}_i) - \mathbf{q}_i^* \mathbf{D}_{T^t} \boldsymbol{\alpha}_i$ .

**if**  $\{\mathbf{p}_1, \dots, \mathbf{p}_l\}$  are given **then**

-Estimate error:  $e_t = \sum_{i=1}^l \|\exp(\mathbf{D}\hat{\boldsymbol{\alpha}}_i^t) - \mathbf{p}_i\|_2^2$ .

**if**  $t > 1$  and  $e_t > e_{t-1}$  **then**

-Set  $t = t - 1$  and break (exit while and return the result of the previous iteration).

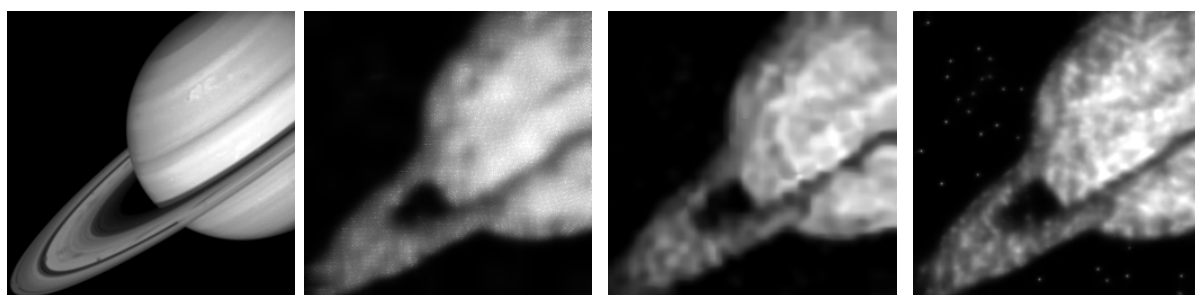
**end if**

**end if**

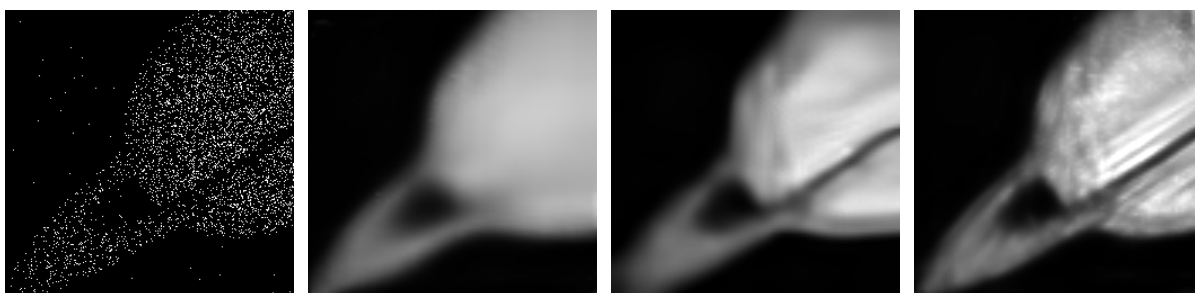
**end while**

-Form the final estimate  $\hat{\mathbf{p}}_i = \exp(\mathbf{D}\hat{\boldsymbol{\alpha}}_i^t), 1 \leq i \leq l$ .

---

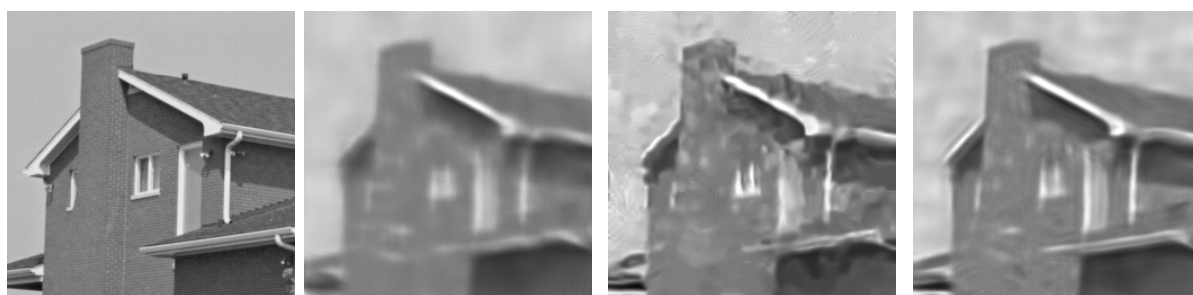


(a) *Saturn* image. (b) NLSPCA. PSNR = 22.98dB. (c) BM3D. PSNR = 21.71dB. (d) SPDA. PSNR = 22.16dB.



(e) Noisy image. Peak = 0.2. (f) NLSPCAbin. PSNR = 20.35dB. (g) BM3Dbin. PSNR = 23.16dB. (h) SPDAbin. PSNR = 23.92dB.

Figure 7.7: Denoising of *Saturn* with peak = 0.2. The PSNR is of the presented recovered images.



(a) *house* image. (b) NLSPCA. PSNR = 23.23dB. (c) BM3D. PSNR = 24.06dB. (d) SPDA. PSNR = **24.87dB**.



(e) Noisy image. Peak = 2. (f) NLSPCAbin. PSNR = 21.28dB. (g) BM3Dbin. PSNR = 24.23dB. (h) SPDAbin. PSNR = 21.39dB.

Figure 7.8: Denoising of *house* with peak = 2. The PSNR is of the presented recovered images.

Method	Peak	Saturn	Flag	Camera	House	Swoosh	Peppers	Bridge	Ridges	Average
NLSPCA		20.86	14.42	16.41	17.81	19.11	16.24	16.59	20.92	17.8
NLSPCAbin		19.13	<b>16.07</b>	<b>17.15</b>	<b>18.71</b>	21.89	16.12	16.93	24.05	18.75
BM3D	0.1	19.42	13.05	15.66	16.28	16.93	15.61	15.68	20.06	16.6
BM3Dbin		21.19	14.23	16.91	18.62	<b>21.90</b>	15.92	16.91	20.40	18.26
SPDA (our work)		18.74	13.70	15.34	16.07	16.57	15.28	15.46	20.83	16.50
<b>SPDAbin (our work)</b>		<b>21.58</b>	15.31	16.82	18.62	20.89	<b>16.34</b>	<b>16.98</b>	<b>24.2</b>	<b>18.84</b>
NLSPCA		22.90	16.48	17.79	18.91	21.10	<b>17.45</b>	17.46	24.22	19.54
NLSPCAbin		20.54	16.54	17.92	<b>19.74</b>	24.00	16.92	17.57	25.91	19.89
BM3D	0.2	22.02	14.28	17.35	18.37	19.95	17.10	17.09	21.27	18.45
BM3Dbin		23.20	16.28	<b>18.25</b>	19.71	<b>24.25</b>	17.44	<b>17.70</b>	23.92	20.09
SPDA (our work)		22.01	16.26	17.26	18.30	19.92	17.10	17.18	23.58	18.95
<b>SPDAbin (our work)</b>		<b>23.59</b>	<b>18.19</b>	17.76	19.31	22.46	17.31	17.57	<b>27.18</b>	<b>20.42</b>
NLSPCA		24.91	18.80	19.23	20.85	23.80	18.78	18.50	28.20	21.63
NLSPCAbin		20.98	17.10	18.32	20.98	26.48	17.77	18.18	26.81	20.83
BM3D	0.5	23.86	15.87	18.83	20.27	22.92	18.49	18.24	23.37	20.29
BM3Dbin		<b>25.70</b>	18.40	<b>19.64</b>	<b>21.71</b>	26.33	<b>19.01</b>	<b>18.67</b>	28.23	22.21
SPDA (our work)		25.42	<b>19.26</b>	19.05	20.49	24.03	18.62	18.45	27.12	21.55
<b>SPDAbin (our work)</b>		25.57	19.24	18.99	21.00	<b>26.56</b>	18.65	18.56	<b>31.03</b>	<b>22.45</b>

Table 7.1: Experiments on simulated data (average over five noise realizations) for peaks 0.1, 0.2 and 0.5.

The figures are the same as those in [20]. Best results are marked.

Method	Peak	Saturn	Flag	Camera	House	Swoosh	Peppers	Bridge	Ridges	Average
NLSPCA		26.89	20.26	20.32	22.09	27.42	19.62	18.94	30.57	23.26
NLSPCAbin		21.18	17.07	18.50	21.26	27.62	17.80	18.20	27.58	21.15
BM3D	1	25.89	18.31	20.37	22.35	26.07	19.89	19.22	26.26	22.42
<b>BM3Dbin</b>		<b>27.41</b>	<b>19.33</b>	<b>20.60</b>	<b>23.19</b>	<b>28.44</b>	<b>20.13</b>	<b>19.38</b>	<b>30.50</b>	<b>23.62</b>
SPDA (our work)		26.85	<b>22.52</b>	20.20	22.61	26.39	20.01	19.18	29.81	23.45
SPDAbin (our work)		27.00	19.85	19.52	21.41	27.42	19.06	18.70	<b>32.41</b>	23.17
NLSPCA		28.22	20.86	20.76	23.86	29.62	20.52	19.47	31.87	24.4
NLSPCAbin		21.49	16.85	18.43	21.41	27.88	17.80	18.34	28.68	21.36
BM3D	2	27.42	20.81	<b>22.13</b>	24.18	28.09	<b>21.97</b>	<b>20.31</b>	29.82	24.59
BM3Dbin		28.84	20.02	21.37	24.49	<b>29.74</b>	21.16	20.17	32.06	24.73
<b>SPDA (our work)</b>		<b>28.93</b>	<b>24.78</b>	21.56	<b>25.10</b>	29.24	21.35	20.19	32.13	<b>25.41</b>
SPDAbin (our work)		28.44	19.87	19.56	21.76	28.64	19.32	18.97	<b>33.39</b>	23.74
NLSPCA		29.44	21.25	21.09	24.89	31.30	21.12	20.16	34.01	25.41
NLSPCAbin		21.20	16.50	18.45	21.44	28.01	17.82	18.34	29.09	21.36
BM3D	4	29.40	23.04	<b>23.94</b>	26.04	30.72	<b>24.07</b>	21.50	32.39	26.89
BM3Dbin		30.19	20.51	21.98	25.48	31.30	22.09	<b>20.80</b>	33.55	25.74
<b>SPDA (our work)</b>		<b>30.71</b>	<b>26.32</b>	21.96	<b>26.26</b>	<b>33.06</b>	22.32	20.59	<b>34.70</b>	<b>26.99</b>
SPDAbin (our work)		29.42	19.67	19.69	21.92	29.93	19.86	19.00	34.38	24.23

Table 7.2: Experiments on simulated data (average over five noise realizations) for peaks 1, 2 and 4.

The figures are the same as those in [20]. Best results are marked.

The recovery error in terms of PSNR for all images and different peak values appears in Tables 7.1 and 7.2. By looking at the overall performance we can see that our proposed strategy provides better performance on average for 5 of 6 tested peak-values. For low peak values SPDAbin behaves better and for larger ones SPDA should be preferred.

The addition of the binning to the algorithms improves their performance significantly in the lower peak values. As the peak raises the effectiveness of the binning reduces (since BM3D relies on the Anscombe, the binning efficiency reduces slower for it).

Concluding this section, SPDA seems to have a good denoising quality for Poisson noisy images with low SNR achieving state-of-the-art recovery performance. We should mention that if we use only the Poisson greedy algorithm for the recovery, without the dictionary learning and the boot-strap stopping criterion, the reconstruction results are degraded by 2.4dB on average (over all images and peak values) if both use binning, and by 2dB on average if not .

## 7.4 Discussion and Summary

In this chapter we have proposed a new scheme for Poisson denoising of images, termed the sparse Poisson denoising algorithm (SPDA). It relies on the Poisson statistical model presented in [20] and uses a dictionary learning strategy with a sparse coding algorithm that employs a boot-strapped stopping criterion. The recovery performance of the SPDA are state-of-the-art and in some scenarios outperform the existing algorithms by more than 1dB.

## Chapter 8

# Epilog

In this dissertation we have considered the performance of greedy algorithms in different sparsity settings. Our main contributions can be summarized as follows:

1. We started with providing near-oracle performance guarantees for the greedy-like schemes: CoSaMP, SP and IHT. The bounds, unlike previous ones for greedy methods, are dependent only on the dictionary properties (RIP constant) and the sparsity level of the sought solution. In addition, those bounds hold also for the MSE of the reconstruction and not only with high probability for the squared error, as has been done in previous works for other algorithms.
2. Motivated by the preceding result, we have developed analysis versions for the greedy-like techniques – CoSaMP, SP, IHT and HTP – for the cosparsity analysis model. By introducing the notion of near-optimal projection and extending the RIP definition, we have provided uniform recovery guarantees for these new schemes in the adversarial noise case. We have shown that, unlike in synthesis, in the analysis model linear dependencies within the dictionary are permitted and even encouraged.
3. As a consequence of our work in the analysis framework, we have realized that as this model sets the focus on the signal, the same is possible also for the synthesis model that classically puts the focus on the representation. With this new approach, we have provided new uniqueness and stability conditions for signal recovery in the synthesis setting. In addition, we have analyzed two new algorithms –  $\epsilon$ -OMP and signal space CoSaMP – showing recovery results that handle high correlations in the synthesis dictionary.
4. For the analysis model we have taken the opposite direction. We have realized that as classical synthesis puts the emphasize on the representation, the same can be done for

analysis by focusing on the coefficients of the signal after applying the analysis dictionary on it. Taking this perspective, we have proposed a new greedy-like technique that operates in the analysis transform domain. This approach provides guarantees for frames both for the adversarial noise and the random Gaussian noise cases. In an unpublished work [105], we show that the same can be done also for the 2D finite difference operator (corresponds to 2D-TV if used with  $\ell_1$  minimization).

5. In the last part of our work we have considered the Poisson image denoising problem. Relying on previous work that proposed Poisson statistics based model, we have developed a denoising scheme that enforces sparse representation on image patches with a global dictionary. This scheme includes a novel sparse coding technique with dictionary learning steps and achieves state-of-the-art results.

We see several directions for further research in this field:

- We found a fundamental gap in analysis between the signal dimension ( $d - r$ ) and the number of measurements required for recovery (order of  $p - \ell$ ). We ask ourselves whether this is a dead-end? With respect to uniform recovery guarantees for the noisy case, the answer seems to be positive [121]. However, this is still an open problem in the other cases.
- Our work on the analysis greedy-like methods assumed the existence of a procedure that finds a cosupport that implies a near optimal projection with a constant  $C_\ell$ . Two examples for optimal cosupport selection schemes were given. However, the existence of an optimal or a near optimal scheme for a general operator is still an open question. The question is: for which types of  $\Omega$  and values of  $C_\ell$  we can find an efficient procedure that implies a near optimal projection. We can ask also whether selection procedures that succeed with high probability exist. Such can be used for developing probabilistic bounds [52].
- The same question holds true also with respect to the signal space near optimal projections. It remains an important and challenging open problem to develop approximate projection techniques which satisfy the assumptions of our main results for SSCoSAMP even when the dictionary is highly coherent in an arbitrary fashion. There are clearly limitations in this regard, as decoding from highly correlated atoms has fundamental

theoretic boundaries. It is unknown, however, how far these limits reach and for what applications accurate reconstruction is still possible.

- An alternative course is to develop greedy methods which do not require such projections, which we believe to be an equally challenging problem. Indeed, initial steps in this direction have been taken with  $\epsilon$ -OMP. However, the proposed guarantees are too restrictive as they are coherence based and depend on the magnitudes of the entries of the original signal.
- As we have seen in the simulations, the thresholding procedure, though not near optimal with the theorems' required constants, provides good reconstruction results for the analysis greedy-like techniques. A theoretical study with this cosupport selection scheme is required. Indeed, we have developed a result for TDIHT. However, it would be interesting to see if the same holds for AIHT and the other analysis greedy-like techniques.
- The first technique for which near-oracle performance guarantees have been proposed in the synthesis context is the Dantzig Selector (DS). As such guarantees have been developed in our work for the analysis framework, it would be interesting to study the analysis version of DS as we expect it to have similar guarantees. We believe that analysis DS should be defined as follows:

$$\underset{\mathbf{v}}{\operatorname{argmin}} \|\mathbf{\Omega}\mathbf{v}\|_1 \quad \text{s.t.} \quad \|\mathbf{M}^*(\mathbf{y} - \mathbf{M}\mathbf{v})\|_\infty \leq \lambda_{DS,\epsilon} \quad (8.1)$$

where  $\lambda_{DS,\epsilon}$  should be a function of the noise statistics and the operator  $\mathbf{\Omega}$ .

- In [113], a result has been developed for signal recovery using  $\ell_1$ -minimization in the case that the signal has sparse representation in the frequency domain and each non-zero frequency is far enough from the other. Using our terminology, this result provides recovery guarantees in the case that a signal has a sparse representation under the redundant DFT as a dictionary and the non-zero locations in the representation corresponds to incoherent atoms. In our results for  $\epsilon$ -OMP we have treated the exact complementary case, where the atoms are highly coherent. It would be interesting to see whether the two proof techniques can be combined to come up with a better theory.
- In our Poisson denoising scheme we have used the same initialization dictionary  $\mathbf{D}$  for all types of images. However, in many applications the type of the images to be observed

is known beforehand, e.g., star in astronomy or cells in fluorescence microscopy. Off-line training of a dictionary which is dedicated to a specific task is expected improve the current results.

- Setting a suitable number of dictionary learning iterations is important for the quality of the reconstruction in the Poisson denoising problem. An automated tuning technique should be considered for this purpose [124, 125].
- Poisson noise appears also in deconvolution problems such as Tomography. Hence, it would be of much value to extend our proposed Poisson denoising algorithm also to the deconvolution setup, where we have a measurement matrix in the noise model.

# Appendix A

## Proofs for Chapter 3

### A.1 Proof of Theorem 3.2.1 – Inequality (3.4)

In the proof of (3.4) we use two main inequalities:

$$\|\boldsymbol{\alpha}_{T-\tilde{T}^t}\|_2 \leq \frac{2\delta_{3k}}{(1-\delta_{3k})^2} \|\boldsymbol{\alpha}_{T-T^{t-1}}\|_2 + \frac{2}{(1-\delta_{3k})^2} \|\mathbf{A}_{T_e}^* \mathbf{e}\|_2, \quad (\text{A.1})$$

and

$$\|\boldsymbol{\alpha}_{T-T^t}\|_2 \leq \frac{1+\delta_{3k}}{1-\delta_{3k}} \|\boldsymbol{\alpha}_{T-\tilde{T}^t}\|_2 + \frac{4}{1-\delta_{3k}} \|\mathbf{A}_{T_e}^* \mathbf{e}\|_2. \quad (\text{A.2})$$

Their proofs are in Sections A.2 and A.3 respectively. The inequality (3.4) is obtained by substituting (A.1) into (A.2) as shown below:

$$\begin{aligned} \|\boldsymbol{\alpha}_{T-T^t}\|_2 &\leq \frac{1+\delta_{3k}}{1-\delta_{3k}} \|\boldsymbol{\alpha}_{T-\tilde{T}^t}\|_2 + \frac{4}{1-\delta_{3k}} \|\mathbf{A}_{T_e}^* \mathbf{e}\|_2 \\ &\leq \frac{1+\delta_{3k}}{1-\delta_{3k}} \left[ \frac{2\delta_{3k}}{(1-\delta_{3k})^2} \|\boldsymbol{\alpha}_{T-T^{t-1}}\|_2 + \frac{2}{(1-\delta_{3k})^2} \|\mathbf{A}_{T_e}^* \mathbf{e}\|_2 \right] + \frac{4}{1-\delta_{3k}} \|\mathbf{A}_{T_e}^* \mathbf{e}\|_2 \\ &\leq \frac{2\delta_{3k}(1+\delta_{3k})}{(1-\delta_{3k})^3} \|\boldsymbol{\alpha}_{T-T^{t-1}}\|_2 + \frac{2(1+\delta_{3k})}{(1-\delta_{3k})^3} \|\mathbf{A}_{T_e}^* \mathbf{e}\|_2 + \frac{4}{1-\delta_{3k}} \|\mathbf{A}_{T_e}^* \mathbf{e}\|_2 \\ &\leq \frac{2\delta_{3k}(1+\delta_{3k})}{(1-\delta_{3k})^3} \|\boldsymbol{\alpha}_{T-T^{t-1}}\|_2 + \frac{6-6\delta_{3k}+4\delta_{3k}^2}{(1-\delta_{3k})^3} \|\mathbf{A}_{T_e}^* \mathbf{e}\|_2, \end{aligned} \quad (\text{A.3})$$

and this concludes this proof.  $\square$

### A.2 Proof of Inequality (A.1)

**Lemma A.2.1** *The following inequality holds true for the SP algorithm:*

$$\|\boldsymbol{\alpha}_{T-\tilde{T}^t}\|_2 \leq \frac{2\delta_{3k}}{(1-\delta_{3k})^2} \|\boldsymbol{\alpha}_{T-T^{t-1}}\|_2 + \frac{2}{(1-\delta_{3k})^2} \|\mathbf{A}_{T_e}^* \mathbf{e}\|_2,$$

*Proof:* We start by the residual-update step in the SP algorithm, and exploit the relation  $\mathbf{y} = \mathbf{A}\boldsymbol{\alpha} + \mathbf{e} = \mathbf{A}_{T-T^{t-1}}\boldsymbol{\alpha}_{T-T^{t-1}} + \mathbf{A}_{T\cap T^{t-1}}\boldsymbol{\alpha}_{T\cap T^{t-1}} + \mathbf{e}$ . This leads to

$$\mathbf{y}_r^{t-1} = \mathbf{Q}_{T^{t-1}}\mathbf{y} = \mathbf{Q}_{T^{t-1}}\mathbf{A}_{T-T^{t-1}}\boldsymbol{\alpha}_{T-T^{t-1}} + \mathbf{Q}_{T^{t-1}}\mathbf{A}_{T\cap T^{t-1}}\boldsymbol{\alpha}_{T\cap T^{t-1}} + \mathbf{Q}_{T^{t-1}}\mathbf{e}. \quad (\text{A.4})$$

Here we have used the linearity of the operator  $\mathbf{Q}_{T^{t-1}}$  with respect to its first entry. The second term in the right-hand-side (rhs) is 0 since  $\mathbf{A}_{T\cap T^{t-1}}\boldsymbol{\alpha}_{T\cap T^{t-1}} \in \text{span}(\mathbf{A}_{T^{t-1}})$ . For the first term in the rhs we have

$$\begin{aligned} \mathbf{Q}_{T^{t-1}}\mathbf{A}_{T-T^{t-1}}\boldsymbol{\alpha}_{T-T^{t-1}} &= \mathbf{A}_{T-T^{t-1}}\boldsymbol{\alpha}_{T-T^{t-1}} - \mathbf{P}_{T^{t-1}}\mathbf{A}_{T-T^{t-1}}\boldsymbol{\alpha}_{T-T^{t-1}} \\ &= \mathbf{A}_{T-T^{t-1}}\boldsymbol{\alpha}_{T-T^{t-1}} + \mathbf{A}_{T^{t-1}}\boldsymbol{\alpha}_{\mathbf{P},T^{t-1}} = [\mathbf{A}_{T-T^{t-1}}, \mathbf{A}_{T^{t-1}}] \begin{bmatrix} \boldsymbol{\alpha}_{T-T^{t-1}} \\ \boldsymbol{\alpha}_{\mathbf{P},T^{t-1}} \end{bmatrix} \triangleq \mathbf{A}_{T\cup T^{t-1}}\boldsymbol{\alpha}_r^{t-1}, \end{aligned} \quad (\text{A.5})$$

where we have defined

$$\boldsymbol{\alpha}_{\mathbf{P},T^{t-1}} = -(\mathbf{A}_{T^{t-1}}^*\mathbf{A}_{T^{t-1}})^{-1}\mathbf{A}_{T^{t-1}}^*\mathbf{A}_{T-T^{t-1}}\boldsymbol{\alpha}_{T-T^{t-1}}. \quad (\text{A.6})$$

Combining (A.4) and (A.5) leads to

$$\mathbf{y}_r^{t-1} = \mathbf{A}_{T\cup T^{t-1}}\boldsymbol{\alpha}_r^{t-1} + \mathbf{Q}_{T^{t-1}}\mathbf{e}. \quad (\text{A.7})$$

By the definition of  $T_\Delta$  in Algorithm 3 we obtain

$$\begin{aligned} \|\mathbf{A}_{T_\Delta}^*\mathbf{y}_r^{t-1}\|_2 &\geq \|\mathbf{A}_T^*\mathbf{y}_r^{t-1}\|_2 \geq \|\mathbf{A}_{T-T^{t-1}}^*\mathbf{y}_r^{t-1}\|_2 \\ &\geq \|\mathbf{A}_{T-T^{t-1}}^*\mathbf{A}_{T\cup T^{t-1}}\boldsymbol{\alpha}_r^{t-1}\|_2 - \|\mathbf{A}_{T-T^{t-1}}^*\mathbf{Q}_{T^{t-1}}\mathbf{e}\|_2 \\ &\geq \|\mathbf{A}_{T-T^{t-1}}^*\mathbf{A}_{T\cup T^{t-1}}\boldsymbol{\alpha}_r^{t-1}\|_2 - \|\mathbf{A}_{T-T^{t-1}}^*\mathbf{e}\|_2 - \|\mathbf{A}_{T-T^{t-1}}^*\mathbf{P}_{T^{t-1}}\mathbf{e}\|_2. \end{aligned} \quad (\text{A.8})$$

We will bound  $\|\mathbf{A}_{T-T^{t-1}}^*\mathbf{P}_{T^{t-1}}\mathbf{e}\|_2$  from above using RIP properties from Section 3.1,

$$\|\mathbf{A}_{T-T^{t-1}}^*\mathbf{P}_{T^{t-1}}\mathbf{e}\|_2 = \|\mathbf{A}_{T-T^{t-1}}^*\mathbf{A}_{T^{t-1}}(\mathbf{A}_{T^{t-1}}^*\mathbf{A}_{T^{t-1}})^{-1}\mathbf{A}_{T^{t-1}}^*\mathbf{e}\|_2 \leq \frac{\delta_{3k}}{1-\delta_{3k}}\|\mathbf{A}_{T^{t-1}}^*\mathbf{e}\|_2. \quad (\text{A.9})$$

Combining (A.8) and (A.9) leads to

$$\begin{aligned} \|\mathbf{A}_{T_\Delta}^*\mathbf{y}_r^{t-1}\|_2 &\geq \|\mathbf{A}_{T-T^{t-1}}^*\mathbf{A}_{T\cup T^{t-1}}\boldsymbol{\alpha}_r^{t-1}\|_2 - \|\mathbf{A}_T^*\mathbf{e}\|_2 - \frac{\delta_{3k}}{1-\delta_{3k}}\|\mathbf{A}_{T^{t-1}}^*\mathbf{e}\|_2 \\ &\geq \|\mathbf{A}_{T-T^{t-1}}^*\mathbf{A}_{T\cup T^{t-1}}\boldsymbol{\alpha}_r^{t-1}\|_2 - \frac{1}{1-\delta_{3k}}\|\mathbf{A}_T^*\mathbf{e}\|_2. \end{aligned} \quad (\text{A.10})$$

By the definition of  $T_\Delta$  and  $\mathbf{y}_r^{t-1}$  it holds that  $T_\Delta \cap T^{t-1} = \emptyset$  since  $\mathbf{A}_{T^{t-1}}^* \mathbf{y}_r^{t-1} = 0$ . Using (A.7), the left-hand-side (lhs) of (A.10) is upper bounded by

$$\begin{aligned} \left\| \mathbf{A}_{T_\Delta}^* \mathbf{y}_r^{t-1} \right\|_2 &\leq \left\| \mathbf{A}_{T_\Delta}^* \mathbf{A}_{T \cup T^{t-1}} \boldsymbol{\alpha}_r^{t-1} \right\|_2 + \left\| \mathbf{A}_{T_\Delta}^* \mathbf{Q}_{T^{t-1}} \mathbf{e} \right\|_2 \\ &\leq \left\| \mathbf{A}_{T_\Delta}^* \mathbf{A}_{T \cup T^{t-1}} \boldsymbol{\alpha}_r^{t-1} \right\|_2 + \left\| \mathbf{A}_{T_\Delta}^* \mathbf{e} \right\|_2 + \left\| \mathbf{A}_{T_\Delta}^* \mathbf{A}_{T^{t-1}} (\mathbf{A}_{T^{t-1}}^* \mathbf{A}_{T^{t-1}})^{-1} \mathbf{A}_{T^{t-1}}^* \mathbf{e} \right\|_2 \\ &\leq \left\| \mathbf{A}_{T_\Delta}^* \mathbf{A}_{T \cup T^{t-1}} \boldsymbol{\alpha}_r^{t-1} \right\|_2 + \left\| \mathbf{A}_{T_\Delta}^* \mathbf{e} \right\|_2 + \frac{\delta_{3k}}{1 - \delta_{3k}} \left\| \mathbf{A}_{T^{t-1}}^* \mathbf{e} \right\|_2 \\ &\leq \left\| \mathbf{A}_{T_\Delta}^* \mathbf{A}_{T \cup T^{t-1}} \boldsymbol{\alpha}_r^{t-1} \right\|_2 + \frac{1}{1 - \delta_{3k}} \left\| \mathbf{A}_{T_e}^* \mathbf{e} \right\|_2. \end{aligned} \quad (\text{A.11})$$

Combining (A.10) and (A.11) gives

$$\left\| \mathbf{A}_{T_\Delta}^* \mathbf{A}_{T \cup T^{t-1}} \boldsymbol{\alpha}_r^{t-1} \right\|_2 + \frac{2}{1 - \delta_{3k}} \left\| \mathbf{A}_{T_e}^* \mathbf{e} \right\|_2 \geq \left\| \mathbf{A}_{T - T^{t-1}}^* \mathbf{A}_{T \cup T^{t-1}} \boldsymbol{\alpha}_r^{t-1} \right\|_2. \quad (\text{A.12})$$

Removing the common rows in  $\mathbf{A}_{T_\Delta}^*$  and  $\mathbf{A}_{T - T^{t-1}}^*$  we get

$$\begin{aligned} \left\| \mathbf{A}_{T_\Delta - T}^* \mathbf{A}_{T \cup T^{t-1}} \boldsymbol{\alpha}_r^{t-1} \right\|_2 + \frac{2}{1 - \delta_{3k}} \left\| \mathbf{A}_{T_e}^* \mathbf{e} \right\|_2 &\geq \left\| \mathbf{A}_{T - T^{t-1} - T_\Delta}^* \mathbf{A}_{T \cup T^{t-1}} \boldsymbol{\alpha}_r^{t-1} \right\|_2 \\ &= \left\| \mathbf{A}_{T - \tilde{T}^t}^* \mathbf{A}_{T \cup T^{t-1}} \boldsymbol{\alpha}_r^{t-1} \right\|_2. \end{aligned} \quad (\text{A.13})$$

The last equality is true because  $T - T^{t-1} - T_\Delta = T - T^{t-1} - (T - \tilde{T}^t) = T - \tilde{T}^t$ .

Now we turn to bound the lhs and rhs terms of (A.13) from below and above, respectively. For the lhs term we exploit the fact that the supports  $T_\Delta - T$  and  $T \cup T^{t-1}$  are disjoint, leading to

$$\left\| \mathbf{A}_{T_\Delta - T}^* \mathbf{A}_{T \cup T^{t-1}} \boldsymbol{\alpha}_r^{t-1} \right\|_2 \leq \delta_{|T_\Delta \cup T^{t-1} \cup T|} \left\| \boldsymbol{\alpha}_r^{t-1} \right\|_2 \leq \delta_{3k} \left\| \boldsymbol{\alpha}_r^{t-1} \right\|_2 \quad (\text{A.14})$$

For the rhs term in (A.13), we obtain

$$\begin{aligned} &\left\| \mathbf{A}_{T - \tilde{T}^t}^* \mathbf{A}_{T \cup T^{t-1}} \boldsymbol{\alpha}_r^{t-1} \right\|_2 \\ &\geq \left\| \mathbf{A}_{T - \tilde{T}^t}^* \mathbf{A}_{T - \tilde{T}^t} (\boldsymbol{\alpha}_r^{t-1})_{T - \tilde{T}^t} \right\|_2 - \left\| \mathbf{A}_{T - \tilde{T}^t}^* \mathbf{A}_{(T \cup T^{t-1}) - (T - \tilde{T}^t)} (\boldsymbol{\alpha}_r^{t-1})_{(T \cup T^{t-1}) - (T - \tilde{T}^t)} \right\|_2 \\ &\geq (1 - \delta_k) \left\| (\boldsymbol{\alpha}_r^{t-1})_{T - \tilde{T}^t} \right\|_2 - \delta_{3k} \left\| \boldsymbol{\alpha}_r^{t-1} \right\|_2 \geq (1 - \delta_{3k}) \left\| (\boldsymbol{\alpha}_r^{t-1})_{T - \tilde{T}^t} \right\|_2 - \delta_{3k} \left\| \boldsymbol{\alpha}_r^{t-1} \right\|_2 \end{aligned} \quad (\text{A.15})$$

Substitution of the two bounds derived above into (A.13) gives

$$2\delta_{3k} \left\| \boldsymbol{\alpha}_r^{t-1} \right\|_2 + \frac{2}{1 - \delta_{3k}} \left\| \mathbf{A}_{T_e}^* \mathbf{e} \right\|_2 \geq (1 - \delta_{3k}) \left\| (\boldsymbol{\alpha}_r^{t-1})_{T - \tilde{T}^t} \right\|_2. \quad (\text{A.16})$$

The above inequality uses  $\boldsymbol{\alpha}_r^{t-1}$ , which was defined in (A.5), and this definition relies on yet another definition for the vector  $\boldsymbol{\alpha}_{\mathbf{P}, T^{t-1}}$  in (A.6). We proceed by bounding  $\left\| \boldsymbol{\alpha}_{\mathbf{P}, T^{t-1}} \right\|_2$  from above,

$$\begin{aligned} \left\| \boldsymbol{\alpha}_{\mathbf{P}, T^{t-1}} \right\|_2 &= \left\| -(\mathbf{A}_{T^{t-1}}^* \mathbf{A}_{T^{t-1}})^{-1} \mathbf{A}_{T^{t-1}}^* \mathbf{A}_{T - T^{t-1}} \boldsymbol{\alpha}_{T - T^{t-1}} \right\|_2 \\ &\leq \frac{1}{1 - \delta_k} \left\| -\mathbf{A}_{T^{t-1}}^* \mathbf{A}_{T - T^{t-1}} \boldsymbol{\alpha}_{T - T^{t-1}} \right\|_2 \leq \frac{\delta_{2k}}{1 - \delta_k} \left\| \boldsymbol{\alpha}_{T - T^{t-1}} \right\|_2 \leq \frac{\delta_{3k}}{1 - \delta_{3k}} \left\| \boldsymbol{\alpha}_{T - T^{t-1}} \right\|_2, \end{aligned} \quad (\text{A.17})$$

and get

$$\|\boldsymbol{\alpha}_r^{t-1}\|_2 \leq \|\boldsymbol{\alpha}_{T-T^{t-1}}\|_2 + \|\boldsymbol{\alpha}_{\mathbf{P}, T^{t-1}}\|_2 \leq \left(1 + \frac{\delta_{3k}}{1 - \delta_{3k}}\right) \|\boldsymbol{\alpha}_{T-T^{t-1}}\|_2 \leq \frac{1}{1 - \delta_{3k}} \|\boldsymbol{\alpha}_{T-T^{t-1}}\|_2. \quad (\text{A.18})$$

In addition, since  $(\boldsymbol{\alpha}_r^{t-1})_{T-T^{t-1}} = \boldsymbol{\alpha}_{T-T^{t-1}}$  then  $(\boldsymbol{\alpha}_r^{t-1})_{T-\tilde{T}^t} = \boldsymbol{\alpha}_{T-\tilde{T}^t}$ . Using this fact and (A.18) with (A.16) leads to

$$\|\boldsymbol{\alpha}_{T-\tilde{T}^t}\|_2 \leq \frac{2\delta_{3k}}{(1 - \delta_{3k})^2} \|\boldsymbol{\alpha}_{T-T^{t-1}}\|_2 + \frac{2}{(1 - \delta_{3k})^2} \|\mathbf{A}_{T_e}^* \mathbf{e}\|_2, \quad (\text{A.19})$$

which proves the inequality in (A.1).  $\square$

### A.3 Proof of Inequality (A.2)

**Lemma A.3.1** *The following inequality holds true for the SP algorithm:*

$$\|\boldsymbol{\alpha}_{T-T^t}\|_2 \leq \frac{1 + \delta_{3k}}{1 - \delta_{3k}} \|\boldsymbol{\alpha}_{T-\tilde{T}^t}\|_2 + \frac{4}{1 - \delta_{3k}} \|\mathbf{A}_{T_e}^* \mathbf{e}\|_2.$$

*Proof:* We will define the smear vector  $\boldsymbol{\epsilon} = \mathbf{w} - \boldsymbol{\alpha}_{\tilde{T}^t}$ , where  $\mathbf{w}$  is the outcome of the representation computation over  $\tilde{T}^t$ , given by

$$\mathbf{w} = \mathbf{A}_{\tilde{T}^t}^\dagger \mathbf{y} = \mathbf{A}_{\tilde{T}^t}^\dagger (\mathbf{A}_T \boldsymbol{\alpha}_T + \mathbf{e}), \quad (\text{A.20})$$

as defined in Algorithm 3. Expanding the first term in the last equality gives:

$$\begin{aligned} \mathbf{A}_{\tilde{T}^t}^\dagger \mathbf{A}_T \boldsymbol{\alpha}_T &= \mathbf{A}_{\tilde{T}^t}^\dagger \mathbf{A}_{T \cap \tilde{T}^t} \boldsymbol{\alpha}_{T \cap \tilde{T}^t} + \mathbf{A}_{\tilde{T}^t}^\dagger \mathbf{A}_{T - \tilde{T}^t} \boldsymbol{\alpha}_{T - \tilde{T}^t} \\ &= \mathbf{A}_{\tilde{T}^t}^\dagger [\mathbf{A}_{T \cap \tilde{T}^t}, \mathbf{A}_{\tilde{T}^t - T}] \begin{bmatrix} \boldsymbol{\alpha}_{T \cap \tilde{T}^t} \\ \mathbf{0} \end{bmatrix} + \mathbf{A}_{\tilde{T}^t}^\dagger \mathbf{A}_{T - \tilde{T}^t} \boldsymbol{\alpha}_{T - \tilde{T}^t} \\ &= \mathbf{A}_{\tilde{T}^t}^\dagger \mathbf{A}_{\tilde{T}^t} \boldsymbol{\alpha}_{\tilde{T}^t} + \mathbf{A}_{\tilde{T}^t}^\dagger \mathbf{A}_{T - \tilde{T}^t} \boldsymbol{\alpha}_{T - \tilde{T}^t} = \boldsymbol{\alpha}_{\tilde{T}^t} + \mathbf{A}_{\tilde{T}^t}^\dagger \mathbf{A}_{T - \tilde{T}^t} \boldsymbol{\alpha}_{T - \tilde{T}^t}. \end{aligned} \quad (\text{A.21})$$

The equalities hold based on the definition of  $\mathbf{A}_{\tilde{T}^t}^\dagger$  and on the fact that  $\boldsymbol{\alpha}$  is 0 outside of  $T$ . Using (A.21) we bound the smear energy from above, obtaining

$$\begin{aligned} \|\boldsymbol{\epsilon}\|_2 &\leq \left\| \mathbf{A}_{\tilde{T}^t}^\dagger \mathbf{A}_T \boldsymbol{\alpha}_T \right\|_2 + \left\| \mathbf{A}_{\tilde{T}^t}^\dagger \mathbf{e} \right\|_2 \\ &= \left\| (\mathbf{A}_{\tilde{T}^t}^* \mathbf{A}_{\tilde{T}^t})^{-1} \mathbf{A}_{\tilde{T}^t}^* \mathbf{A}_{T - \tilde{T}^t} \boldsymbol{\alpha}_{T - \tilde{T}^t} \right\|_2 + \left\| (\mathbf{A}_{\tilde{T}^t}^* \mathbf{A}_{\tilde{T}^t})^{-1} \mathbf{A}_{\tilde{T}^t}^* \mathbf{e} \right\|_2 \\ &\leq \frac{\delta_{3k}}{1 - \delta_{3k}} \|\boldsymbol{\alpha}_{T - \tilde{T}^t}\|_2 + \frac{1}{1 - \delta_{3k}} \|\mathbf{A}_{\tilde{T}^t}^* \mathbf{e}\|_2. \end{aligned} \quad (\text{A.22})$$

We now turn to bound  $\|\boldsymbol{\epsilon}\|_2$  from below. We denote the support of the  $k$  smallest coefficients in  $\mathbf{w}$  by  $\Delta T \triangleq \tilde{T}^t - T^t$ . Thus, for any set  $T' \subset \tilde{T}^t$  of cardinality  $k$ , it holds that  $\|(\mathbf{w})_{\Delta T}\|_2 \leq \|(\mathbf{w})_{T'}\|_2$ . In particular, we shall choose  $T'$  such that  $T' \cap T = \emptyset$ , which necessarily exists

because  $\tilde{T}^t$  is of cardinality  $2k$  and therefore there must be at  $k$  entries in this support that are outside  $T$ . Thus, using the relation  $\boldsymbol{\epsilon} = \mathbf{w} - \boldsymbol{\alpha}_{\tilde{T}^t}$  we get

$$\|(\mathbf{w})_{\Delta T}\|_2 \leq \|(\mathbf{w})_{T'}\|_2 = \|(\boldsymbol{\alpha}_{\tilde{T}^t})_{T'} + \boldsymbol{\epsilon}_{T'}\|_2 = \|\boldsymbol{\epsilon}_{T'}\|_2 \leq \|\boldsymbol{\epsilon}\|_2. \quad (\text{A.23})$$

Because  $\boldsymbol{\alpha}$  is supported on  $T$  we have that  $\|\boldsymbol{\alpha}_{\Delta T}\|_2 = \|\boldsymbol{\alpha}_{\Delta T \cap T}\|_2$ . An upper bound for this vector is reached by

$$\begin{aligned} \|\boldsymbol{\alpha}_{\Delta T \cap T}\|_2 &= \|(\mathbf{w})_{\Delta T \cap T} - \boldsymbol{\epsilon}_{\Delta T \cap T}\|_2 \\ &\leq \|(\mathbf{w})_{\Delta T \cap T}\|_2 + \|\boldsymbol{\epsilon}_{\Delta T \cap T}\|_2 \leq \|(\mathbf{w})_{\Delta T}\|_2 + \|\boldsymbol{\epsilon}\|_2 \leq 2\|\boldsymbol{\epsilon}\|_2, \end{aligned} \quad (\text{A.24})$$

where the last step uses (A.23). The vector  $\boldsymbol{\alpha}_{T-\tilde{T}^t}$  can be decomposed as  $\boldsymbol{\alpha}_{T-\tilde{T}^t} = \left[ \boldsymbol{\alpha}_{T \cap \Delta T}^*, \boldsymbol{\alpha}_{T-\tilde{T}^t}^* \right]^*$ . Using (A.22) and (A.24) we get

$$\begin{aligned} \|\boldsymbol{\alpha}_{T-\tilde{T}^t}\|_2 &\leq \|\boldsymbol{\alpha}_{T \cap \Delta T}\|_2 + \|\boldsymbol{\alpha}_{T-\tilde{T}^t}\|_2 \leq 2\|\boldsymbol{\epsilon}\|_2 + \|\boldsymbol{\alpha}_{T-\tilde{T}^t}\|_2 \\ &\leq \left(1 + \frac{2\delta_{3k}}{1-\delta_{3k}}\right) \|\boldsymbol{\alpha}_{T-\tilde{T}^t}\|_2 + \frac{2}{1-\delta_{3k}} \|\mathbf{A}_{\tilde{T}^t}^* \mathbf{e}\|_2 \\ &= \frac{1+\delta_{3k}}{1-\delta_{3k}} \|\boldsymbol{\alpha}_{T-\tilde{T}^t}\|_2 + \frac{4}{1-\delta_{3k}} \|\mathbf{A}_{T_e}^* \mathbf{e}\|_2, \end{aligned}$$

where the last step uses the property  $\|\mathbf{A}_{\tilde{T}^t}^* \mathbf{e}\|_2 \leq 2\|\mathbf{A}_{T_e}^* \mathbf{e}\|_2$  taken from Section 3.1, and this concludes the proof.  $\square$

## A.4 Proof of Inequality (3.15)

**Lemma A.4.1** *The following inequality holds true for the CoSaMP algorithm:*

$$\|\boldsymbol{\alpha} - \hat{\boldsymbol{\alpha}}_{\text{CoSaMP}}^t\|_2 \leq \frac{4\delta_{4k}}{(1-\delta_{4k})^2} \|\boldsymbol{\alpha} - \hat{\boldsymbol{\alpha}}_{\text{CoSaMP}}^{t-1}\|_2 + \frac{14-6\delta_{4k}}{(1-\delta_{4k})^2} \|\mathbf{A}_{T_e}^* \mathbf{e}\|_2. \quad (\text{A.25})$$

*Proof:* We denote  $\hat{\boldsymbol{\alpha}}_{\text{CoSaMP}}^t$  as the solution of CoSaMP in the  $t$ -th iteration:  $\hat{\boldsymbol{\alpha}}_{\text{CoSaMP},(T^t)^c}^t = 0$  and  $\hat{\boldsymbol{\alpha}}_{\text{CoSaMP},T^t}^t = \mathbf{w}_{T^t}$ . We further define  $\mathbf{r}^t \triangleq \boldsymbol{\alpha} - \hat{\boldsymbol{\alpha}}_{\text{CoSaMP}}^t$  and use the definition of  $T_{e,b}$  (Equation (3.25)). Our proof is based on the proof of Theorem 4.1 in [39] and the Lemmas used with it.

Since we choose  $T_\Delta$  to contain the biggest  $2k$  elements in  $\mathbf{A}^* \mathbf{y}_r^t$  and  $|T^{t-1} \cup T| \leq 2k$  it holds true that  $\|(\mathbf{A}^* \mathbf{y}_r^t)_{T^t \cup T}\|_2 \leq \|(\mathbf{A}^* \mathbf{y}_r^t)_{T_\Delta}\|_2$ . Removing the common elements from both sides we get

$$\|(\mathbf{A}^* \mathbf{y}_r^t)_{(T^t \cup T) - T_\Delta}\|_2 \leq \|(\mathbf{A}^* \mathbf{y}_r^t)_{T_\Delta - (T^t \cup T)}\|_2. \quad (\text{A.26})$$

We proceed by bounding the rhs and lhs of (A.26), from above and from below respectively, using the triangle inequality. We use Propositions 3.1.1 and 3.1.2, the definition of  $T_{e,2}$ , and the

fact that  $\|\mathbf{r}^t\|_2 = \|\mathbf{r}_{T^t \cup T}^t\|_2$  (this holds true since the support of  $\mathbf{r}^t$  is over  $T \cup T^t$ ). For the rhs we obtain

$$\begin{aligned} \left\| (\mathbf{A}^* \mathbf{y}_r^t)_{T_\Delta - (T^t \cup T)} \right\|_2 &= \left\| \mathbf{A}_{T_\Delta - (T^t \cup T)}^* (\mathbf{A} \mathbf{r}^t + \mathbf{e}) \right\|_2 \\ &\leq \left\| \mathbf{A}_{T_\Delta - (T^t \cup T)}^* \mathbf{A}_{T^t \cup T} \mathbf{r}_{T^t \cup T}^t \right\|_2 + \left\| \mathbf{A}_{T_\Delta - (T^t \cup T)}^* \mathbf{e} \right\|_2 \leq \delta_{4k} \|\mathbf{r}^t\|_2 + \left\| \mathbf{A}_{T_{e,2}}^* \mathbf{e} \right\|_2. \end{aligned} \quad (\text{A.27})$$

and for the lhs:

$$\begin{aligned} \left\| (\mathbf{A}^* \mathbf{y}_r^t)_{(T^t \cup T) - T_\Delta} \right\|_2 &= \left\| \mathbf{A}_{(T^t \cup T) - T_\Delta}^* (\mathbf{A} \mathbf{r}^t + \mathbf{e}) \right\|_2 \\ &\geq \left\| \mathbf{A}_{(T^t \cup T) - T_\Delta}^* \mathbf{A}_{(T^t \cup T) - T_\Delta} \mathbf{r}_{(T^t \cup T) - T_\Delta}^t \right\|_2 - \left\| \mathbf{A}_{(T^t \cup T) - T_\Delta}^* \mathbf{A}_{T_\Delta} \mathbf{r}_{T_\Delta}^t \right\|_2 - \left\| \mathbf{A}_{(T^t \cup T) - T_\Delta}^* \mathbf{e} \right\|_2 \\ &\geq (1 - \delta_{2k}) \left\| \mathbf{r}_{(T^t \cup T) - T_\Delta}^t \right\|_2 - \delta_{4k} \|\mathbf{r}_{T_\Delta}^t\|_2 - \left\| \mathbf{A}_{T_{e,2}}^* \mathbf{e} \right\|_2. \end{aligned} \quad (\text{A.28})$$

Because  $\mathbf{r}^t$  is supported over  $T \cup T^t$ , it holds true that  $\left\| \mathbf{r}_{(T^t \cup T) - T_\Delta}^t \right\|_2 = \left\| \mathbf{r}_{T_\Delta}^t \right\|_2$ . Combining (A.28) and (A.27) with (A.26), gives

$$\left\| \mathbf{r}_{T_\Delta}^t \right\|_2 \leq \frac{2\delta_{4k} \|\mathbf{r}^t\|_2 + 2 \left\| \mathbf{A}_{T_{e,2}}^* \mathbf{e} \right\|_2}{1 - \delta_{2k}} \leq \frac{2\delta_{4k} \|\mathbf{r}^t\|_2 + 4 \left\| \mathbf{A}_{T_e}^* \mathbf{e} \right\|_2}{1 - \delta_{4k}}.$$

For brevity of notations, we denote hereafter  $\tilde{T}^t$  as  $\tilde{T}$ . Using  $\mathbf{y} = \mathbf{A} \boldsymbol{\alpha} + \mathbf{e} = \mathbf{A}_{\tilde{T}} \boldsymbol{\alpha}_{\tilde{T}} + \mathbf{A}_{\tilde{T}^c} \boldsymbol{\alpha}_{\tilde{T}^c} + \mathbf{e}$ , we observe that

$$\begin{aligned} \|\boldsymbol{\alpha}_{\tilde{T}} - \mathbf{w}_{\tilde{T}}\|_2 &= \left\| \boldsymbol{\alpha}_{\tilde{T}} - \mathbf{A}_{\tilde{T}}^\dagger (\mathbf{A}_{\tilde{T}} \boldsymbol{\alpha}_{\tilde{T}} + \mathbf{A}_{\tilde{T}^c} \boldsymbol{\alpha}_{\tilde{T}^c} + \mathbf{e}) \right\|_2 = \left\| \mathbf{A}_{\tilde{T}}^\dagger (\mathbf{A}_{\tilde{T}^c} \boldsymbol{\alpha}_{\tilde{T}^c} + \mathbf{e}) \right\|_2 \\ &\leq \left\| (\mathbf{A}_{\tilde{T}}^* \mathbf{A}_{\tilde{T}})^{-1} \mathbf{A}_{\tilde{T}}^* \mathbf{A}_{\tilde{T}^c} \boldsymbol{\alpha}_{\tilde{T}^c} \right\|_2 + \left\| (\mathbf{A}_{\tilde{T}}^* \mathbf{A}_{\tilde{T}})^{-1} \mathbf{A}_{\tilde{T}}^* \mathbf{e} \right\|_2 \\ &\leq \frac{1}{1 - \delta_{3k}} \left\| \mathbf{A}_{\tilde{T}}^* \mathbf{A}_{\tilde{T}^c} \boldsymbol{\alpha}_{\tilde{T}^c} \right\|_2 + \frac{1}{1 - \delta_{3k}} \left\| \mathbf{A}_{T_{e,3}}^* \mathbf{e} \right\|_2 \leq \frac{\delta_{4k}}{1 - \delta_{4k}} \|\boldsymbol{\alpha}_{\tilde{T}^c}\|_2 + \frac{3}{1 - \delta_{4k}} \left\| \mathbf{A}_{T_e}^* \mathbf{e} \right\|_2, \end{aligned} \quad (\text{A.29})$$

where the last inequality holds true because of Proposition 3.1.4 and that  $|\tilde{T}| = 3k$ . Using the triangle inequality and the fact that  $\mathbf{w}$  is supported on  $\tilde{T}$ , we obtain

$$\|\boldsymbol{\alpha} - \mathbf{w}\|_2 \leq \|\boldsymbol{\alpha}_{\tilde{T}^c}\|_2 + \|\boldsymbol{\alpha}_{\tilde{T}} - \mathbf{w}_{\tilde{T}}\|_2, \quad (\text{A.30})$$

which leads to

$$\begin{aligned} \|\boldsymbol{\alpha} - \mathbf{w}\|_2 &\leq \left( 1 + \frac{\delta_{4k}}{1 - \delta_{4k}} \right) \|\boldsymbol{\alpha}_{\tilde{T}^c}\|_2 + \frac{3}{1 - \delta_{4k}} \left\| \mathbf{A}_{T_e}^* \mathbf{e} \right\|_2 \\ &= \frac{1}{1 - \delta_{4k}} \|\boldsymbol{\alpha}_{\tilde{T}^c}\|_2 + \frac{3}{1 - \delta_{4k}} \left\| \mathbf{A}_{T_e}^* \mathbf{e} \right\|_2. \end{aligned} \quad (\text{A.31})$$

Having the above results we can obtain (3.15) by

$$\begin{aligned}
\|\boldsymbol{\alpha} - \hat{\boldsymbol{\alpha}}_{\text{CoSaMP}}^t\|_2 &\leq 2\|\boldsymbol{\alpha} - \mathbf{w}\|_2 \leq 2\left(\frac{1}{1-\delta_{4k}}\|\boldsymbol{\alpha}_{\bar{T}^c}\|_2 + \frac{3}{1-\delta_{4k}}\|\mathbf{A}_{T_e}^*\mathbf{e}\|_2\right) \\
&\leq \frac{2}{1-\delta_{4k}}\|\mathbf{r}_{T_\Delta}^{t-1}\|_2 + \frac{6}{1-\delta_{4k}}\|\mathbf{A}_{T_e}^*\mathbf{e}\|_2 \\
&\leq \frac{2}{1-\delta_{4k}}\left(\frac{2\delta_{4k}}{1-\delta_{4k}}\|\mathbf{r}^{t-1}\|_2 + \frac{4}{1-\delta_{4k}}\|\mathbf{A}_{T_e}^*\mathbf{e}\|_2\right) + \frac{6}{1-\delta_{4k}}\|\mathbf{A}_{T_e}^*\mathbf{e}\|_2 \\
&= \frac{4\delta_{4k}}{(1-\delta_{4k})^2}\|\mathbf{r}^{t-1}\|_2 + \frac{14-6\delta_{4k}}{(1-\delta_{4k})^2}\|\mathbf{A}_{T_e}^*\mathbf{e}\|_2,
\end{aligned} \tag{A.32}$$

where the inequalities are based on Lemma 4.5 from [39], (A.31), Lemma 4.3 from [39] and (A.29) respectively.  $\square$



# Appendix B

## Proofs for Chapter 4

### B.1 Proofs of Theorem 4.1.7 and Theorem 4.1.8

*Theorem 4.1.7 (Theorem 3.3 in [95]):* Let  $\mathbf{M} \in \mathbb{R}^{m \times d}$  be a random matrix that satisfies that for any  $\mathbf{z} \in \mathbb{R}^d$  and  $0 < \tilde{\varepsilon} \leq \frac{1}{3}$

$$P\left(\left|\|\mathbf{M}\mathbf{z}\|_2^2 - \|\mathbf{z}\|_2^2\right| \geq \tilde{\varepsilon} \|\mathbf{z}\|_2^2\right) \leq e^{-\frac{C_M m \tilde{\varepsilon}}{2}},$$

where  $C_M > 0$  is a constant. For any value of  $\varepsilon_r > 0$ , if

$$m \geq \frac{32}{C_M \varepsilon_r^2} \left( \log(|\mathcal{L}_r^{\text{corank}}|) + (d-r) \log(9/\varepsilon_r) + t \right),$$

then  $\delta_r^{\text{corank}} \leq \varepsilon_r$  with probability exceeding  $1 - e^{-t}$ .

*Theorem 4.1.8:* Under the same setup of Theorem 4.1.7, for any  $\varepsilon_\ell > 0$  if

$$m \geq \frac{32}{C_M \varepsilon_\ell^2} \left( (p-\ell) \log\left(\frac{9p}{(p-\ell)\varepsilon_\ell}\right) + t \right),$$

then  $\delta_\ell \leq \varepsilon_\ell$  with probability exceeding  $1 - e^{-t}$ .

*Proof:* Let  $\tilde{\varepsilon} = \varepsilon_r/4$ ,  $B^{d-r} = \{\mathbf{z} \in \mathbb{R}^{d-r}, \|\mathbf{z}\|_2 \leq 1\}$  and  $\Psi$  an  $\tilde{\varepsilon}$ -net for  $B^{d-r}$  with size  $|\Psi| \leq \left(1 + \frac{2}{\tilde{\varepsilon}}\right)^{d-r}$  [96]. For any subspace  $\mathcal{W}_\Lambda^B = \mathcal{W}_\Lambda \cap B^{d-r}$  such that  $\Lambda \in \mathcal{L}_r^{\text{corank}}$  we can build an orthogonal matrix  $\mathbf{U}_\Omega \in \mathbb{R}^{d \times (d-r)}$  such that  $\mathcal{W}_\Lambda^B = \{\mathbf{U}_\Omega \mathbf{z}, \mathbf{z} \in \mathbb{R}^{d-r}, \|\mathbf{z}\|_2 \leq 1\} = \mathbf{U}_\Omega B^{d-r}$ . It is easy to see that  $\Psi_\Lambda = \mathbf{U}_\Omega \Psi^{d-r}$  is an  $\tilde{\varepsilon}$ -net for  $\mathcal{W}_\Lambda^B$  and that  $\Psi_{\mathcal{A}_r^{\text{corank}}} = \cup_{\Lambda \in \mathcal{L}_r^{\text{corank}}} \Psi_\Lambda$  is an  $\tilde{\varepsilon}$ -net for  $\mathcal{A}_r^{\text{corank}} \cap B^d$ , where  $|\Psi_{\mathcal{A}_r^{\text{corank}}}| \leq |\mathcal{L}_r^{\text{corank}}| \left(1 + \frac{2}{\tilde{\varepsilon}}\right)^{d-r}$ .

We could stop here and use directly Theorem 2.1 from [96] to get the desired result for Theorem 4.1.7. However, we present the remaining of the proof using a proof technique from [98, 76]. Using union bound and the properties of  $\mathbf{M}$  we have that with probability exceeding  $1 - |\mathcal{L}_r^{\text{corank}}| \left(1 + \frac{2}{\tilde{\varepsilon}}\right)^{d-r} e^{-\frac{C_M m \tilde{\varepsilon}^2}{2}}$  every  $\mathbf{v} \in \Psi_{\mathcal{A}_r^{\text{corank}}}$  satisfies

$$(1 - \tilde{\varepsilon}) \|\mathbf{v}\|_2^2 \leq \|\mathbf{M}\mathbf{v}\|_2^2 \leq (1 + \tilde{\varepsilon}) \|\mathbf{v}\|_2^2. \quad (\text{B.1})$$

According to the definition of  $\delta_r^{\text{corank}}$  it holds that  $\sqrt{1 + \delta_r^{\text{corank}}} = \sup_{\mathbf{v} \in \mathcal{A}_r^{\text{corank}} \cap B^d} \|\mathbf{M}\mathbf{v}\|_2$ . Since  $\mathcal{A}_r^{\text{corank}} \cap B^d$  is a compact set there exists  $\mathbf{v}_0 \in \mathcal{A}_r^{\text{corank}} \cap B^d$  that achieves the supremum. Denoting by  $\tilde{\mathbf{v}}$  its closest vector in  $\Psi_{\mathcal{A}_r^{\text{corank}}}$  and using the definition of  $\Psi_{\mathcal{A}_r^{\text{corank}}}$  we have  $\|\mathbf{v}_0 - \tilde{\mathbf{v}}\|_2 \leq \tilde{\varepsilon}$ . This yields

$$\begin{aligned} \sqrt{1 + \delta_r^{\text{corank}}} = \|\mathbf{M}\mathbf{v}_0\|_2 &\leq \|\mathbf{M}\tilde{\mathbf{v}}\|_2 + \|\mathbf{M}(\mathbf{v}_0 - \tilde{\mathbf{v}})\|_2 \\ &\leq \sqrt{1 + \tilde{\varepsilon}} + \left\| \mathbf{M} \frac{\mathbf{v}_0 - \tilde{\mathbf{v}}}{\|\mathbf{v}_0 - \tilde{\mathbf{v}}\|_2} \right\|_2 \|\mathbf{v}_0 - \tilde{\mathbf{v}}\|_2 \leq \sqrt{1 + \tilde{\varepsilon}} + \sqrt{1 + \delta_r^{\text{corank}}} \tilde{\varepsilon}. \end{aligned} \quad (\text{B.2})$$

The first inequality is due to the triangle inequality; the second one follows from (B.1) and arithmetics; and the last inequality follows from the definition of  $\delta_r^{\text{corank}}$ , the properties of  $\tilde{\varepsilon}$ -net and the fact that  $\left\| \frac{\mathbf{v}_0 - \tilde{\mathbf{v}}}{\|\mathbf{v}_0 - \tilde{\mathbf{v}}\|_2} \right\|_2 = 1$ . Reordering (B.2) gives

$$1 + \delta_r^{\text{corank}} \leq \frac{1 + \tilde{\varepsilon}}{(1 - \tilde{\varepsilon})^2} \leq 1 + 4\tilde{\varepsilon} = 1 + \varepsilon_r. \quad (\text{B.3})$$

where the inequality holds because  $\varepsilon_r \leq 0.5$  and  $\tilde{\varepsilon} = \frac{\varepsilon_r}{4} \leq \frac{1}{8}$ . Since we want (B.3) to hold with probability greater than  $1 - e^{-t}$  it remains to require  $|\mathcal{L}_r^{\text{corank}}| \left(1 + \frac{8}{\varepsilon_r}\right)^{d-r} e^{-\frac{C_M m \varepsilon_r^2}{32}} \leq e^{-t}$ . Using the fact that  $(1 + \frac{8}{\varepsilon_r}) \geq \frac{9}{\varepsilon_r}$  and some arithmetics we get (4.13) and this completes the proof of the theorem.

We turn now to the proof of Theorem 4.1.8. Its proof is almost identical to the previous proof but with the difference that instead of  $r$ ,  $\mathcal{L}_r^{\text{corank}}$  and  $\delta_r^{\text{corank}}$  we look at  $\ell$ ,  $\mathcal{L}_\ell$  and  $\delta_\ell$ . In this case we do not know what is the dimension of the subspace that each cosupport implies. However, we can have a lower bound on it using  $p - \ell$ . Therefore, we use  $B^{p-\ell}$  instead of  $B^{d-r}$ . This change provides us with a condition similar to (4.13) but with  $p - \ell$  in the second coefficient instead of  $d - r$ . By using some arithmetics, noticing that the size of  $\mathcal{L}_\ell$  is  $\binom{p}{\ell}$  and using Stirling's formula for upper bounding it we get (4.14) and this completes the proof.

## B.2 Proof of Lemma 4.4.6

*Lemma 4.4.6:* Consider the problem  $\mathcal{P}$ -Analysis and apply either AIHT or AHTP with a constant step size  $\mu$  satisfying  $\frac{1}{\mu} \geq 1 + \delta_{2\ell-p}$  or an optimal step size. Then, at the  $t$ -th iteration, the following holds:

$$\begin{aligned} \|\mathbf{y} - \mathbf{M}\hat{\mathbf{x}}^t\|_2^2 - \|\mathbf{y} - \mathbf{M}\hat{\mathbf{x}}^{t-1}\|_2^2 &\leq C_\ell \left( \|\mathbf{y} - \mathbf{M}\mathbf{x}\|_2^2 - \|\mathbf{y} - \mathbf{M}\hat{\mathbf{x}}^{t-1}\|_2^2 \right) \\ &+ C_\ell \left( \frac{1}{\mu(1 - \delta_{2\ell-p})} - 1 \right) \|\mathbf{M}(\mathbf{x} - \hat{\mathbf{x}}^{t-1})\|_2^2 + (C_\ell - 1)\mu\sigma_{\mathbf{M}}^2 \|\mathbf{y} - \mathbf{M}\hat{\mathbf{x}}^{t-1}\|_2^2. \end{aligned} \quad (\text{B.4})$$

For the optimal step size the bound is achieved with the value  $\mu = \frac{1}{1 + \delta_{2\ell-p}}$ .

*Proof:* We consider the AIHT algorithm first. We take similar steps to those taken in the proof of Lemma 3 in [95]. Since  $\frac{1}{\mu} \geq 1 + \delta_{2\ell-p}$ , we have, from the O-RIP of  $\mathbf{M}$ ,

$$\left\| \mathbf{M}(\hat{\mathbf{x}}^t - \hat{\mathbf{x}}^{t-1}) \right\|_2^2 \leq \frac{1}{\mu} \left\| \hat{\mathbf{x}}^t - \hat{\mathbf{x}}^{t-1} \right\|_2^2.$$

Thus,

$$\begin{aligned} \left\| \mathbf{y} - \mathbf{M}\hat{\mathbf{x}}^t \right\|_2^2 - \left\| \mathbf{y} - \mathbf{M}\hat{\mathbf{x}}^{t-1} \right\|_2^2 &= -2\langle \mathbf{M}(\hat{\mathbf{x}}^t - \hat{\mathbf{x}}^{t-1}), \mathbf{y} - \mathbf{M}\hat{\mathbf{x}}^{t-1} \rangle + \left\| \mathbf{M}(\hat{\mathbf{x}}^t - \hat{\mathbf{x}}^{t-1}) \right\|_2^2 \\ &\leq -2\langle \mathbf{M}(\hat{\mathbf{x}}^t - \hat{\mathbf{x}}^{t-1}), \mathbf{y} - \mathbf{M}\hat{\mathbf{x}}^{t-1} \rangle + \frac{1}{\mu} \left\| \hat{\mathbf{x}}^t - \hat{\mathbf{x}}^{t-1} \right\|_2^2 \\ &= -2\langle \hat{\mathbf{x}}^t - \hat{\mathbf{x}}^{t-1}, \mathbf{M}^*(\mathbf{y} - \mathbf{M}\hat{\mathbf{x}}^{t-1}) \rangle + \frac{1}{\mu} \left\| \hat{\mathbf{x}}^t - \hat{\mathbf{x}}^{t-1} \right\|_2^2 \\ &= -\mu \left\| \mathbf{M}^*(\mathbf{y} - \mathbf{M}\hat{\mathbf{x}}^{t-1}) \right\|_2^2 + \frac{1}{\mu} \left\| \hat{\mathbf{x}}^t - \hat{\mathbf{x}}^{t-1} - \mu \mathbf{M}^*(\mathbf{y} - \mathbf{M}\hat{\mathbf{x}}^{t-1}) \right\|_2^2. \end{aligned}$$

Note that by definition,  $\hat{\mathbf{x}}^t = \mathbf{Q}_{\mathcal{S}_\ell}(\hat{\mathbf{x}}^{t-1} + \mu \mathbf{M}^*(\mathbf{y} - \mathbf{M}\hat{\mathbf{x}}^{t-1}))$ . Hence, by the  $C_\ell$ -near optimality of the projection, we get

$$\begin{aligned} \left\| \mathbf{y} - \mathbf{M}\hat{\mathbf{x}}^t \right\|_2^2 - \left\| \mathbf{y} - \mathbf{M}\hat{\mathbf{x}}^{t-1} \right\|_2^2 & \tag{B.5} \\ & \leq -\mu \left\| \mathbf{M}^*(\mathbf{y} - \mathbf{M}\hat{\mathbf{x}}^{t-1}) \right\|_2^2 + \frac{C_\ell}{\mu} \left\| \mathbf{x} - \hat{\mathbf{x}}^{t-1} - \mu \mathbf{M}^*(\mathbf{y} - \mathbf{M}\hat{\mathbf{x}}^{t-1}) \right\|_2^2. \end{aligned}$$

Now note that

$$\begin{aligned} \left\| \mathbf{x} - \hat{\mathbf{x}}^{t-1} - \mu \mathbf{M}^*(\mathbf{y} - \mathbf{M}\hat{\mathbf{x}}^{t-1}) \right\|_2^2 & \tag{B.6} \\ &= \left\| \mathbf{x} - \hat{\mathbf{x}}^{t-1} \right\|_2^2 - 2\mu \langle \mathbf{M}(\mathbf{x} - \hat{\mathbf{x}}^{t-1}), \mathbf{y} - \mathbf{M}\hat{\mathbf{x}}^{t-1} \rangle + \mu^2 \left\| \mathbf{M}^*(\mathbf{y} - \mathbf{M}\hat{\mathbf{x}}^{t-1}) \right\|_2^2 \\ &\leq \frac{1}{1 - \delta_{2\ell-p}} \left\| \mathbf{M}(\mathbf{x} - \hat{\mathbf{x}}^{t-1}) \right\|_2^2 - 2\mu \langle \mathbf{M}(\mathbf{x} - \hat{\mathbf{x}}^{t-1}), \mathbf{y} - \mathbf{M}\hat{\mathbf{x}}^{t-1} \rangle + \mu^2 \left\| \mathbf{M}^*(\mathbf{y} - \mathbf{M}\hat{\mathbf{x}}^{t-1}) \right\|_2^2 \\ &= \frac{1}{1 - \delta_{2\ell-p}} \left\| \mathbf{M}(\mathbf{x} - \hat{\mathbf{x}}^{t-1}) \right\|_2^2 + \mu \left( \left\| \mathbf{y} - \mathbf{M}\mathbf{x} \right\|_2^2 - \left\| \mathbf{y} - \mathbf{M}\hat{\mathbf{x}}^{t-1} \right\|_2^2 - \left\| \mathbf{M}(\mathbf{x} - \hat{\mathbf{x}}^{t-1}) \right\|_2^2 \right) \\ &\quad + \mu^2 \left\| \mathbf{M}^*(\mathbf{y} - \mathbf{M}\hat{\mathbf{x}}^{t-1}) \right\|_2^2. \end{aligned}$$

Putting this into (B.5), we obtain the desired result for the AIHT algorithm.

We can check that the same holds true for the AHTP algorithm as follows: suppose that  $\hat{\mathbf{x}}_{\text{AHTP}}^{t-1}$  is the  $(t-1)$ -st estimate from the AHTP algorithm. If we now initialize the AIHT algorithm with this estimate and obtain the next estimate  $\hat{\mathbf{x}}_{\text{AIHT}}^t$ , then the inequality of the lemma holds true with  $\hat{\mathbf{x}}_{\text{AIHT}}^t$  and  $\hat{\mathbf{x}}_{\text{AHTP}}^{t-1}$  in place of  $\hat{\mathbf{x}}^t$  and  $\hat{\mathbf{x}}^{t-1}$  respectively. On the other hand, from the algorithm description, we know that the  $t$ -th estimate  $\hat{\mathbf{x}}_{\text{AHTP}}^t$  of the AHTP satisfies

$$\left\| \mathbf{y} - \mathbf{M}\hat{\mathbf{x}}_{\text{AHTP}}^t \right\|_2^2 \leq \left\| \mathbf{y} - \mathbf{M}\hat{\mathbf{x}}_{\text{AIHT}}^t \right\|_2^2.$$

This means that the result holds for the AHTP algorithm as well.

Using a similar argument for the optimal changing step size we note that it selects the cosupport that minimizes  $\|\mathbf{M}\mathbf{x} - \mathbf{M}\hat{\mathbf{x}}^t\|_2^2$ . Thus, for AIHT and AHTP we have that  $\|\mathbf{M}\mathbf{x} - \mathbf{M}\hat{\mathbf{x}}_{\text{Opt}}^t\|_2^2 \leq \|\mathbf{M}\mathbf{x} - \mathbf{M}\hat{\mathbf{x}}_\mu^t\|_2^2$  for any value of  $\mu$ , where  $\hat{\mathbf{x}}_{\text{Opt}}^t$  and  $\hat{\mathbf{x}}_\mu^t$  are the recovery results of AIHT or AHTP with an optimal changing step-size and a constant step-size  $\mu$  respectively. This yields that any theoretical result for a constant step-size selection with a constant  $\mu$  holds true also to the optimal changing-step size selection. In particular this is true also for  $\mu = \frac{1}{1+\delta_{2\ell-p}}$ . This choice is justified in the proof of Lemma 4.4.7.  $\square$

### B.3 Proof of Lemma 4.4.7

*Lemma 4.4.7:* Suppose that the same conditions of Theorem 4.4.5 hold true. If  $\|\mathbf{y} - \mathbf{M}\hat{\mathbf{x}}^{t-1}\|_2^2 \leq \eta^2 \|\mathbf{e}\|_2^2$ , then  $\|\mathbf{y} - \mathbf{M}\hat{\mathbf{x}}^t\|_2^2 \leq \eta^2 \|\mathbf{e}\|_2^2$ . Furthermore, if  $\|\mathbf{y} - \mathbf{M}\hat{\mathbf{x}}^{t-1}\|_2^2 > \eta^2 \|\mathbf{e}\|_2^2$ , then

$$\|\mathbf{y} - \mathbf{M}\hat{\mathbf{x}}^t\|_2^2 \leq c_4 \|\mathbf{y} - \mathbf{M}\hat{\mathbf{x}}^{t-1}\|_2^2$$

where

$$c_4 := \left(1 + \frac{1}{\eta}\right)^2 \left(\frac{1}{\mu(1 - \delta_{2\ell-p})} - 1\right) C_\ell + (C_\ell - 1)(\mu\sigma_{\mathbf{M}}^2 - 1) + \frac{C_\ell}{\eta^2} < 1.$$

*Proof:* First, suppose that  $\|\mathbf{y} - \mathbf{M}\hat{\mathbf{x}}^{t-1}\|_2^2 > \eta^2 \|\mathbf{e}\|_2^2$ . From Lemma 4.4.6, we have

$$\begin{aligned} \|\mathbf{y} - \mathbf{M}\hat{\mathbf{x}}^t\|_2^2 &\leq C_\ell \|\mathbf{y} - \mathbf{M}\mathbf{x}\|_2^2 + (C_\ell - 1)(\mu\sigma_{\mathbf{M}}^2 - 1) \|\mathbf{y} - \mathbf{M}\hat{\mathbf{x}}^{t-1}\|_2^2 \\ &\quad + C_\ell \left(\frac{1}{\mu(1 - \delta_{2\ell-p})} - 1\right) \|\mathbf{M}(\mathbf{x} - \hat{\mathbf{x}}^{t-1})\|_2^2. \end{aligned} \quad (\text{B.7})$$

Remark that all the coefficients in the above are positive because  $1 + \delta_{2\ell-p} \leq \frac{1}{\mu} \leq \sigma_{\mathbf{M}}^2$  and  $C_\ell \geq 1$ . Since  $\mathbf{y} - \mathbf{M}\mathbf{x} = \mathbf{e}$ , we note

$$\|\mathbf{y} - \mathbf{M}\mathbf{x}\|_2^2 < \frac{1}{\eta^2} \|\mathbf{y} - \mathbf{M}\hat{\mathbf{x}}^{t-1}\|_2^2$$

and, by the triangle inequality,

$$\|\mathbf{M}(\mathbf{x} - \hat{\mathbf{x}}^{t-1})\|_2 \leq \|\mathbf{y} - \mathbf{M}\mathbf{x}\|_2 + \|\mathbf{y} - \mathbf{M}\hat{\mathbf{x}}^{t-1}\|_2 < \left(1 + \frac{1}{\eta}\right) \|\mathbf{y} - \mathbf{M}\hat{\mathbf{x}}^{t-1}\|_2.$$

Therefore, from (B.7),

$$\|\mathbf{y} - \mathbf{M}\hat{\mathbf{x}}^t\|_2^2 < c_4 \|\mathbf{y} - \mathbf{M}\hat{\mathbf{x}}^{t-1}\|_2^2.$$

This is the second part of the lemma.

Now, suppose that  $\|\mathbf{y} - \mathbf{M}\hat{\mathbf{x}}^{t-1}\|_2^2 \leq \eta^2 \|\mathbf{e}\|_2^2$ . This time we have

$$\|\mathbf{M}(\mathbf{x} - \hat{\mathbf{x}}^{t-1})\|_2 \leq \|\mathbf{y} - \mathbf{M}\mathbf{x}\|_2 + \|\mathbf{y} - \mathbf{M}\hat{\mathbf{x}}^{t-1}\|_2 \leq (1 + \eta) \|\mathbf{e}\|_2.$$

Applying this to (B.7), we obtain

$$\begin{aligned} \|\mathbf{y} - \mathbf{M}\hat{\mathbf{x}}^t\|_2^2 &\leq C_\ell \|\mathbf{e}\|_2^2 + (C_\ell - 1)(\mu\sigma_M^2 - 1)\eta^2 \|\mathbf{e}\|_2^2 + C_\ell \left( \frac{1}{\mu(1 - \delta_{2\ell-p})} - 1 \right) (1 + \eta)^2 \|\mathbf{e}\|_2^2 \\ &= \left( C_\ell + (C_\ell - 1)(\mu\sigma_M^2 - 1)\eta^2 + C_\ell \left( \frac{1}{\mu(1 - \delta_{2\ell-p})} - 1 \right) (1 + \eta)^2 \right) \|\mathbf{e}\|_2^2 = c_4 \eta^2 \|\mathbf{e}\|_2^2. \end{aligned}$$

Thus, the proof is complete as soon as we show  $c_4 < 1$ , or  $c_4 - 1 < 0$ .

To see  $c_4 - 1 < 0$ , we first note that it is equivalent to—all the subscripts are dropped from here on for simplicity of notation—

$$\frac{1}{\mu^2} - \frac{2(1 - \delta)}{1 + \frac{1}{\eta}} \frac{1}{\mu} + \frac{(C - 1)\sigma^2(1 - \delta)}{C \left(1 + \frac{1}{\eta}\right)^2} < 0,$$

or

$$\frac{1}{\mu^2} - 2(1 - \delta)b_1 \frac{1}{\mu} + (1 - \delta)^2 b_2 < 0.$$

Solving this quadratic equation in  $\frac{1}{\mu}$ , we want

$$(1 - \delta) \left( b_1 - \sqrt{b_1^2 - b_2} \right) < \frac{1}{\mu} < (1 - \delta) \left( b_1 + \sqrt{b_1^2 - b_2} \right).$$

Such  $\mu$  exists only when  $\frac{b_2}{b_1^2} < 1$ . Furthermore, we have already assumed  $1 + \delta \leq \frac{1}{\mu}$  and we know  $(1 - \delta) \left( b_1 - \sqrt{b_1^2 - b_2} \right) < 1 + \delta$ , and hence the condition we require is

$$1 + \delta \leq \frac{1}{\mu} < (1 - \delta) \left( b_1 + \sqrt{b_1^2 - b_2} \right), \quad (\text{B.8})$$

which is what we desired to prove.

For a changing optimal step-size selection, in a similar way to what we have in Lemma 4.4.6, (4.41) holds for any value of  $\mu$  that satisfies the conditions in (B.8). Thus, in the bound of changing optimal step-size we put a value of  $\mu$  that minimizes  $c_4$ . This minimization result with  $\frac{1}{\mu} = \sqrt{b_2}(1 - \delta_{2\ell-p})$ . However, since we need  $\frac{1}{\mu} \geq 1 + \delta_{2\ell-p}$  and have that  $\sqrt{b_2}(1 - \delta_{2\ell-p}) < b_1(1 - \delta_{2\ell-p}) < 1 + \delta_{2\ell-p}$  we set  $\frac{1}{\mu} = 1 + \delta_{2\ell-p}$  in  $c_4$  for the bound in optimal changing step-size case.  $\square$

## B.4 Proof of Lemma 4.4.10

*Lemma 4.4.10:* Consider the problem  $\mathcal{P}$ -Analysis and apply ACoSaMP with  $a = \frac{2\ell-p}{\ell}$ . For each iteration we have

$$\|\mathbf{x} - \mathbf{w}\|_2 \leq \frac{1}{\sqrt{1 - \delta_{4\ell-3p}^2}} \|\mathbf{P}_{\tilde{\Lambda}^t}(\mathbf{x} - \mathbf{w})\|_2 + \frac{\sqrt{1 + \delta_{3\ell-2p}}}{1 - \delta_{4\ell-3p}} \|\mathbf{e}\|_2.$$

*Proof:* Since  $\mathbf{w}$  is the minimizer of  $\|\mathbf{y} - \mathbf{M}\mathbf{v}\|_2^2$  with the constraint  $\mathbf{\Omega}_{\tilde{\Lambda}^t}\mathbf{v} = 0$ , then

$$\langle \mathbf{M}\mathbf{w} - \mathbf{y}, \mathbf{M}\mathbf{u} \rangle = 0, \quad (\text{B.9})$$

for any vector  $\mathbf{u}$  such that  $\mathbf{\Omega}_{\tilde{\Lambda}^t}\mathbf{u} = 0$ . Substituting  $\mathbf{y} = \mathbf{M}\mathbf{x} + \mathbf{e}$  and moving terms from the LHS to the RHS gives

$$\langle \mathbf{w} - \mathbf{x}, \mathbf{M}^*\mathbf{M}\mathbf{u} \rangle = \langle \mathbf{e}, \mathbf{M}\mathbf{u} \rangle, \quad (\text{B.10})$$

where  $\mathbf{u}$  is a vector satisfying  $\mathbf{\Omega}_{\tilde{\Lambda}^t}\mathbf{u} = 0$ . Turning to look at  $\|\mathbf{Q}_{\tilde{\Lambda}^t}(\mathbf{x} - \mathbf{w})\|_2^2$  and using (B.10) with  $\mathbf{u} = \mathbf{Q}_{\tilde{\Lambda}^t}(\mathbf{x} - \mathbf{w})$ , we have

$$\begin{aligned} \|\mathbf{Q}_{\tilde{\Lambda}^t}(\mathbf{x} - \mathbf{w})\|_2^2 &= \langle \mathbf{x} - \mathbf{w}, \mathbf{Q}_{\tilde{\Lambda}^t}(\mathbf{x} - \mathbf{w}) \rangle \\ &= \langle \mathbf{x} - \mathbf{w}, (\mathbf{I} - \mathbf{M}^*\mathbf{M})\mathbf{Q}_{\tilde{\Lambda}^t}(\mathbf{x} - \mathbf{w}) \rangle - \langle \mathbf{e}, \mathbf{M}\mathbf{Q}_{\tilde{\Lambda}^t}(\mathbf{x} - \mathbf{w}) \rangle \\ &\leq \|\mathbf{x} - \mathbf{w}\|_2 \|\mathbf{Q}_{\Lambda \cap \tilde{\Lambda}^t}(\mathbf{I} - \mathbf{M}^*\mathbf{M})\mathbf{Q}_{\tilde{\Lambda}^t}\|_2 \|\mathbf{Q}_{\tilde{\Lambda}^t}(\mathbf{x} - \mathbf{w})\|_2 + \|\mathbf{e}\|_2 \|\mathbf{M}\mathbf{Q}_{\tilde{\Lambda}^t}(\mathbf{x} - \mathbf{w})\|_2 \\ &\leq \delta_{4\ell-3p} \|\mathbf{x} - \mathbf{w}\|_2 \|\mathbf{Q}_{\tilde{\Lambda}^t}(\mathbf{x} - \mathbf{w})\|_2 + \|\mathbf{e}\|_2 \sqrt{1 + \delta_{3\ell-2p}} \|\mathbf{Q}_{\tilde{\Lambda}^t}(\mathbf{x} - \mathbf{w})\|_2. \end{aligned} \quad (\text{B.11})$$

where the first inequality follows from the Cauchy-Schwartz inequality, the projection property that  $\mathbf{Q}_{\tilde{\Lambda}^t} = \mathbf{Q}_{\tilde{\Lambda}^t}\mathbf{Q}_{\tilde{\Lambda}^t}$  and the fact that  $\mathbf{x} - \mathbf{w} = \mathbf{Q}_{\Lambda \cap \tilde{\Lambda}^t}(\mathbf{x} - \mathbf{w})$ . The last inequality is due to the O-RIP properties, Corollary 4.1.6 and that according to Table 4.1  $|\tilde{\Lambda}^t| \geq 3\ell - 2p$  and  $|\Lambda \cap \tilde{\Lambda}^t| \geq 4\ell - 3p$ . After simplification of (B.11) by  $\|\mathbf{Q}_{\tilde{\Lambda}^t}(\mathbf{x} - \mathbf{w})\|_2$  we have

$$\|\mathbf{Q}_{\tilde{\Lambda}^t}(\mathbf{x} - \mathbf{w})\|_2 \leq \delta_{4\ell-3p} \|\mathbf{x} - \mathbf{w}\|_2 + \sqrt{1 + \delta_{3\ell-2p}} \|\mathbf{e}\|_2. \quad (\text{B.12})$$

Utilizing the last inequality with the fact that  $\|\mathbf{x} - \mathbf{w}\|_2^2 = \|\mathbf{P}_{\tilde{\Lambda}^t}(\mathbf{x} - \mathbf{w})\|_2^2 + \|\mathbf{Q}_{\tilde{\Lambda}^t}(\mathbf{x} - \mathbf{w})\|_2^2$  gives

$$\|\mathbf{x} - \mathbf{w}\|_2^2 \leq \|\mathbf{P}_{\tilde{\Lambda}^t}(\mathbf{x} - \mathbf{w})\|_2^2 + \left( \delta_{4\ell-3p} \|\mathbf{x} - \mathbf{w}\|_2 + \sqrt{1 + \delta_{3\ell-2p}} \|\mathbf{e}\|_2 \right)^2. \quad (\text{B.13})$$

By moving all terms to the LHS we get a quadratic function of  $\|\mathbf{x} - \mathbf{w}\|_2$ . Thus,  $\|\mathbf{x} - \mathbf{w}\|_2$  is bounded from above by the larger root of that function; this with a few simple algebraic steps gives the inequality in (4.50).  $\square$

## B.5 Proof of Lemma 4.4.11

*Lemma 4.4.11:* Consider the problem  $\mathcal{P}$ -Analysis and apply ACoSaMP with  $a = \frac{2\ell-p}{\ell}$ . For each iteration we have

$$\|\mathbf{x} - \hat{\mathbf{x}}^t\|_2 \leq \rho_1 \|\mathbf{P}_{\tilde{\Lambda}^t}(\mathbf{x} - \mathbf{w})\|_2 + \eta_1 \|\mathbf{e}\|_2,$$

where  $\eta_1$  and  $\rho_1$  are the same constants as in Theorem 4.4.8.

*Proof:* We start with the following observation

$$\|\mathbf{x} - \hat{\mathbf{x}}^t\|_2^2 = \|\mathbf{x} - \mathbf{w} + \mathbf{w} - \hat{\mathbf{x}}^t\|_2^2 = \|\mathbf{x} - \mathbf{w}\|_2^2 + \|\hat{\mathbf{x}}^t - \mathbf{w}\|_2^2 + 2(\mathbf{x} - \mathbf{w})^*(\mathbf{w} - \hat{\mathbf{x}}^t), \quad (\text{B.14})$$

and turn to bound the second and last terms in the RHS. For the second term, using the fact that  $\hat{\mathbf{x}}^t = \mathbf{Q}_{\hat{\Sigma}_t(\mathbf{w})}\mathbf{w}$  with (4.17) gives

$$\|\hat{\mathbf{x}}^t - \mathbf{w}\|_2^2 \leq C_\ell \|\mathbf{x} - \mathbf{w}\|_2^2. \quad (\text{B.15})$$

For bounding the last term, we look at its absolute value and use (B.10) with  $\mathbf{u} = \mathbf{w} - \hat{\mathbf{x}}^t = \mathbf{Q}_{\tilde{\Lambda}^t}(\mathbf{w} - \hat{\mathbf{x}}^t)$ . This leads to

$$|(\mathbf{x} - \mathbf{w})^*(\mathbf{w} - \hat{\mathbf{x}}^t)| = |(\mathbf{x} - \mathbf{w})^*(\mathbf{I} - \mathbf{M}^*\mathbf{M})(\mathbf{w} - \hat{\mathbf{x}}^t) - \mathbf{e}^*\mathbf{M}(\mathbf{w} - \hat{\mathbf{x}}^t)|.$$

By using the triangle and Cauchy-Schwartz inequalities with the fact that  $\mathbf{x} - \mathbf{w} = \mathbf{Q}_{\Lambda \cap \tilde{\Lambda}^t}(\mathbf{x} - \mathbf{w})$  and  $\mathbf{w} - \hat{\mathbf{x}}^t = \mathbf{Q}_{\tilde{\Lambda}^t}(\mathbf{w} - \hat{\mathbf{x}}^t)$  we have

$$\begin{aligned} |(\mathbf{x} - \mathbf{w})^*(\mathbf{w} - \hat{\mathbf{x}}^t)| & \quad (\text{B.16}) \\ & \leq \|\mathbf{x} - \mathbf{w}\|_2 \|\mathbf{Q}_{\Lambda \cap \tilde{\Lambda}^t}(\mathbf{I} - \mathbf{M}^*\mathbf{M})\mathbf{Q}_{\tilde{\Lambda}^t}\|_2 \|\mathbf{w} - \hat{\mathbf{x}}^t\|_2 + \|\mathbf{e}\|_2 \|\mathbf{M}(\mathbf{w} - \hat{\mathbf{x}}^t)\|_2 \\ & \leq \delta_{4\ell-3p} \|\mathbf{x} - \mathbf{w}\|_2 \|\mathbf{w} - \hat{\mathbf{x}}^t\|_2 + \sqrt{1 + \delta_{3\ell-2p}} \|\mathbf{e}\|_2 \|\mathbf{w} - \hat{\mathbf{x}}^t\|_2, \end{aligned}$$

where the last inequality is due to the O-RIP definition and Corollary 4.1.6.

By substituting (B.15) and (B.16) into (B.14) we have

$$\begin{aligned} \|\mathbf{x} - \hat{\mathbf{x}}^t\|_2^2 & \quad (\text{B.17}) \\ & \leq (1 + C_\ell) \|\mathbf{x} - \mathbf{w}\|_2^2 + 2\delta_{4\ell-3p} \sqrt{C_\ell} \|\mathbf{x} - \mathbf{w}\|_2^2 + 2\sqrt{1 + \delta_{3\ell-2p}} \sqrt{C_\ell} \|\mathbf{e}\|_2 \|\mathbf{x} - \mathbf{w}\|_2 \\ & \leq \left( (1 + 2\delta_{4\ell-3p} \sqrt{C_\ell} + C_\ell) \|\mathbf{x} - \mathbf{w}\|_2 + 2\sqrt{(1 + \delta_{3\ell-2p})C_\ell} \|\mathbf{e}\|_2 \right) \|\mathbf{x} - \mathbf{w}\|_2 \\ & \leq \frac{1 + 2\delta_{4\ell-3p} \sqrt{C_\ell} + C_\ell}{1 - \delta_{4\ell-3p}^2} \|\mathbf{P}_{\tilde{\Lambda}^t}(\mathbf{x} - \mathbf{w})\|_2^2 + \frac{(1 + \delta_{3\ell-2p})(1 + 2\sqrt{C_\ell} + C_\ell)}{(1 - \delta_{4\ell-3p})^2} \|\mathbf{e}\|_2^2 \\ & \quad + \frac{2\sqrt{1 + \delta_{3\ell-2p}}(1 + (1 + \delta_{4\ell-3p})\sqrt{C_\ell} + C_\ell)}{(1 - \delta_{4\ell-3p})\sqrt{1 - \delta_{4\ell-3p}^2}} \|\mathbf{P}_{\tilde{\Lambda}^t}(\mathbf{x} - \mathbf{w})\|_2 \|\mathbf{e}\|_2 \\ & \leq \left( \frac{\sqrt{1 + 2\delta_{4\ell-3p} \sqrt{C_\ell} + C_\ell}}{\sqrt{1 - \delta_{4\ell-3p}^2}} \|\mathbf{P}_{\tilde{\Lambda}^t}(\mathbf{x} - \mathbf{w})\|_2 + \frac{\sqrt{\frac{2+C_\ell}{1+C_\ell} + 2\sqrt{C_\ell} + C_\ell} \sqrt{1 + \delta_{3\ell-2p}}}{1 - \delta_{4\ell-3p}} \|\mathbf{e}\|_2 \right)^2, \end{aligned}$$

where for the second inequality we use the fact that  $\delta_{4\ell-3p} \leq 1$  combined with the inequality of Lemma 4.4.10, and for the last inequality we use the fact that  $(1 + (1 + \delta_{4\ell-3p})\sqrt{C_\ell} + C_\ell)^2 \leq (1 + 2\delta_{4\ell-3p}\sqrt{C_\ell} + C_\ell)(\frac{2+C_\ell}{1+C_\ell} + 2\sqrt{C_\ell} + C_\ell)$  together with a few algebraic steps. Taking square-root on both sides of (B.17) provides the desired result.  $\square$

## B.6 Proof of Lemma 4.4.12

*Lemma 4.4.12:* Consider the problem  $\mathcal{P}$ -Analysis and apply ACoSaMP with  $a = \frac{2\ell-p}{\ell}$ . if

$$C_{2\ell-p} < \frac{\sigma_{\mathbf{M}}^2(1+\gamma)^2}{\sigma_{\mathbf{M}}^2(1+\gamma)^2 - 1},$$

then there exists  $\tilde{\delta}_{\text{ACoSaMP}}(C_{2\ell-p}, \sigma_{\mathbf{M}}^2, \gamma) > 0$  such that for any  $\delta_{2\ell-p} < \tilde{\delta}_{\text{ACoSaMP}}(C_{2\ell-p}, \sigma_{\mathbf{M}}^2, \gamma)$

$$\|\mathbf{P}_{\tilde{\Lambda}^t}(\mathbf{x} - \mathbf{w})\|_2 \leq \eta_2 \|\mathbf{e}\|_2 + \rho_2 \|\mathbf{x} - \hat{\mathbf{x}}^{t-1}\|_2.$$

The constants  $\eta_2$  and  $\rho_2$  are as defined in Theorem 4.4.8.

In the proof of the lemma we use the following Proposition.

**Proposition B.6.1** For any two given vectors  $\mathbf{x}_1, \mathbf{x}_2$  and a constant  $c > 0$  it holds that

$$\|\mathbf{x}_1 + \mathbf{x}_2\|_2^2 \leq (1+c) \|\mathbf{x}_1\|_2^2 + \left(1 + \frac{1}{c}\right) \|\mathbf{x}_2\|_2^2. \quad (\text{B.18})$$

The proof of the proposition is immediate using the inequality of arithmetic and geometric means. We turn to the proof of the lemma.

*Proof:* Looking at the step of finding new cosupport elements one can observe that  $\mathbf{Q}_{\Lambda_\Delta}$  is a near optimal projection for  $\mathbf{M}^* \mathbf{y}_{\text{resid}}^{t-1} = \mathbf{M}^*(\mathbf{y} - \mathbf{M}\hat{\mathbf{x}}^{t-1})$  with a constant  $C_{2\ell-p}$ . The fact that  $|\hat{\Lambda}^{t-1} \cap \Lambda| \geq 2\ell - p$  combined with (4.17) gives

$$\left\| (\mathbf{I} - \mathbf{Q}_{\Lambda_\Delta}) \mathbf{M}^*(\mathbf{y} - \mathbf{M}\hat{\mathbf{x}}^{t-1}) \right\|_2^2 \leq C_{2\ell-p} \left\| (\mathbf{I} - \mathbf{Q}_{\hat{\Lambda}^{t-1} \cap \Lambda}) \mathbf{M}^*(\mathbf{y} - \mathbf{M}\hat{\mathbf{x}}^{t-1}) \right\|_2^2.$$

Using simple projection properties and the fact that  $\tilde{\Lambda}^t \subseteq \Lambda_\Delta$  with  $\mathbf{z} = \mathbf{M}^*(\mathbf{y} - \mathbf{M}\hat{\mathbf{x}}^{t-1})$  we have

$$\begin{aligned} \|\mathbf{Q}_{\tilde{\Lambda}^t} \mathbf{z}\|_2^2 &\geq \|\mathbf{Q}_{\Lambda_\Delta} \mathbf{z}\|_2^2 = \|\mathbf{z}\|_2^2 - \|(\mathbf{I} - \mathbf{Q}_{\Lambda_\Delta}) \mathbf{z}\|_2^2 \geq \|\mathbf{z}\|_2^2 - C_{2\ell-p} \|(\mathbf{I} - \mathbf{Q}_{\hat{\Lambda}^{t-1} \cap \Lambda}) \mathbf{z}\|_2^2 \\ &= \|\mathbf{z}\|_2^2 - C_{2\ell-p} \left( \|\mathbf{z}\|_2^2 - \|\mathbf{Q}_{\hat{\Lambda}^{t-1} \cap \Lambda} \mathbf{z}\|_2^2 \right) = C_{2\ell-p} \|\mathbf{Q}_{\hat{\Lambda}^{t-1} \cap \Lambda} \mathbf{z}\|_2^2 - (C_{2\ell-p} - 1) \|\mathbf{z}\|_2^2. \end{aligned} \quad (\text{B.19})$$

We turn to bound the LHS of (B.19) from above. Noticing that  $\mathbf{y} = \mathbf{M}\mathbf{x} + \mathbf{e}$  and using (B.18) with a constant  $\gamma_1 > 0$  gives

$$\left\| \mathbf{Q}_{\tilde{\Lambda}^t} \mathbf{M}^* (\mathbf{y} - \mathbf{M}\hat{\mathbf{x}}^{t-1}) \right\|_2^2 \leq \left( 1 + \frac{1}{\gamma_1} \right) \left\| \mathbf{Q}_{\tilde{\Lambda}^t} \mathbf{M}^* \mathbf{e} \right\|_2^2 + (1 + \gamma_1) \left\| \mathbf{Q}_{\tilde{\Lambda}^t} \mathbf{M}^* \mathbf{M} (\mathbf{x} - \hat{\mathbf{x}}^{t-1}) \right\|_2^2. \quad (\text{B.20})$$

Using (B.18) again, now with a constant  $\alpha > 0$ , we have

$$\begin{aligned} & \left\| \mathbf{Q}_{\tilde{\Lambda}^t} \mathbf{M}^* \mathbf{M} (\mathbf{x} - \hat{\mathbf{x}}^{t-1}) \right\|_2^2 & (\text{B.21}) \\ & \leq (1 + \alpha) \left\| \mathbf{Q}_{\tilde{\Lambda}^t} (\mathbf{x} - \hat{\mathbf{x}}^{t-1}) \right\|_2^2 + \left( 1 + \frac{1}{\alpha} \right) \left\| \mathbf{Q}_{\tilde{\Lambda}^t} (\mathbf{I} - \mathbf{M}^* \mathbf{M}) (\mathbf{x} - \hat{\mathbf{x}}^{t-1}) \right\|_2^2 \\ & \leq (1 + \alpha) \left\| \mathbf{x} - \hat{\mathbf{x}}^{t-1} \right\|_2^2 - (1 + \alpha) \left\| \mathbf{P}_{\tilde{\Lambda}^t} (\mathbf{x} - \hat{\mathbf{x}}^{t-1}) \right\|_2^2 + \left( 1 + \frac{1}{\alpha} \right) \left\| \mathbf{Q}_{\tilde{\Lambda}^t} (\mathbf{I} - \mathbf{M}^* \mathbf{M}) (\mathbf{x} - \hat{\mathbf{x}}^{t-1}) \right\|_2^2. \end{aligned}$$

Putting (B.21) into (B.20) and using (4.11) and Corollary 4.1.3 gives

$$\begin{aligned} & \left\| \mathbf{Q}_{\tilde{\Lambda}^t} \mathbf{M}^* (\mathbf{y} - \mathbf{M}\hat{\mathbf{x}}^{t-1}) \right\|_2^2 \leq \frac{(1 + \gamma_1)(1 + \delta_{3\ell-2p})}{\gamma_1} \left\| \mathbf{e} \right\|_2^2 & (\text{B.22}) \\ & \quad - (1 + \alpha)(1 + \gamma_1) \left\| \mathbf{P}_{\tilde{\Lambda}^t} (\mathbf{x} - \hat{\mathbf{x}}^{t-1}) \right\|_2^2 + \left( 1 + \alpha + \delta_{4\ell-3p} + \frac{\delta_{4\ell-3p}}{\alpha} \right) (1 + \gamma_1) \left\| \mathbf{x} - \hat{\mathbf{x}}^{t-1} \right\|_2^2. \end{aligned}$$

We continue with bounding the RHS of (B.19) from below. For the first element of the RHS we use an altered version of (B.18) with a constant  $\gamma_2 > 0$  and have

$$\left\| \mathbf{Q}_{\hat{\Lambda}^{t-1} \cap \Lambda} \mathbf{M}^* (\mathbf{y} - \mathbf{M}\hat{\mathbf{x}}^{t-1}) \right\|_2^2 \geq \frac{1}{1 + \gamma_2} \left\| \mathbf{Q}_{\hat{\Lambda}^{t-1} \cap \Lambda} \mathbf{M}^* \mathbf{M} (\mathbf{x} - \hat{\mathbf{x}}^{t-1}) \right\|_2^2 - \frac{1}{\gamma_2} \left\| \mathbf{Q}_{\hat{\Lambda}^{t-1} \cap \Lambda} \mathbf{M}^* \mathbf{e} \right\|_2^2. \quad (\text{B.23})$$

Using the altered form again, for the first element in the RHS of (B.23), with a constant  $\beta > 0$  gives

$$\left\| \mathbf{Q}_{\hat{\Lambda}^{t-1} \cap \Lambda} \mathbf{M}^* \mathbf{M} (\mathbf{x} - \hat{\mathbf{x}}^{t-1}) \right\|_2^2 \geq \frac{1}{1 + \beta} \left\| \mathbf{x} - \hat{\mathbf{x}}^{t-1} \right\|_2^2 - \frac{1}{\beta} \left\| \mathbf{Q}_{\hat{\Lambda}^{t-1} \cap \Lambda} (\mathbf{M}^* \mathbf{M} - \mathbf{I}) (\mathbf{x} - \hat{\mathbf{x}}^{t-1}) \right\|_2^2. \quad (\text{B.24})$$

Putting (B.24) in (B.23) and using the RIP properties and (4.11) provide

$$\left\| \mathbf{Q}_{\hat{\Lambda}^{t-1} \cap \Lambda} \mathbf{M}^* (\mathbf{y} - \mathbf{M}\hat{\mathbf{x}}^{t-1}) \right\|_2^2 \geq \left( \frac{1}{1 + \beta} - \frac{\delta_{2\ell-p}}{\beta} \right) \frac{1}{1 + \gamma_2} \left\| \mathbf{x} - \hat{\mathbf{x}}^{t-1} \right\|_2^2 - \frac{(1 + \delta_{2\ell-p})}{\gamma_2} \left\| \mathbf{e} \right\|_2^2. \quad (\text{B.25})$$

Using (B.18), with a constant  $\gamma_3 > 0$ , (4.2), and some basic algebraic steps we have for the second element in the RHS of (B.19)

$$\begin{aligned} \left\| \mathbf{M}^* (\mathbf{y} - \mathbf{M}\hat{\mathbf{x}}^{t-1}) \right\|_2^2 & \leq (1 + \gamma_3) \left\| \mathbf{M}^* \mathbf{M} (\mathbf{x} - \hat{\mathbf{x}}^{t-1}) \right\|_2^2 + \left( 1 + \frac{1}{\gamma_3} \right) \left\| \mathbf{M}^* \mathbf{e} \right\|_2^2 & (\text{B.26}) \\ & \leq (1 + \gamma_3)(1 + \delta_{2\ell-p}) \sigma_{\mathbf{M}}^2 \left\| (\mathbf{x} - \hat{\mathbf{x}}^{t-1}) \right\|_2^2 + \left( 1 + \frac{1}{\gamma_3} \right) \sigma_{\mathbf{M}}^2 \left\| \mathbf{e} \right\|_2^2. \end{aligned}$$

By combining (B.22), (B.25) and (B.26) with (B.19) we have

$$\begin{aligned}
(1 + \alpha)(1 + \gamma_1) \left\| \mathbf{P}_{\hat{\Lambda}^t}(\mathbf{x} - \hat{\mathbf{x}}^{t-1}) \right\|_2^2 &\leq \frac{(1 + \gamma_1)(1 + \delta_{3\ell-2p})}{\gamma_1} \|\mathbf{e}\|_2^2 \\
&+ C_{2\ell-p} \frac{(1 + \delta_{2\ell-p})}{\gamma_2} \|\mathbf{e}\|_2^2 + (C_{2\ell-p} - 1) \left(1 + \frac{1}{\gamma_3}\right) \sigma_{\mathbf{M}}^2 \|\mathbf{e}\|_2^2 \\
&+ \left(1 + \alpha + \delta_{4\ell-3p} + \frac{\delta_{4\ell-3p}}{\alpha}\right) (1 + \gamma_1) \left\| \mathbf{x} - \hat{\mathbf{x}}^{t-1} \right\|_2^2 \\
&+ (C_{2\ell-p} - 1)(1 + \gamma_3)(1 + \delta_{2\ell-p}) \sigma_{\mathbf{M}}^2 \left\| (\mathbf{x} - \hat{\mathbf{x}}^{t-1}) \right\|_2^2 \\
&- C_{2\ell-p} \left( \frac{1}{1 + \beta} - \frac{\delta_{2\ell-p}}{\beta} \right) \frac{1}{1 + \gamma_2} \left\| \mathbf{x} - \hat{\mathbf{x}}^{t-1} \right\|_2^2.
\end{aligned} \tag{B.27}$$

Dividing both sides by  $(1 + \alpha)(1 + \gamma_1)$  and gathering coefficients give

$$\begin{aligned}
\left\| \mathbf{P}_{\hat{\Lambda}^t}(\mathbf{x} - \hat{\mathbf{x}}^{t-1}) \right\|_2^2 &\leq \left( \frac{1 + \delta_{3\ell-2p}}{\gamma_1(1 + \alpha)} + \frac{(1 + \delta_{2\ell-p})C_{2\ell-p}}{\gamma_2(1 + \alpha)(1 + \gamma_1)} + \frac{(C_{2\ell-p} - 1)(1 + \gamma_3)\sigma_{\mathbf{M}}^2}{(1 + \alpha)(1 + \gamma_1)\gamma_3} \right) \|\mathbf{e}\|_2^2 \\
&+ \left( 1 + \frac{\delta_{4\ell-3p}}{\alpha} + \frac{(C_{2\ell-p} - 1)(1 + \gamma_3)(1 + \delta_{2\ell-p})\sigma_{\mathbf{M}}^2}{(1 + \alpha)(1 + \gamma_1)} \right. \\
&\quad \left. - \frac{C_{2\ell-p}}{(1 + \alpha)(1 + \gamma_1)(1 + \gamma_2)} \left( \frac{1}{1 + \beta} - \frac{\delta_{2\ell-p}}{\beta} \right) \right) \left\| \mathbf{x} - \hat{\mathbf{x}}^{t-1} \right\|_2^2.
\end{aligned} \tag{B.28}$$

The smaller the coefficient of  $\left\| \mathbf{x} - \hat{\mathbf{x}}^{t-1} \right\|_2^2$ , the better convergence guarantee we obtain. Thus, we choose  $\beta = \frac{\sqrt{\delta_{2\ell-p}}}{1 - \sqrt{\delta_{2\ell-p}}}$  and  $\alpha = \frac{\sqrt{\delta_{4\ell-3p}}}{\sqrt{\frac{C_{2\ell-p}}{(1 + \gamma_1)(1 + \gamma_2)}(1 - \sqrt{\delta_{2\ell-p}})^2 - \frac{(C_{2\ell-p} - 1)(1 + \gamma_3)(1 + \delta_{2\ell-p})\sigma_{\mathbf{M}}^2}{1 + \gamma_1}} - \sqrt{\delta_{4\ell-3p}}}$  so that the coefficient is minimized. The values of  $\gamma_1, \gamma_2, \gamma_3$  provide a trade-off between the convergence rate and the size of the noise coefficient. For smaller values we get better convergence rate but higher amplification of the noise. We make no optimization on their values and choose them to be  $\gamma_1 = \gamma_2 = \gamma_3 = \gamma$  for an appropriate  $\gamma > 0$ . Thus, the above yields

$$\begin{aligned}
\left\| \mathbf{P}_{\hat{\Lambda}^t}(\mathbf{x} - \hat{\mathbf{x}}^{t-1}) \right\|_2^2 &\leq \left( \frac{1 + \delta_{3\ell-2p}}{\gamma(1 + \alpha)} + \frac{(1 + \delta_{2\ell-p})C_{2\ell-p}}{\gamma(1 + \alpha)(1 + \gamma)} + \frac{(C_{2\ell-p} - 1)(1 + \gamma)\sigma_{\mathbf{M}}^2}{(1 + \alpha)(1 + \gamma)\gamma} \right) \|\mathbf{e}\|_2^2 \\
&+ \left( 1 - \left( \sqrt{\delta_{4\ell-3p}} - \sqrt{\frac{C_{2\ell-p}}{(1 + \gamma)^2} (1 - \sqrt{\delta_{2\ell-p}})^2 - (C_{2\ell-p} - 1)(1 + \delta_{2\ell-p})\sigma_{\mathbf{M}}^2} \right)^2 \right) \left\| \mathbf{x} - \hat{\mathbf{x}}^{t-1} \right\|_2^2.
\end{aligned} \tag{B.29}$$

Since  $\mathbf{P}_{\hat{\Lambda}^t}\mathbf{w} = \mathbf{P}_{\hat{\Lambda}^t}\hat{\mathbf{x}}^{t-1} = 0$  the above inequality holds also for  $\left\| \mathbf{P}_{\hat{\Lambda}^t}(\mathbf{x} - \hat{\mathbf{x}}^{t-1}) \right\|_2^2$ . Inequality (4.53) follows since the right-hand side of (B.29) is smaller than the square of the right-hand side of (4.53).

Before ending the proof, we notice that  $\rho_2$ , the coefficient of  $\left\| \mathbf{x} - \hat{\mathbf{x}}^{t-1} \right\|_2^2$  is defined only when

$$(C_{2\ell-p} - 1)(1 + \delta_{2\ell-p})\sigma_{\mathbf{M}}^2 \leq \frac{C_{2\ell-p}}{(1 + \gamma)^2} \left( 1 - \sqrt{\delta_{2\ell-p}} \right)^2. \tag{B.30}$$

First we notice that since  $1 + \delta_{2\ell-p} \geq (1 - \sqrt{\delta_{2\ell-p}})^2$  a necessary condition for (B.30) to hold is  $(C_{2\ell-p} - 1)\sigma_{\mathbf{M}}^2 < \frac{C_{2\ell-p}}{(1+\gamma)^2}$  which is equivalent to (4.52). By moving the terms in the RHS to the LHS we get a quadratic function of  $\sqrt{\delta_{2\ell-p}}$ . The condition in (4.52) guarantees that its constant term is smaller than zero and thus there exists a positive  $\delta_{2\ell-p}$  for which the function is smaller than zero. Therefore, for any  $\delta_{2\ell-p} < \tilde{\delta}_{\text{ACoSAMP}}(C_{2\ell-p}, \sigma_{\mathbf{M}}^2, \gamma)$  (B.30) holds, where  $\tilde{\delta}_{\text{ACoSAMP}}(C_{2\ell-p}, \sigma_{\mathbf{M}}^2, \gamma) > 0$  is the square of the positive solution of the quadratic function.

□



# Appendix C

## Proofs for Chapter 5

### C.1 Proof of Lemma 5.8.5

*Lemma 5.8.5:* If  $\mathbf{M}$  has the  $\mathbf{D}$ -RIP with constants  $\delta_{3\zeta k}, \delta_{(3\zeta+1)k}$ , then

$$\|\mathbf{x}_p - \mathbf{x}\|_2 \leq \frac{1}{\sqrt{1 - \delta_{(3\zeta+1)k}^2}} \|\mathbf{Q}_{\tilde{T}^t}(\mathbf{x}_p - \mathbf{x})\|_2 + \frac{\sqrt{1 + \delta_{3\zeta k}}}{1 - \delta_{(3\zeta+1)k}} \|\mathbf{e}\|_2.$$

*Proof:* Since  $\mathbf{x}_p \triangleq \mathbf{D}\boldsymbol{\alpha}_p$  is the minimizer of  $\|\mathbf{y} - \mathbf{M}\mathbf{u}\|_2$  with the constraints  $\mathbf{u} = \mathbf{D}\mathbf{w}$  and  $\mathbf{w}_{(\tilde{T}^t)^c} = 0$ , then

$$\langle \mathbf{M}\mathbf{x}_p - \mathbf{y}, \mathbf{M}\mathbf{v} \rangle = 0 \tag{C.1}$$

for any vector  $\mathbf{v} = \mathbf{D}\mathbf{w}$  such that  $\mathbf{w}_{(\tilde{T}^t)^c} = 0$ . Substituting  $\mathbf{y} = \mathbf{M}\mathbf{x} + \mathbf{e}$  with simple arithmetics gives

$$\langle \mathbf{x}_p - \mathbf{x}, \mathbf{M}^*\mathbf{M}\mathbf{v} \rangle = \langle \mathbf{e}, \mathbf{M}\mathbf{v} \rangle \tag{C.2}$$

where  $\mathbf{v} = \mathbf{D}\mathbf{w}$  and  $\mathbf{w}_{(\tilde{T}^t)^c} = 0$ . Turning to look at  $\|\mathbf{P}_{\tilde{T}^t}(\mathbf{x}_p - \mathbf{x})\|_2^2$  and using (C.2) with  $\mathbf{v} = \mathbf{P}_{\tilde{T}^t}(\mathbf{x}_p - \mathbf{x})$ , we have

$$\begin{aligned} \|\mathbf{P}_{\tilde{T}^t}(\mathbf{x}_p - \mathbf{x})\|_2^2 &= \langle \mathbf{x}_p - \mathbf{x}, \mathbf{P}_{\tilde{T}^t}(\mathbf{x}_p - \mathbf{x}) \rangle & \tag{C.3} \\ &= \langle \mathbf{x}_p - \mathbf{x}, (\mathbf{I}_d - \mathbf{M}^*\mathbf{M})\mathbf{P}_{\tilde{T}^t}(\mathbf{x}_p - \mathbf{x}) \rangle + \langle \mathbf{e}, \mathbf{M}\mathbf{P}_{\tilde{T}^t}(\mathbf{x}_p - \mathbf{x}) \rangle \\ &\leq \|\mathbf{x}_p - \mathbf{x}\|_2 \|\mathbf{P}_{\tilde{T}^t \cup T}(\mathbf{I}_d - \mathbf{M}^*\mathbf{M})\mathbf{P}_{\tilde{T}^t}\|_2 \|\mathbf{P}_{\tilde{T}^t}(\mathbf{x}_p - \mathbf{x})\|_2 + \|\mathbf{e}\|_2 \|\mathbf{M}\mathbf{P}_{\tilde{T}^t}(\mathbf{x}_p - \mathbf{x})\|_2 \\ &\leq \delta_{(3\zeta+1)k} \|\mathbf{x}_p - \mathbf{x}\|_2 \|\mathbf{P}_{\tilde{T}^t}(\mathbf{x}_p - \mathbf{x})\|_2 + \|\mathbf{e}\|_2 \sqrt{1 + \delta_{3\zeta k}} \|\mathbf{P}_{\tilde{T}^t}(\mathbf{x}_p - \mathbf{x})\|_2. \end{aligned}$$

where the first inequality follows from the Cauchy-Schwartz inequality, the projection property that  $\mathbf{P}_{\tilde{T}^t} = \mathbf{P}_{\tilde{T}^t}\mathbf{P}_{\tilde{T}^t}$  and the fact that  $\mathbf{x}_p - \mathbf{x} = \mathbf{P}_{\tilde{T}^t \cup T}(\mathbf{x}_p - \mathbf{x})$ . The last inequality is due to the

D-RIP property, the fact that  $|\tilde{T}^t| \leq 3\zeta k$  and Corollary 5.2.4. After simplification of (C.3) by  $\|\mathbf{P}_{\tilde{T}^t}(\mathbf{x}_p - \mathbf{x})\|_2$  we have

$$\|\mathbf{P}_{\tilde{T}^t}(\mathbf{x}_p - \mathbf{x})\|_2 \leq \delta_{(3\zeta+1)k} \|\mathbf{x}_p - \mathbf{x}\|_2 + \sqrt{1 + \delta_{3\zeta k}} \|\mathbf{e}\|_2.$$

Utilizing the last inequality with the fact that  $\|\mathbf{x}_p - \mathbf{x}\|_2^2 = \|\mathbf{Q}_{\tilde{\Lambda}^t}(\mathbf{x}_p - \mathbf{x})\|_2^2 + \|\mathbf{P}_{\tilde{\Lambda}^t}(\mathbf{x}_p - \mathbf{x})\|_2^2$  gives

$$\|\mathbf{x}_p - \mathbf{x}\|_2^2 \leq \|\mathbf{Q}_{\tilde{T}^t}(\mathbf{x}_p - \mathbf{x})\|_2^2 + \left( \delta_{(3\zeta+1)k} \|\mathbf{x}_p - \mathbf{x}\|_2 + \sqrt{1 + \delta_{3\zeta k}} \|\mathbf{e}\|_2 \right)^2. \quad (\text{C.4})$$

The last equation is a second order polynomial of  $\|\mathbf{x}_p - \mathbf{x}\|_2$ . Thus its larger root is an upper bound for it and this gives the inequality in (5.46). For more details look at the derivation of (13) in [45].  $\square$

## C.2 Proof of Lemma 5.8.6

*Lemma 5.8.6:* apply ACoSaMP with  $a = 2$ . For each iteration we have

$$\|\mathbf{x} - \mathbf{x}^t\|_2 \leq \rho_1 \|\mathbf{Q}_{\tilde{T}^t}(\mathbf{x} - \mathbf{x}_p)\|_2 + \eta_1 \|\mathbf{e}\|_2,$$

where  $\eta_1$  and  $\rho_1$  are the same constants as in Theorem 5.8.3.

*Proof:* Denote  $\mathbf{w} = \mathbf{x}_p$ . We start with the following observation

$$\|\mathbf{x} - \mathbf{x}^t\|_2^2 = \|\mathbf{x} - \mathbf{w} + \mathbf{w} - \mathbf{x}^t\|_2^2 = \|\mathbf{x} - \mathbf{w}\|_2^2 + \|\mathbf{x}^t - \mathbf{w}\|_2^2 + 2(\mathbf{x} - \mathbf{w})^*(\mathbf{w} - \mathbf{x}^t), \quad (\text{C.5})$$

and turn to bound the second and last terms in the RHS. For the second term, using the fact that  $\mathbf{x}^t = \mathbf{P}_{\hat{\mathcal{S}}_{\zeta k, 2}(\mathbf{w})} \mathbf{w}$  with (5.39) gives

$$\|\mathbf{x}^t - \mathbf{w}\|_2^2 \leq C_k \|\mathbf{x} - \mathbf{w}\|_2^2. \quad (\text{C.6})$$

For bounding the last term, we look at its absolute value and use (C.2) with  $\mathbf{u} = \mathbf{w} - \mathbf{x}^t = \mathbf{P}_{\tilde{T}^t}(\mathbf{w} - \mathbf{x}^t)$ . This leads to

$$|(\mathbf{x} - \mathbf{w})^*(\mathbf{w} - \mathbf{x}^t)| = |(\mathbf{x} - \mathbf{w})^*(\mathbf{I} - \mathbf{M}^*\mathbf{M})(\mathbf{w} - \mathbf{x}^t) - \mathbf{e}^*\mathbf{M}(\mathbf{w} - \mathbf{x}^t)|.$$

By using the triangle and Cauchy-Schwartz inequalities with the fact that  $\mathbf{x} - \mathbf{w} = \mathbf{P}_{T \cup \tilde{T}^t}(\mathbf{x} - \mathbf{w})$  and  $\mathbf{w} - \mathbf{x}^t = \mathbf{P}_{\tilde{T}^t}(\mathbf{w} - \mathbf{x}^t)$  we have

$$\begin{aligned} |(\mathbf{x} - \mathbf{w})^*(\mathbf{w} - \mathbf{x}^t)| &\leq \|\mathbf{x} - \mathbf{w}\|_2 \|\mathbf{P}_{T \cup \tilde{T}^t}(\mathbf{I} - \mathbf{M}^*\mathbf{M})\mathbf{P}_{\tilde{T}^t}\|_2 \|\mathbf{w} - \mathbf{x}^t\|_2 + \|\mathbf{e}\|_2 \|\mathbf{M}(\mathbf{w} - \mathbf{x}^t)\|_2 \\ &\leq \delta_{(3\zeta+1)k} \|\mathbf{x} - \mathbf{w}\|_2 \|\mathbf{w} - \mathbf{x}^t\|_2 + \sqrt{1 + \delta_{3\zeta k}} \|\mathbf{e}\|_2 \|\mathbf{w} - \mathbf{x}^t\|_2, \end{aligned} \quad (\text{C.7})$$

where the last inequality is due to the **D**-RIP definition, the fact that  $|\tilde{T}^t| \leq 3\zeta k$  and Corollary 5.2.4.

By substituting (C.6) and (C.7) into (C.5) we have

$$\begin{aligned}
\|\mathbf{x} - \mathbf{x}^t\|_2^2 &\leq (1 + C_k) \|\mathbf{x} - \mathbf{w}\|_2^2 + 2\delta_{(3\zeta+1)k} \sqrt{C_k} \|\mathbf{x} - \mathbf{w}\|_2^2 + 2\sqrt{1 + \delta_{3\zeta k}} \sqrt{C_k} \|\mathbf{e}\|_2 \|\mathbf{x} - \mathbf{w}\|_2 \quad (\text{C.8}) \\
&\leq \left( (1 + 2\delta_{(3\zeta+1)k} \sqrt{C_k} + C_k) \|\mathbf{x} - \mathbf{w}\|_2 + 2\sqrt{(1 + \delta_{3\zeta k}) C_k} \|\mathbf{e}\|_2 \right) \|\mathbf{x} - \mathbf{w}\|_2 \\
&\leq \frac{1 + 2\delta_{(3\zeta+1)k} \sqrt{C_k} + C_k}{1 - \delta_{(3\zeta+1)k}^2} \|\mathbf{Q}_{\tilde{T}^t}(\mathbf{x} - \mathbf{w})\|_2^2 \\
&\quad + \frac{2\sqrt{1 + \delta_{3\zeta k}}(1 + (1 + \delta_{(3\zeta+1)k})\sqrt{C_k} + C_k)}{(1 - \delta_{(3\zeta+1)k})\sqrt{1 - \delta_{4k}^2}} \|\mathbf{Q}_{\tilde{T}^t}(\mathbf{x} - \mathbf{w})\|_2 \|\mathbf{e}\|_2 \\
&\quad + \frac{(1 + \delta_{3\zeta k})(1 + 2\sqrt{C_k} + C_k)}{(1 - \delta_{(3\zeta+1)k})^2} \|\mathbf{e}\|_2^2 \\
&\leq \left( \frac{\sqrt{1 + 2\delta_{(3\zeta+1)k} \sqrt{C_k} + C_k}}{\sqrt{1 - \delta_{(3\zeta+1)k}^2}} \|\mathbf{Q}_{\tilde{T}^t}(\mathbf{x} - \mathbf{w})\|_2 + \frac{\sqrt{\frac{2+C_k}{1+C_k} + 2\sqrt{C_k} + C_k} \sqrt{1 + \delta_{3\zeta k}}}{1 - \delta_{(3\zeta+1)k}} \|\mathbf{e}\|_2 \right)^2,
\end{aligned}$$

where for the second inequality we use the fact that  $\delta_{(3\zeta+1)k} \leq 1$  combined with the inequality of Lemma 5.8.5, and for the last inequality we use the fact that  $(1 + (1 + \delta_{(3\zeta+1)k})\sqrt{C_k} + C_k)^2 \leq (1 + 2\delta_{(3\zeta+1)k} \sqrt{C_k} + C_k)(\frac{2+C_k}{1+C_k} + 2\sqrt{C_k} + C_k)$  together with a few algebraic steps. Taking square-root on both sides of (C.8) provides the desired result.  $\square$

### C.3 Proof of Lemma 5.8.7

*Lemma 5.8.7:* Given that  $S_{2\zeta k, 1}$  is a near optimal support selection scheme with a constant  $\tilde{C}_{2k}$ , if  $\mathbf{M}$  has the **D**-RIP with constants  $\delta_{(3\zeta+1)k}$ ,  $\delta_{3\zeta k}$  and  $\delta_{(\zeta+1)k}$  then

$$\|\mathbf{Q}_{\tilde{T}^t}(\mathbf{x}_p - \mathbf{x})\|_2 \leq \eta_2 \|\mathbf{e}\|_2 + \rho_2 \|\mathbf{x} - \mathbf{x}^{t-1}\|_2.$$

*Proof:* Looking at the step of finding new support elements one can observe that  $\mathbf{P}_{\Lambda_\Delta}$  is a near optimal projection operator for  $\mathbf{M}^* \mathbf{y}_r^{t-1} = \mathbf{M}^*(\mathbf{y} - \mathbf{M}\mathbf{x}^{t-1})$ . Noticing that  $T_\Delta \subseteq \tilde{T}^t$  and then using (5.40) with  $\mathbf{P}_{T^{t-1} \cup T}$  gives

$$\left\| \mathbf{P}_{\tilde{T}^t} \mathbf{M}^*(\mathbf{y} - \mathbf{M}\mathbf{x}^{t-1}) \right\|_2^2 \geq \left\| \mathbf{P}_{T_\Delta} \mathbf{M}^*(\mathbf{y} - \mathbf{M}\mathbf{x}^{t-1}) \right\|_2^2 \geq \tilde{C}_{2k} \left\| \mathbf{P}_{T^{t-1} \cup T} \mathbf{M}^*(\mathbf{y} - \mathbf{M}\mathbf{x}^{t-1}) \right\|_2^2. \quad (\text{C.9})$$

We start by bounding the lhs of (C.9) from above. Using Proposition B.6.1 with  $\gamma_1 > 0$  and

$\alpha > 0$  we have

$$\begin{aligned}
\left\| \mathbf{P}_{\tilde{T}^t} \mathbf{M}^* (\mathbf{y} - \mathbf{M} \mathbf{x}^{t-1}) \right\|_2^2 &\leq \left(1 + \frac{1}{\gamma_1}\right) \left\| \mathbf{P}_{\tilde{T}^t} \mathbf{M}^* \mathbf{e} \right\|_2^2 + (1 + \gamma_1) \left\| \mathbf{P}_{\tilde{T}^t} \mathbf{M}^* \mathbf{M} (\mathbf{x} - \mathbf{x}^{t-1}) \right\|_2^2 \quad (\text{C.10}) \\
&\leq \frac{1 + \gamma_1}{\gamma_1} \left\| \mathbf{P}_{\tilde{T}^t} \mathbf{M}^* \mathbf{e} \right\|_2^2 + (1 + \alpha)(1 + \gamma_1) \left\| \mathbf{P}_{\tilde{T}^t} (\mathbf{x} - \mathbf{x}^{t-1}) \right\|_2^2 \\
&\quad + \left(1 + \frac{1}{\alpha}\right)(1 + \gamma_1) \left\| \mathbf{P}_{\tilde{T}^t} (\mathbf{I}_d - \mathbf{M}^* \mathbf{M}) (\mathbf{x} - \mathbf{x}^{t-1}) \right\|_2^2 \\
&\leq \frac{(1 + \gamma_1)(1 + \delta_{3\zeta k})}{\gamma_1} \left\| \mathbf{e} \right\|_2^2 - (1 + \alpha)(1 + \gamma_1) \left\| \mathbf{Q}_{\tilde{T}^t} (\mathbf{x} - \mathbf{x}^{t-1}) \right\|_2^2 \\
&\quad + \left(1 + \alpha + \delta_{(3\zeta+1)k} + \frac{\delta_{(3\zeta+1)k}}{\alpha}\right) (1 + \gamma_1) \left\| \mathbf{x} - \mathbf{x}^{t-1} \right\|_2^2,
\end{aligned}$$

where the last inequality is due to Corollary 5.2.1 and (5.12).

We continue with bounding the rhs of (C.9) from below. For the first element we use Proposition B.6.1 with constants  $\gamma_2 > 0$  and  $\beta > 0$ , and (5.12) to achieve

$$\begin{aligned}
\left\| \mathbf{P}_{T^{t-1} \cup T} \mathbf{M}^* (\mathbf{y} - \mathbf{M} \mathbf{x}^{t-1}) \right\|_2^2 &\geq \frac{1}{1 + \gamma_2} \left\| \mathbf{P}_{T^{t-1} \cup T} \mathbf{M}^* \mathbf{M} (\mathbf{x} - \mathbf{x}^t) \right\|_2^2 - \frac{1}{\gamma_2} \left\| \mathbf{P}_{T^{t-1} \cup T} \mathbf{M}^* \mathbf{e} \right\|_2^2 \quad (\text{C.11}) \\
&\geq \frac{1}{1 + \beta} \frac{1}{1 + \gamma_2} \left\| \mathbf{x} - \mathbf{x}^{t-1} \right\|_2^2 - \frac{1}{\gamma_2} \left\| \mathbf{P}_{T^{t-1} \cup T} \mathbf{M}^* \mathbf{e} \right\|_2^2 - \frac{1}{\beta} \frac{1}{1 + \gamma_2} \left\| \mathbf{P}_{T^{t-1} \cup T} (\mathbf{M}^* \mathbf{M} - \mathbf{I}_d) (\mathbf{x} - \mathbf{x}^{t-1}) \right\|_2^2 \\
&\geq \left(\frac{1}{1 + \beta} - \frac{\delta_{(\zeta+1)k}}{\beta}\right) \frac{1}{1 + \gamma_2} \left\| \mathbf{x} - \mathbf{x}^{t-1} \right\|_2^2 - \frac{(1 + \delta_{(\zeta+1)k})}{\gamma_2} \left\| \mathbf{e} \right\|_2^2.
\end{aligned}$$

By combining (C.10) and (C.11) with (C.9) we have

$$\begin{aligned}
(1 + \alpha)(1 + \gamma_1) \left\| \mathbf{Q}_{\tilde{T}^t} (\mathbf{x} - \mathbf{x}^{t-1}) \right\|_2^2 &\leq \frac{(1 + \gamma_1)(1 + \delta_{3\zeta k})}{\gamma_1} \left\| \mathbf{e} \right\|_2^2 + \tilde{C}_{2k} \frac{(1 + \delta_{(1+\zeta)k})}{\gamma_2} \left\| \mathbf{e} \right\|_2^2 \quad (\text{C.12}) \\
&+ \left(1 + \alpha + \delta_{(3\zeta+1)k} + \frac{\delta_{(3\zeta+1)k}}{\alpha}\right) (1 + \gamma_1) \left\| \mathbf{x} - \mathbf{x}^{t-1} \right\|_2^2 - \tilde{C}_k \left(\frac{1}{1 + \beta} - \frac{\delta_{(1+\zeta)k}}{\beta}\right) \frac{1}{1 + \gamma_2} \left\| \mathbf{x} - \mathbf{x}^{t-1} \right\|_2^2.
\end{aligned}$$

Division of both sides by  $(1 + \alpha)(1 + \gamma_1)$  yields

$$\begin{aligned}
\left\| \mathbf{Q}_{\tilde{T}^t} (\mathbf{x} - \mathbf{x}^{t-1}) \right\|_2^2 &\leq \left(\frac{1 + \delta_{3\zeta k}}{\gamma_1(1 + \alpha)} + \frac{(1 + \delta_{(\zeta+1)k})\tilde{C}_{2k}}{\gamma_2(1 + \alpha)(1 + \gamma_1)}\right) \left\| \mathbf{e} \right\|_2^2 \quad (\text{C.13}) \\
&+ \left(1 + \frac{\delta_{(3\zeta+1)k}}{\alpha} - \frac{\tilde{C}_{2k}}{(1 + \alpha)(1 + \gamma_1)(1 + \gamma_2)} \left(\frac{1}{1 + \beta} - \frac{\delta_{(\zeta+1)k}}{\beta}\right)\right) \left\| \mathbf{x} - \mathbf{x}^{t-1} \right\|_2^2.
\end{aligned}$$

Substituting  $\beta = \frac{\sqrt{\delta_{(\zeta+1)k}}}{1 - \sqrt{\delta_{(\zeta+1)k}}}$  gives

$$\begin{aligned}
\left\| \mathbf{Q}_{\tilde{T}^t} (\mathbf{x} - \mathbf{x}^{t-1}) \right\|_2^2 &\leq \left(\frac{1 + \delta_{3\zeta k}}{\gamma_1(1 + \alpha)} + \frac{(1 + \delta_{(\zeta+1)k})\tilde{C}_{2k}}{\gamma_2(1 + \alpha)(1 + \gamma_1)}\right) \left\| \mathbf{e} \right\|_2^2 \quad (\text{C.14}) \\
&+ \left(1 + \frac{\delta_{(3\zeta+1)k}}{\alpha} - \frac{\tilde{C}_{2k}}{(1 + \alpha)(1 + \gamma_1)(1 + \gamma_2)} \left(1 - \sqrt{\delta_{(\zeta+1)k}}\right)^2\right) \left\| \mathbf{x} - \mathbf{x}^{t-1} \right\|_2^2,
\end{aligned}$$

Using  $\alpha = \frac{\sqrt{\delta_{(3\zeta+1)k}}}{\sqrt{\frac{\tilde{C}_{2k}}{(1+\gamma_1)(1+\gamma_2)}(1-\sqrt{\delta_{(\zeta+1)k}})-\sqrt{\delta_{(3\zeta+1)k}}}}$  yields

$$\begin{aligned} \left\| \mathbf{Q}_{\tilde{\Lambda}^t}(\mathbf{x} - \mathbf{x}^{t-1}) \right\|_2^2 &\leq \left( \frac{1 + \delta_{3\zeta k}}{\gamma_1(1 + \alpha)} + \frac{(1 + \delta_{(\zeta+1)k})\tilde{C}_{2k}}{\gamma_2(1 + \alpha)(1 + \gamma_1)} \right) \|\mathbf{e}\|_2^2 \\ &\quad + \left( - \left( \sqrt{\delta_{(3\zeta+1)k}} - \sqrt{\frac{\tilde{C}_{2k}}{(1 + \gamma_1)(1 + \gamma_2)}(1 - \sqrt{\delta_{(\zeta+1)k}})} \right)^2 + 1 \right) \|\mathbf{x} - \mathbf{x}^{t-1}\|_2^2, \end{aligned} \quad (\text{C.15})$$

The values of  $\gamma_1, \gamma_2$  give a tradeoff between the convergence rate and the size of the noise coefficient. For smaller values we get better convergence rate but higher amplification of the noise. We make no optimization on them and choose them to be  $\gamma_1 = \gamma_2 = \gamma$  where  $\gamma$  is an arbitrary number greater than 0. Thus we have

$$\begin{aligned} \left\| \mathbf{Q}_{\tilde{T}^t}(\mathbf{x} - \mathbf{x}^{t-1}) \right\|_2^2 &\leq \left( \frac{1 + \delta_{3\zeta k}}{\gamma(1 + \alpha)} + \frac{(1 + \delta_{(\zeta+1)k})\tilde{C}_{2k}}{\gamma(1 + \alpha)(1 + \gamma)} \right) \|\mathbf{e}\|_2^2 \\ &\quad + \left( - \left( \sqrt{\delta_{(3\zeta+1)k}} - \frac{\sqrt{\tilde{C}_{2k}}}{1 + \gamma} (1 - \sqrt{\delta_{(\zeta+1)k}}) \right)^2 + 1 \right) \|\mathbf{x} - \mathbf{x}^{t-1}\|_2^2, \end{aligned} \quad (\text{C.16})$$

Using the triangle inequality and the fact that  $\mathbf{Q}_{\tilde{T}^t} \mathbf{x}_p = \mathbf{Q}_{\tilde{T}^t} \mathbf{x}^{t-1} = 0$  gives the desired result.  $\square$



# Bibliography

- [1] R. Giryes and M. Elad, "RIP-based near-oracle performance guarantees for SP, CoSaMP, and IHT," *IEEE Trans. Signal Process.*, vol. 60, no. 3, pp. 1465–1468, March 2012.
- [2] R. Giryes and V. Cevher, "Online performance guarantees for sparse recovery," in *IEEE International Conference on Acoustics, Speech and Signal Processing (ICASSP)*, 2011, pp. 2020–2023.
- [3] R. Giryes and M. Elad, "Denoising with greedy-like pursuit algorithms," in *The 19th European Signal Processing Conference (EUSIPCO-2011)*, Barcelona, Spain, 2011.
- [4] R. Giryes, S. Nam, M. Elad, R. Gribonval, and M. E. Davies, "Greedy-like algorithms for the cospase analysis model," *to appear in the Special Issue in Linear Algebra and its Applications on Sparse Approximate Solution of Linear Systems*, 2013.
- [5] R. Giryes, S. Nam, R. Gribonval, and M. E. Davies, "Iterative cospase projection algorithms for the recovery of cospase vectors," in *The 19th European Signal Processing Conference (EUSIPCO-2011)*, Barcelona, Spain, 2011.
- [6] R. Giryes and M. Elad, "CoSaMP and SP for the cospase analysis model," in *The 20th European Signal Processing Conference (EUSIPCO-2012)*, Bucharest, Romania, 2012.
- [7] —, "Can we allow linear dependencies in the dictionary in the synthesis framework?" in *IEEE International Conference on Acoustics, Speech and Signal Processing (ICASSP)*, 2013.
- [8] —, "Iterative hard thresholding for signal recovery using near optimal projections?" in *10th Int. Conf. on Sampling Theory Appl. (SAMPTA)*, 2013.
- [9] —, "OMP with highly coherent dictionaries," in *10th Int. Conf. on Sampling Theory Appl. (SAMPTA)*, 2013.
- [10] —, "Sparsity based poisson denoising," in *IEEE 27th Convention of Electrical Electronics Engineers in Israel (IEEEI)*, 2012, 2012, pp. 1–5.

- [11] R. Giryes and D. Needell, "Greedy signal space methods for incoherence and beyond," *CoRR*, vol. abs/1309.2676, 2013.
- [12] R. Giryes, "Greedy algorithm for the analysis transform domain," *CoRR*, vol. abs/1309.7298, 2013.
- [13] R. Giryes and M. Elad, "Sparsity based poisson denoising with dictionary learning," *CoRR*, vol. abs/1309.4306, 2013.
- [14] D. L. Donoho, M. Elad, and V. N. Temlyakov, "Stable recovery of sparse overcomplete representations in the presence of noise," *IEEE Trans. Inf. Theory*, vol. 52, no. 1, pp. 6–18, Jan. 2006.
- [15] K. Dabov, A. Foi, V. Katkovnik, and K. Egiazarian, "Image denoising with block-matching and 3d filtering," in *Proc. SPIE*, vol. 6064, 2006, pp. 606 414–606 414–12.
- [16] A. Danielyan, V. Katkovnik, and K. Egiazarian, "BM3D frames and variational image deblurring," *IEEE Trans. Image Process.*, vol. 21, no. 4, pp. 1715–1728, 2012.
- [17] R. Zeyde, M. Elad, and M. Protter, "On single image scale-up using sparse-representations," in *Proceedings of the 7th international conference on Curves and Surfaces*. Berlin, Heidelberg: Springer-Verlag, 2012, pp. 711–730.
- [18] A. Fannjiang, T. Strohmer, and P. Yan, "Compressed remote sensing of sparse objects," *SIAM Journal on Imaging Sciences*, vol. 3, no. 3, pp. 595–618, 2010.
- [19] M. Lustig, D. Donoho, J. Santos, and J. Pauly, "Compressed sensing MRI," *IEEE Signal Processing Magazine*, vol. 25, no. 2, pp. 72–82, 2008.
- [20] J. Salmon, Z. Harmany, C.-A. Deledalle, and R. Willett, "Poisson noise reduction with non-local PCA," *Journal of Mathematical Imaging and Vision*, pp. 1–16, 2013.
- [21] A. M. Bruckstein, D. L. Donoho, and M. Elad, "From sparse solutions of systems of equations to sparse modeling of signals and images," *SIAM Review*, vol. 51, no. 1, pp. 34–81, 2009.
- [22] M. Elad, P. Milanfar, and R. Rubinstein, "Analysis versus synthesis in signal priors," *Inverse Problems*, vol. 23, no. 3, pp. 947–968, June 2007.

- [23] S. Nam, M. Davies, M. Elad, and R. Gribonval, "The cosparsity analysis model and algorithms," *Appl. Comput. Harmon. Anal.*, vol. 34, no. 1, pp. 30 – 56, 2013.
- [24] E. J. Candès, Y. C. Eldar, D. Needell, and P. Randall, "Compressed sensing with coherent and redundant dictionaries," *Appl. Comput. Harmon. Anal.*, vol. 31, no. 1, pp. 59 – 73, 2011.
- [25] S. Vaiter, G. Peyre, C. Dossal, and J. Fadili, "Robust sparse analysis regularization," *IEEE Trans. Inf. Theory*, vol. 59, no. 4, pp. 2001–2016, 2013.
- [26] L. I. Rudin, S. Osher, and E. Fatemi, "Nonlinear total variation based noise removal algorithms," *Phys. D*, vol. 60, no. 1-4, pp. 259–268, Nov. 1992.
- [27] D. Needell and R. Ward, "Stable image reconstruction using total variation minimization," *SIAM Journal on Imaging Sciences*, vol. 6, no. 2, pp. 1035–1058, 2013.
- [28] E. J. Candès and T. Tao, "Near-optimal signal recovery from random projections: Universal encoding strategies?" *IEEE Trans. Inf. Theory*, vol. 52, no. 12, pp. 5406 –5425, Dec. 2006.
- [29] E. Candès and T. Tao, "Decoding by linear programming," *IEEE Trans. Inf. Theory*, vol. 51, no. 12, pp. 4203 – 4215, dec. 2005.
- [30] ———, "The Dantzig selector: Statistical estimation when  $p$  is much larger than  $n$ ," *Annals Of Statistics*, vol. 35, p. 2313, 2007.
- [31] P. Bickel, Y. Ritov, and A. Tsybakov, "Simultaneous analysis of lasso and dantzig selector," *Annals of Statistics*, vol. 37, no. 4, pp. 1705–1732, 2009.
- [32] E. Candès, "Modern statistical estimation via oracle inequalities," *Acta Numerica*, vol. 15, pp. 257–325, 2006.
- [33] G. Davis, S. Mallat, and M. Avellaneda, "Adaptive greedy approximations," *Journal of Constructive Approximation*, vol. 50, pp. 57–98, 1997.
- [34] S. S. Chen, D. L. Donoho, and M. A. Saunders, "Atomic decomposition by basis pursuit," *SIAM Journal on Scientific Computing*, vol. 20, no. 1, pp. 33–61, 1998.
- [35] D. L. Donoho and M. Elad, "On the stability of the basis pursuit in the presence of noise," *Signal Process.*, vol. 86, no. 3, pp. 511–532, 2006.

- [36] R. Tibshirani, "Regression shrinkage and selection via the lasso," *J. Roy. Statist. Soc. B*, vol. 58, no. 1, pp. 267–288, 1996.
- [37] S. Chen, S. A. Billings, and W. Luo, "Orthogonal least squares methods and their application to non-linear system identification," *International Journal of Control*, vol. 50, no. 5, pp. 1873–1896, 1989.
- [38] S. Mallat and Z. Zhang, "Matching pursuits with time-frequency dictionaries," *IEEE Trans. Signal Process.*, vol. 41, pp. 3397–3415, 1993.
- [39] D. Needell and J. Tropp, "CoSaMP: Iterative signal recovery from incomplete and inaccurate samples," *Appl. Comput. Harmon. A.*, vol. 26, no. 3, pp. 301 – 321, May 2009.
- [40] W. Dai and O. Milenkovic, "Subspace pursuit for compressive sensing signal reconstruction," *IEEE Trans. Inf. Theory*, vol. 55, no. 5, pp. 2230 –2249, May 2009.
- [41] T. Blumensath and M. Davies, "Iterative hard thresholding for compressed sensing," *Appl. Comput. Harmon. Anal.*, vol. 27, no. 3, pp. 265 – 274, 2009.
- [42] S. Foucart, "Hard thresholding pursuit: an algorithm for compressive sensing," *SIAM J. Numer. Anal.*, vol. 49, no. 6, pp. 2543–2563, 2011.
- [43] D. L. Donoho and M. Elad, "Optimal sparse representation in general (nonorthogonal) dictionaries via  $l_1$  minimization," *Proceedings of the National Academy of Science*, vol. 100, pp. 2197–2202, Mar 2003.
- [44] T. Zhang, "Sparse recovery with orthogonal matching pursuit under RIP," *IEEE Trans. Inf. Theory*, vol. 57, no. 9, pp. 6215 –6221, Sept. 2011.
- [45] S. Foucart, "Sparse recovery algorithms: sufficient conditions in terms of restricted isometry constants," in *Approximation Theory XIII*. Springer Proceedings in Mathematics, 2010, pp. 65–77.
- [46] Z. Ben-Haim, Y. Eldar, and M. Elad, "Coherence-based performance guarantees for estimating a sparse vector under random noise," *IEEE Trans. Signal Process.*, vol. 58, no. 10, pp. 5030 –5043, Oct. 2010.
- [47] M. Rudelson and R. Vershynin, "Sparse reconstruction by convex relaxation: Fourier and gaussian measurements," in *Information Sciences and Systems, 2006 40th Annual Conference on*, 22-24 2006, pp. 207 –212.

- [48] T. Strohmer and R. W. Heath Jr., "Grassmannian frames with applications to coding and communication," *Appl. Comput. Harmon. A.*, vol. 14, no. 3, pp. 257–275, 2003.
- [49] T. Cai, L. Wang, and G. Xu, "Stable recovery of sparse signals and an oracle inequality," *IEEE Trans. Inf. Theory*, vol. 56, no. 7, pp. 3516–3522, Jul. 2010.
- [50] Y. Liu, T. Mi, and S. Li, "Compressed sensing with general frames via optimal-dual-based  $l_1$ -analysis," *IEEE Trans. Inf. Theory*, vol. 58, no. 7, pp. 4201–4214, 2012.
- [51] M. Kabanava and H. Rauhut, "Analysis  $l_1$ -recovery with frames and Gaussian measurements," *Preprint*, 2013.
- [52] T. Peleg and M. Elad, "Performance guarantees of the thresholding algorithm for the cospase analysis model," *IEEE Trans. Inf. Theory*, vol. 59, no. 3, pp. 1832–1845, Mar. 2013.
- [53] J. Salmon, C.-A. Deledalle, R. Willett, and Z. T. Harmany, "Poisson noise reduction with non-local PCA," in *IEEE International Conference on Acoustics, Speech and Signal Processing (ICASSP)*, March 2012, pp. 1109–1112.
- [54] J. Mairal, G. Sapiro, and M. Elad, "Multiscale sparse image representation with learned dictionaries," vol. 3, sep. 2007, pp. III–105–III–108.
- [55] G. Yu, G. Sapiro, and S. Mallat, "Solving inverse problems with piecewise linear estimators: From Gaussian mixture models to structured sparsity," *IEEE Trans. on Image Processing*, vol. 21, no. 5, pp. 2481–2499, may 2012.
- [56] R. Giryes and M. Elad, "Rip-based near-oracle performance guarantees for subspace pursuit, cosamp, and iterative hard-thresholding," *Technion CS-2010-23 Technical Report*, 2010.
- [57] Y. Lu and M. Do, "A theory for sampling signals from a union of subspaces," *IEEE Trans. Signal Process.*, vol. 56, no. 6, pp. 2334–2345, Jun. 2008.
- [58] D. Donoho and M. Elad, "Optimally sparse representation in general (nonorthogonal) dictionaries via  $\ell^1$  minimization," *Proc. Nat. Aca. Sci.*, vol. 100, no. 5, pp. 2197–2202, Mar. 2003.
- [59] R. Gribonval and M. Nielsen, "Sparse representations in unions of bases," *IEEE Trans. Inf. Theory*, vol. 49, no. 12, pp. 3320–3325, Dec. 2003.

- [60] J. Tropp, "Just relax: Convex programming methods for identifying sparse signals," *IEEE Trans. Inf. Theory*, vol. 52, no. 3, pp. 1030–1051, Mar. 2006.
- [61] B. Natarajan, "Sparse approximate solutions to linear systems," *SIAM Journal on Computing*, vol. 24, pp. 227–234, 1995.
- [62] Y. Pati, R. Rezaeiifar, and P. Krishnaprasad, "Orthonormal matching pursuit : recursive function approximation with applications to wavelet decomposition," in *Proceedings of the 27<sup>th</sup> Annual Asilomar Conf. on Signals, Systems and Computers*, Nov. 1993.
- [63] D. Needell and R. Vershynin, "Signal recovery from incomplete and inaccurate measurements via regularized orthogonal matching pursuit," *IEEE Journal of Selected Topics in Signal Processing*, vol. 4, no. 2, pp. 310–316, Apr. 2010.
- [64] A. Kyrillidis and V. Cevher, "Recipes on hard thresholding methods," in *4th Int. Workshop on Computational Advances in Multi-Sensor Adaptive Processing (CAMSAP)*, Dec. 2011, pp. 353–356.
- [65] T. Blumensath, "Accelerated iterative hard thresholding," *Signal Processing*, vol. 92, no. 3, pp. 752–756, 2012.
- [66] H. Rauhut, "Stability results for random sampling of sparse trigonometric polynomials," *IEEE Trans. Inf. Theory*, vol. 54, no. 12, pp. 5661–5670, 2008.
- [67] J. Tropp, J. Laska, M. Duarte, J. Romberg, and R. Baraniuk, "Beyond nyquist: Efficient sampling of sparse bandlimited signals," *IEEE Trans. Inf. Theory*, vol. 56, no. 1, pp. 520–544, 2010.
- [68] H. Rauhut, J. Romberg, and J. A. Tropp, "Restricted isometries for partial random circulant matrices," *Appl. Comput. Harmon. A.*, vol. 32, no. 2, pp. 242–254, 2012.
- [69] F. Krahmer, S. Mendelson, and H. Rauhut, "Suprema of chaos processes and the restricted isometry property," *to appear in Comm. Pure Appl. Math.*, 2013.
- [70] J. Tropp, "Just relax: convex programming methods for identifying sparse signals in noise," *IEEE Trans. Inf. Theory*, vol. 52, no. 3, pp. 1030–1051, March 2006.
- [71] E. Candès, J. K. Romberg, and T. Tao, "Stable signal recovery from incomplete and inaccurate measurements," *Communications on Pure and Applied Mathematics*, vol. 59, no. 8, pp. 1207–1223, 2006.

- [72] E. J. Candès, "The restricted isometry property and its implications for compressed sensing," *Comptes-rendus de l'Académie des Sciences, Paris, Series I*, vol. 346, no. 9–10, pp. 589 – 592, 2008.
- [73] Q. Mo and S. Li, "New bounds on the restricted isometry constant," *Appl. Comput. Harmon. A.*, vol. 31, no. 3, pp. 460 – 468, 2011.
- [74] T. Cai, L. Wang, and G. Xu, "Shifting inequality and recovery of sparse signals," *IEEE Trans. Signal Process.*, vol. 58, no. 3, pp. 1300 –1308, march 2010.
- [75] ———, "New bounds for restricted isometry constants," *To appear in IEEE Trans. Inf. Theory*, 2010.
- [76] H. Rauhut, K. Schnass, and P. Vandergheynst, "Compressed sensing and redundant dictionaries," *IEEE Trans. Inf. Theory*, vol. 54, no. 5, pp. 2210 –2219, May 2008.
- [77] A. Chistov and D. Grigoriev, "Complexity of quantifier elimination in the theory of algebraically closed fields," in *Mathematical Foundations of Computer Science 1984*, ser. Lecture Notes in Computer Science, M. Chytil and V. Koubek, Eds. Springer Berlin Heidelberg, 1984, vol. 176, pp. 17–31.
- [78] E. J. Candès and B. Recht, "Exact matrix completion via convex optimization," *Found. Comput. Math.*, vol. 9, no. 6, pp. 717–772, Dec. 2009.
- [79] M. Michenková, "Numerical algorithms for low-rank matrix completion problems," *Technical Report*, May 2011.
- [80] K. Lee and Y. Bresler, "ADMiRA: Atomic decomposition for minimum rank approximation," *IEEE Trans. Inf. Theory*, vol. 56, no. 9, pp. 4402 –4416, Sept. 2010.
- [81] W. Dai, O. Milenkovic, and E. Kerman, "Subspace evolution and transfer (SET) for low-rank matrix completion," *IEEE Trans. Signal Process.*, vol. 59, no. 7, pp. 3120 –3132, July 2011.
- [82] J. Tanner and K. Wei, "Normalized iterative hard thresholding for matrix completion," *to appear in SIAM J. on Scientific Computing*, 2013.
- [83] S. Nam, M. Davies, M. Elad, and R. Gribonval, "Cospase analysis modeling - uniqueness and algorithms," in *IEEE International Conference on Acoustics, Speech and Signal Processing (ICASSP)*, May 2011.

- [84] —, “Cospase analysis modeling,” in *9th Int. Conf. on Sampling Theory Appl. (SAMPTA)*, Singapore, 2011.
- [85] I. Daubechies, R. DeVore, M. Fornasier, and C. S. Gntk, “Iteratively reweighted least squares minimization for sparse recovery,” *Communications on Pure and Applied Mathematics*, vol. 63, no. 1, pp. 1–38, 2010.
- [86] R. Rubinstein, T. Peleg, and M. Elad, “Analysis K-SVD: A dictionary-learning algorithm for the analysis sparse model,” *IEEE Trans. on Signal Process.*, vol. 61, no. 3, pp. 661–677, Feb. 2013.
- [87] J. Boulanger, C. Kervrann, P. Bouthemy, P. Elbau, J.-B. Sibarita, and J. Salamero, “Patch-based nonlocal functional for denoising fluorescence microscopy image sequences,” *IEEE Trans. on Med. Imag.*, vol. 29, no. 2, pp. 442–454, Feb. 2010.
- [88] M. Makitalo and A. Foi, “Optimal inversion of the Anscombe transformation in low-count Poisson image denoising,” *IEEE Trans. on Image Proces.*, vol. 20, no. 1, pp. 99–109, Jan. 2011.
- [89] B. Zhang, J. Fadili, and J. Starck, “Wavelets, ridgelets, and curvelets for poisson noise removal,” *IEEE Trans. on Image Processing*, vol. 17, no. 7, pp. 1093–1108, July 2008.
- [90] F. J. Anscombe, “The transformation of Poisson, Binomial and negative-Binomial data,” *Biometrika*, vol. 35, no. 3-4, pp. 246–254, 1948.
- [91] M. Fisz, “The limiting distribution of a function of two independent random variables and its statistical application,” *Colloquium Mathematicum*, vol. 3, pp. 138–146, 1955.
- [92] K. Dabov, A. Foi, V. Katkovnik, and K. Egiazarian, “Image denoising by sparse 3-d transform-domain collaborative filtering,” *IEEE Trans. on Image Processing*, vol. 16, no. 8, pp. 2080–2095, 2007.
- [93] J. Mairal, F. Bach, J. Ponce, G. Sapiro, and A. Zisserman, “Non-local sparse models for image restoration,” in *ICCV, 2009*, 2009, pp. 2272–2279.
- [94] Z. Ben-Haim and Y. C. Eldar, “The Cramèr?-Rao bound for estimating a sparse parameter vector,” *IEEE Trans. Signal Process.*, vol. 58, no. 6, pp. 3384–3389, june 2010.

- [95] T. Blumensath and M. Davies, "Sampling theorems for signals from the union of finite-dimensional linear subspaces," *IEEE Trans. Inf. Theory*, vol. 55, no. 4, pp. 1872–1882, april 2009.
- [96] S. Mendelson, A. Pajor, and N. Tomczak-Jaegermann, "Uniform uncertainty principle for bernoulli and subgaussian ensembles," *Constructive Approximation*, vol. 28, pp. 277–289, 2008.
- [97] F. Krahmer and R. Ward, "New and improved Johnson-Lindenstrauss embeddings via the restricted isometry property," *SIAM J. Math. Analysis*, vol. 43, no. 3, pp. 1269–1281, 2011.
- [98] R. Baraniuk, M. Davenport, R. DeVore, and M. Wakin, "A simple proof of the restricted isometry property for random matrices," *Constructive Approximation*, vol. 28, no. 3, pp. 253–263, 2008.
- [99] R. Gribonval, M. E. Pfetsch, and A. M. Tillmann, "Projection onto the k-cosparse set is NP-hard," *submitted to IEEE Trans. Inf. Theory*, 2013.
- [100] T. Han, S. Kay, and T. Huang, "Optimal segmentation of signals and its application to image denoising and boundary feature extraction," in *IEEE International Conference on Image Processing (ICIP)*, vol. 4, oct. 2004, pp. 2693 – 2696 Vol. 4.
- [101] R. Tibshirani, M. Saunders, S. Rosset, J. Zhu, and K. Knight, "Sparsity and smoothness via the fused Lasso," *Journal of the Royal Statistical Society: Series B (Statistical Methodology)*, vol. 67, no. 1, pp. 91–108, 2005.
- [102] R. Garg and R. Khandekar, "Gradient descent with sparsification: an iterative algorithm for sparse recovery with restricted isometry property," in *ICML '09*. New York, NY, USA: ACM, 2009, pp. 337–344.
- [103] M. Rudelson and R. Vershynin, "Non-asymptotic theory of random matrices: extreme singular values," in *International Congress of Mathematicians*, 2010.
- [104] D. L. Donoho and J. Tanner, "Counting faces of randomly-projected polytopes when the projection radically lowers dimension," *J. of the AMS*, pp. 1–53, 2009.
- [105] R. Giryes, "Sampling in the analysis transform domain," 2013, in preparation.

- [106] J. A. Tropp, "Greed is good: algorithmic results for sparse approximation," *IEEE Trans. Inf. Theory*, vol. 50, no. 10, pp. 2231–2242, 2004.
- [107] M. Elad and A. Bruckstein, "A generalized uncertainty principle and sparse representation in pairs of bases," *IEEE Trans. Inf. Theory*, vol. 48, no. 9, pp. 2558–2567, Sep 2002.
- [108] M. Davenport, D. Needell, and M. Wakin, "Signal space CoSaMP for sparse recovery with redundant dictionaries," *To appear in IEEE Trans. Inf. Theory*, 2013.
- [109] T. Blumensath, "Sampling and reconstructing signals from a union of linear subspaces," *IEEE Trans. Inf. Theory*, vol. 57, no. 7, pp. 4660–4671, 2011.
- [110] M. Elad, *Sparse and Redundant Representations: From Theory to Applications in Signal and Image Processing*, 1st ed. Springer Publishing Company, Incorporated, 2010.
- [111] R. O. Schmidt, "Multiple emitter location and signal parameter estimation," *IEEE Trans. Atten. Prop.*, vol. 34, no. 3, pp. 276–280, Apr. 1986.
- [112] A. Fannjiang and W. Liao, "Coherence-pattern guided compressive sensing with unresolved grids," *IAM J. Imaging Sci.*, vol. 5, pp. 179–202, 2012.
- [113] E. J. Candès and C. Fernandez-Granda, "Towards a mathematical theory of super-resolution," *Commun. Pur. Appl. Math*, 2013, to appear.
- [114] L. Demanet, D. Needell, and N. Nguyen, "Super-resolution via superset selection and pruning," in *10th Int. Conf. on Sampling Theory Appl. (SAMPTA)*, 2013.
- [115] A. Divekar and D. Needell, "Using correlated subset structure for compressive sensing recovery," in *10th Int. Conf. on Sampling Theory Appl. (SAMPTA)*, 2013.
- [116] R. Baraniuk, V. Cevher, M. Duarte, and C. Hegde, "Model-based compressive sensing," *IEEE Trans. Inf. Theory*, vol. 56, no. 4, pp. 1982–2001, 2010.
- [117] M. Davenport and M. Wakin, "Compressive sensing of analog signals using discrete prolate spheroidal sequences," *Appl. Comput. Harmon. A.*, vol. 33, no. 3, pp. 438–472, 2012.
- [118] B. Ophir, M. Lustig, and M. Elad, "Multi-scale dictionary learning using wavelets," *IEEE Journal of Selected Topics in Signal Processing*, vol. 5, no. 5, pp. 1014–1024, 2011.

- [119] S. Ravishankar and Y. Bresler, "MR image reconstruction from highly undersampled k-space data by dictionary learning," *IEEE Trans. Medical Imaging*, vol. 30, no. 5, pp. 1028–1041, 2011.
- [120] —, "Sparsifying transform learning for compressed sensing MRI," in *2013 IEEE 10th International Symposium on Biomedical Imaging (ISBI)*, 2013, pp. 17–20.
- [121] Y. Plan, R. Vershynin, and R. Giryes, "Limitations of low-dimensional manifold models for the analysis version of compressed sensing," 2013.
- [122] Z. T. Harmany, R. F. Marcia, and R. M. Willett, "This is SPIRAL-TAP: Sparse poisson intensity reconstruction algorithms – theory and practice," *Trans. Img. Proc.*, vol. 21, no. 3, pp. 1084–1096, Mar. 2012.
- [123] H. Burger and S. Harmeling, "Improving denoising algorithms via a multi-scale meta-procedure," in *Pattern Recognition*, ser. Lecture Notes in Computer Science, R. Mester and M. Felsberg, Eds. Springer Berlin Heidelberg, 2011, vol. 6835, pp. 206–215.
- [124] C.-A. Deledalle, F. Tupin, and L. Denis, "Poisson NL means: Unsupervised non local means for poisson noise," in *IEEE International Conference on Image Processing (ICIP)*, sept. 2010, pp. 801 –804.
- [125] R. Giryes, M. Elad, and Y. C. Eldar, "The projected GSURE for automatic parameter tuning in iterative shrinkage methods," *Appl. Comput. Harmon. A.*, vol. 30, no. 3, pp. 407 – 422, 2011.